



Tsagkari, Erifyli (2017) *The role of physical and biological processes in biofilms in drinking water*. PhD thesis.

<http://theses.gla.ac.uk/8557/>

Copyright and moral rights for this work are retained by the author

A copy can be downloaded for personal non-commercial research or study, without prior permission or charge

This work cannot be reproduced or quoted extensively from without first obtaining permission in writing from the author

The content must not be changed in any way or sold commercially in any format or medium without the formal permission of the author

When referring to this work, full bibliographic details including the author, title, awarding institution and date of the thesis must be given

Enlighten:Theses
<http://theses.gla.ac.uk/>
theses@gla.ac.uk



University
of Glasgow

The role of physical and biological processes in biofilms in drinking water

Erifyli Tsagkari

Submitted in fulfilment of the requirements for the Degree of
Doctor of Philosophy

School of Engineering
College of Science and Engineering
University of Glasgow

October, 2017

Abstract

Microorganisms, such as bacteria, fungi, viruses and protozoa, colonise the inner surfaces of drinking water pipes and form biofilms. Drinking water biofilms act to protect the microorganisms that they house from the harsh conditions that we impose such as disinfection. Biofilms are generally thought of as being detrimental in drinking water distribution systems; they can harbour pathogens that intermittently emerge at the tap and they can affect the aesthetics of drinking water. The formation and dissolution of biofilms are intricately linked with the flow conditions and therefore, if we are to manage biofilms in drinking water systems, then it is imperative that we understand the crucial role that hydrodynamics play. Thus, my thesis focuses on the growth of biofilms in drinking water under three distinct flow regimes: turbulent, transition and laminar, and under stagnant conditions, and reveals the role that hydrodynamics play in shaping biofilms in drinking water distribution systems.

Not all bacteria are merely passive tracers in flow whose fate is governed by the physical flow alone. This thesis presents evidence that there might be key bacteria in aggregation in drinking water, whose biology acts to enhance the formation of multi-species biofilms. I explored that by testing the role that the *Methylobacterium* strain DSM 18358 played in the formation of biofilms on surfaces that starts with the formation of aggregates in the bulk water. I also explored whether the ability of this *Methylobacterium* strain to form aggregates was influenced by the flow regime. Ultimately, this research reveals whether the formation and structure of those aggregates in drinking water is influenced by the subtle interplay between biological and physical processes.

Given that they are bacteria that can degrade various dangerous chlorine disinfection by-products I explored the role of the *Methylobacterium* strain DSM 18358 in the concentration of trihalomethanes in drinking water as these chlorine disinfection by-products can cause serious problems to human health when they occur at high concentrations in drinking water. Overall, I identified whether the presence of this *Methylobacterium* strain in drinking water can actually deliver a service that contributes to better drinking water quality.

Table of Contents

The role of physical and biological processes in biofilms in drinking water	1
Abstract	2
Table of Contents	3
List of Tables.....	8
List of Figures	9
Acknowledgments	15
Declaration	16
Abbreviations	17
1 Introduction	20
1.1 Problem Statement.....	20
1.2 Research aims and objectives	20
1.3 Research outlines.....	22
2 Literature Review	25
2.1 Biofilms	25
2.2 Biofilms in pipes	26
2.2.1 Biofilms in drinking water distribution systems	26
2.2.2 Biofilms in wastewater systems	28
2.2.3 Biofilms in indwelling tubular medical devices	29
2.2.4 Biofilms in oil and gas pipelines	30
2.2.5 Biofilms in fire protection pipes.....	31
2.2.6 Biofilms in cooling and heating water systems	32
2.3 Biofilm structures	33
2.3.1 Mushroom structures	34
2.3.2 Flat structures	35
2.3.3 Filamentous structures	35
2.3.4 Ripple structures	36
2.3.5 Pellicle structures	37
2.3.6 Hollow structures.....	38
2.3.7 Wrinkled structures	38
2.3.8 Clusters	39
2.4 Bacterial Adhesion.....	40
2.5 Biofilm formation and development	42
2.5.1 The role of the extracellular polymeric substances	42

2.5.2	The role of quorum sensing	43
2.5.3	Other control factors.....	44
2.6	Detachment	45
2.7	Flow in a rotating annular reactor and in a pipe	45
2.7.1	Flow in a rotating annular reactor	46
2.7.2	Flow in a pipe	47
3	The role of flow regime in biofilms in drinking water	49
3.1	Introduction	49
3.2	Materials and Methods	51
3.2.1	Reactor conditions.....	51
3.2.2	Reactor medium	53
3.2.3	Experimental processes.....	54
3.2.4	Gravimetric measurements	57
3.2.5	Microcolonies count measurements.....	57
3.2.6	Biofilm structure measurements	59
3.2.7	Statistical analysis.....	60
3.2.8	Spatial statistics	61
3.3	Results and Discussion	64
3.3.1	Development process	64
3.3.2	Formation process.....	67
3.3.3	Changes of flow regime process.....	68
3.3.4	Biofilm structures.....	70
3.3.5	Semi-variograms	71
3.3.6	Autocorrelation function diagrams.....	72
3.3.7	Batch versus recirculation mode	75
3.3.8	Stagnant conditions	75
3.4	Conclusions	78
4	The role of <i>Methylobacterium</i> in aggregation in drinking water	80
4.1	Introduction	80
4.2	Materials and Methods	82
4.2.1	<i>Methylobacterium</i> culture	82
4.2.2	Drinking water culture	84
4.2.3	Inoculation of <i>Methylobacterium</i> into drinking water culture.....	84
4.2.4	Analysis of aggregates	85
4.2.5	Statistical analysis.....	86

4.3	Results and Discussion	86
4.3.1	Growth of cultures	86
4.3.2	Aggregation in drinking water	88
4.4	Conclusions	94
5	The role of <i>Methylobacterium</i> in aggregation in drinking water under two distinct flow regimes.....	95
5.1	Introduction	95
5.2	Materials and Methods	96
5.2.1	Operating system	96
5.2.2	Analysis of samples	97
5.2.3	Statistical analysis.....	98
5.3	Results	99
5.3.1	Differences between control and inoculated cultures	99
5.3.2	Differences between turbulent and laminar flow	102
5.3.3	Differences between the time periods of growth.....	102
5.4	Discussion	103
5.5	Conclusions	105
6	The structures of drinking water aggregates under stagnant and flow conditions.....	106
6.1	Introduction	106
6.2	Materials and Methods	107
6.2.1	DNA extraction.....	107
6.2.2	PCR for <i>Methylobacterium</i> DSM 18358	107
6.2.2.1	Initial amplification of a 369 bp region of the 16S gene from <i>Methylobacterium</i> DSM 18358 via general primers.....	107
6.2.2.2	Designing <i>Methylobacterium</i> DSM 18358-specific primers.....	108
6.2.2.3	PCR amplification of the 16S rRNA gene	109
	<i>In situ</i> hybridization.....	110
6.2.3	110
6.2.3.1	Fixation, storage and preparation of samples.....	110
6.2.3.2	Hybridization with oligonucleotide probes	110
6.2.3.3	Washing and microscopy.....	111
6.2.3.4	Control reactions	112
6.3	Results	117
6.3.1	Areas in which <i>Methylobacterium</i> was present	118
6.3.2	Areas in which <i>Methylobacterium</i> was not present	121

6.4	Discussion	124
6.5	Conclusions	125
7	The role of motility of <i>Methylobacterium</i> in aggregation	127
7.1	Introduction	127
7.2	Materials and Methods	129
7.2.1	Pure <i>Methylobacterium</i> colonies	129
7.2.2	Mixed drinking water and pure <i>Methylobacterium</i> colonies	131
7.3	Results and Discussion	132
7.3.1	Motility of pure <i>Methylobacterium</i> colonies.....	132
7.3.2	Interactions of mixed drinking water and pure <i>Methylobacterium</i> colonies	135
7.4	Conclusions	136
8	Effect of <i>Methylobacterium</i> on trihalomethanes concentration in drinking water	138
8.1	Introduction	138
8.2	Materials and Methods	141
8.2.1	Chlorine and trihalomethanes measurements at different times of water sampling.....	142
8.2.2	Chlorine and trihalomethanes measurements under different <i>Methylobacterium</i> concentrations	142
8.2.3	Chlorine and trihalomethanes measurements in drinking water under different organic matter concentrations.....	143
8.2.4	Trihalomethanes measurements in drinking water under different chlorine concentrations	143
8.3	Results	144
8.3.1	Chlorine and trihalomethanes concentrations in raw drinking water	144
8.3.2	The role of <i>Methylobacterium</i> in chlorine and trihalomethanes concentrations	144
8.3.3	The role of organic matter in chlorine and trihalomethanes concentrations	147
8.3.4	The role of chlorine in trihalomethanes concentration.....	150
8.4	Discussion	151
8.5	Conclusions	153
9	Conclusions and Future Work	155
9.1	Conclusions	155
9.2	Future Work	158

10	Appendix	160
10.1	Chapter 3.....	160
10.1.1	Protocol for fixation of biofilms on surfaces	160
10.1.2	Microcolonies and entropy measurements in the changes of flow regime process.....	161
10.1.3	Semi-Variograms	162
10.1.4	Autocorrelation function diagrams	165
10.2	Chapter 4.....	178
10.2.1	Protocol for the revival of the freeze-dried <i>Methylobacterium</i> culture	178
10.2.2	Culture medium R2A.....	178
10.2.3	Images from the analysis of aggregates.....	179
10.3	Chapter 5.....	180
10.3.1	Microcolonies attached on the reactor slides	180
10.3.2	Surface area of biofilms on the reactor slides.....	181
10.4	Chapter 6.....	182
10.4.1	Protocol for DNA extraction	182
10.4.2	Protocol for PCR.....	183
10.4.3	Protocol for agarose gel electrophoresis	184
10.4.4	Protocol for <i>in situ</i> hybridization	184
10.4.5	Amoeba protozoa	187
10.5	Chapter 8.....	189
10.5.1	Protocol for total chlorine concentration measurements	189
10.5.2	Protocol for trihalomethanes concentration measurements.....	189
	References.....	192

List of Tables

Table 3-1 Conditions for turbulent, transition and laminar flow.	53
Table 3-2 Development process for A, B and C experiments.	55
Table 3-3 Formation process for A, B and C experiments.	55
Table 3-4 Changes of flow regime each of which lasted for 24 hours for A, B and C experiments.	56
Table 4-1 Size of aggregates (mm ²) of the different liquid cultures at 24, 48 and 72 hours.	89
Table 4-2 Number of aggregates of the different liquid cultures at 24, 48 and 72 hours.	89
Table 4-3 Surface area (mm ²) that aggregates from the different liquid cultures occupied on membrane filters at 24, 48 and 72 hours.	90
Table 4-4 Aggregation scores of the different liquid cultures at 24, 48 and 72 hours.	91
Table 4-5 Cell concentrations in the bulk water of the different liquid cultures at 24, 48 and 72 hours.	93
Table 5-1 Significant differences that were found in the various measures between control and inoculated drinking water cultures in turbulent and laminar flow.	99
Table 5-2 Significant differences that were found in the various measures between turbulent and laminar flow for the control and inoculated drinking water cultures.	102
Table 5-3 Significant differences that were found in the various measures in turbulent and laminar flow between the different time periods.	103
Table 7-1 Summary of conditions of the first set of experiments.	131
Table 7-2 Summary of conditions of the second set of experiments.	132

List of Figures

Figure 2-1 Drinking water pipe in Denmark with a rough inner surface of iron and calcium precipitates. Source: (Boe-Hansen, 2001)	27
Figure 2-2 Typical morphologies of initially adhered cells and 24-hour biofilms found in wastewater treatment systems. Source: (Andersson et al., 2008). 29	
Figure 2-3 <i>Candida parapsilosis</i> on silicone tubing after 2 hours of exposure to urine. Source: (Percival et al., 2011)	30
Figure 2-4 Biofilm formation after 40 days on X52 steel coupon exposed to crude oil flow as revealed by scanning electron microscopy. Source: (Neria-Gonzalez et al., 2006).....	31
Figure 2-5 Formation of tubercles (corrosion deposits) on the surfaces of a carbon steel fire protection pipe. Sources: (Kraigsley et al., 2014)	32
Figure 2-6 Biofilm formation on stainless steel surface after 30 days of <i>in situ</i> exposure to cooling water as revealed by scanning electron microscopy. Source: (Wang et al., 2013)	33
Figure 2-7 Mushroom structures of biofilms in hydrothermal hot springs. Source: (Hall-Stoodley et al., 2004).....	34
Figure 2-8 Final formation of a flat <i>Pseudomonas aeruginosa</i> biofilm (bottom right of the image) as revealed by confocal laser scanning microscopy. Sources: (Klausen et al., 2003b, Klausen et al., 2006)	35
Figure 2-9 Streamers formed in hydrothermal hot springs biofilms. Source: (Hall-Stoodley et al., 2004)	36
Figure 2-10 Ripple structures of biofilms in laboratory flow cells. Source: (Hall-Stoodley et al., 2004)	37
Figure 2-11 Pellicle formation by <i>Pseudomonas fluorescens</i> isolates. Source: (Ude et al., 2006).....	37
Figure 2-12 Hollow structures of <i>Pseudomonas aeruginosa</i> biofilms after 72 and 144 hours of growth (A and B), respectively as revealed by scanning electron microscopy. Source: (Read et al., 2010)	38
Figure 2-13 Wrinkled structures of <i>Bacillus subtilis</i> pellicles. Source: (Trejo et al., 2013).....	39
Figure 2-14 Formation of clusters of drinking water biofilms after four weeks of growth in a rotating annular reactor as revealed by light microscopy in this study.	39

Figure 3-1 The rotating annular reactor used in this study.	51
Figure 3-2 Diagram of the experimental processes conducted at each experiment.....	54
Figure 3-3 Images and relevant ACF images. Source: (Russ, 2011)	63
Figure 3-4 Biofilm thickness and density after 4 weeks of biofilm growth at the end of the development process.....	65
Figure 3-5 Concentration of microcolonies on the reactor surfaces in the development and formation processes.	65
Figure 3-6 Percentage of surface area of biofilms in the development and formation processes.	66
Figure 3-7 Entropy of biofilms in the development and formation processes. ...	66
Figure 3-8 Percentage of surface area of EPS in the development and formation processes.	67
Figure 3-9 Percentage of surface area of biofilms in the changes of flow regime process.....	69
Figure 3-10 Percentage of surface area of EPS in the changes of flow regime process.....	69
Figure 3-11 Biofilm structures as revealed by microscopy using the 100X objective lens.....	70
Figure 3-12 Semi-variograms in the biofilm development process.	71
Figure 3-13 Autocorrelation function diagrams in the development process.	74
Figure 3-14 Biofilm thickness and density for both stagnant and flow conditions after 4 weeks of biofilm growth.	77
Figure 3-15 Percentage of surface area of biofilms for both stagnant and flow conditions after 4 weeks of biofilm growth.	77
Figure 3-16 Entropy of biofilms for both stagnant and flow conditions after 4 weeks of biofilm growth.	78
Figure 4-1 Growth curve of pure <i>Methylobacterium</i> culture.	87
Figure 4-2 Growth curve of drinking water culture.	87
Figure 5-1 Concentration of microcolonies in the bulk water of reactor for both the control and inoculated drinking water cultures at 0, 24, 48 and 72 hours.	100
Figure 5-2 Number of aggregates on the reactor slides for both the control and inoculated drinking water cultures at 24, 48 and 72 hours.	101

Figure 5-3 Percentage of surface area of biofilms from the bulk water of reactor on the membrane filters for both the control and inoculated drinking water cultures at 0, 24, 48 and 72 hours.	102
Figure 6-1 Positive control image for 5'-DIG labelled probe MethF in pure <i>Methylobacterium</i> DSM 18358 culture as revealed by <i>in situ</i> hybridization using the 100X objective lens.	112
Figure 6-2 Pure <i>Methylobacterium</i> DSM 18358 culture stained with DAPI as revealed by fluorescence microscopy using the 100X objective lens.	113
Figure 6-3 Negative control image for 5'-DIG labelled probe MethF in pure <i>E. coli</i> MG 1655 culture as revealed by <i>in situ</i> hybridization using the 100X objective lens.....	114
Figure 6-4 Pure <i>E. coli</i> MG 1655 culture stained with DAPI and visualised using the TRITC filter as revealed by fluorescence microscopy using the 100X objective lens.....	114
Figure 6-5 Pure <i>E. coli</i> MG 1655 culture stained with DAPI as revealed by fluorescence microscopy using the 100X objective lens.	115
Figure 6-6 Positive control image for 5'-CY3 labelled EUB338 probe in drinking water culture without any added <i>Methylobacterium</i> as revealed by <i>in situ</i> hybridization using the 100X objective lens.	116
Figure 6-7 Positive control image for 5'-CY3 labelled EUB338 probe in pure <i>Methylobacterium</i> DSM 18358 culture as revealed by <i>in situ</i> hybridization using the 100X objective lens.	116
Figure 6-8 Negative control image for 5'-CY3 labelled probe EUB338 in protozoa culture as revealed by <i>in situ</i> hybridization using the 100X objective lens.	117
Figure 6-9 Protozoa culture stained with DAPI as revealed by fluorescence microscopy using the 100X objective lens.....	117
Figure 6-10 Amount of DNA from the pure <i>Methylobacterium</i> DSM 18358 culture quantified based on the Qubit® DNA assay for different optical densities.	118
Figure 6-11 Structures of drinking water aggregates under stagnant conditions as revealed by <i>in situ</i> hybridization using the 100X objective lens.	119
Figure 6-12 Structures of drinking water aggregates in laminar flow as revealed by <i>in situ</i> hybridization using the 100X objective lens - Liquid sample.	120
Figure 6-13 Structures of drinking water aggregates in laminar flow as revealed by <i>in situ</i> hybridization using the 100X objective lens - Slide sample.	120

Figure 6-14 Structures of drinking water aggregates in turbulent flow as revealed by <i>in situ</i> hybridization using the 100X objective lens - Liquid sample.	121
Figure 6-15 Structures of drinking water aggregates in turbulent flow as revealed by <i>in situ</i> hybridization using the 100X objective lens - Slide sample.	121
Figure 6-16 Structures of drinking water aggregates under stagnant conditions as revealed by <i>in situ</i> hybridization using the 100X objective lens.	122
Figure 6-17 Structures of drinking water aggregates in laminar flow as revealed by <i>in situ</i> hybridization using the 100X objective lens - Liquid sample.	122
Figure 6-18 Structures of drinking water aggregates in laminar flow as revealed by <i>in situ</i> hybridization using the 100X objective lens - Slide sample.	123
Figure 6-19 Structures of drinking water aggregates in turbulent flow as revealed by <i>in situ</i> hybridization using the 100X objective lens - Liquid sample.	123
Figure 6-20 Structures of drinking water aggregates in turbulent flow as revealed by <i>in situ</i> hybridization using the 100X objective lens - Slide sample.	124
Figure 7-1 Motility of <i>Methylobacterium</i> at 0.2% agar medium after 12, 24, 48 and 72 hours of incubation at 28°C.	133
Figure 7-2 Maximum diameter of pure <i>Methylobacterium</i> colonies at 0.2% agar medium after 12 hours of incubation at 28°C.	133
Figure 7-3 Motility of <i>Methylobacterium</i> in different substrate conditions at 0.2% agar medium after 12 hours of incubation at 28°C.	135
Figure 7-4 Interactions of mixed drinking water colonies with and without <i>Methylobacterium</i> addition after 12 hours of incubation.	135
Figure 7-5 Interactions of mixed drinking water colonies with and without <i>Methylobacterium</i> , and of pure <i>Methylobacterium</i> colonies after 12 hours of incubation.	136
Figure 8-1 Chlorine and THM concentrations in raw drinking water at different times of water sampling from 8.00 hours to 18.00 hours every 2 hours. ...	144
Figure 8-2 Chlorine and THM concentrations in drinking water with <i>Methylobacterium</i> after 0, 1, 3, 6 and 24 hours at 4°C.	146
Figure 8-3 Concentration of THM in a THM standard solution with <i>Methylobacterium</i> addition after 0, 1, 3, 6 and 24 hours at 4°C.	146
Figure 8-4 Chlorine and THM concentrations in autoclaved drinking water after 0, 1, 3, 6 and 24 hours at 4°C.	148
Figure 8-5 Percentage of surface area of EPS in drinking water after 0, 1, 3, 6 and 24 hours at 4°C.	149

Figure 8-6 Chlorine and THM concentrations in drinking water with 1% glucose addition after 0, 1, 3, 6 and 24 hours at 4°C.....	150
Figure 8-7 Chlorine and THM concentrations in drinking water with sodium thiosulphate addition after 0, 5 and 10 minutes at 4°C.	151
Figure 10-2 Concentration of microcolonies on the reactor surfaces in the changes of flow regime process.....	161
Figure 10-3 Entropy of biofilms in the changes of flow regime process.	161
Figure 10-4 Semi-variograms for A experiment for the formation process.	162
Figure 10-5 Semi-variograms for A experiment for the changes of flow regime process.....	162
Figure 10-6 Semi-variograms for B experiment for the formation process.....	163
Figure 10-7 Semi-variograms for B experiment for the changes of flow regime process.....	163
Figure 10-8 Semi-variograms for C experiment for the formation process.	164
Figure 10-9 Semi-variograms for C experiment for the changes of flow regime process.....	164
Figure 10-10 Autocorrelation function diagrams for A experiment for the formation process.	167
Figure 10-11 Autocorrelation function diagrams for A experiment for the changes of flow regime process.	168
Figure 10-12 Autocorrelation function diagrams for B experiment for the formation process.	171
Figure 10-13 Autocorrelation function diagrams for B experiment for the changes of flow regime process.	173
Figure 10-14 Autocorrelation function diagrams for C experiment for the formation process.	175
Figure 10-15 Autocorrelation function diagrams for C experiment for the changes of flow regime process.	177
Figure 10-16 BRAND [®] culture tube (Sigma-Aldrich, Irvine, UK) containing 10 ml of drinking water bacterial culture.....	179
Figure 10-17 Cellulose nitrate filter of 0.2 μm pore size with 3 mm^2 squares (Sartorius, England, UK) used for the analysis of aggregates.....	179
Figure 10-18 Concentration of microcolonies on the reactor slides for both the control and inoculated drinking water cultures at 24, 48 and 72 hours. ...	180

Figure 10-19 Percentage of surface area of biofilms on the reactor slides for both the control and inoculated drinking water cultures at 24, 48 and 72 hours.

..... 181

Acknowledgments

I wish to sincerely thank and express my gratitude to my principal PhD supervisor Professor William T. Sloan for helping and supporting me along these years of my PhD study. It was a great honour to learn from such bright supervisor. I will be forever grateful to have got the chance to work with him providing me intimate knowledge, useful advice and constructive feedback in all our meetings. His guidance, patience, encouragement, kindness and smile were always a motivation for me for more and more work.

I would like to thank the College of Science and Engineering and in particular, the School of Engineering for the James Watt 2013 Scholarship, which was my financial support for three-and-a-half years. Also, I wish to thank the University of Glasgow for the overall great experience that I gain from my research program with its great personnel, IT services, facilities, training and development opportunities, institutional standards and seminar programs. I am very thankful to Mrs Elaine MacNamara for her great help with the administrative things. Finally, I would like to thank Mr Peter McKenna for printing my posters.

I would like to thank Dr Ciara Keating for training me for FISH, Dr Jillian M. Couto for designing the PCR primers and Mrs Julie Russell for conducting the purification of the PCR products. Also, I thank Dr Rungrach Sungthong, Dr Aoife Duff and Dr Gavin Collins for their help with some of my Laboratory work. A special thanks to the two technicians in the Water and Environment Lab, Ms Anne McGarrity and Mrs Julie Russell, who were keen to help and offer me their kind advice. Finally, thanks to all my colleagues at the two PhD offices, Yiannis, Zahur, Pradeep, Carol, Ahmet, Thomas, Remi, Stephanie, Asha, Maria, Dot, Mathieu, Alex, Fabien and Kevin, for the nice time we had together. You made this period to be fun and enjoyable for me.

I would also like to express my great thanks to my colleagues Melina, Ignatis, Dimitris and Caroline for their friendship, which was a big support for me. I also thank my boyfriend Nikos for his constant support and care. Finally, I am very grateful to my father Takis, my mother Koula and my sister Eirini for their love and courage. You were everyday here with me with my thoughts.

Declaration

This is a declaration to state that this thesis entitled “The role of physical and biological processes in biofilms in drinking water” is submitted in fulfillment of the requirements for the degree of Doctor of Philosophy at the School of Engineering at the College of Science and Engineering of the University of Glasgow in the United Kingdom. The thesis is an account of the author’s work and has not been submitted for any other degree of qualification.

Erifyli Tsagkari

Glasgow, October 2017.

Abbreviations

Abbreviation	Meaning	Units
Chapter 2		
EPS	Extracellular polymeric substances	
DWDS	Drinking water distribution systems	
DLVO	Derjaguin-Landau-Verwey-Overbeek	
QS	Quorum sensing	
AHL	Acyl homoserine lactones	
RAR	Rotating annular reactor	
u	Velocity in reactor	m/s
r	Distance from the centre of reactor	m
A, B	Constants A, B	
$\Omega_{1,2}$	Rotational speed in reactor of inner and outer cylinder, respectively	rpm
$R_{1,2}$	Radius of inner and outer cylinder of reactor, respectively	m
Ta	Taylor number	
R_m	Average radius of reactor	m
ν	Kinematic viscosity of fluid	m ² /s
Re	Reynolds number	
τ	Shear stress in reactor	Pa
μ	Dynamic viscosity of fluid	kg/sm
u_p	Mean velocity of fluid in pipe	m/s
u_v	Velocity of fluid in pipe	m/s
D	Diameter of pipe	m
R	Radius of pipe	m
τ_p	Wall shear stress in pipe	Pa
r_v	Distance from the centre of pipe	m
f	Friction factor of pipe	
$f_{1,2}$	Friction factor of pipe in laminar and turbulent flow, respectively	
τ_v	Shear stress in pipe	Pa
Chapter 3		
m_{WF}	Wet biofilm mass	mg
m_{DF}	Dry biofilm mass	mg
L_F	Biofilm thickness	μm
A_F	Surface area of reactor slide	cm ²
ρ_{WF}	Density of water	kg/m ³
ρ_F	Biofilm density	mg/cm ²
DAPI	4', 6-diamidino-2-phenylindole	$\mu\text{g/ml}$
$\Sigma x/n$	Average number	

s	Standard deviation	
A_{memb}	Surface area of filter membrane	cm^2
A_{field}	Surface area of the microscopic viewing field	μm^2
V_{filt}	Filtered volume	ml
d	Dilution factor	
V_{susp}	Suspension volume	ml
A_{bio}	Surface area of biomaterial	cm^2
d_{XY}	Lateral resolution	nm
d_z	Axial resolution	nm
λ	Wavelength	nm
NA	Numerical aperture	
E	Entropy	
p	Pixel intensity	
ACF	Autocorrelation function	
Chapter 4		
DSMZ	Deutsche Sammlung von Mikroorganismen und Zellkulturen	
OD	Optical density	
μ^*	Specific growth rate	h^{-1}
$N_{1,2}$	Optical densities at the beginning and end of the exponential phase of growth	
$t_{1,2}$	Time of the beginning and end of the exponential phase of growth	h
DT	Doubling time	h
Chapter 6		
FISH	Fluorescence <i>in situ</i> hybridization	
CARD-FISH	Catalysed reporter deposition- FISH	
MethF	<i>Methylobacterium</i> forward primer	μM
MethR	<i>Methylobacterium</i> reverse primer	μM
RNA	Ribonucleic acid	
rRNA	Ribosomal RNA	
DNA	Deoxyribonucleic acid	
PCR	Polymerase Chain Reaction	
bp	Base pairs	
Tris	Tris(hydroxymethyl)aminomethane	mM
EDTA	Ethylenediaminetetraacetic acid	mM
TAE	Tris-acetate-EDTA	mM
dNTPs	Deoxy-nucleoside-triphosphates	mM
MgCl_2	Magnesium chloride	mM
PBS	Phosphate-buffered saline	M
DIG	Digoxigenin	
CY3	Cyanine dye	

NaCl	Sodium chloride	M
Tris-HCl	Tris-hydrochloride	M
CH ₃ NO	Formamide	%
SDS	Sodium dodecyl sulphate	%
<i>EF</i>	Efficiency of 5'-DIG labelled probe MethF	%
SA	Surface area of biomaterial	%
Chapter 8		
Cl ₂	Chlorine	
CHCl ₃	Chloramines	
ClO ₂	Chlorine dioxide	
H	Hydrogen	
CH ₄	Methane	
F/Br/I/At	Fluorine/Bromine/Iodine/Astatine	
CH ₃ COOH	Acetic acids	
CHCl ₃	Chloroform	
CHBr ₃	Bromoform	
CHBr ₂ Cl	Dibromochloromethane	
CHBrCl ₂	Bromodichloromethane	
C ₂ H ₃ ClO ₂	Monochloroacetic acid	
C ₂ H ₂ Cl ₂ O ₂	Dichloroacetic acid	
C ₂ HCl ₃ O ₂	Trichloroacetic acid	
C ₂ H ₃ BrO ₂	Monobromoacetic acid	
C ₂ H ₂ Br ₂ O ₂	Dibromoacetic acid	
C ₁₀ H ₁₆ N ₂	N,N-diethyl-p-phenylenediamine	
C ₁₀ H ₁₄ N ₂ O	N, N,-diethylnicotinamide	
Na ₂ S ₂ O ₃	Sodium thiosulphate	
Appendix		
SD	Standard deviation	
NaOH	Sodium hydroxide	ml
CrK ₈ S ₂	Chromium potassium sulphate	g

1 Introduction

1.1 Problem Statement

Safe drinking water is essential for human health and its provision in a changing climate is one of the global most pressing problems. Research communities, governments and drinking water supplying companies are working on improving the quality of drinking water and reducing its cost. This is achieved firstly, by monitoring the physicochemical and biological quality parameters of drinking water and secondly, by developing strategies for the improvement of the design and operational management of the water distribution systems.

Although drinking water is closely monitored in the developed countries, waterborne disease outbreaks are still being reported in drinking water systems. These outbreaks may be associated with pathogenic bacteria and viruses as biofilms in the pipe networks create favourable conditions for the survival and growth of pathogens. In addition, the sloughing of biofilms from pipe walls is associated with changes in the water taste, odour and colour, which form the basis of most complaints from costumers received by water companies. Despite the best efforts of water utilities to eradicate biofilms from filtration systems and pipe networks by physical and chemical means, it has proved impossible to eradicate biofilms from the inner surfaces of water pipes and bacteria from the water. Thus, it is imperative that we find new ways of managing the biofilms that will inevitably form in drinking water systems.

1.2 Research aims and objectives

Biofilms are ubiquitous in drinking water systems and are thought to be the source of most of the bacteria that appear at our taps. Biofilms impact drinking water quality and, therefore, it is essential to understand biofilm processes if we are to develop ways to control biofilm formation at the inner surfaces of drinking water pipes. However, little is known about the role of the interaction between physical and biological processes in biofilms in drinking water. Therefore, this study was set up to look at these processes and understand the behaviour of biofilms under various environmental conditions. Both the physical and biological processes in biofilms are here hypothesised to be of great

importance for biofilm formation at the inner surfaces of drinking water pipes. From the engineering view, the study of those processes can contribute to the successful management and control of their formation in order to avoid biocorrosion problems that lead to material deterioration and subsequent reduced life of these pipes. The main hypotheses of this study was that flow conditions play key role in the formation of biofilms in drinking water and that there are key species in bacterial aggregation in drinking water whose behaviour should be explored as they might have significant influences on the formation of biofilms and the quality of drinking water.

Firstly, the thesis focuses on the effect of different flow conditions on biofilm growth in drinking water with the objective to understand whether controlling the flow conditions can play an important role in the growth of biofilms in drinking water. Specifically, turbulent flow is hypothesised to be the flow regime under which biofilms could grow most in drinking water. This study will allow comparison of the initial biofilm formation, the development of biofilms and their structures between three very distinct flow regimes: the turbulent, transition and laminar. Secondly, the role of the *Methylobacterium* strain DSM 18358 in bacterial aggregation is studied under different flow conditions, with the aim of determining whether it is a key strain in aggregation and subsequently, in the formation of biofilms in drinking water. It is hypothesised that this specific strain is key in bacterial aggregation in drinking water. Such knowledge will allow us to understand whether there are key species in aggregation and whether their presence in drinking water is responsible for the formation of biofilms on the available surfaces. Finally, the effect of this *Methylobacterium* strain on the concentration of trihalomethanes in drinking water is studied, as these are the most common chlorine disinfection by-products that occur in drinking water systems. Specifically, it is hypothesised that the specific *Methylobacterium* strain can impact the fate of trihalomethanes in drinking water. The potential presence of key species in bacterial aggregation is considered detrimental for drinking water quality due to the subsequent presence of biofilms on the available surfaces. However, this last part of this thesis will indicate whether these key species can be, from the other side, beneficial to some point for the quality of drinking water resulting in the

potential consumption of trihalomethanes that are undesired for health related issues.

1.3 Research outlines

The following section provides an overview of this thesis with a short summary of each individual chapter. The chapters that this work consists of are the following:

- Chapter 2 provides a literature review on biofilms that are found in various pipe systems and in drinking water systems. Also, the biofilm structures that have been observed under a variety of different environmental conditions are discussed. Then, the main growth stages of a biofilm, which are the initial bacterial attachment to surfaces, the formation and development of the biofilm and the biofilm detachment, are described. This section continues with a description of the flow in a rotating annular reactor, which is the type of bioreactor used in most experiments in this study. Finally, there is a description of the flow conditions that occur in a pipe, which are simulated by this bioreactor.
- Chapter 3 includes a study, which investigates the effect of different flow regimes on biofilms that were grown in drinking water. Specifically, the effect of three distinct flow regimes: turbulent, transition and laminar, developed in a bioreactor, and of stagnant conditions is studied on biofilm growth. Biofilms are characterised based on their thickness and density, and by determining other biofilm-related measures. Finally, the biofilm spatial structures are revealed and compared under the different flow conditions.
- Chapter 4 presents a study on bacterial aggregation by the *Methylobacterium* strain DSM 18358, which is hypothesised to be a key strain in aggregation in drinking water. The aggregation ability of this *Methylobacterium* strain in drinking water is studied here under different conditions. These conditions include different inoculation concentrations of this *Methylobacterium* strain in drinking water, both oligotrophic and

eutrophic conditions, both stagnant and shaking conditions, and different time periods in which aggregation is studied.

- Chapter 5 extends the previous study and focuses on the effect of different flow regimes on the aggregation ability of the *Methylobacterium* strain DSM 18358 in drinking water, as a factor that may cause significant changes in aggregation. Specifically, turbulent and laminar flow regimes are developed using the bioreactor, and bacterial aggregation is studied as an important factor for the formation of biofilms on surfaces.
- Chapter 6 presents the spatial structures of the aggregates of the *Methylobacterium* strain DSM 18358 and of the other drinking water bacteria from the bulk water under stagnant conditions, and from both the bulk water and the surfaces of bioreactor in turbulent and laminar flow conditions. Here, it is studied whether the flow conditions play a key role in shaping the structures of drinking water aggregates.
- Chapter 7 includes the study of the motility of the *Methylobacterium* strain DSM 18358 on agar plates under differing conditions in order to characterise the behaviour of this strain. These conditions include different substrates, different viscosities of the substrate and different temperatures. Also, the presence of this *Methylobacterium* strain in mixed drinking water colonies is studied whether it contributes to the communication between drinking water bacteria and the formation of aggregates in drinking water.
- Chapter 8 investigates the role of the *Methylobacterium* strain DSM 18358 in the concentration of trihalomethanes in drinking water. Since *Methylobacterium* species have been previously found to be able to degrade some chlorine disinfection by-products, here the potential ability of the *Methylobacterium* strain DSM 18358 to impact the fate of trihalomethanes is studied under different inoculation concentrations of *Methylobacterium* and different chlorine and organic matter concentrations.

- Chapter 9 is the final part of this thesis where there is the summary of the impact of this research and an outline of how this work can be continued in a future project.
- The Appendix includes all the materials, methods, procedures and protocols followed during this study and are not included in the relevant chapters. Also, some results, which are not included in the relevant chapters because they were not of prime importance, are provided to give some additional relevant information.

2 Literature Review

2.1 Biofilms

The main challenge to drinking water industries is to deliver water that is microbiologically and chemically safe, aesthetically pleasing and adequate in quantity (Simões, 2012). Biofilms are ubiquitous as they are found on virtually every wetted surface on earth. Even though the term “biofilm” may not form part of the popular lexicon, most people are familiar with biofilms in one way or another, in particular with those biofilms that can be seen by naked eye. The plaque that is formed on teeth is a biofilm, the slime on contact lenses, bathroom walls or rotting food is also a biofilm. Similarly, the green or brown coating on rocks, pebbles or sand in a natural river system are biofilms (Hall-Stoodley et al., 2004).

A biofilm consists of a group of microorganisms, such as bacteria, archaea, fungi, algae and protozoa, which adhere to a surface, usually housed in a matrix of extracellular polymeric substances (EPS). The EPS are biopolymers including polysaccharides, proteins, nucleic acids and lipids (Flemming, 2011). In most biofilms, the microorganisms may account for less than 10% of the total biofilm dry mass, whereas the EPS matrix may account for over 90% of that. The biofilm matrix has been characterised as a three-dimensional polymer network that interconnects and immobilises the cells that it consists of. It also acts as an external digestive system because it keeps the extracellular enzymes close to the cells and this mechanism enables them to metabolise various biopolymers (Flemming and Wingender, 2010).

It is estimated that 99% of the total population of bacteria in the world are found in the form of a biofilm. Bacteria in biofilms differ from planktonic bacteria. In addition, bacteria demonstrate vast heterogeneity in terms of metabolism, gene expression and physiology even in mono-species biofilms due to the different conditions that might be present at the different locations of the biofilm (Florjanic and Kristl, 2011).

Biofilms can be useful, especially in the field of bioremediation. Organisms may be used for contaminant removal, such as metals and oil spills, and for the

purification of industrial wastewater. On the other hand, biofilms can result in heavy costs for the cleaning and maintenance of the industrial and domestic pipes that they colonise. Examples of industrial pipes include those in which wastewater, drinking water and oil are being transported. However, the environment in which people are mostly exposed to biofilms is the domestic environment (Garrett et al., 2008).

2.2 Biofilms in pipes

Of particular importance in industry are the biofilms that grow on the inside of pipes, which walls are made of different materials, transporting a variety of substances, such as drinking water, wastewater, oil, or fire extinguishing agents.

2.2.1 Biofilms in drinking water distribution systems

At the inner surfaces of the pipes of drinking water distribution systems (DWDS) biofilms are formed and bacterial communities are found to be very diverse (Douterelo et al., 2013). In DWDS, Gram-negative bacteria are dominant over Gram-positive bacteria and *Pseudomonas* species are the most abundant organisms in most water supply systems. Proteobacteria are a major group of Gram-negative bacteria that are found in DWDS (Simões, 2012, Douterelo et al., 2014b, Bautista-de Los Santos et al., 2016a).

Of particular interest from a public health perspective is the contamination events that may occur in DWDS. After a contamination event, biofilm bacterial communities may be composed of enteric bacteria, such as *Escherichia coli*, *Enterobacter cloacae* and *Enterococcus faecalis*, and environmental bacteria that become opportunistic pathogens, such as *Legionella pneumophila*, *Pseudomonas aeruginosa*, *Aeromonas hydrophila* and *Mycobacterium avium*. Water discoloration, taste and odour degradation may occur due to the presence of bacterial pathogens and parasitic protozoa. The activity of opportunistic pathogens can induce serious diseases to people (Simões, 2012). The quality of drinking water is also related to the time that the water spends in DWDS. The age of drinking water influences the water colour, taste and odour, corrosion rates, material precipitation, disinfection by-product formation and biological activities (Machell et al., 2009, Machell and Boxall, 2014).

The exact structure of drinking water biofilms is still unclear and has not yet been described in detail due to difficulties in investigating such a small amount of biomass without disturbing it. This process is rendered even more complicated by the presence of debris, corrosion products and mineral deposits, which provide new niches for bacteria to colonise (Batté et al., 2003). An example of the presence of these compounds in a drinking water pipe can be seen in Figure 2-1. Organic and inorganic particles can accumulate in low-flow areas or dead-ends of DWDS and enhance microbial activities by providing protection for bacteria against harsh conditions. Any inorganic particles passing nearby may be incorporated in biofilms. There are inorganic particles such as sand that promote the erosion of biofilms whereas others such as clay may result in thicker and stronger biofilms (Simões, 2012, Douterelo et al., 2013).



Figure 2-1 Drinking water pipe in Denmark with a rough inner surface of iron and calcium precipitates. Source: (Boe-Hansen, 2001)

However, one of the most beneficial aspects of biofilms is to use them in water cleaning systems. In biofilm filtration systems, the filter medium presents a surface for the microbes to attach to and to feed on the organic material in the water being treated. Such cleaning systems are biologically more stable and their disinfectant demand is lower than that of conventionally treated systems. Less microorganism induced contamination is likely to occur in water that passes through a biofilm based filter than there is in water that passes through another alternative treatment system (Campos et al., 2002).

Biofilms in drinking water are generally thin but the thicknesses that can be reached are variable. Thicknesses that have been recorded for biofilms in DWDS

range from a few tens of micrometres (Srinivasan et al., 2008) to a few hundreds of micrometres (Momba et al., 2000). Biofilms may be formed on the surfaces within a few days or months and may reach a cell concentration of 10^7 - 10^9 cells/cm² (Manuel, 2007). The vast majority of bacteria, estimated at 95% of the total cell population, are attached to the surfaces, whereas only 5% are found in the water phase (Flemming et al., 2002).

Drinking water distribution networks are designed for liquid velocities of about 0.2 to 0.5 m/s. Flow conditions can range from laminar to turbulent flow but stagnant waters also occur in places in which the water consumption is low (Manuel et al., 2007). In low flow conditions, the transport of bacteria from the bulk water to the exposed surfaces occurs due to Brownian diffusion, sedimentation and cell motility. In high flow conditions, which are mostly experienced in such systems, microorganisms are transported by eddies in the flow (Derlon et al., 2008, Paul et al., 2012, Kumarasamy and Maharaj, 2015). Changes in the hydraulic conditions affect the quality of drinking water and thus, different pipes should be treated differently to obtain optimum operational effectiveness and minimise discoloration risk depending on their material composition (Husband and Boxall, 2010). Finally, the abundance, structure and composition of planktonic bacterial assemblages are also affected by the hydraulic conditions (Sekar et al., 2012).

2.2.2 Biofilms in wastewater systems

Biofilms can play a very important role in the bioremediation of wastewater systems. They can be used to convert organic pollutants into biomass, carbon dioxide and other harmless products. It is the bacteria and archaea within such biofilms that are responsible for the removal of organic matter, whereas protozoa are mainly responsible for the removal of suspended solids. Heavy metals, such as copper and iron, are typical pollutants in wastewater. Biofilms are capable of eliminating heavy metals from the surrounding liquid by binding metal ions to the EPS matrix (Kornaros and Lyberatos, 2006). An example of bacteria and biofilm that can be found in a wastewater system can be seen in Figure 2-2.

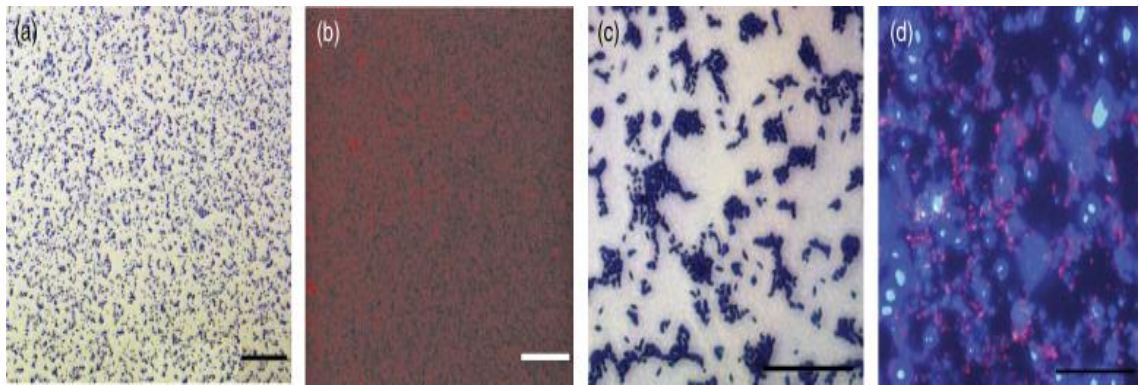


Figure 2-2 Typical morphologies of initially adhered cells and 24-hour biofilms found in wastewater treatment systems. Source: (Andersson et al., 2008)
 (a and c) Adherence of *Acinetobacter calcoaceticus* and *Comamonas denitrificans* 110, respectively stained with crystal violet by light microscopy and (b and d) biofilms formed from the same taxa, respectively after 24 hours consisted of cells, stained in red, and EPS, stained in blue, using fluorescence *in situ* hybridization by confocal laser scanning microscopy (scale bar = 40 μm).

Biofilm based wastewater treatment systems are advantageous because the microbial communities are resistant to changing environmental conditions, which makes them resilient to variations in toxicity concentrations. These systems are being improved because there is more and more research on biofilm processes, such as biofilm formation and species interactions (Simões et al., 2007, Andersson et al., 2008, Kloc and González, 2012).

2.2.3 Biofilms in indwelling tubular medical devices

Depending on the medical device, biofilms may be composed of single or multiple bacterial species. Characteristic medical devices, in which biofilms are formed, are the central venous and urinary catheters. Examples of commonly found organisms in central venous catheters are *Staphylococcus epidermidis*, *Candida albicans* and *Pseudomonas aeruginosa*. They can enter the catheter port from the skin of the patient or personnel (Kokare et al., 2009). Examples of commonly found organisms in urinary catheters are *Enterococcus faecalis*, *Escherichia coli* and *Klebsiella pneumonia* (Percival et al., 2011). A characteristic example is shown in Figure 2-3.

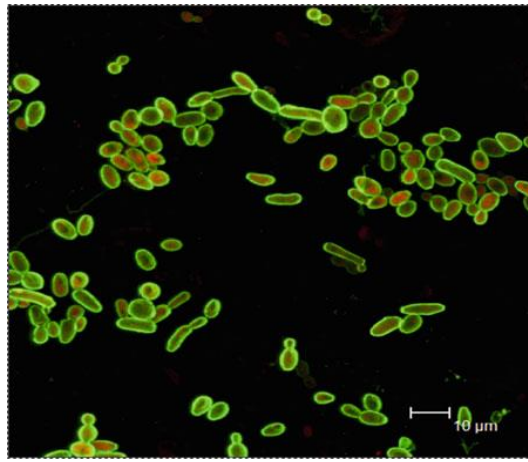


Figure 2-3 *Candida parapsilosis* on silicone tubing after 2 hours of exposure to urine.
Source: (Percival et al., 2011)

Biofilms that are formed in urinary catheters include organisms that react with the urea and form free ammonia. The consequence is that ammonia then raises the pH at the interface between biofilm and flow and this finally results in the precipitation of minerals. These minerals can be entrapped within the biofilm and cause encrustation of the catheter (Donlan, 2002). Even though the thickness of a biofilm is quite difficult to define, medical biofilms tend to be thinner than biofilms encountered in industry (Percival et al., 2011). Although equipment contamination constitutes an economic problem, public health is the most detrimental impact of these biofilms as pathogenic organisms are transmitted from biofilms to susceptible people (Stickler, 2008, Kokare et al., 2009).

2.2.4 Biofilms in oil and gas pipelines

A serious problem encountered in oil and gas industry is the pipe deterioration caused by biofilms. Microorganisms that occur in pipelines alter the chemistry at the interface between the pipe material and the bulk fluid. The most extensively studied microorganisms in relation to corrosion in these pipelines are the sulphate reducing bacteria that live in biofilms causing sulphuric acid and sticky exopolymers production, which corrodes pipes and results in serious leaks (Chan et al., 2002, Jan-Roblero et al., 2004). A typical morphology of a biofilm formed in an oil pipeline can be seen in Figure 2-4.

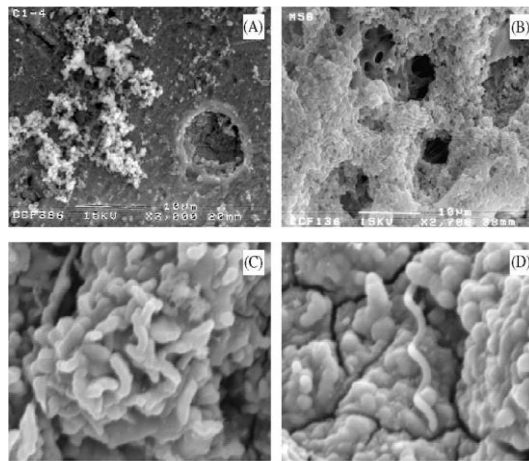


Figure 2-4 Biofilm formation after 40 days on X52 steel coupon exposed to crude oil flow as revealed by scanning electron microscopy. Source: (Neria-Gonzalez et al., 2006)
 (a) Biofilm formed on the surface of a coupon, (b) the morphology of biofilm grown on a surface, (c) a microcolony into a biofilm and (d) example of a specimen of a biofilm.

This corrosion that is influenced by the presence and metabolic activity of microorganisms on a metallic surface is called biocorrosion. The obvious consequence is the pipeline failure. Even in heavy pipelines, parts of the metallic surface can be detached causing significant industrial financial losses. However, some microbes are able to break down the particles of oil slowly. Since oil is primarily made of carbon, there is a wide variety of bacteria that break down small oil molecules and use them as food. In this way biofilms can be considered as a valuable tool to clean up environmental pollution through cleaning up oil spills (Neria-Gonzalez et al., 2006). Most of the research on biocorrosion has been focused on the action of sulphate reducing bacteria; however, there are other types of bacteria such as methanogens involved in biocorrosion (Zhang et al., 2003, Zhu et al., 2003).

2.2.5 Biofilms in fire protection pipes

In fire protection pipelines, occlusion might occur and cause the completely blocking of flow (Kraigsley et al., 2014). These systems represent a complex challenge for the control and prevention of the accumulation of microorganisms on their surfaces. An extremely localised corrosion in those pipes might penetrate the mass of the pipe material and lead to the creation of small holes in carbon steel and copper, which is known as pitting corrosion. Presence of such corrosion in a carbon steel fire protection pipe is shown in Figure 2-5. This corrosion is caused by the activities of iron reducing bacteria, and sulphur and

manganese oxidizing bacteria (Wang and Melchers, 2017). There are several costs included in the cleaning and replacement of these corroded pipes (Kraigsley et al., 2014).

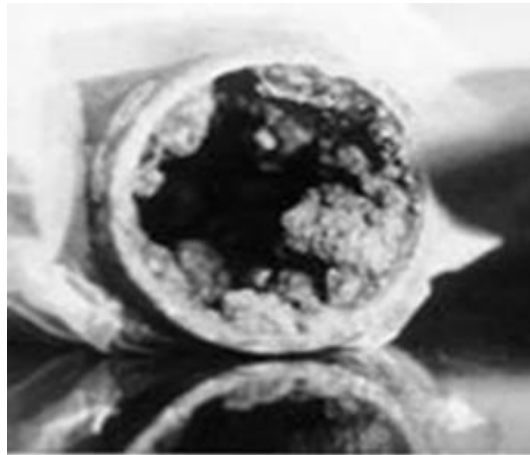


Figure 2-5 Formation of tubercles (corrosion deposits) on the surfaces of a carbon steel fire protection pipe. Sources: (Kraigsley et al., 2014)

2.2.6 Biofilms in cooling and heating water systems

Biofilms within cooling and heating water systems form a layer, which creates a barrier between the recirculating cooling or heating water and the inner pipe surfaces. The subsequent increase in frictional resistance in such systems results in the increase in the power required to operate the recirculating pumps. In these systems, it is again the action of sulphate reducing bacteria that is important as these bacteria can cause corrosion of the metallic surfaces (O'Neal and Guillemot, 2010). Particular example of such systems, for which the microbial accumulation is a major problem, is the cooling towers that transfer heat from the recirculated water to the atmosphere (Hsieh et al., 2010, Wang et al., 2013). In Figure 2-6 a biofilm formed in a cooling system is shown.

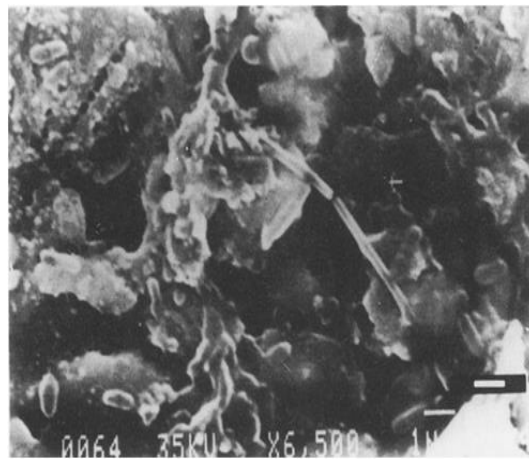


Figure 2-6 Biofilm formation on stainless steel surface after 30 days of *in situ* exposure to cooling water as revealed by scanning electron microscopy. Source: (Wang et al., 2013)

2.3 Biofilm structures

There are many types of biofilm heterogeneity (Bishop et al., 1997, Picioreanu et al., 2000, Wimpenny et al., 2000, Stewart and Franklin, 2008). Firstly, there is the geometrical heterogeneity (e.g., biofilm thickness, biofilm surface roughness, biofilm porosity, substratum surface coverage with biofilms). Secondly, there is the chemical heterogeneity (e.g., nutrients, metabolic products and inhibitors, pH variations, diversity of aerobic and anaerobic reactions). Thirdly, there is the biological heterogeneity (e.g., microbial diversity, activity of cells and EPS). Finally, there is the physical heterogeneity (e.g., biofilm density, biofilm strength, permeability, viscoelasticity, viscosity, EPS properties, solute concentration, solute diffusivity, presence of abiotic solids).

Biofilms are found to form very complex and heterogeneous structures, which are influenced by many factors. The study of these factors is motivated by a wide range of practical problems and thus, a wide range of hypotheses are emerging. Hydrodynamic conditions are one of the most significant factors affecting biofilm structures because they influence important variables, such as substrate loading rate and developing shear stresses (van Loodsrecht et al., 1995). The recent development of improved imaging techniques such as confocal laser scanning microscopy has allowed the visualisation of three-dimensional biofilm structures and spatial arrangement of different microbial species within them. There are at least four major influences on biofilm structures: surface

properties, such as hydrophobicity and roughness, hydrodynamic environment, nutrient availability and finally, biofilm consortia such as microbes (Stoodley et al., 1997). Below, there is a description of the different biofilm structures that have been observed under different environmental conditions.

2.3.1 Mushroom structures

A very common structure is the mushroom-shaped structure, which is formed in quiescent or low shear stress environments (Hall-Stoodley et al., 2004). It has been showed that immotile *Pseudomonas aeruginosa* cells can form stalks that are subsequently capped by migrating bacteria to form mushroom-like biofilms. This bacterial migration requires a particular cell motion, which is called twitching motility (Craig et al., 2004). Other factors that contribute to the development of these structures are cell activities such as chemotaxis, which describes certain movements of bacteria towards favourable conditions due to chemicals existing in their surrounding environment, and other factors like cell attachments and detachments (Picioreanu et al., 2007, Son et al., 2015). Mushroom structures of biofilms are shown in Figure 2-7.



Figure 2-7 Mushroom structures of biofilms in hydrothermal hot springs. Source: (Hall-Stoodley et al., 2004)

At the centre of the mushroom caps, which is the upper part of this structure, there might be the highest concentration of cell signals (Battin et al., 2007), which are substances that cells secrete in order to communicate with one another (Jefferson, 2004). This happens because in that place the biomass accumulation protects cell signals from flow-induced losses (Battin et al., 2007). The stalks, the other part of this structure, appear as columns. At the outer

layers of stalks there might be a high proportion of non-viable cells surrounding the inner core of viable cells (Hope and Wilson, 2006).

2.3.2 Flat structures

The tendency of motile cells to form flat biofilms spreading out on the exposed substratum has been reported. In contrast, immotile cells have been found to form round biofilm structures (Klausen et al., 2003a). It has been shown that the flux of substrate transferred to a flat biofilm was higher than that transferred to an irregularly shaped biofilm, which resulted in a higher growth rate of cells in the flat and thin biofilm compared to the irregular biofilm (Piciooreanu et al., 2007). Many studies have previously shown flat patterns that *Pseudomonas aeruginosa* species formed as a response to the available nutrients in the substratum (Heydorn et al., 2000, Banin et al., 2005, Parsek and Tolker-Nielsen, 2008). A typical formation of a flat biofilm structure is shown in Figure 2-8.

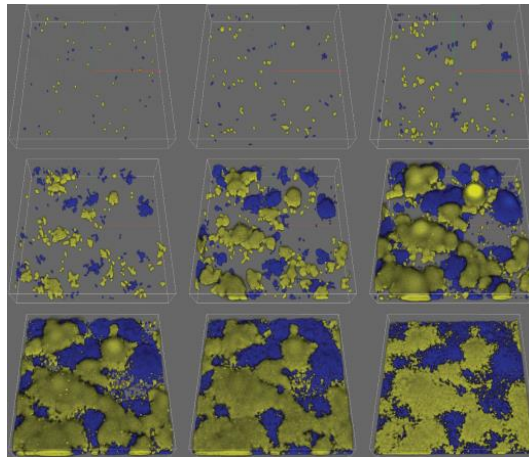


Figure 2-8 Final formation of a flat *Pseudomonas aeruginosa* biofilm (bottom right of the image) as revealed by confocal laser scanning microscopy. Sources: (Klausen et al., 2003b, Klausen et al., 2006)
Cyan and yellow fluorescent protein-tagged cells after 23 hours of growth in a flow chamber (Boxes of 230 μm x 44 μm).

2.3.3 Filamentous structures

In fast moving waters, turbulent flows and eddies that are characterized by high shear stresses, biofilms tend to form filamentous structures that are also called streamers (Besemer et al., 2009). Streamers are attached to the exposed surface by an upstream "head" and a downstream "tail" oscillates in the turbulent current. In Figure 2-9, the morphology of filamentous biofilm structures is

shown. The formation of these oscillating streamers has been implicated with increased energy losses and heat transfer in pipelines (Hall-Stoodley et al., 2004). Streamers are mainly found in environments, such as rivers (Hall-Stoodley et al., 2004), acidic metal rich waters (Edwards et al., 2000, Hallberg et al., 2006) and hydrothermal hot springs (Reysenbach and Cady, 2001). However, streamers have been also identified in laminar flow conditions (Rusconi et al., 2010).

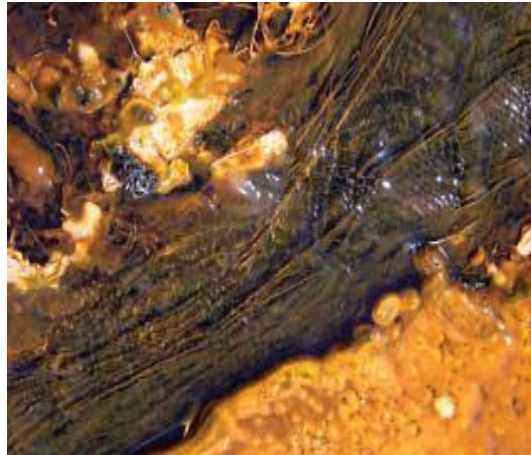


Figure 2-9 Streamers formed in hydrothermal hot springs biofilms. Source: (Hall-Stoodley et al., 2004)

2.3.4 Ripple structures

Ripple structures are found in high shear flows. They are described as regularly spaced ridges running perpendicularly to the flow direction. These structures have been reported in medical applications, such as endotracheal tubes and catheters (Hall-Stoodley et al., 2004). The morphology and migration velocity of these structures has been found to vary with changes in the bulk liquid velocity. Ripples are consisted of a large number of viable microorganisms, which can be detached into the bulk fluid, resulting in serious implications for microbiological contamination on solid surfaces (Stoodley et al., 1999b). Examples of studies on traveling ripples have been for myxobacteria (Sager and Kaiser, 1994) and cells from *Pseudomonas aeruginosa* biofilms (Purevdorj et al., 2002). This ripple structure can be seen in Figure 2-10.

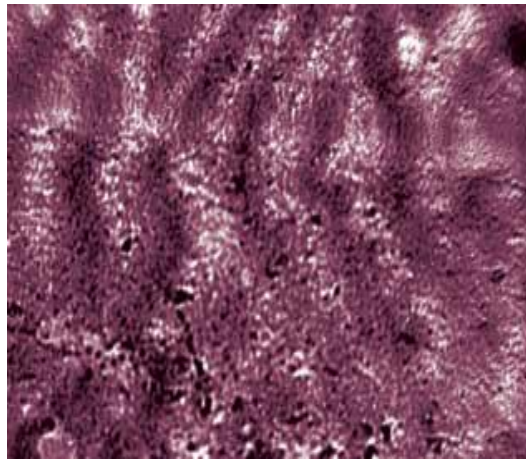


Figure 2-10 Ripple structures of biofilms in laboratory flow cells. Source: (Hall-Stoodley et al., 2004)

2.3.5 Pellicle structures

Pellicle structures are encountered at liquid and air interfaces. They mainly consist of a continuous thin film formed by cultures growing on the surface of liquid media. Most studies on pellicle structures have been focused on Gram-positive bacteria and especially on *Bacillus subtilis*. However, Gram-negative bacteria, such as *Acetobacter*, *Pseudomonas* and *Salmonella* species, are also found to be able to form pellicle structures (Armitano et al., 2014). Pellicle structures formed by *Pseudomonas* species are shown in Figure 2-11. For Gram-negative bacteria, flagella cell appendages were found to play an important role in pellicle formation and integrity (Hung et al., 2013, Visick et al., 2013).

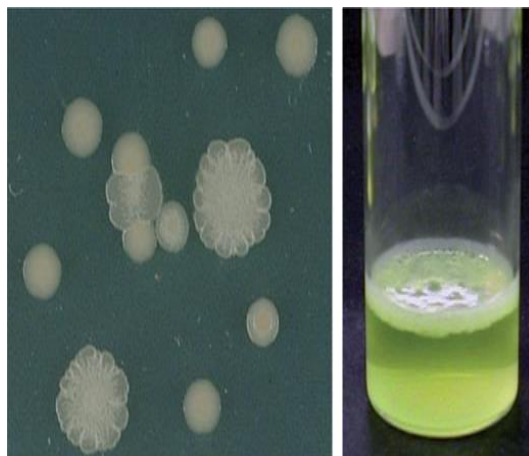


Figure 2-11 Pellicle formation by *Pseudomonas fluorescens* isolates. Source: (Ude et al., 2006)

2.3.6 Hollow structures

Hollow structures are formed out of bacterial microcolonies that leave the interior areas of a biomass. Immotile cells have been found to form the rigid walls surrounding these structures with occasional free-floating cells in the centre of the biomass (Purevdorj and Stoodley, 2004). Such structures have been found in *Pseudomonas putida* biofilms (Tolker-Nielsen et al., 2000) and *Pseudomonas aeruginosa* biofilms (Read et al., 2010). A typical example of hollow structures can be seen in Figure 2-12. These structures are mostly formed during seeding dispersal, also known as central hollowing, which refers to the rapid release of cells from inside the biofilm colony (Kaplan, 2010).

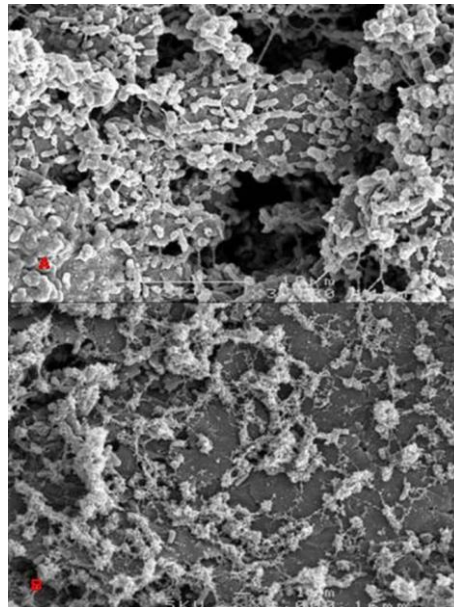


Figure 2-12 Hollow structures of *Pseudomonas aeruginosa* biofilms after 72 and 144 hours of growth (A and B), respectively as revealed by scanning electron microscopy. Source: (Read et al., 2010)

2.3.7 Wrinkled structures

Wrinkled patterns are created on the solid surfaces of pipes. During the formation of this structure localised cell deaths, exopolysaccharides production and DNA release may occur as revealed by high resolution imaging techniques (DePas et al., 2013, Haussler and Fuqua, 2013). The origin of the wrinkles has been found to be controlled by the mechanical properties of the biofilm, which are governed by the production of EPS (Espeso et al., 2015). Direct measurements on the elasticity of biofilms have revealed that the presence of wrinkles is a consequence of that elasticity and that EPS plays a key role in this

elasticity (Trejo et al., 2013). Wrinkled structures formed by *Bacillus subtilis* are shown in Figure 2-13.

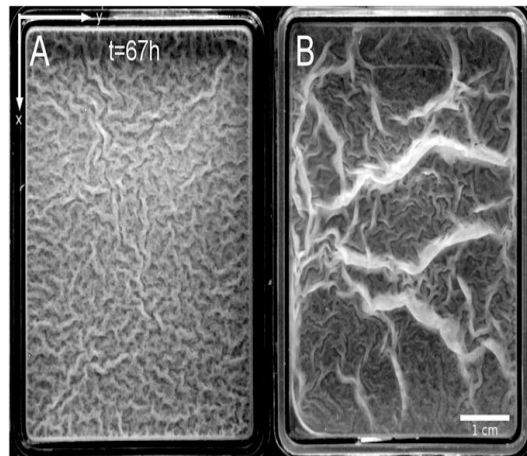


Figure 2-13 Wrinkled structures of *Bacillus subtilis* pellicles. Source: (Trejo et al., 2013)

2.3.8 Clusters

Drinking water bacteria tend to form clusters, which are microcolonies that consist of densely packed cells held together by EPS. The composition of these structures can range from a few cells to hundreds of micrometre-high cell clumps (Boe-Hansen, 2001). Tap water biofilms are found to form discrete mound-shaped cell clusters, which might be elongated in the downstream direction and finally, form filamentous streamers (Stoodley et al., 2001). The formation of these structures has important effects on both the mass transport and oxygen distribution in the bulk liquid (De Beer et al., 1994). An example of a cluster structure is shown in Figure 2-14.

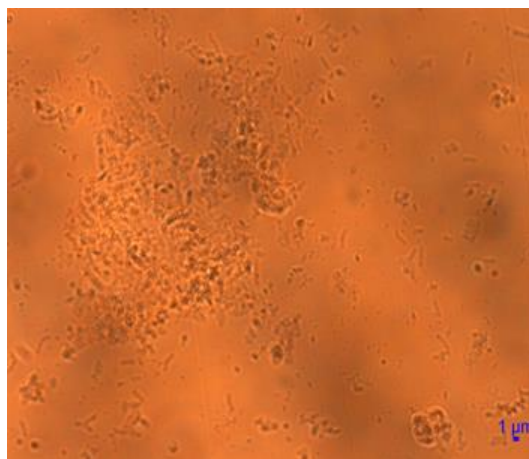


Figure 2-14 Formation of clusters of drinking water biofilms after four weeks of growth in a rotating annular reactor as revealed by light microscopy in this study.

2.4 Bacterial Adhesion

Adhesion is the attachment of a cell to a substrate and the initial stage of biofilm formation. Actual bacterial adhesion is an extremely complicated process and frequently deviates from the adhesion models that have been developed. Microorganisms adhere to surfaces forming layers, which are called conditioning films. The physicochemical properties of conditioning films are quite different from those of original bare surfaces, and the interactions of microorganisms with conditioning films also differ between different microorganisms and surfaces (Hori and Matsumoto, 2010).

There are two types of bacterial adhesion: the reversible and irreversible adhesion. If the repulsive forces are greater than the attractive forces, the bacteria will detach from the surface; this is more likely to occur before the conditioning of a surface. However, a number of the reversibly adsorbed cells will remain immobilised and become irreversibly adsorbed (Characklis and Marshall, 1990). Also, there are two types of adhesion measurements: the adhesion number, which includes counting of the cells before and after the adhesion event, and the critical force, which includes measurements during the adhesion event. For the adhesion number measurements, different imaging techniques such as confocal laser scanning microscopy have been used. These measurements although powerful, do not measure directly the adhesion of bacteria. For the critical force measurements, atomic force microscopy has been used that allows the direct interaction with bacteria. This way, the force required to move bacteria can be determined (Fang et al., 2000, Garrett et al., 2008).

One physicochemical approach to describe the complexity of bacterial adhesion is the Derjaguin-Landau-Verwey-Overbeek (DLVO) theory, based on which the interaction between a surface and a particle is the summary of their van der Waals and Coulomb interactions. When the van der Waals force (attractive force) is dominant in the vicinity of a surface, particles adhere to the surface irreversibly. The Coulomb force (electrostatic repulsive force, which occurs due to the negative charge of cells and surface) then becomes dominant at a distance away from the surface because the van der Waals force decreases

sharply with distance (Vanloosdrecht et al., 1989, Hermansson, 1999, Wu et al., 1999, Abu-Lail and Camesano, 2003).

Other models have also been developed in order to predict bacterial adhesion such as the extended DLVO theory since the classical DLVO theory was found not to be able to fully explain bacterial adhesion. In the extended DLVO theory, the hydrophobic or hydrophilic interactions and osmotic interactions are also included in the calculation of bacterial adhesion. However, for cells the osmotic interactions are considered negligible. The extended DLVO theory seems to qualitatively predict bacterial adhesion better than the classical DLVO theory because it takes into account the acid-base interactions, whereas adhesion is not expected to occur according to the classical DLVO theory (Vanoss, 1993, Yotsumoto and Yoon, 1993b, Yotsumoto and Yoon, 1993a).

Factors that influence bacterial adhesion can be divided into three main categories: those associated with the bacteria, those associated with the surfaces of colonisation and finally, those associated with the ambient environment. As far as the bacteria-associated factors are concerned, the bacterial appendages, such as flagella, fimbriae and pili, function as bridges between cells and surfaces and might contribute so that bacteria attach to the surfaces (Garrett et al., 2008). Examples of other such factors are the cell hydrophobicity, cell surface charge and the ability of bacteria to produce polysaccharides (Douterelo et al., 2014a). Bacteria with a hydrophobic cell surface are found to prefer hydrophobic material surfaces, whereas those with a hydrophilic cell surface are found to prefer hydrophilic material surfaces (Hori and Matsumoto, 2010).

It has been reported that as the roughness of the surface increases, bacterial adhesion also increases because the roughness works as shelter for microbes against shear forces (Percival et al., 2011). Temperature and pH are found to be important environmental factors that affect bacterial adhesion. The individual microbial ability to produce EPS, which are compounds that enhance cell adherence, can be affected by temperature (Else et al., 2003). The optimum temperature for bacterial adhesion depends on the individual species. Bacteria also respond to changes in pH by adjusting the activity and synthesis of proteins. The optimum pH for polysaccharide production depends on the individual species

(Garrett et al., 2008, Liu et al., 2016). Finally, the use of antimicrobial agents might be an effective strategy preventing adhesion of microorganisms. For instance, chlorine residuals present in DWDS are found to affect bacterial adhesion (Hori and Matsumoto, 2010).

2.5 Biofilm formation and development

One of the main reasons why bacteria opt for the biofilm, rather than the planktonic mode of life, is the protection that the biofilm offers to them. This might include protection against harsh conditions, such as nutrient deprivation, shear stresses, ultraviolet or acid exposure, metal toxicity, dehydration, salinity, antibiotics and other antimicrobial agents (Hall-Stoodley et al., 2004, Percival et al., 2011). Biofilms are considered to be an ideal environment for exchange of genetic material between cells (Jefferson, 2004).

The attachment of bacteria to the exposed surface is followed by microbial growth, development of microcolonies and recruitment of additional microorganisms. While this occurs, the colonising bacteria grow with the production and accumulation of EPS. The initial biofilm diversity is high because planktonic bacteria attach to the surfaces. During biofilm growth, diversity is reduced as more competitive organisms dominate the mixed microbial community (Jackson et al., 2001, Martiny et al., 2003). When the biofilm reaches a certain thickness, which might range from a few micrometres to millimetres, the biofilm approaches a state of maturity, which describes a condition of high species diversity and stability (Percival et al., 2011). The development of a mature biofilm is a multi-stage process and is dependent on a number of variables, such as the microorganisms, surface and environmental factors (Dunne, 2002).

2.5.1 The role of the extracellular polymeric substances

The matrix of EPS is mainly composed of polysaccharides and proteins, but also includes other macromolecules, such as DNA, lipids and humic substances. The composition and quantity of EPS varies, depending on the type of microorganisms, biofilm age and environmental conditions under which the biofilms grow (Vu et al., 2009). There are two types of EPS in biofilms; the one

that constitutes most of the EPS matrix and is loosely associated with the microbial cells, and the one that is tightly bound to the cell surfaces. To isolate the tightly bound EPS chemical methods are needed, but the loosely bound EPS can be separated from cells using physical methods (Lewandowski and Beyenal, 2013). The EPS matrix may account for 50 to 90% of the biofilm total organic carbon but little is known about the chemical structure of EPS that can be found in a biofilm (Characklis and Marshall, 1990). The physical properties of the biofilm are largely determined by EPS, while the physiological properties are determined by cells (De Beer and Stoodley, 2006).

It has been reported that when there is lack of nutrients in the environment, the production of EPS on the exposed surfaces is increased and that allows greater chances for adsorption of organics to the surfaces (Vu et al., 2009). The role of polysaccharides, proteins and DNA of the EPS matrix is very important for the long-term biofilm existence on surfaces. Also, EPS promote the cell-to-cell communication and development of high cell densities in the biofilm. Polysaccharides and proteins that EPS contain may help biofilms to withstand water-deficient environments by maintaining a hydrated microenvironment around them. Finally, proteins of EPS may also contribute to the release of cells from biofilms allowing enzymatic activities (Lewandowski and Beyenal, 2013).

2.5.2 The role of quorum sensing

An important factor that has been found to regulate bacterial colonisation and control biofilm growth is quorum sensing (QS); the cell-to-cell communication using chemical molecules, which is mainly a cell density-dependent regulation of gene expression. Quorum sensing signals, which are also termed as autoinducers, are acyl homoserine lactones (AHL) released by Gram-negative bacteria, and oligopeptides released by Gram-positive bacteria. When these signals are present at a critical concentration they induce the expression of certain genes (Jefferson, 2004). These small molecules are excreted by cells and accumulate in cultures as a function of cell density, which is termed the quorum (Percival et al., 2011). By using these signals, bacteria synchronize particular behaviours and function as multi-cellular organisms (Waters and Bassler, 2005). Cell-to-cell signalling might enable not only self-recognition but also recognition and

identification of other microbial colonies. Thus, this signalling may regulate the microbial colonisation (Battin et al., 2007, Liu et al., 2016).

The main drawback of the techniques used to detect cell-to-cell signalling is that they ignore the actual diversity of real biofilms and the complexity of the system, which is under study. Most studies have examined QS regulated by a limited number of bacterial species under controlled laboratory conditions (Douterelo et al., 2014a). A common method to record the presence of QS activities is the use of specific organisms that can sense QS molecules. Various methods such as the gas chromatography mass spectrometry have been used to identify the specific QS compounds being present (Ramalingam, 2012).

2.5.3 Other control factors

There are several factors that are found to control biofilm formation and growth in DWDS. One of them is the use of disinfectants (Garrett et al., 2008). Disinfectants should be used at appropriate concentrations to remove microorganisms because otherwise they can enhance the formation of substances that can be utilised by microorganisms and thus, promote biofilm formation. It has been shown that some bacteria not only survive but also multiply with the presence of disinfectants at certain concentrations (Momba et al., 2000).

Substances that may be used by the microorganisms and control the biofilm formation and development are biodegradable compounds, which are either present in water or originate from materials in contact with water (Momba et al., 2000, Horemans et al., 2013). The biodegradable organic matter that can be used by microorganisms can be divided into the dissolved organic carbon, which can be metabolised by bacteria within a period of a few days to months, and the assimilable organic carbon, which can be converted into new cellular material and thus, increase the formation of biofilms (Escobar and Randall, 2001, Liu et al., 2016). Finally, temperature plays an important role in the control of biofilm formation and growth; there is a wide range of temperatures under which bacteria can grow (Momba et al., 2000, Liu et al., 2016).

2.6 Detachment

Detachment is a random process, which is caused by local instabilities within the physical biofilm structure in combination with external forces. It is important to study detachment as it has various consequences in biofilms such as changes in the EPS matrix. There are many factors influencing detachment, such as cell properties, grazing activity, hydrodynamics, synthesis and release of EPS and substrate properties (Boe-Hansen, 2001). Other factors influencing detachment are pH, oxygen concentration and nutrient conditions (Simões, 2012).

There are two mechanisms of dispersal: the active dispersal, which occurs due to cell motility and the passive dispersal, which occurs due to shear forces. The dispersal strategies are: the seeding or swarming dispersal or central hollowing, in which there is a rapid release of individual cells from the microcolonies to the bulk water, the clumping dispersal or sloughing, in which there is a rapid detachment of large microcolonies of cells from biofilms, and the surface dispersal, which can be achieved by different types of cell motility, such as the gliding and the twitching motility (Hall-Stoodley and Stoodley, 2005).

The three modes of dispersal are the erosion, abrasion and grazing. Erosion is a process in which there is a continuous release of single cells or small clusters of cells into the aqueous phase due to shear forces (Kaplan, 2010). Abrasion occurs due to direct physical contact of the medium with the biofilm structure, for instance during backwashing. Grazing is caused by large organisms, which feed on biofilms. Different detachment patterns have significant effects on the spatial distribution of microorganisms within biofilms and cause biofilm thicknesses to vary with space and time. In various mathematical models, detachment has been described as a function of biofilm thickness and density, biofilm growth rate, and shear stress. However, it is difficult to model such complex process because it is affected by many variables in real systems (Morgenroth and Wilderer, 2000, Cogan et al., 2016).

2.7 Flow in a rotating annular reactor and in a pipe

In this study, a rotating annular reactor (RAR) was used to investigate the role of the flow regime in biofilms in drinking water. This reactor presents various

advantages, such as simple sampling process and the fact that the shear stress conditions can be applied simply by the rotational speed of its inner rotating cylinder (Gomes et al., 2014). Also, the liquid phase of the reactor is well mixed, which ensures that there is uniform distribution of bacteria in the liquid phase (Characklis and Marshall, 1990). The exact description of flow conditions in the reactor is complicated because of the presence of Taylor vortices (Gomes et al., 2014) and the geometry of the reactor (Gjaltema et al., 1994). Here, some key aspects regarding the flow in the reactor and the pipe are described.

2.7.1 Flow in a rotating annular reactor

The flow that is developed in such a bioreactor is the Taylor-Couette flow, which is a flow confined in the gap between two rotating cylinders, but most often with the inner cylinder rotating and the outer cylinder fixed, as in this study. By applying the Navier-Stokes equations and assuming that the velocity in the radial and axial direction is negligible compared to the azimuthal direction, the velocity in the reactor is given by (Childs, 2011):

$$u = Ar + \frac{B}{r} \quad 2-1$$

where,

$$A = \frac{\Omega_2 R_2^2 - \Omega_1 R_1^2}{R_2^2 - R_1^2}, \quad 2-2$$

$$B = (\Omega_1 - \Omega_2) \frac{R_1^2 R_2^2}{R_2^2 - R_1^2}, \quad 2-3$$

u is the velocity (m/s) in the reactor, r is the distance (m) from the centre of the pipe, R_1 and R_2 are the radii (m) of the inner and outer cylinders, respectively, and Ω_1 and Ω_2 are the rotational speeds (rpm) of the inner and outer cylinders, respectively. These reactors are also named Taylor-Couette reactors as Taylor vortices can be generated in the annular gap of the reactor. The Taylor number is used to define the appearance of those vortices in the reactor. When only the inner cylinder rotates the Taylor number is given by (Childs, 2011):

$$Ta = \frac{\Omega_1 R_m^{0.5} (R_2 - R_1)^{1.5}}{\nu} \quad 2-4$$

where,

$$R_m = \frac{(R_1 + R_2)}{2}, \quad 2-5$$

Ta is the Taylor number, ν is the kinematic viscosity (m^2/s) of fluid, and R_m is the average radius (m) of the two reactor cylinders. When the Taylor number is equal to 41.19 pairs of counter-rotating axisymmetric vortices are formed in the radial and axial directions, while the principal flow continues to be around the azimuth. Also, the onset of turbulence can be defined by the Taylor number. For narrow annuli only with the ratio of width (the gap between the two cylinders) to mean radius close to 0.198, when the rotational speed of the inner cylinder of the reactor is around 53.8 rpm and the Taylor number is around 418, that indicates the onset of turbulent flow (Kaye and Elgar, 1957). The Reynolds number, which is also used in order to define the transition from laminar to turbulent flow, is given by:

$$Re = \Omega_1 R_1 \frac{2(R_2 - R_1)}{\nu} \quad 2-6$$

where Re is the Reynolds number. For Reynolds number equal to approximately 2000 the transition flow occurs, for Reynolds number lower than 2000 the flow is laminar and for Reynolds number higher than 2000 the flow is turbulent (Bird et al., 1960). Finally, the shear stress in the reactor is given by (Childs, 2011):

$$\tau = -\mu \frac{2B}{r^2} \quad 2-7$$

where τ is the shear stress (Pa) in the reactor, μ is the dynamic viscosity (kg/sm) of fluid and B was described earlier (see Equation 2-3).

2.7.2 Flow in a pipe

In the pipe the transition from laminar to turbulent flow is defined based on the Reynolds number, which is defined by:

$$Re = u_p \frac{D}{\nu} \quad 2-8$$

where u_p is the mean velocity (m/s) in the pipe and D is the diameter (m) of the pipe. For Reynolds number lower than approximately 2000 the flow is laminar, for Reynolds number greater than 4000 the flow is turbulent, and for Reynolds number between 2000 and 4000 the flow is transitional (Holman, 2002). The velocity in the pipe is defined by (Munson B. R. et al., 1998):

$$u_v = \frac{\tau_p D}{4\mu} \left(1 - \frac{r_v^2}{R^2}\right) \quad 2-9$$

where u_v is the velocity (m/s) in the pipe, τ_p is the wall shear stress (Pa) in the pipe, R is the radius (m) of the pipe, and r_v is the distance (m) from the centre of the pipe. The wall shear stress in the pipe is defined by (Munson B. R. et al., 1998):

$$\tau_p = \frac{f \rho u_p^2}{8} \quad 2-10$$

where τ_p is the wall shear stress (Pa) in the pipe at $r=R$, and f is the friction factor. For Reynolds number lower than 2100, the friction factor in the pipe is determined by (Characklis and Marshall, 1990):

$$f_1 = \frac{64}{Re} \quad 2-11$$

For Reynolds number higher than 2100 and lower than 100000, the friction factor in the pipe is determined by (Characklis and Marshall, 1990),

$$f_2 = \frac{0.0791}{Re^{0.25}} \quad 2-12$$

Finally, the shear stress in the pipe is given by (Munson B. R. et al., 1998):

$$\tau_v = \frac{2\tau_p r_v}{D} \quad 2-13$$

3 The role of flow regime in biofilms in drinking water

3.1 Introduction

The provision of safe drinking water is a top priority in all societies. Managing biofilms that are formed on the inside surface of drinking water pipes is a concern of water utilities around the world as these biofilms can affect the aesthetics of drinking water (Batté et al., 2003, Abe et al., 2012, Douterelo et al., 2013). Hydrodynamics exert a significant influence on biofilms (Percival et al., 1999, Manuel, 2007, Manuel et al., 2007, Rochex et al., 2008, Fish et al., 2016) and in particular, on the spatial distribution of bacteria (Saur et al., 2017). The hydrodynamics in real DWDS may dramatically vary between different locations, alternating from laminar to turbulent flow and vice versa (Manuel et al., 2007, Liu et al., 2016). Stagnation and laminar flow occur mainly at the dead ends of service lines of DWDS (Romero-Gomez and Choi, 2011). Most water flow in most engineered systems, including the mains of DWDS, is turbulent (Percival et al., 1999). Within the DWDS between the two extremes of flow, the laminar one in the dead ends of the service lines part of DWDS and the turbulent one in the main part of DWDS, transition flow may occur (Percival et al., 1999). Therefore, this study was set up to look at how biofilms grow under 3 distinct flow regimes: turbulent, transition and laminar flow, and under stagnant conditions.

There is a wealth of literature that supports the fact that biofilm structure is intimately linked with hydrodynamics (Stoodley et al., 1999a, Liu and Tay, 2002, Pereira et al., 2002, Purevdorj et al., 2002, Simoes et al., 2007b). These studies have been mostly focused on the growth and detachment of bacteria under a constant flow regime. In laminar flows, biofilms are found to create patchy structures (Stoodley et al., 1999a), whereas in turbulent flows, biofilms are found to create elongated streamers (Hall-Stoodley et al., 2004). The formation of streamers has been suggested to cause firmer adhesion of bacteria to the available surfaces and promotion of microcolonies formation. Streamers may consist mainly of EPS and are found to improve the resistance of the biofilm to the external shear (Percival et al., 1999). The structure of biofilms may impact

biofilm development, mass transfer processes, oxygen distribution and frictional resistance in pipelines (Stoodley et al., 1997) and thus, it is important for researchers to extend the existing knowledge.

Hydrodynamics are found to affect biofilm thickness and density. High detachment forces, caused by increased shear stresses, have been shown to lead to denser biofilms that are mechanically more stable (Garny et al., 2008, Rochex et al., 2008). As far as the effect of hydrodynamics on biofilm thickness is concerned, there is limited knowledge regarding biofilms in drinking water systems. The prevailing view is that biofilm development is hindered by higher shear stresses due to higher detachment forces, which are applied to the biofilm (Percival et al., 1999, Liu and Tay, 2002, Rickard et al., 2004). However, turbulence has been also found to promote the development of thick biofilms (Rochex et al., 2008) probably due to the increased transport of nutrients and oxygen to the biofilm surface (Percival et al., 1999). It has also been proposed that biofilms respond to shear stress by regulating metabolic pathways and become stronger (Liu and Tay, 2001).

This unexpected result of the development of thick biofilms in turbulent flow might be attributed to several other factors. The change in the substrate flux is one of those factors. High shear stress conditions are found to cause a double effect on mass transfer properties; on the one hand, turbulence facilitates high substrate diffusion in biofilms and on the other hand, the resulting denser biofilm reduces the diffusivity of substrate (Liu and Tay, 2002). Another factor is the role of bacterial aggregation in biofilms. Bacterial aggregation is an important biological process between bacteria under which they come together (attach to one another) in the bulk water before they attach to the exposed surfaces as biofilms (Karunakaran et al., 2011). Evidence from freshwater samples (Rickard et al., 2003, Rickard et al., 2004) suggests that there is a strong relationship between aggregation and flow regime. In the fluvial environment multi-species aggregates in the bulk flow have been shown to present distinct growth dynamics that are shear dependent (Niederdorfer et al., 2016).

Little is known regarding the initial colonisation of bacteria, which is a precursor to the formation of biofilms (Garrett et al., 2008, Hori and Matsumoto, 2010),

and how it is affected by the flow regime (Saur et al., 2017). In the present study, the influence of different flow regimes was studied on biofilms grown for 4 weeks in drinking water with the hypothesis that turbulent flow is more likely to enhance their growth. Initial formation of biofilms was characterised as a function of the flow regime with the hypothesis that biofilms can be established on the surfaces even after a short time period of 10 hours. Finally, the robustness of already established biofilms which were grown for 4 weeks under a constant flow regime was studied to changes to the flow regime, each of which lasted 24 hours, assuming that biofilms would be able to respond to those changes.

3.2 Materials and Methods

3.2.1 Reactor conditions

Biofilms were grown in a jacketed rotating annular reactor (model 1320 LJ, BioSurface Technologies, USA) (Figure 3-1). The main advantage of this reactor is that the shear stress conditions can be easily controlled by its motor device, and the flow rate can be controlled independently of the shear stress. It has been suggested that reactors cannot accurately simulate the flow conditions of real drinking water distribution systems due to their geometry (Deines et al., 2010, Gomes et al., 2014). However, the generic relationships between biofilms and flow regimes were the focus of this study and those flow regimes were confidently created in this reactor.

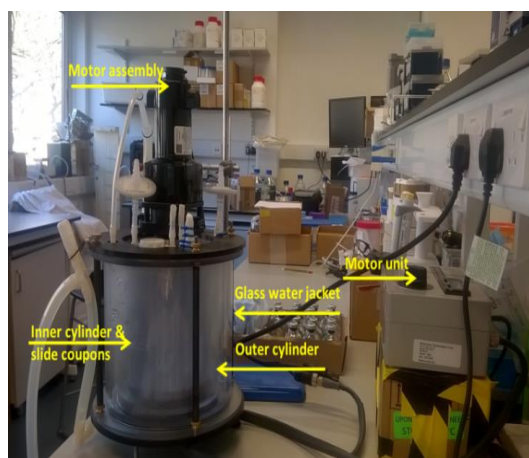


Figure 3-1 The rotating annular reactor used in this study.

The reactor held 20 removable polycarbonate slides (BST-503-PC) that were attached to its inner drum. The beveled edges of the slides were dropped into the beveled slots on the reactor inner cylinder and they were removed from it using a sterilized hook. The slides were filled in the inner cylinder in a symmetric way in order to avoid imbalances. They had a height of 14.986 cm, a width of 1.168 cm, an area of 17.51 cm² and a volume of 2.80 cm³. The polycarbonate material was chosen as one of the plastic materials used in drinking water systems, which does not have a rough surface of corroded material (Szabo et al., 2007, Garny et al., 2008). The jacket of the reactor allowed the temperature to be maintained in the system via heated water from a bath circulator (Isotemp Bath Circulator, Fisher Scientific, England, UK). The temperature was chosen at 16°C as the representative temperature of DWDS in the United Kingdom for spring and summer (Douterelo et al., 2013). The reactor was covered with aluminium foil in order to achieve dark conditions for biofilm growth.

This reactor was used to simulate flow conditions similar to those in a pipe with a radius equal to the gap between the two cylinders of the reactor, and mean velocity equal to the mean velocity of the reactor. The inner drum of the reactor was rotated at 3 different speeds to induce Taylor-Couette flows (Kaye and Elgar, 1957, Bird et al., 1960, Childs, 2011); at 30 rpm (the Reynolds number, $Re = 960$ and the Taylor number, $Ta = 233$), which corresponds to laminar flow; at 57 rpm ($Re = 1800$ and $Ta = 439$), which corresponds to transition flow; at 217 rpm ($Re = 6800$ and $Ta = 1682$), which corresponds to turbulent flow. These 3 speeds of the reactor were used to simulate 3 different flow conditions in a pipe of 30.3 mm diameter with: average velocity of 0.03 m/s and shear stress at the wall of 0.007 Pa in laminar flow, average velocity of 0.07 m/s and shear stress at the wall of 0.02 Pa in transition flow, and average velocity of 0.25 m/s and shear stress at the wall of 0.07 Pa in turbulent flow (Characklis et al., 1990, Munson B. R. et al., 1998, Holman, 2002). These conditions, which are described in Table 3-1, were determined using the equations described in Section 2.7.

Flow regime	Rotation speed (RPM)	Reynolds number	Taylor number	Average velocity (m/s)	Shear stress at the wall (Pa)
Turbulent	217	6800	1682	0.25	0.07
Transition	57	1800	439	0.07	0.02
Laminar	30	960	233	0.03	0.007

Table 3-1 Conditions for turbulent, transition and laminar flow.

The choice of the diameter of the pipe at 30.3 mm corresponds to the extremities of drinking water pipes where the service lines start (NRCouncil, 2006, Hall et al., 2009, SAWater, 2011). In those parts of DWDS the control of flow conditions is very important as the disinfectant residual has been depleted and microbial activities are higher than in the mains of DWDS (Chowdhury, 2012). Also, the conditions in service lines are characterised by longer residence times, higher stagnation periods, reduced flow rates and higher temperatures compared to the mains (Zheng et al., 2015).

3.2.2 Reactor medium

The medium that the reactor was filled with consisted of 150 ml of nutrient medium and 850 ml of drinking water that was sampled from a domestic tap in Glasgow. The concentrations for mineral salts of the reactor medium were: ammonium sulphate (1.2 mg/l), ammonium chloride (0.9 mg/l), magnesium sulphate heptahydrate (0.3 mg/l), manganese chloride tetrahydrate (0.003 mg/l), copper sulphate pentahydrate (0.002 mg/l), cobalt sulphate heptahydrate (0.001 mg/l), sodium molybdate dehydrate (0.001 mg/l), zinc sulphate heptahydrate (0.01 mg/l), and boric acid (0.75 mg/l) (Milferstedt et al., 2006), and the concentration for glucose of the reactor medium was 1.5 mg/l. These concentrations kept the bulk water conditions in the reactor oligotrophic (Batté et al., 2003).

The concentration of total chlorine of the drinking water, that was sampled from the tap, was measured immediately after its sampling using the USEPA DPD Method 8167 (Chamberlain and Adams, 2006) and a colorimeter (DR 900 Hach) and was found at 0.36 mg/l. The total organic carbon of the reactor medium was monitored during the reactor operation using a TOC-L analyser (Shimadzu, Japan) as the difference between the total carbon and the total inorganic

carbon and it was found to be 1.59 ± 0.88 mg/l. Finally, the concentration of cells and microcolonies in the bulk water of the reactor was found to be $(5.8 \pm 0.2) \times 10^5$ cells/ml and $(7.6 \pm 0.1) \times 10^3$ microcolonies/ml, respectively (see Section 4.2.1 for the analytical method for the calculation of the concentrations).

3.2.3 Experimental processes

Three experiments were conducted, which are described here as “A”, “B” and “C” experiments. In each experiment, the same processes were followed. An overview of the experimental processes can be seen in Figure 3-2.

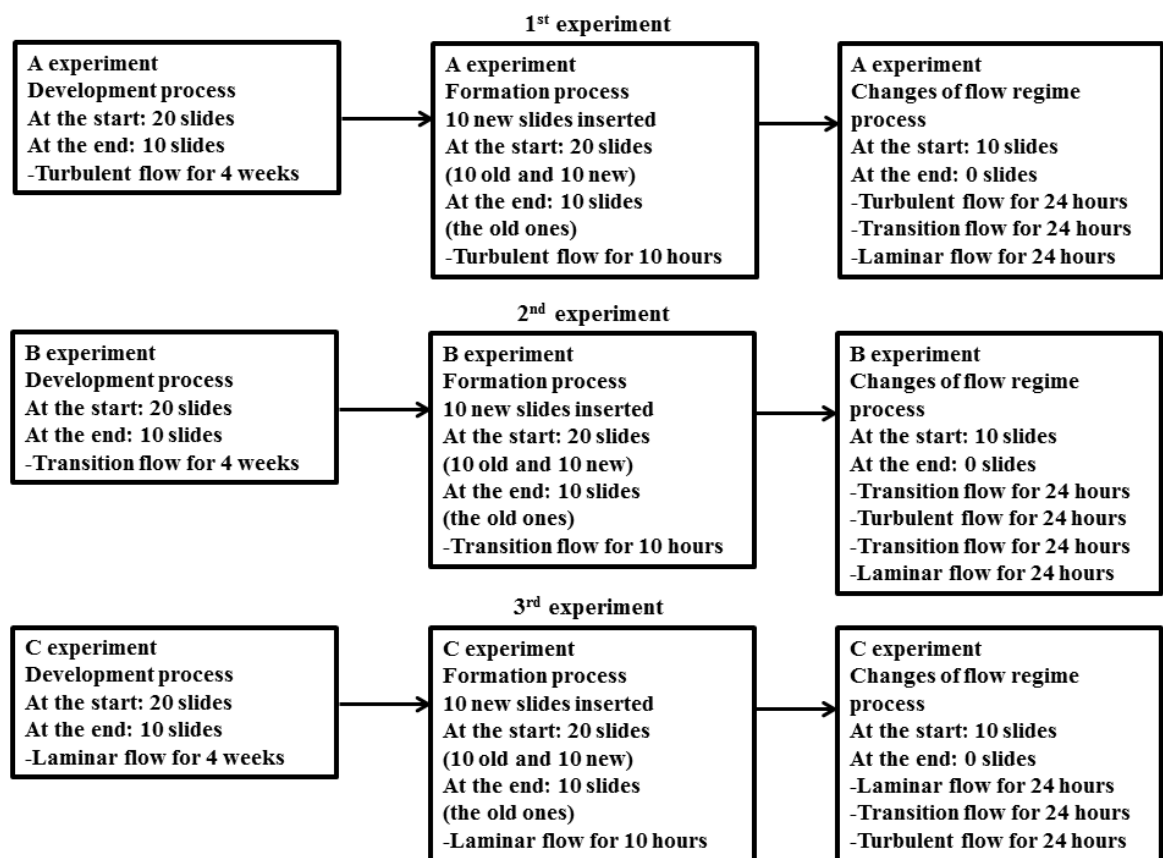


Figure 3-2 Diagram of the experimental processes conducted at each experiment.

The first process, which is described here as “development”, is the process in which biofilm development was studied after 4 weeks of reactor operation (Table 3-2). During these 4 weeks, the reactor was operating under batch mode (zero flow rate) as a closed system in order to retain the biomass and ensure that biofilms would be established on its surfaces. In each experiment, the medium was manually added to the reactor and immediately after that the

reactor started to operate under the specific rotation speed associated with experiment A, B or C. The 10 out of the 20 slides of the reactor were sacrificed for sampling at the end of this process.

Name of experiment	Flow regime Development process	Total time (weeks)	10 out of 20 slides were used at the end of this process
A	Turbulent	4	
B	Transition	4	
C	Laminar	4	

Table 3-2 Development process for A, B and C experiments.

The second process, which is described here as “formation”, is the process in which the biofilm initial formation was studied after 10 hours (Table 3-3). The reactor was operating again under batch mode, without changing the reactor medium after the 4 weeks of reactor operation, under the same rotation speed as in the development process. Clearly during the 4 weeks that the biofilms became established there would have been “formation” of biofilms on the surfaces, but it was thought that this might be atypical formation because both the bulk water environment and the neighbouring surfaces would not have been conditioned by the presence of biofilms. In a real system, any new uncolonised surfaces would be placed into a distribution system where biofilms were already established up and downstream. It is for this reason that the formation process on clean slides was studied after the 4 weeks where biofilms had become established on the surfaces of the bioreactor. The 10 slides that were sacrificed at the development process were replaced by 10 new sterile slides at the start of the formation process. These were removed for analysis in pairs at 2 hourly intervals.

Name of experiment	Flow regime Formation process	Total time (hours)	10 new slides were used at this process
A	Turbulent	10	
B	Transition	10	
C	Laminar	10	

Table 3-3 Formation process for A, B and C experiments.

The last process, which is described here as “changes of flow regime”, lasted 72 hours for A and C experiments and 96 hours for B experiment. The aim of this process was to test how the already established biofilms after the 4 weeks of the reactor operation responded to changes in the shear stress conditions each of which lasted only 24 hours. During this process, the reactor was operating under recirculation mode. One litre of a similar medium that initially filled the reactor was recycled; the differences being that distilled water was used instead of drinking water and the recycling medium here was 10 times more diluted. This meant that bulk liquid initially contained few planktonic bacteria and the bacteria that did appear were primarily derived from eroding biofilms on the surfaces. That medium was recirculated with flow rate at 22 ml/min and retention time at 45 minutes, in order to minimise suspended cell growth and enhance biofilm growth on the reactor surfaces (Rochex et al., 2008). During this process, the rotation speed of reactor was changed every 24 hours to switch to one of the 3 distinct flow regimes: turbulent, transition and laminar.

In Table 3-4 there is description of the changes in the flow regime that were imposed for each of the 3 experiments conducted. The rationale behind the decision about the flow regime in each 24-hour interval was the following: the first flow regime was the same as the one in the development and formation processes. This allowed us to establish whether there were differences in biofilm growth due to the change of the mode of flow from batch to recirculation. After 24 hours, the flow regime was ramped down for experiment A, ramped up for experiment C and set higher then lower for experiment B. Finally, for the changes of flow regime process the 10 slides that had remained in the reactor untouched from the start of each experiment were used.

Name of experiment	Flow regimes Changes of flow regime process				Total time (hours)	The left 10 out of 20 slides were used at this process
	Turbulent	Transition	Laminar	n/a		
A	Turbulent	Transition	Laminar	n/a	72	
B	Transition	Turbulent	Transition	Laminar	96	
C	Laminar	Transition	Turbulent	n/a	72	

Table 3-4 Changes of flow regime each of which lasted for 24 hours for A, B and C experiments.

3.2.4 Gravimetric measurements

Gravimetric measurements were used to characterise the thickness and density of the biofilms (Staudt et al., 2004). The measurements were taken after 4 weeks of the reactor operation at the end of the development process. In brief, two slides were removed from the reactor, drained for 5 minutes at a vertical position, and weighed for the determination of the wet mass. Then, the slides were dried for 24 hours at 65°C in an oven and weighed again. After that, the dried biofilm was washed off the slides with distilled water and laboratory tissues. The clean slides were dried again for 24 hours at 65°C and then weighed again. The dry mass was determined by the weight difference of the slides with and without the dried biofilm. The biofilm thickness, L_F , was determined by:

$$L_F = \frac{m_{WF}}{\rho_{WF}A_F} \quad 3-1$$

and the biofilm density, ρ_F , was determined by:

$$\rho_F = \frac{m_{DF}}{\left(\frac{m_{WF}}{\rho_{WF}}\right)} \quad 3-2$$

where m_{WF} and m_{DF} are the wet and dry mass of the biofilm respectively, ρ_{WF} is the density of biofilm, for which there is the assumption that it is equal to that of water at 16°C at 998.946 kg/m³ (CRChandbook, 1984), and A_F is the surface area of the slide, which is equal to 17.51 cm². Finally, the areal biofilm density was calculated as the product of the biofilm thickness (Equation 3-1) and the volumetric biofilm density (Equation 3-2).

3.2.5 Microcolonies count measurements

Two slides were used for each of the 3 processes of each experiment for these measurements. The biomaterial attached on the reactor slides was gently scraped from the reactor slides using a sterile cell scraper of 30 mm blade length and 390 mm handle length (ThermoFisher Scientific, England, UK), and diluted in 5 ml distilled water. Then, the 5 ml samples were fixed with 0.5 ml of 2% formaldehyde (Kepner and Pratt, 1994) and filtered on Whatman® 0.2 µm membrane filters (Sigma-Aldrich, Irvine, UK). A solution of 1 ml of 10 µg/ml 4',

6-diamidino-2-phenylindole (DAPI) (ThermoFisher Scientific, Loughborough, England, UK) was used to stain the microcolonies for 20 minutes in the dark. After that, the solution was filtered and the membrane filters were dried and prepared for visualisation. Images were obtained for the microcolonies on the membrane filters using fluorescence microscopy (Olympus IX71, Japan, Asia) with the UPlanFLN objective lens (Japan, Asia) with 10X magnification/0.30 numerical aperture. The filter used was the DAPI filter with excitation at 358 nm and emission at 461 nm. The microcolonies visualised had a diameter of approximately 10 μm and consisted of approximately 10 cells. More than 30 images per membrane filter were obtained in order to calculate the concentration of microcolonies. The concentration of microcolonies was calculated from (Brunk et al., 1979):

$$\frac{\text{microcolonies}}{\text{cm}^2} = \frac{\left(\frac{\sum x}{n} \pm s\right) A_{\text{memb}} d V_{\text{susp}}}{A_{\text{field}} V_{\text{filt}} A_{\text{biof}}} \quad 3-3$$

where, $\sum x/n$ is the mean number, s is the standard deviation, A_{memb} is the surface area of the membrane filter, d is the dilution factor, V_{susp} is the total suspension volume, A_{field} is the surface area of the microscope field, V_{filt} is the volume of liquid sample that is filtered and A_{biof} is the area from which the biomaterial was scraped.

The concentration of cells on the reactor slides was also calculated following the same process as that described for the microcolonies. The only difference is that after the biomaterial attached on the reactor slides was scraped from the reactor slides, it was homogenised in vortex for 2 minutes in 5 ml distilled water. Also, the membrane filters were covered with 1 ml of 0.1% Triton X-100 solution (ThermoFisher Scientific, Loughborough, England, UK) in order to evenly disperse the cells before DAPI staining was applied. Cells were finally visualised on the membrane filters using the oil immersion UPlanFLN objective lens with 100X magnification/1.30 numerical aperture. The filter used was the DAPI filter with excitation at 358 nm and emission at 461 nm. Their concentration was calculated at $(5.4 \pm 0.6) \cdot 10^5$ cells/cm².

3.2.6 Biofilm structure measurements

For these measurements 2 slides were used for the development process, 3 slides for the formation process and 3 slides for the changes of flow regime process. The biofilms on the reactor slides were firstly fixed with 0.5 ml of 4% paraformaldehyde (Chao and Zhang, 2011) (see Appendix 10.1.1 for the analytical fixation protocol). The samples were firstly covered with 1 ml of 10 µg/ml Fluorescein Aleuria aurantia lectin (Vector laboratories, Peterborough, England, UK) for 10 minutes in the dark to stain the EPS (Garny et al., 2008, Flemming and Wingender, 2010). Then, they were covered with 1 ml of 10 µg/ml DAPI for 20 minutes in the dark to stain the cells. Biofilm structures were visualised directly on the slides using fluorescence microscopy with the oil immersion UPlanFLN objective lens with 100X magnification/1.30 numerical aperture. The filters used was the DAPI filter with excitation at 358 nm and emission at 461 nm for cells visualisation, and the FITC filter with excitation at 495 nm and emission at 525 nm for EPS visualisation. The lateral resolution (i.e. d_{XY}) and the axial resolution (i.e. d_z) were calculated from Equations 3-4 and 3-5 (Nicewarner-Pena et al., 2001, Vijayakmar et al., 2016):

$$d_{XY} = \lambda / (2NA) \quad 3-4$$

$$d_z = 2\lambda / NA^2 \quad 3-5$$

In Equations 3-4 and 3-5, λ is the excitation wavelength band in fluorescence and NA is the numerical aperture. For cells visualisation, the lateral and axial resolutions were calculated at 137 nm and 423 nm, respectively. For EPS visualisation, the lateral and axial resolutions were calculated at 190 and 585 nm, respectively.

The composite image of biofilms was created using the Matlab command called “imfuse”. The surface area of biofilms on the reactor surfaces was then calculated. Also, the surface area that only the EPS occupied on the reactor surfaces was calculated. These surface areas were calculated in Matlab by processing more than 30 images per slide obtained from fluorescence microscopy. The original images were firstly converted to gray-scale images using the Matlab command called “rgb2gray” and then to binary images using

the Matlab command called “im2bw” in order to separate the biomaterial (the biofilms in one case and only the EPS in the other case) from the background of the image. After the surface areas were calculated, they were divided to the total surface area of the image in order to finally calculate the percentages of these surface areas (%).

3.2.7 Statistical analysis

All measures were analysed in IBM SPSS Statistics using one of the following tests: i. the one-way ANOVA test in conjunction with the Tukey's and Duncan-Waller's tests, ii. the Kruskal-Wallis by ranks test, iii. the Jonckheere-Terpstra test and finally, iv. the Pearson's chi-squared test in conjunction with the Phi and Cramer's test, depending on the fitness of the data under comparison to the assumptions of the tests. All statistical calculations were based on the confidence level of 95%, which means that a *P* value lower than 0.05 was considered statistically significant.

Where the data sets were normally distributed and there was homogeneity of variances, then significant differences between data were tested using the one-way ANOVA test in conjunction with the Post-hoc Tukey's and Duncan-Waller's tests that would further validate the statistical result of one-way ANOVA. Comparisons of the surface area of biofilms between the batch and recirculation mode of flow were tested using one-way ANOVA in conjunction with the Tukey's and Duncan-Waller's tests.

Where the data sets were not normally distributed, then the Kruskal-Wallis test was used, in which the variances of the populations should be equal across the samples. Comparisons of the surface area of biofilms between the different flow regimes for the changes of flow regime process were made using this test.

For the data in which the condition for the variances of the Kruskal-Wallis test was not met, the Jonckheere-Terpstra test was deployed, in which there should be a priori ordering of the populations. Comparisons of the microcolonies that were attached on the reactor slides between the different flow regimes for the development process were made using this test. The same test was used for the

comparisons of the surface area of EPS between the different flow regimes for the formation process.

In the case in which the data sets did not validate the assumptions of any of the previous tests, the Pearson's chi-squared test in conjunction with the Phi and Cramer's test were performed for large size samples for which there was the assumption that the data sets were consistent with a theoretical distribution. For all the rest comparisons described in Section 3.3 these two tests were used.

3.2.8 Spatial statistics

Textural entropy was one of the measures used in this study to characterise the biofilm structures. It is used to describe the randomness of the components of a gray-scale image by comparing the intensity of the image pixels. The higher is the value of the entropy, the more heterogeneous is the biofilm. This means that more complex biofilm structures are demonstrated in the image. Entropy refers to the gray levels, which the individual pixels can adopt. In an 8-bit pixel image, for example, there are 256 such levels. If all of the pixels of the image have the same value, or the image has no structures, or the image is composed of only white pixels or voids, the entropy of the image is zero showing there is no gray scale variation in the pixels or heterogeneity. Increased numbers of cell clusters in the image increase entropy due to increased gray level variability and heterogeneity in the image. Thus, the surface area of biofilm structures in the image is related to the entropy (Yang et al., 2000, Beyenal et al., 2004). The entropy, E , of an image is here defined:

$$E = - \sum p \log_2 p \quad 3-6$$

where, p is the pixel intensity associated with the gray level. Entropy was here calculated using the Matlab function called "entropy".

Semi-variograms were used here as another measure to characterise the spatial variance of biofilm structures within gray-scale images and quantify the spatial dependencies in the data sets. Their function relates the semi-variance of the data points to the distance that separates them. Large distance of the data points means more data pairs for estimation of the semi-variance but less amount of detail in the semi-variogram. In other words, semi-variograms are a

way of graphically capturing the spatial variance of points on a landscape as a function of their distance. All combinations of points at a distance are collated and their variance is determined for all possible separation distances (Carr and de Miranda, 1998, Olea, 1999).

An important part of a semi-variogram is the “origin”; the closest points of the diagram. In theory, the semi-variogram value at the origin should be zero. If it is significantly different from zero for lags very close to zero, then this semi-variogram value is the “nugget”. Where values are co-located, for example in clusters, the variances at short distances are low as the values are similar. At the characteristic cluster length the variance will step up. Another important part of a semi-variogram is the “sill”; the variogram upper bound that is equal to the variance of the dataset and reflects the amount of variability. The sill is usually at large distances where there is no gradient in the diagram (Cohen et al., 1990, Cressie, 1993). The lag distance at which the semi-variogram reaches the sill value is the “range”. In total, 12000 points were used for the calculation of each semi-variogram. They were calculated using the Matlab function called “variogram.m” and they were created only for the most representative images obtained from fluorescence microscopy. These images were obtained from the biofilm structure measurements described in Section 3.2.6. The whole biofilm (combined proportion of cells and EPS) was taken into account for the calculation of the semi-variogram. The representative images were those in which their entropy was found to be equal to the average entropy of all the images obtained.

Autocorrelation function (ACF) diagrams were used as the last measure to characterise the biofilm structures. The ACF diagrams are, in essence, a two-dimensional extension of the semi-variograms. They allow us to assess how the spatial autocorrelation changes with distance. They correlate pixel intensities within gray-scale images and detect the repetitive structures within the images under consideration by combining together all parts of them. The ACF diagrams are real-space images, so that their dimensions have the same meaning as in the original images. Interpretation of the ACF diagrams can be understood by imagining the image to be printed on transparency and placed on top of itself but rotated by 180°. By sliding the top image laterally in any direction, the

degree of match with the underlying original image is measured by this function. When features align with themselves, the match will be high. Similarly, when a large shift brings a feature onto another feature similar to the previous one, the match will be again high (Heilbronner and Barrett, 2014). Below, there are two examples of images and their relevant ACF plots (Figure 3-1).

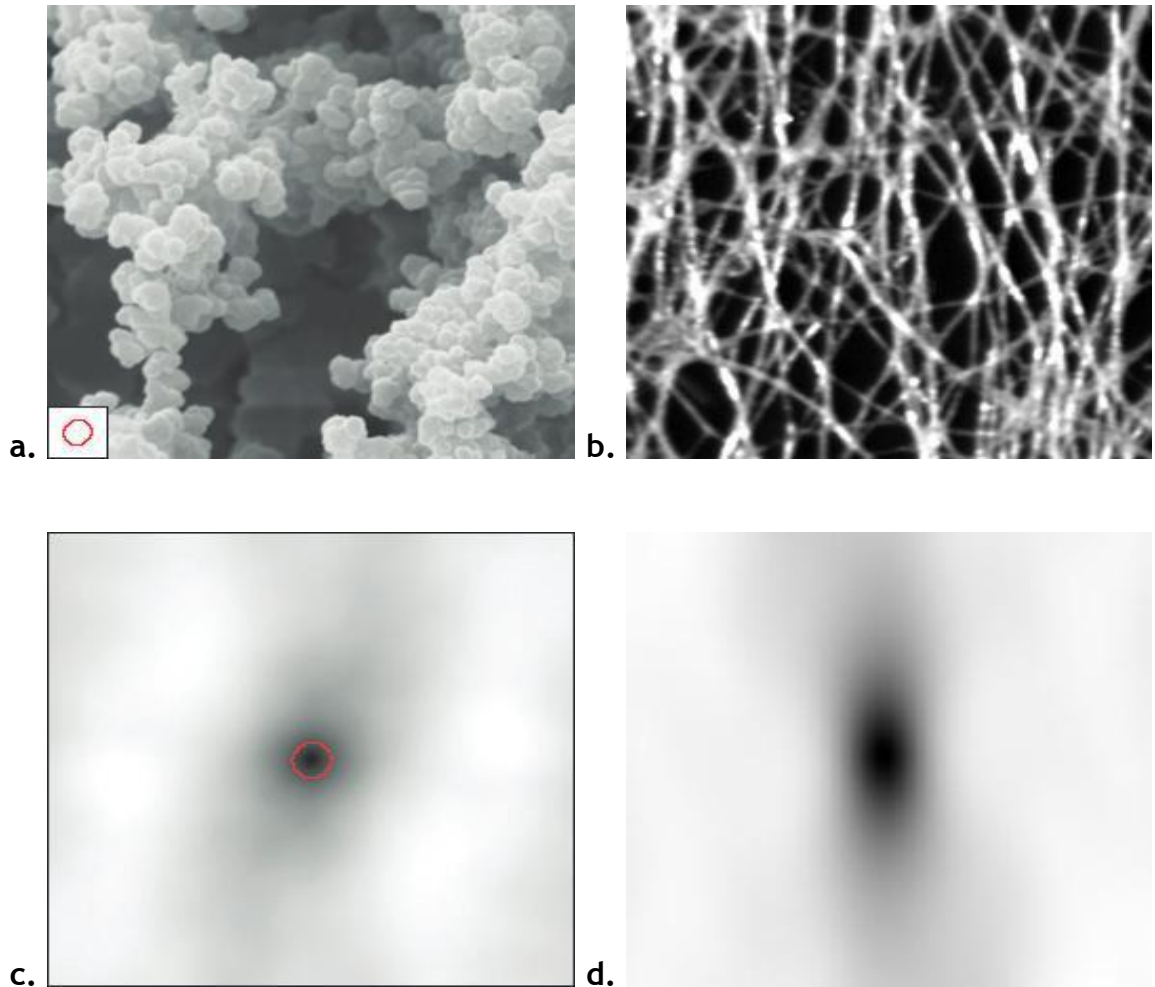


Figure 3-3 Images and relevant ACF images. Source: (Russ, 2011)
(a) Image of a cheese consisting of different size curds, (b) image of felted textile fibers, (c) autocorrelation image for image a. and (d) autocorrelation image for image b.

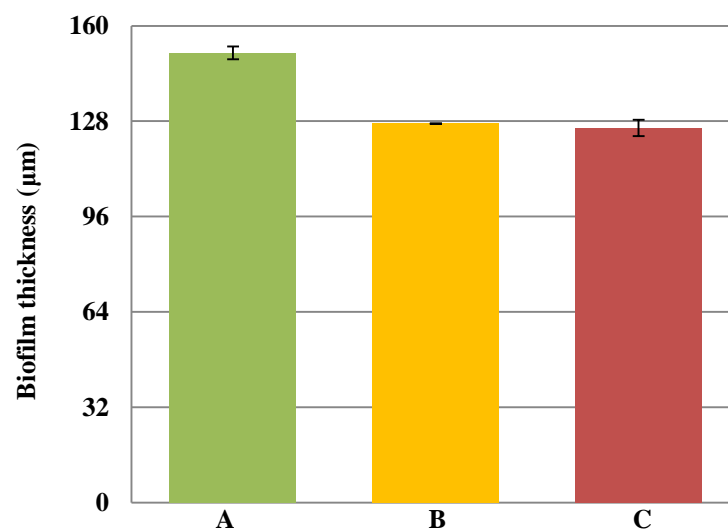
In these diagrams, represented here as contour plots, the central element provides a measure of the size and shape of the basic element that dominates the original images. The rest contour lines reflect the size and shape of the neighbourhood elements of the original images. Finally, the bar on the right side of the diagrams provides a measure of the autocorrelation. The darker is the colour on the bar, the less is the autocorrelation value with its lowest value to be 0 and the highest one to be 1 (Russ, 2011). The ACF diagrams were calculated using the Matlab function called “autocorr2d.m” and again created only for the

most representative images. Again, the whole biofilm (combined proportion of cells and EPS) was taken into account for the calculation of the ACF diagrams. The algorithm for the calculation of the ACF diagram is based on the Wiener-Khintchine theorem (Wiener, 1930).

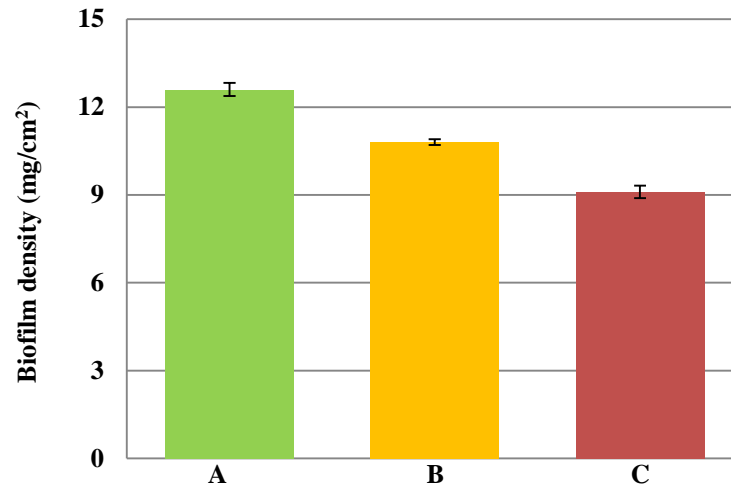
3.3 Results and Discussion

3.3.1 Development process

The biofilm thickness (Figure 3-2a) and biofilm density (Figure 3-2b) were determined for all 3 experiments at the end of the development process. It was found that the highest thickness and density were for the biofilms developed in turbulent flow. Also, at the end of the development process the number of microcolonies attached on the reactor slides (Figure 3-3), the surface area of biofilms (Figure 3-4) and the entropy of biofilms (Figure 3-5) were found to be significantly higher ($P < 0.05$) in turbulent flow compared to transition and laminar flow. No significant differences were found in these measures between the transition and laminar flow.



a.



b.

Figure 3-4 Biofilm thickness and density after 4 weeks of biofilm growth at the end of the development process.

(a) Biofilm thickness and (b) biofilm density. “A” describes turbulent flow, “B” describes transition flow and “C” describes laminar flow. The error bars represent the standard deviation of the measurements.

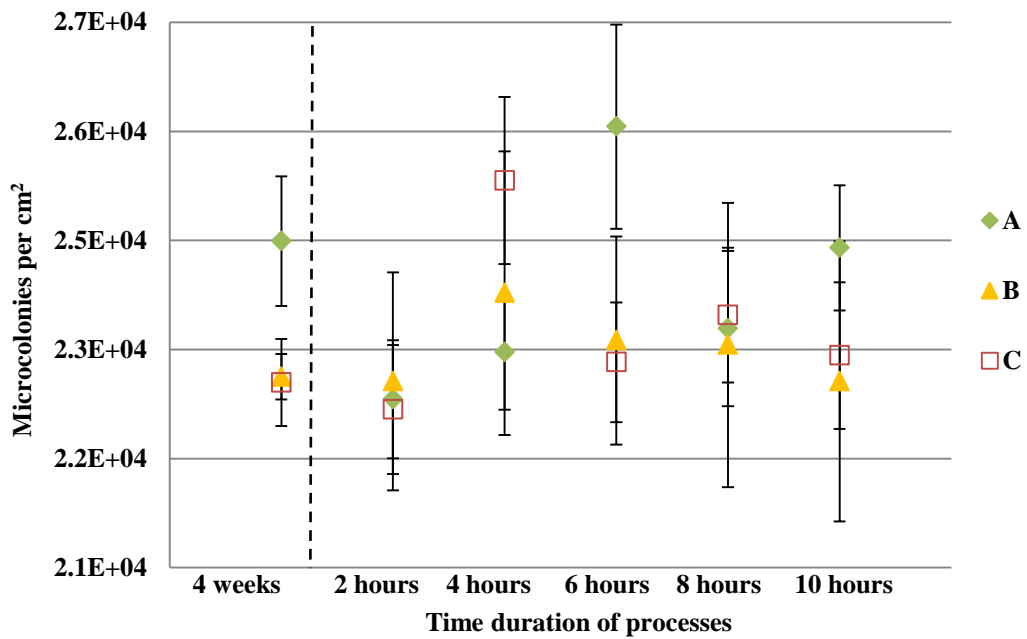


Figure 3-5 Concentration of microcolonies on the reactor surfaces in the development and formation processes.

The dashed line indicates the move from the development to the formation process. “A” describes turbulent flow, “B” describes transition flow and “C” describes laminar flow. The error bars represent the standard deviation of the measurements.

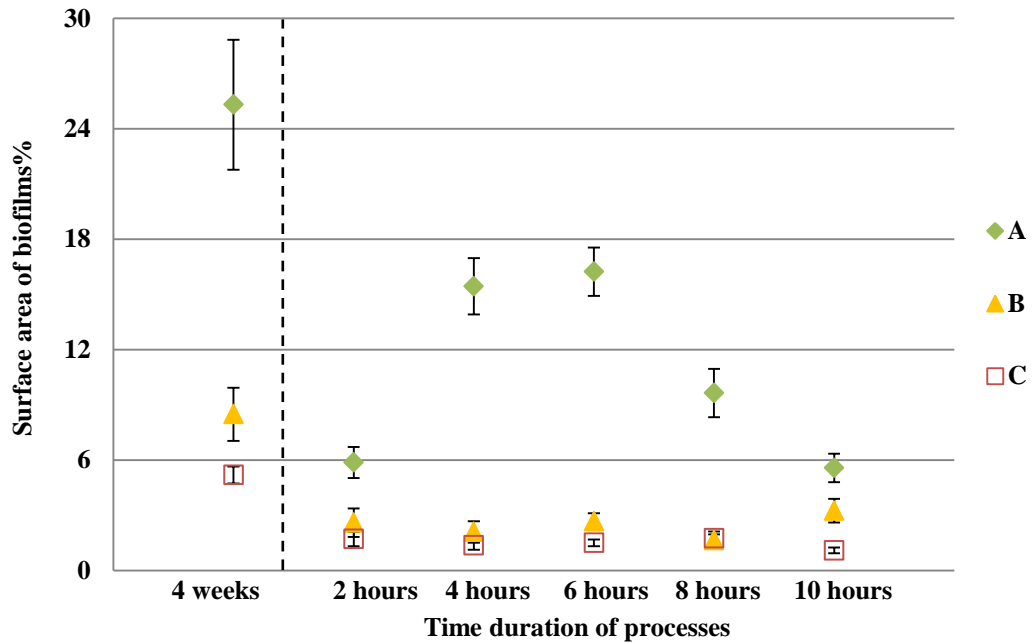


Figure 3-6 Percentage of surface area of biofilms in the development and formation processes.

The dashed line indicates the move from the development to the formation process. “A” describes turbulent flow, “B” describes transition flow and “C” describes laminar flow. The error bars represent the standard deviation of the measurements.

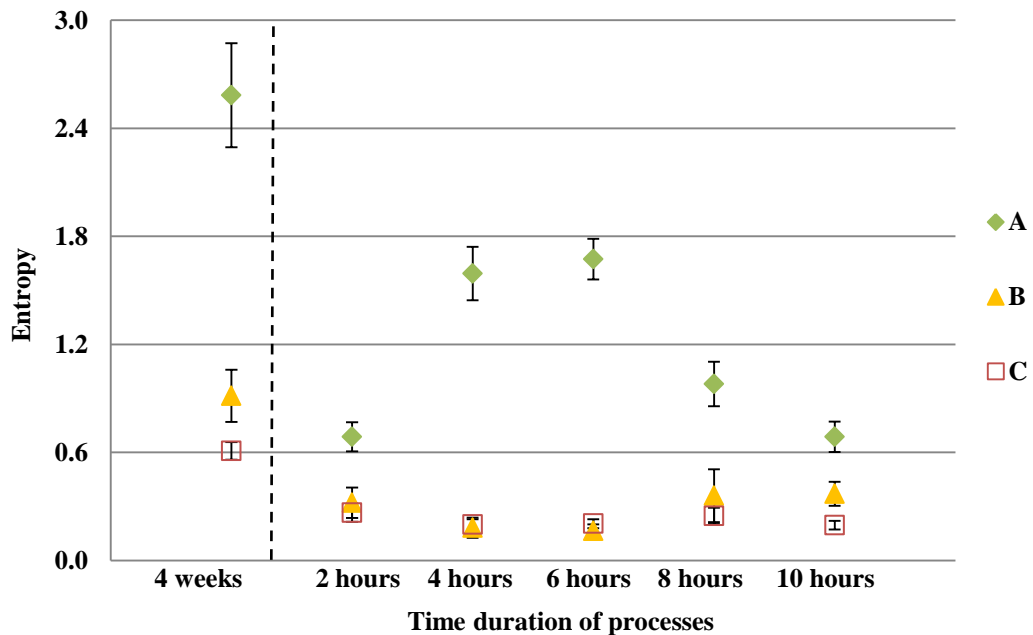


Figure 3-7 Entropy of biofilms in the development and formation processes.

The dashed line indicates the move from the development to the formation process. “A” describes turbulent flow, “B” describes transition flow and “C” describes laminar flow. The error bars represent the standard deviation of the measurements.

These measurements proved our hypothesis correct that turbulent flow was the one to enhance the development of biofilms more than the rest two flow regimes. With the increase in shear stress associated with faster flows one might

have expected biofilms to be smoother in the turbulent regime; where the biofilm protrudes into the flow the high stress could potentially shear off pieces of the biofilm eroding any “lumps” on the surface. However, this did not appear to be the case. The measure of roughness here was the entropy and the entropy of biofilms was greatest in the turbulent regime. The increased number of microcolonies attached on the reactor slides and the increased growth of biofilms on the surfaces might mean that in turbulent flow more microcolonies actually come from the bulk liquid and land on the surfaces.

3.3.2 Formation process

The surface area of biofilms (Figure 3-4) and the entropy of biofilms (Figure 3-5) were found to be significantly higher ($P < 0.05$) in turbulent flow compared to the rest two flow regimes in the formation process. Again, no significant differences for these measures were found between the transition and laminar flow. Also, the surface area of EPS (Figure 3-6) was found to be significantly higher ($P < 0.05$) in turbulent flow compared to transition and laminar flow in the formation process. Again, no significant differences were found in the surface area of EPS between the transition and laminar flow.

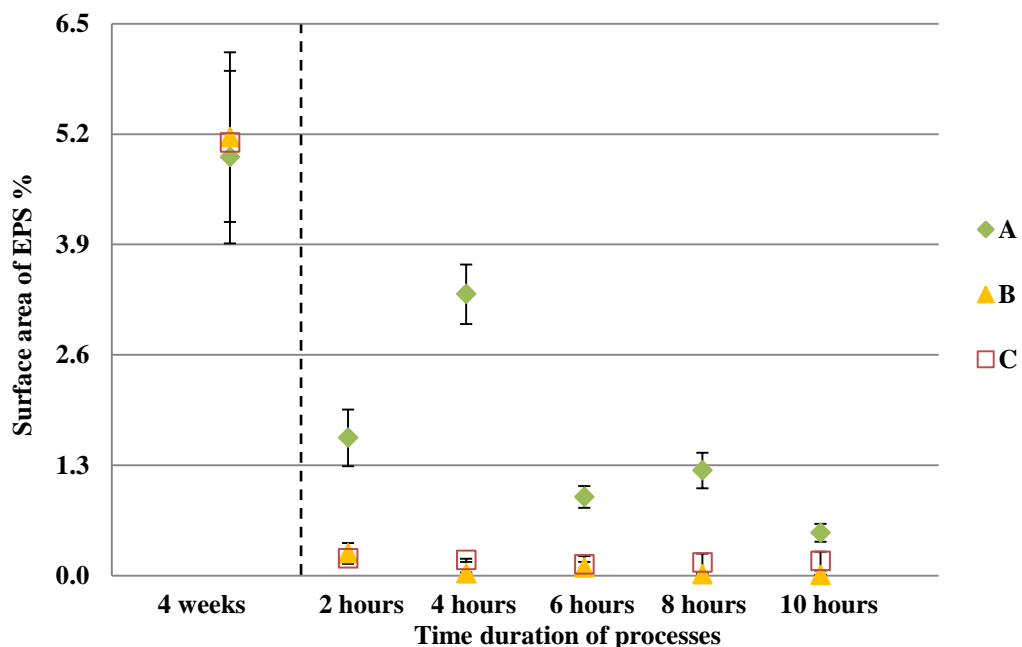


Figure 3-8 Percentage of surface area of EPS in the development and formation processes. The dashed line indicates the move from the development to the formation process. “A” describes turbulent flow, “B” describes transition flow and “C” describes laminar flow. The error bars represent the standard deviation of the measurements.

It was shown that in turbulent flow the entropy and surface area of biofilms peaked at 6 hours, and the surface area of EPS peaked at 4 hours. So, again turbulence was found to be critical in shaping the structure of the biofilm with area and roughness being consistently higher than in the other flow regimes. The peak found in those measures might show that in the early stage of formation, microcolonies that were already rich in EPS were deposited on the slides. As the deposits grew the surface area of biofilms increased and so did the entropy. With increased roughness and surface area of biofilms came increased and more heterogeneous shear stresses and thus, erosion served to decrease both the entropy and the surface area of biofilms and subsequently that of EPS over the latter part of the 10-hour formation period. These changes in the structure of biofilms for the different time periods of the formation process were significant only in turbulent flow. For the entropy and the surface area of biofilms, significant differences ($P < 0.05$) were found between 2-4, 2-6, 2-8, 4-8, 4-10, 6-8, 6-10 and 8-10 hours. Finally, for the surface area of EPS, significant differences ($P < 0.05$) were found between 2-4, 2-10, 4-6, 4-8 and 4-10 hours.

3.3.3 Changes of flow regime process

When the flow went through discrete changes in the flow regime, significant differences ($P < 0.05$) were found in the surface area of biofilms between the different flow regimes in each of the 3 experiments (Figure 3-7). Also, significant differences ($P < 0.05$) were found in the surface area of EPS between the different flow regimes in each of the 3 experiments (Figure 3-8).

From the development process, which lasted 4 weeks, it was clear that the coverage of biofilms was increased with the flow speed. Also, when the bulk water was conditioned by the presence of biofilms, it was found that in the formation process the coverage of EPS was increased with the flow speed. It was shown from Figure 3-7 and Figure 3-8 that where rapid changes in the flow regime were applied even over a 24-hour period, biofilms covered more surface area and produced more EPS as the flow speed was increased. Consequently, it was shown that biofilms that were grown under a constant flow regime in the development process responded finally to the 24-hour changes to shear stress by converging to the characteristic morphology they had developed when that flow

regime was constant for the long time period of 4 weeks (see Appendix 10.1.2 for the measures for which no significant differences were found).

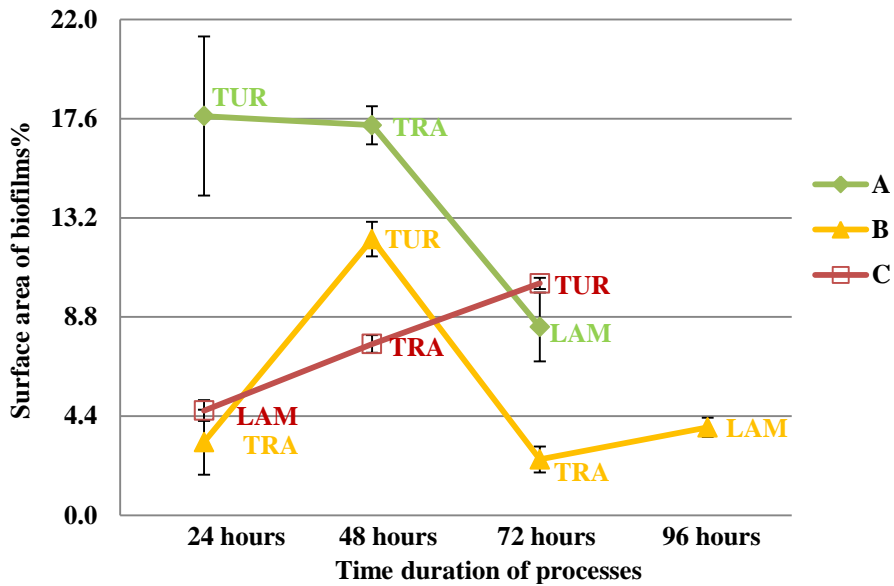


Figure 3-9 Percentage of surface area of biofilms in the changes of flow regime process. “TUR” describes the turbulent flow regime, “TRA” describes the transition flow regime and “LAM” describes the laminar flow regime in all three experiments (A, B & C). The error bars represent the standard deviation of the measurements.

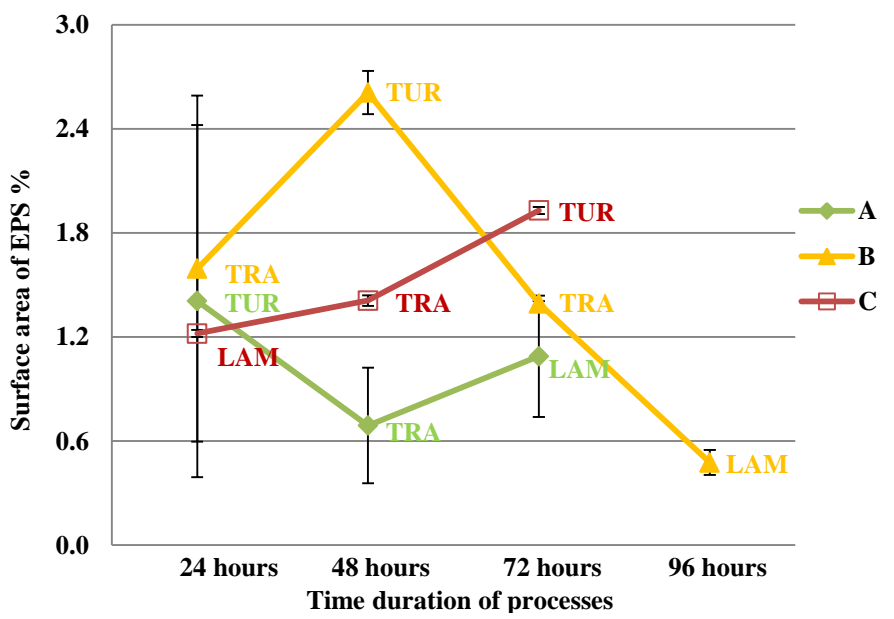


Figure 3-10 Percentage of surface area of EPS in the changes of flow regime process. “TUR” describes the turbulent flow regime, “TRA” describes the transition flow regime and “LAM” describes the laminar flow regime in all three experiments (A, B & C). The error bars represent the standard deviation of the measurements.

3.3.4 Biofilm structures

Biofilms were found to form either patchy (Figure 3-9a) structures in turbulent flow (experiment A) or linear structures consisting of strands or streamers, possibly of EPS, with which the bacteria were associated (Figure 3-9b) in transition (experiment B) and laminar flow (experiment C), as revealed by phase contrast microscopy. Biofilms were also stained in order to reveal the cells and EPS of their structures with fluorescence microscopy using DAPI and Fluorescein *Aleuria aurantia* lectin, respectively (experiment A) (Figure 3-9c). The hazy part in Figure 3-9c is probably the rest DNA of the sample, which occurred due to diffuse staining of the sample.

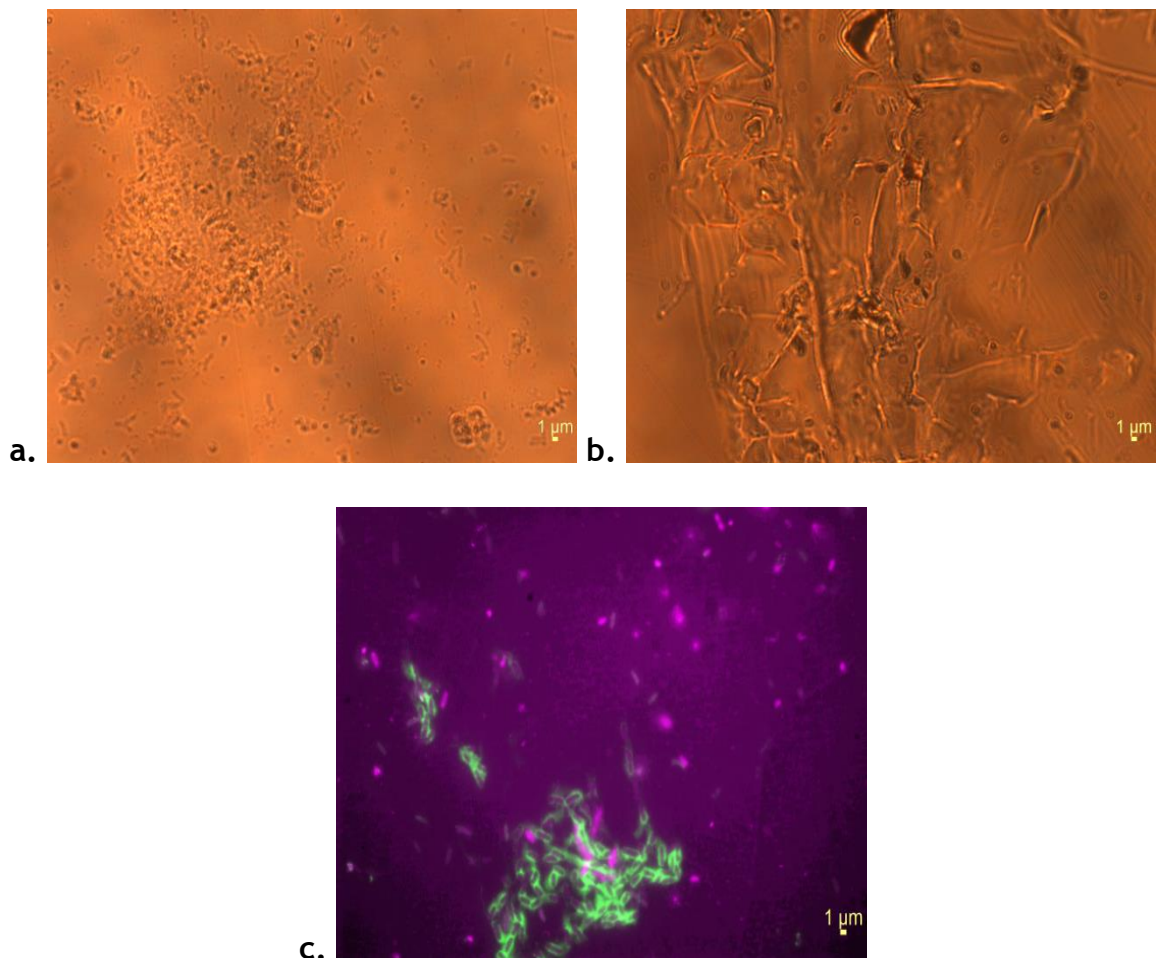


Figure 3-11 Biofilm structures as revealed by microscopy using the 100X objective lens. (a) Patchy structures in turbulent flow, (b) linear structures in transition and laminar flow revealed by phase-contrast microscopy, and (c) stained cells (rods of purple colour) and stained EPS (green colour) structures revealed by fluorescence microscopy in turbulent flow. The bar which appears at the right bottom of the images indicates 1 μm distance.

3.3.5 Semi-variograms

The semi-variograms of the development process for all 3 experiments are here demonstrated (Figure 3-10). The highest variance, represented by the sill of the semi-variograms, was found in turbulent flow and it was reached at about 60 micrometres. This suggests that there was a low degree of correlation between distant points on the biofilm surface topography, which is in agreement with the previous indication from the entropy measurements that the biofilm under turbulent flow conditions was the most heterogeneous.

The gradient in the variance close to the origin (nugget effect) was the highest in turbulent flow. This shows that the topography of the biofilm was the most heterogeneous in turbulent flow. Specifically, the gradient in variance dropped after about 20 micrometres, which shows that there was a prevalence of topographic structures with a characteristic radius (or length scale) of approximately 20 micrometres. For the laminar and transition flows, the heterogeneity in the topography was much lower and there was a shallow linear gradient on the semi-variograms. This indicates a smoother surface potentially with features that extended over longer length scales than in the turbulent regime.

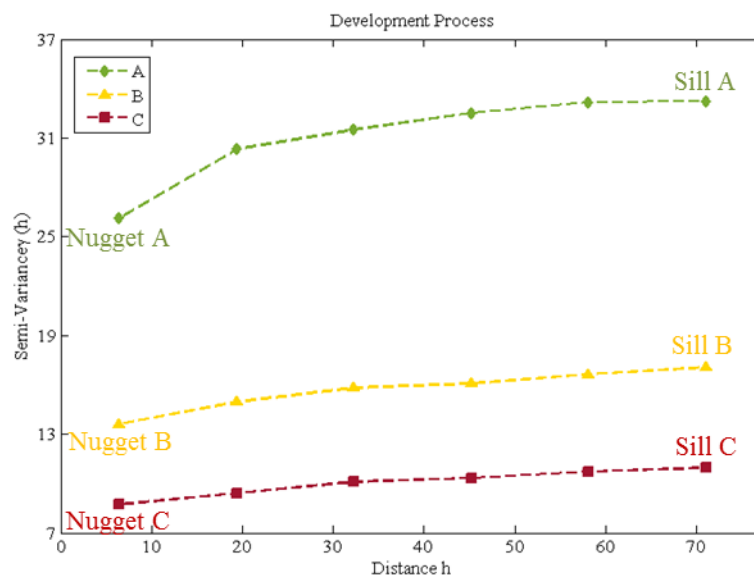


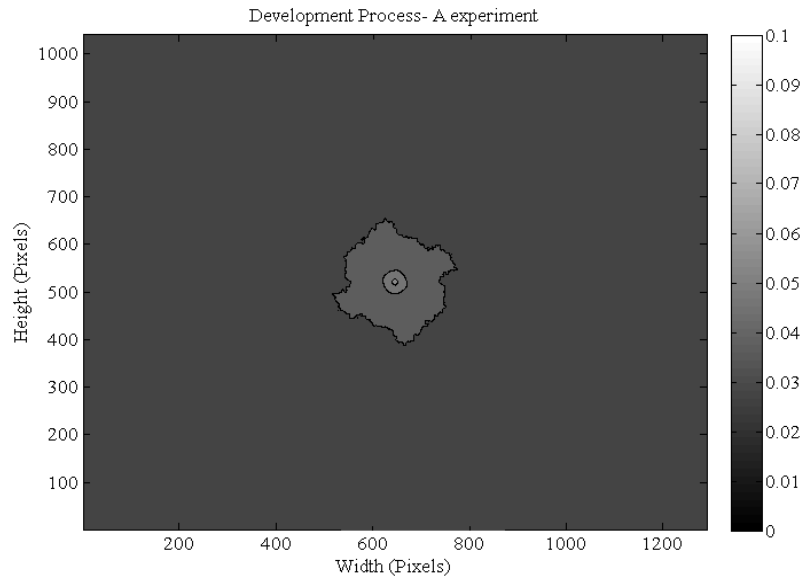
Figure 3-12 Semi-variograms in the biofilm development process. In the vertical axis is the semi-variance and in the horizontal axis is the distance for the calculation of the semi-variogram in micrometres. “A” describes turbulent flow, “B” describes transition flow and “C” describes laminar flow.

For the formation and changes of flow regimes processes, the data are changing rapidly so the semi-variograms are less informative since the overall variance fluctuated between time points in a way that made it difficult to draw any further conclusions; nonetheless they are displayed in the Appendix 10.1.3. The semi-variograms in the formation and changes of flow regimes processes indicate broadly similar patterns with those in the development process. The biofilm irregularity was the highest in the development process, after biofilms were established on the reactor surfaces for 4 weeks, as the variance was found to be higher in the development process than in the other two processes.

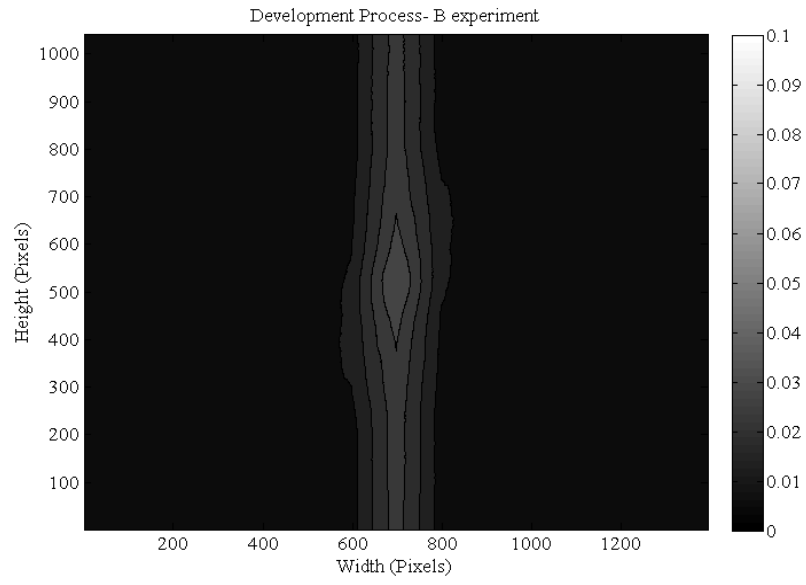
3.3.6 Autocorrelation function diagrams

The ACF diagrams of the development process for all 3 experiments are here demonstrated (Figure 3-11). In Figure 3-11a radially symmetric (circular) contours in autocorrelation are presented for turbulent flow conditions. This diagram is not suggesting that there is one spatially-correlated “lump” at the centre of the image. It is the average autocorrelation for all pixels on the image. It demonstrates that on-average pixels are spatially correlated with their neighbours and this diminishes at about 100 pixels, which corresponds to approximately 10 micrometres. It suggests that radially symmetrical lumps are the prevalent topographical feature, which could be associated with microcolonies.

In transition (Figure 3-11b) and laminar flow (Figure 3-11c) there is a much higher degree of correlation at the direction perpendicular to the flow direction than along the flow direction. This indicates that the biofilm is arranged in linear structures that run perpendicular to the direction of flow. There does not seem to be any strong morphological feature at the centre of the contour plots rather than linear features that are spaced consistently across the surface. If there was such a strong morphological structure in the ACF diagram, the diagram would have exhibited bands of higher correlation running both parallel and either side of that main structure. Finally, the highest degree of autocorrelation was found in turbulent flow, which suggests that in turbulent flow the biofilms consisted of cells that were piled up rather than dispersed as in the other two flow conditions.



a.



b.

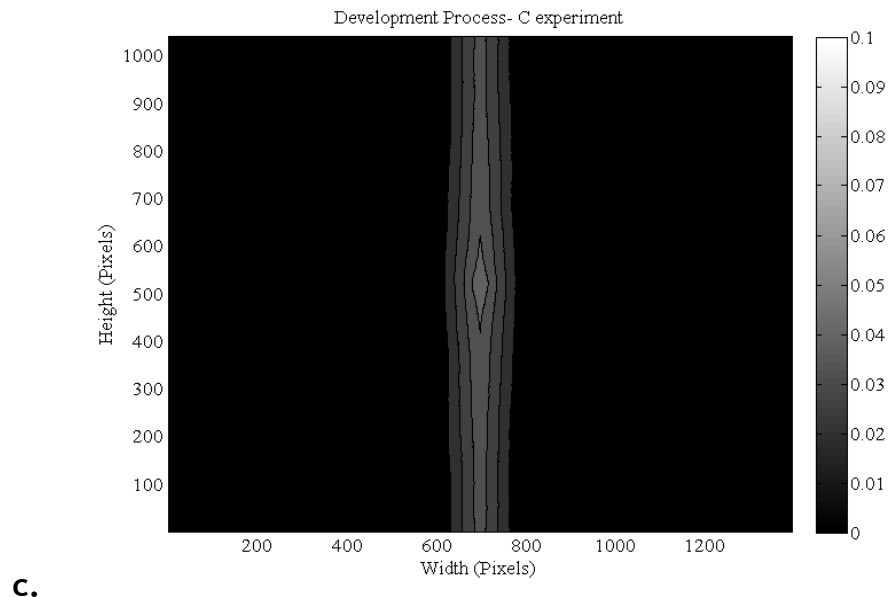


Figure 3-13 Autocorrelation function diagrams in the development process. (a) In A experiment, (b) in B experiment and (c) C experiment. “A” describes turbulent flow, “B” describes transition flow and “C” describes laminar flow. The size in pixels of the contour plots is the same as of the original images based on which they were produced.

The ACF diagrams are most useful in determining the structures that have been established over the development phase, rather than the rapidly changing formation or changes of flow regime processes of the 3 experiments. In both these processes, the only spatial structure identified for all 3 experiments was that of microcolonies. Again, the autocorrelation of biofilm structures was the highest in turbulent flow. These results only marginally strengthen the arguments made here and so, they have been demoted to the Appendix 10.1.4. The ACF diagrams in Figure 10-10 of the Appendix 10.1.4 for the formation process, in which the autocorrelation appears to decrease from 2 to 6 hours, present an inverse relationship of what was expected from figures in 3.3.2, in which the surface area of biofilms and the entropy of biofilms present a peak at the 6-hour time point. This might be explained by the fact that ACF diagrams are less informative in the formation process where data are changing rapidly with time. This is the reason they can only be used as an indication of the structure of the main feature in the original microscope image rather than as a comparison of the autocorrelation between the different short time periods from 2 to 10 hours based on the bar in the ACF diagram.

3.3.7 Batch versus recirculation mode

Biofilms were studied for 4 weeks (development process) and for 10 hours (formation process) while the reactor was operating under batch mode, which is not a typical condition for DWDS. The reason to do that was to emphasise the important differences that can be detected in biofilms under the different flow regimes in a closed well controlled system. By the comparison between the batch mode at the end of 4 weeks of the development process and the recirculation mode at the end of the first 24 hours of the changes of flow regimes process of each experiment, it was found that the surface area of biofilms, and the one of EPS were significantly higher ($P < 0.05$) in batch mode than in recirculation mode.

These differences might be explained by the fact that the surface area of the system was larger in the recirculation than in the batch mode. In the recirculation mode of flow, the system consisted not only of the reactor as in the batch mode, but also of the inlet and outlet polycarbonate pipes used to recycle the medium and the bottle in which the recycled medium was placed into. This means that biofilms could either be dispersed within the recycled medium or be attached to the additional surface area of the pipes. However, this was an unexpected result since the initial motivation to change the mode of flow in the changes of flow regime process was to favour the growth of biofilms with the extra recycled medium and the potential better recirculation of nutrients within the reactor.

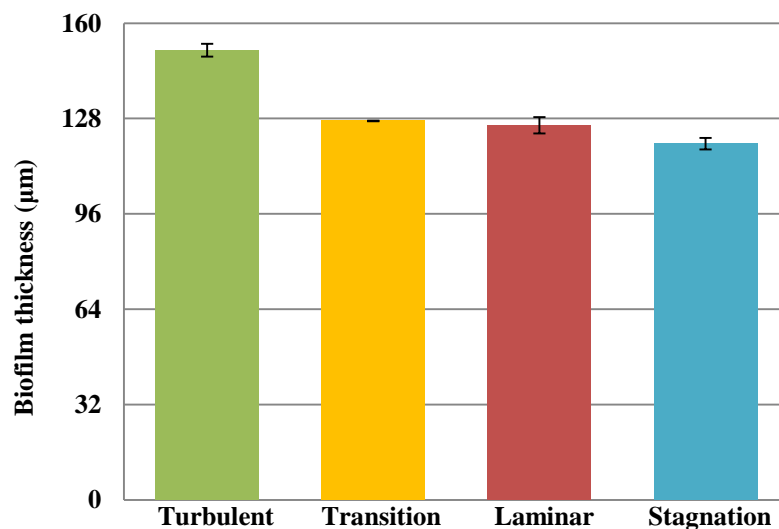
3.3.8 Stagnant conditions

Stagnant conditions occur regularly in drinking water systems (i.e. during overnight periods or near closed valves and flanges) when the water consumption is low and little is known about biofilm growth under such conditions (Wingender and Flemming, 2004, Manuel et al., 2007, Chen et al., 2013, Liu et al., 2016). It is suspected that the biofilm growth characteristics would be similar to those in laminar flow, where shear stresses are low and the transport of nutrients and oxygen is driven by diffusion. Here, it was studied whether biofilms grown under stagnant conditions have the same characteristics as those grown in flowing water. Given that the bacteria are not transported

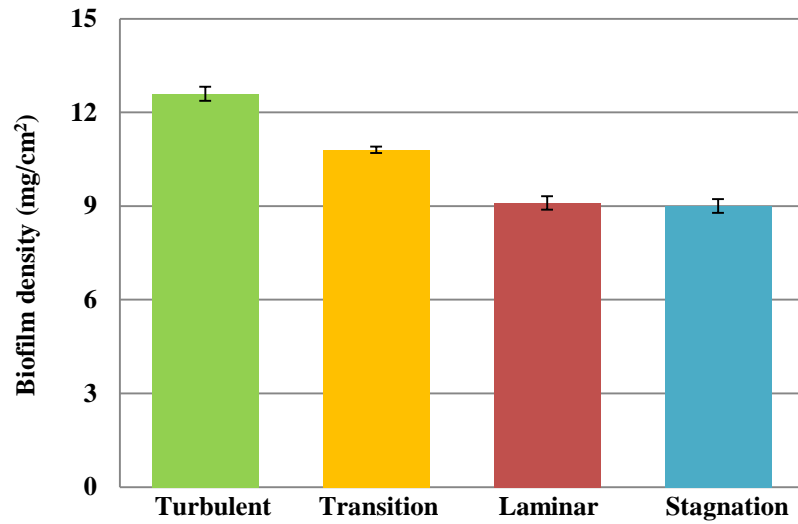
onto surfaces by flowing water, then one might expect gravity to have an effect; thus, the vertical slides of reactor to be less prone to cell colonisation.

Biofilms were grown here for 4 weeks under stagnant conditions; all the other environmental (and media) conditions were the same as those used in the flowing conditions in the development process. After 4 weeks, the slides of the reactor were weighed in their wet and dry state in order to characterise the biofilms developed on their surface in terms of thickness and density, as it was described in Section 3.2.4. Also, the coverage of biofilms was determined as described in Section 3.2.6. Finally, the spatial entropy of biofilms was determined as described in Section 3.2.8.

The biofilm thickness and density (Figure 3-12), the surface area of biofilms (Figure 3-13) and finally, the entropy of biofilms (Figure 3-14) under stagnant conditions were compared to those under flow conditions. It is clear that biofilms were found to be the thickest and densest (Figure 3-12), the most extensive (Figure 3-13) and heterogeneous (Figure 3-14) in turbulent flow compared to all other studied conditions. This agrees with a previous study in which it was shown that biofilms in drinking water were grown less under stagnant than flow conditions (Manuel et al., 2007). By this comparison it was also indicated that the biofilm growth was similar for the lower shear stress conditions and stagnant conditions.



a.



b.

Figure 3-14 Biofilm thickness and density for both stagnant and flow conditions after 4 weeks of biofilm growth.
(a) Biofilm thickness and (b) biofilm density. The error bars represent the standard deviation of the measurements.

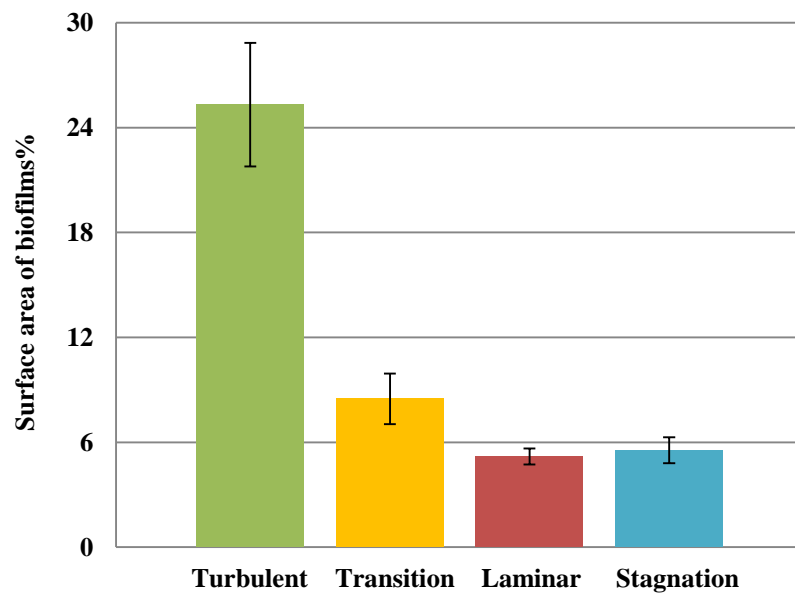


Figure 3-15 Percentage of surface area of biofilms for both stagnant and flow conditions after 4 weeks of biofilm growth.
 The error bars represent the standard deviation of the measurements.

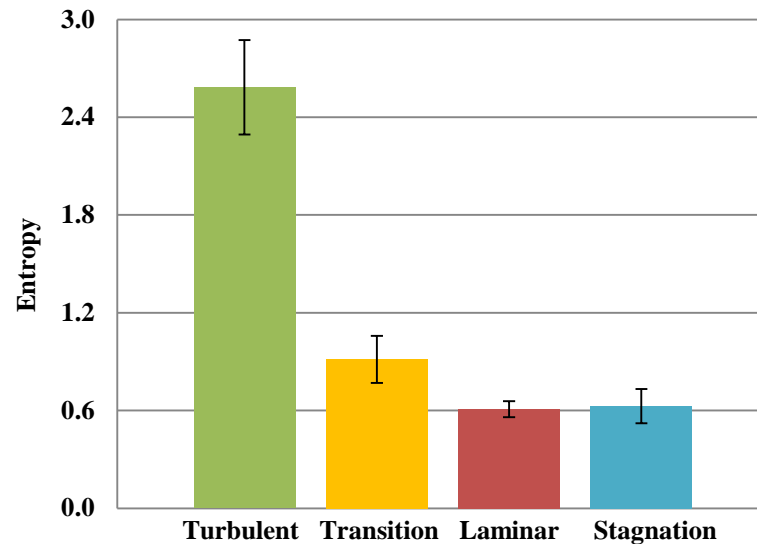


Figure 3-16 Entropy of biofilms for both stagnant and flow conditions after 4 weeks of biofilm growth.

The error bars represent the standard deviation of the measurements.

3.4 Conclusions

A rotating annular reactor allowed us to grow biofilms in drinking water under three distinct flow regimes: turbulent, transition and laminar, and under stagnant conditions, which are all conditions that occur in real DWDS as described in Section 3.1. Understanding the impact of the flow regime on biofilms may be helpful in providing an insight on the functionality and mechanisms of biofilms during the early (hours) and moderate (weeks) stages of their life. This study will help in the consideration of future design of management strategies to control the flow conditions in real drinking water systems. Managing the flow, and especially changes in flow regime, by manipulating flow rate and shear stress, will help in managing the density of microorganisms that finally appear at the tap. To effectively control biofilms by different strategies (i.e. process conditions and disinfection) it is essential to understand how they form and develop and the role that the flow conditions play. Our experiments suggest that:

- i. Denser and thicker, more extensive and heterogenous biofilms were found in turbulent flow than in the other two flow regimes and stagnant conditions after 4 weeks of growth. Biofilm structures were found to be the most irregular in turbulent flow where colonisation of microcolonies was the most evident.

ii. The extent and heterogeneity of biofilms that colonised the clean surfaces of reactor after only 10 hours were the greatest in turbulent flow. Turbulence was also found to enhance the formation of EPS on the exposed surfaces of reactor.

iii. When already established biofilms developed over 4 weeks were exposed to 24-hour changes of flow regime, they were found to respond to these changes as significant differences were detected in the surface area they covered, and in the surface area of EPS under the different short flow regimes.

From the conclusions of this study it is clear that the control of flow conditions is very important for DWDS as it was indicated that in turbulent flow, which mainly occurs in these systems, biofilms form and develop to the highest extent. Thus, it is essential that we found a way to carefully control turbulent flow (perhaps by reducing the shear stresses) in parts of DWDS if we are to control or even prevent biofilm formation.

4 The role of *Methylobacterium* in aggregation in drinking water

4.1 Introduction

The formation of biofilms on the pipe walls is controlled by physical, biological and chemical processes (Jefferson, 2004). One important biological process is bacterial aggregation, where microorganisms interact with each other forming a cluster that is free-floating and can be attached to a substratum as part-of or a precursor-to a biofilm (Karunakaran et al., 2011). This adhesion mechanism has been suggested to influence the formation of complex multi-species biofilms in several diverse habitats (Rickard et al., 2003). Aggregation conveys many advantages to microorganisms in drinking water systems, such as enhanced transfer of chemical signals, exchange of genetic information, protection against harsh conditions and metabolic cooperation (Simões et al., 2008).

Most drinking water bacteria are nonculturable. More specifically, there are about 99.9% of nonculturable bacteria in drinking water and adjoining biofilms. However, members of one species may coexist in the same ecosystem in different physiological states, one being culturable on standard media, whereas the other phenotype is nonculturable but metabolically active (Roszak et al., 1984, Roszak and Colwell, 1987, Byrd et al., 1991, McDougald et al., 1998, Szewzyk et al., 2000). It has been well documented for pathogens like *Salmonella enteritidis*, *Vibrio cholera* and *Vibrio vulnificus* that bacteria may quickly enter a nonculturable state upon exposure to freshwater (Roszak et al., 1984, Oliver et al., 1991, Amann et al., 1995). Other bacteria that are in viable but nonculturable state are *Legionella pneumophila*, *Escherichia*, *Campylobacter* and *Shigella* (Xu et al., 1982, Colwell et al., 1985, Rollins and Colwell, 1986, Byrd et al., 1991). The determination of cell numbers by direct microscopic methods, which avoid growth-dependent steps, can result in values 100- to 10000-fold higher than the results from heterotrophic plate count assays. Other commonly used techniques to study microorganisms in DWDS, which are culture independent, are fingerprinting and high-throughput sequencing techniques. These molecular methods replace the culture-dependent techniques and they are implemented by water companies to detect pathogens in drinking water

(Douterelo et al., 2014a). From sequencing studies of bulk drinking water samples in full-scale DWDS it was found that Proteobacteria, particularly Alpha- and Beta-Proteobacteria, dominate drinking water bacterial communities irrespective of origin of study and presence/absence of or disinfectant residual type (Bautista-de los Santos et al., 2016b).

Culture-dependent methods are useful for monitoring drinking water quality for faecal contamination providing water utilities with data at a reasonable cost, even though they provide limited information about the total cell counts (lower than 1% of the total bacterial diversity) (Douterelo et al., 2014a). Among culturable bacteria, the most commonly found genera in drinking water are *Pseudomonas* (Martiny et al., 2003, Emtiazi et al., 2004, Williams et al., 2004, Simoes et al., 2007a, Soge et al., 2009, Kormas et al., 2010, Sekar et al., 2012), *Sphingomonas* (Martiny et al., 2003, Williams et al., 2004, Simoes et al., 2007a, Simões et al., 2007, Simões et al., 2008, Kormas et al., 2010), *Methylobacterium* (Williams et al., 2004, Simoes et al., 2007a, Simões et al., 2007, Simões et al., 2008, Kormas et al., 2010), *Aeromonas* (Scoaris et al., 2008, Kormas et al., 2010), *Acinetobacter* (Simoes et al., 2007a, Kormas et al., 2010, Sekar et al., 2012) and *Bacillus* (Olson and Nagy, 1984). A small number of species, such as *Methylobacterium* species (Simões et al., 2007), *Acinetobacter calcoaceticus* (Simões et al., 2008), *Mycobacterium* species (Rickard et al., 2004, Simões et al., 2007), have been implicated in promoting aggregation in pure or simple mixed cultures.

Species of *Methylobacterium* are found in a wide variety of environments, such as soil, dust, freshwater, lake sediments, leaf surfaces, air, root nodules, rice grains and hospital environments (Lidstrom and Chistoserdova, 2002, Omer et al., 2004, Van Aken et al., 2004, Gallego et al., 2005b, Xu et al., 2014). They exhibit resistance to chlorination in drinking water, which might explain their prevalence in domestic water-associated environments such as DWDS, shower curtains and showerhead biofilms (Gallego et al., 2005c, Falkinham et al., 2016). They are classified as opportunistic pathogens in clinical settings, such as dental water lines, blood bank purification and urinary units, causing serious threat to ill patients (Korvick et al., 1989, Sanders et al., 2000). It has been shown that *Methylobacterium* species belong to the group of amoeba-resisting bacteria in

drinking water (Thomas et al., 2006) and that their presence at taps and showerheads inhibits the presence of *Mycobacterium* species, which are opportunistic pathogens in household, hospital plumbing and in instruments with water reservoirs (Falkinham et al., 2016).

In this study, it is hypothesised that the *Methylobacterium* strain DSMZ (Deutsche Sammlung von Mikroorganismen und Zellkulturen)18358 is capable of promoting aggregation not only in simple mixed-species cultures but also in complex mixed drinking water microbial communities. To test this hypothesis, this *Methylobacterium* strain was inoculated into a drinking water microbial community, obtained from a domestic tap in Glasgow (the same as the one in Section 3.2.2) at different relative abundances of 1, 10 and 20%. At this stage, flowing conditions were not considered in the study of aggregation. Rather aggregation was explored under stagnant and shaking conditions. However, aggregation, especially where no external physical forces are pushing the bacteria together, might rely on bacterial motility, which is an energy intensive process (Harshey, 2003). Thus, aggregation was explored under oligotrophic conditions that typify water distribution systems and conditions where extra energy, in the form of added glucose, was available.

4.2 Materials and Methods

4.2.1 *Methylobacterium* culture

The *Methylobacterium* strain DSM 18358 was chosen for experimental analysis in this study. This strain was previously isolated from a drinking water network in Seville (Gallego et al., 2005b). The culture received from DSMZ was first reactivated (WHO, 2004) (see Appendix 10.2.1 for the analytical culture revival protocol) and then, *Methylobacterium* was cultured in R2A agar plates at 28°C in the incubator for 72 hours (Gallego et al., 2005c). A colony, which was created by streaking on the agar plates (Thiel, 1999), was inoculated into 10 ml R2A medium (Simões et al., 2007), and incubated at 28°C at 150 rpm speed for 72 hours (Gallego et al., 2005c). The R2A is a low-nutrient medium, which has been used for viable bacterial count and isolation of bacteria from drinking water (see Appendix 10.2.2 for the composition of R2A medium) (Reasoner and Geldreich,

1985, Kalmbach et al., 1997, Sandle, 2004) like *Methylobacterium* (Hiraishi et al., 1995, Gallego et al., 2005a).

The optical density (OD) of the culture was monitored using the Infinite® m200 Pro automated micro-plate reader (Tecan Group Ltd., Männedorf, Switzerland). The 10 ml *Methylobacterium* culture was divided into 500 µl samples and placed in the micro-plate with 3 control samples of 500 µl containing only the R2A medium. The OD was monitored every 3 hours for 72 hours in total (Ramalingam, 2012). The process of monitoring the growth was repeated 3 times. The specific growth rate and doubling time were calculated from the OD readings during the exponential phase of growth in order to determine the growth characteristics of *Methylobacterium*, and were determined by:

$$\mu_* = \frac{\ln\left(\frac{N_2}{N_1}\right)}{t_2 - t_1}, \quad 4-1$$

$$DT = \frac{\ln(2)}{\mu_*} \quad 4-2$$

respectively, where μ_* is the specific growth rate (h^{-1}), N_1 and N_2 are the optical densities measured at the beginning and at the end of the exponential phase of growth, respectively, t_1 and t_2 are the beginning and the end of the exponential phase of growth, respectively (h), and DT is the doubling time (h). In this way, the *Methylobacterium* inoculum was prepared for the inoculation experiments.

To inoculate the *Methylobacterium* strain in drinking water at different relative abundances it was necessary to conduct cell count measurements of the pure culture at the exponential phase of growth. For these measurements, 3 samples of 5 ml of the pure culture were filtered through 47 mm Whatman® 0.2 µm membrane filters (Sigma-Aldrich, Irvine, UK) after they were fixed with 0.5 ml of 2% formaldehyde (Kepner and Pratt, 1994). The membrane filters were then covered with 1 ml of 0.1% Triton X-100 solution in order to evenly disperse the cells. The cells on the membrane filters were then stained with 1 ml of 10 µg/ml DAPI for 20 minutes in the dark and visualised using fluorescence microscopy (Olympus IX71, Japan, Asia) with the oil immersion UPlanFLN objective lens with 100X magnification/1.30 numerical aperture. The filter used was the DAPI filter

with excitation at 358 nm and emission at 461 nm. More than 30 images per membrane filter were obtained in order to calculate the concentration of cells. The concentration of cells was calculated from (Brunk et al., 1979):

$$\frac{\text{cells}}{\text{ml}} = \frac{\left(\frac{\sum x}{n} \pm s\right) A_{\text{memb}} d}{A_{\text{field}} V_{\text{filt}}} \quad 4-3$$

where all the parameters have been described in Section 3.2.5.

4.2.2 Drinking water culture

Drinking water was sampled from the domestic tap in Glasgow early in the morning after flushing the tap for 10 minutes. The density of bacteria in drinking water was low. It was determined at $(4.9 \pm 1.5) \times 10^5$ cells/ml as described in Section 4.2.1. To increase the density and, hopefully, the likelihood of seeing aggregation events, the samples were enriched with cells and this was achieved by adding glucose to drinking water. Bacterial growth was achieved through the inoculation of 5% glucose in 10 ml drinking water (Deighton and Balkau, 1990, Stepanovic et al., 2000). Liquid cultures were incubated at 28°C at 150 rpm for 72 hours, as with the *Methylobacterium* pure culture. In order to ensure that the drinking water cultures were successfully enriched with cells by the addition of glucose, the OD was monitored every 3 hours for 72 hours in total and then, the specific growth rate and doubling time were calculated (Simões et al., 2007) in the same way as with the *Methylobacterium* pure culture. Then, in order to conduct the inoculation experiments it was necessary to measure the cell concentration of the drinking water culture at the exponential phase of growth. This was measured using fluorescence microscopy as described in Section 4.2.1.

4.2.3 Inoculation of *Methylobacterium* into drinking water culture

The drinking water culture without the addition of *Methylobacterium* is described as “control” culture, and the drinking water cultures with the addition of *Methylobacterium* are described as “inoculated” cultures. For both control and inoculated cultures, drinking water cells were harvested from the enriched cell drinking water culture that was at the exponential phase of growth (so that the cells are active) by centrifugation for 20 minutes at 13,000 x g speed,

washed 3 times in 0.1 M of phosphate-buffered saline (PBS) (Simões et al., 2007), and re-suspended in 10 ml of drinking water, that was sampled again from the domestic tap in Glasgow. For the inoculated cultures, *Methylobacterium* cells were harvested from the pure *Methylobacterium* culture that was at the exponential phase of growth and re-suspended in the 10 ml of drinking water.

The relative abundances at which the *Methylobacterium* strain was inoculated into the drinking water were 1%, 10% and 20%. This was decided because for species that are rare, their relative abundances are within the range of 0.1% to 1% (Fuhrman, 2009). Thus, a relative abundance of a strain at 1% is considered to be a low abundance in a mixed population. Also, *Methylobacterium* species have been found to be present in drinking water in the United Kingdom (Douterelo et al., 2014b, Douterelo et al., 2014c) but they have not been found to be abundant in Glasgow tap water (Bautista-de Los Santos et al., 2016a); their relative abundance in Glasgow tap water was lower than 0.005% (personal communication with Bautista-de Los Santos).

4.2.4 Analysis of aggregates

Both control and inoculated cultures were placed in BRAND[®] culture tubes (Sigma-Aldrich, Irvine, UK) (see Appendix 10.2.3 for the image of the tubes) and incubated at 28°C, as this was the optimal growth temperature for *Methylobacterium* (Gallego et al., 2005c). After 24, 48 and 72 hours aggregation analysis was carried out (Ramalingam et al., 2013). Firstly, aggregation scores were recorded by visual observation of the different liquid cultures (Rickard et al., 2004). The cultures were homogenised in vortex for 10 seconds and then rolled gently for 30 seconds before determining the scores. Aggregates were found to have a yellowish colour and thus, they were discriminable in the water. They also had a rectangular-like shape of variable length and width and thus, it was quite easy to quantify them (see Appendix 10.2.3). For the visual aggregation assay the scoring criteria were as follows: 0 for no aggregates in suspension, 1 for small uniform aggregates in a turbid suspension, 2 for easily visible aggregates in a turbid suspension, 3 for clearly visible aggregates which settle, leaving a clear supernatant and finally 4 for large flocs of aggregates that settle almost instantaneously, leaving a clear supernatant.

The liquid cultures were then filtered on gridded membrane filters (cellulose nitrate filters of 0.2 μm pore size with 3 mm^2 squares, Sartorius, England, UK) (see Appendix 10.2.3 for the image of the membrane filters). The number of aggregates was determined visually on the membrane filters. The size of aggregates was measured as the product of the length and width of the aggregates on the membrane filters. From the number and size of aggregates, the surface area that the aggregates occupied on the membrane filters was calculated. For each of those measurements, triplicates of samples were used.

4.2.5 Statistical analysis

All statistics were performed in SPSS Statistics as described in Section 3.2.7. Four measures regarding the aggregation were tested using the Pearson's Chi-squared and Phi and Cramer's tests to see if there were significant differences in aggregation under four different conditions. The four measures were: 1. the size of aggregates on the membrane filters, 2. the number of aggregates on the membrane filters, 3. the surface area that aggregates occupied on the membrane filters, and 4. the aggregation scores of the different liquid cultures. The four conditions were: 1. the different inoculation conditions, 2. the oligotrophic versus the eutrophic conditions; conditions for cultures in which there was drinking water with 1% glucose are described as eutrophic and those in which there was no glucose addition to drinking water are described as oligotrophic, 3. the stagnant versus the shaking conditions at 150 rpm and 4. the time period of growth of the different liquid cultures at 24, 48 and 72 hours.

4.3 Results and Discussion

4.3.1 Growth of cultures

For the pure *Methylobacterium* culture, the specific growth rate was calculated at $0.17 \pm 0.02 \text{ h}^{-1}$ and the doubling time was calculated at $4.24 \pm 0.42 \text{ h}$ (Figure 4-1). The cell concentrations after 6, 10.5 and 15 hours of growth were found at $(1 \pm 0.3) \cdot 10^8$, $(3.2 \pm 0.8) \cdot 10^8$ and $(10 \pm 3) \cdot 10^8$ cells/ml, respectively.

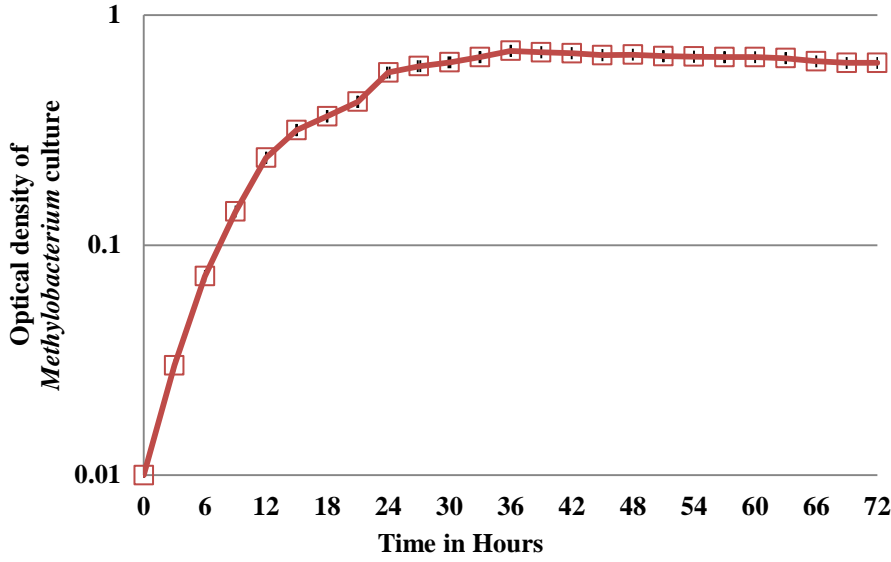


Figure 4-1 Growth curve of pure *Methylobacterium* culture. Growth curve of 1:50 dilution with OD values taken every 3 hours for 72 hours in total at 595 nm wavelength. The error bars represent the standard deviation of the measurements.

For the drinking water culture, the specific growth rate was calculated at $0.18 \pm 0.02 \text{ h}^{-1}$ and the doubling time at $3.96 \pm 0.40 \text{ h}$ (Figure 4-2). The cell concentration of the culture after 15, 19.5 and 24 hours of growth was at $(1.2 \pm 0.8) \times 10^8$, $(3.8 \pm 1.2) \times 10^8$ and $(9.2 \pm 0.6) \times 10^8$ cells/ml, respectively.

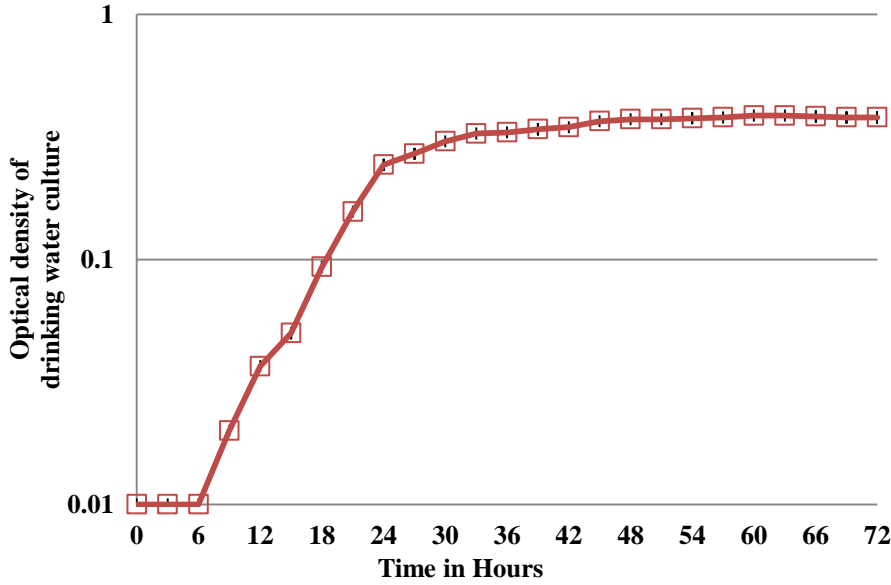


Figure 4-2 Growth curve of drinking water culture. Growth curve of 1:50 dilution with OD values taken every 3 hours for 72 hours in total at 595 nm wavelength. The error bars represent the standard deviation of the measurements.

The growth curves of the pure *Methylobacterium* culture and the complex drinking water culture are quite similar. One might suggest that this can mean

that the drinking water culture is not a complex culture and its growth curve is the outcome from a key species that might be present. For this reason, the growth curve of the drinking water culture was calculated not only in triplicates but several other times in duration of a year. The outcome was that all the times the growth curve was similar to the one in Figure 4-2. If the growth curve in Figure 4-2 was the outcome of a specific key species then during one whole year that the measurements were periodically taken, then the growth curve would have been changed due to the expected considerable differences in the microbial communities in drinking water with time.

The reason that the growth curves were calculated in this study was only to harvest the bacteria during the exponential phase of growth so that they are more active for our subsequent aggregation experiments. Mixed species cultures like the one of our case of drinking water sampled from the tap can still remain mixed cultures without any taxa outcompete in the culture after enrichment (Jackson et al., 1998, Gehring et al., 2012, Singla et al., 2014). In addition, the reason to create the enrichment drinking water culture was only to harvest the cells at the exponential phase of growth in order to introduce them to drinking water sampled from the tap, which is a mixed bacterial community, at the main aggregation experiments.

4.3.2 Aggregation in drinking water

The aggregation measures for the different liquid cultures are outlined in the following Tables. By the product of the size of aggregates (Table 4-1) and the number of aggregates (Table 4-2), the surface area that the aggregates occupied on membrane filters (Table 4-3) was determined. Finally, the aggregation scores of the different liquid cultures (Table 4-4) were recorded.

Size of aggregates (mm ²) (standard deviation)						
	Stagnant			Shaking		
Eutrophic	24 h	48 h	72 h	24 h	48 h	72 h
C	0 (-)	0 (-)	0 (-)	0 (-)	0 (-)	0 (-)
I/ 1% M.	0 (-)	30.1 (1.1)	30 (1.4)	4.1 (1.08)	4 (1.32)	46.8 (0.76)
I/ 10% M.	0 (-)	15.7 (1.15)	80.5 (1.52)	15.4 (1.4)	92 (1.04)	17.4 (1.43)
I/ 20% M.	0 (-)	32.1 (1.2)	28.6 (1.58)	19.6 (1.62)	24.9 (1.89)	10 (1.03)
Oligotrophic	24 h	48 h	72 h	24 h	48 h	72 h
C	0.2 (0.015)	0.3 (0.081)	0.1 (-)	0.3 (0.063)	0.1 (0.06)	0.1 (0.056)
I/ 1% M.	0.3 (0.026)	0.6 (0.048)	0.2 (-)	0.3 (0.073)	0.4 (0.05)	0.1 (-)
I/ 10% M.	0.7 (0.075)	1.8 (0.055)	0.7 (0.061)	0.4 (0.056)	0.1 (-)	0.2 (0.058)
I/ 20% M.	0.8 (0.005)	1.7 (0.06)	0.4 (0.013)	0.8 (0.009)	1.7 (0.65)	1.1 (-)

Table 4-1 Size of aggregates (mm²) of the different liquid cultures at 24, 48 and 72 hours. "M" refers to *Methylobacterium*, "C" refers to control, and "I" refers to inoculated drinking water cultures.

Number of aggregates (standard deviation)						
	Stagnant			Shaking		
Eutrophic	24 h	48 h	72 h	24 h	48 h	72 h
C	0 (-)	0 (-)	0 (-)	0 (-)	0 (-)	0 (-)
I/ 1% M.	0 (-)	3 (0.816)	2 (0.816)	25 (0.816)	3 (0.816)	3 (0.816)
I/ 10% M.	0 (-)	6 (0.816)	1 (-)	7 (-)	3 (0.816)	22 (-)
I/ 20% M.	0 (-)	3 (-)	3 (-)	15 (-)	13 (-)	2 (-)
Oligotrophic	24 h	48 h	72 h	24 h	48 h	72 h
C	1 (-)	5 (-)	1 (-)	3 (-)	13 (0.816)	5 (0.816)
I/ 1% M.	4 (-)	6 (-)	2 (-)	4 (-)	21 (-)	7 (-)
I/ 10% M.	7 (-)	5 (0.816)	2 (-)	3 (-)	13 (-)	9 (0.816)
I/ 20% M.	7 (0.816)	9 (0.816)	5 (0.816)	7 (0.816)	10 (0.816)	5 (-)

Table 4-2 Number of aggregates of the different liquid cultures at 24, 48 and 72 hours. "M" refers to *Methylobacterium*, "C" refers to control, and "I" refers to inoculated drinking water cultures.

Surface area of aggregates (mm ²) (standard deviation)						
	Stagnant			Shaking		
Eutrophic	24 h	48 h	72 h	24 h	48 h	72 h
C	0 (-)	0 (-)	0 (-)	0 (-)	0 (-)	0 (-)
I/ 1% M.	0 (-)	90.3 (24.7)	60 (24.6)	102.5 (27.2)	12 (5.24)	140.4 (38.2)
I/ 10% M.	0 (-)	94.2 (14.5)	80.5 (1.52)	107.8 (9.82)	276 (7.5)	382.8 (31.4)
I/ 20% M.	0 (-)	96.3 (3.61)	85.8 (4.74)	294 (24.3)	323.7 (24.5)	20 (2.06)
Oligotrophic	24 h	48 h	72 h	24 h	48 h	72 h
C	0.2 (0.015)	1.5 (0.405)	0.1 (-)	0.9 (0.189)	1.3 (0.785)	0.5 (0.295)
I/ 1% M.	1.2 (0.104)	3.6 (0.288)	0.4 (-)	1.2 (0.292)	8.4 (1.05)	0.7 (-)
I/ 10% M.	4.9 (0.525)	9 (1.49)	1.4 (0.122)	1.2 (0.168)	1.3 (-)	1.8 (0.548)
I/ 20% M.	5.6 (0.653)	15.3 (1.48)	2.0 (0.332)	5.6 (0.655)	17 (6.66)	5.5 (-)

Table 4-3 Surface area (mm²) that aggregates from the different liquid cultures occupied on membrane filters at 24, 48 and 72 hours.

“M” refers to *Methylobacterium*, “C” refers to control, and “I” refers to inoculated drinking water cultures.

Aggregation scores (standard deviation)						
	Stagnant			Shaking		
Eutrophic	24 h	48 h	72 h	24 h	48 h	72 h
C	1 (-)	2 (0.471)	2 (0.471)	1 (-)	2 (0.471)	2 (-)
I/ 1% M.	2 (-)	4 (-)	4 (-)	4 (-)	4 (-)	4 (-)
I/ 10% M.	3 (-)	4 (0.471)	4 (-)	4 (-)	4 (-)	4 (-)
I/ 20% M.	3 (0.471)	4 (-)	4 (-)	4 (-)	4 (-)	4 (0.471)
Oligotrophic	24 h	48 h	72 h	24 h	48 h	72 h
C	1 (-)	2 (-)	2 (-)	2 (-)	2 (-)	2 (-)
I/ 1% M.	2 (-)	3 (0.471)	3 (0.471)	2 (-)	3 (0.471)	3 (0.471)
I/ 10% M.	2 (-)	3 (0.471)	3 (-)	3 (0.471)	4 (-)	3 (-)
I/ 20% M.	3 (0.471)	4 (-)	4 (-)	4 (-)	4 (-)	4 (0.471)

Table 4-4 Aggregation scores of the different liquid cultures at 24, 48 and 72 hours. “M” refers to *Methylobacterium*, “C” refers to control, and “I” refers to inoculated drinking water cultures. Scoring criteria: 0 for no aggregates in suspension, 1 for small uniform aggregates in a turbid suspension, 2 for easily visible aggregates in a turbid suspension, 3 for clearly visible aggregates which settle, leaving a clear supernatant and 4 for large flocs of aggregates that settle almost instantaneously, leaving a clear supernatant.

The first critical question was, did the addition of the *Methylobacterium* at different concentrations influence the aggregation in the drinking water culture? It is clear that even without adding the *Methylobacterium*, aggregates were formed in the drinking water culture. However, when the *Methylobacterium* was added, the size of aggregates, the area of aggregates and the aggregation scores were found to be significantly higher ($P < 0.05$) in the inoculated cultures than in the control ones. Specifically, these differences were found for: 0%-1%, 0%-10%, 0%-20%, and 1%-20%. This showed that the most important inoculation concentration of the *Methylobacterium* for bacterial aggregation was the lowest one at 1%, as no significant differences in aggregation were found for the successive concentrations at 1%-10% and 10%-20%. These results make one speculate that this *Methylobacterium* strain must not be abundant in the drinking water from the Glasgow tap.

It is important to mention that this increase in the aggregation that was found in the drinking water culture when the *Methylobacterium* was inoculated into it

(from the first critical question) can be attributed to either autoaggregation of *Methylobacterium* or coaggregation of *Methylobacterium* with other drinking water bacteria. Had we have been interested in drawing that distinction on the specific type of aggregation then an additional control experiment would be required, where *Methylobacterium* is inoculated into autoclaved drinking water. However, we were merely interested in demonstrating that the *Methylobacterium* was a key strain in bacterial aggregation in drinking water.

Our results showed that aggregation occurred in a complex drinking water microbial community even under stagnant conditions. This might suggest that some form of chemotaxis occurs, perhaps quorum sensing, that causes the bacteria to move towards one another and then to adhere to one another. What is clear is that the process was enhanced by inoculating the *Methylobacterium* strain and it has been shown that the production of QS molecules is widespread amongst *Methylobacterium* species (Penalver et al., 2006, Poonguzhali et al., 2007, Ramalingam, 2012).

The second critical question was, did the addition of glucose in the liquid cultures influence the aggregation in drinking water? All measures were found to be significantly higher ($P < 0.05$) under the eutrophic than oligotrophic conditions. This showed that the addition of 1% glucose in drinking water enhanced bacterial aggregation. This might lead one to speculate that aggregation is an energy intensive process and that increasing the available energy increases cell motility, which speeds up aggregation; this is explored in Chapter 7. On the other hand, it may just reflect the fact that the glucose allows for more growth in the population. From our measurements on the concentration of cells of the different cultures (Table 4-5), conducted as it was described in Section 4.2.1, this was not the case. However, the relationship between sugars and aggregation is not necessarily straight forward; it was previously shown that the coaggregation ability of pairs of freshwater strains was inhibited by the presence of sugars (Rickard et al., 2000).

Cells/ml (*10 ⁸)						
	Stagnant			Shaking		
Eutrophic	24 h	48 h	72 h	24 h	48 h	72 h
C	1.1	1.3	1.4	1.2	1.2	1.3
I/ 1% M.	1.2	1.4	1.4	1.2	1.3	1.3
I/ 10% M.	1.3	1.4	1.5	1.3	1.3	1.4
I/ 20% M.	1.4	1.5	1.5	1.4	1.4	1.5
Oligotrophic	24 h	48 h	72 h	24 h	48 h	72 h
C	1.1	1.1	1.1	1.1	1.2	1.2
I/ 1% M.	1.1	1.2	1.2	1.2	1.2	1.3
I/ 10% M.	1.2	1.3	1.3	1.3	1.3	1.3
I/ 20% M.	1.3	1.3	1.4	1.3	1.4	1.4

Table 4-5 Cell concentrations in the bulk water of the different liquid cultures at 24, 48 and 72 hours.

“M” refers to *Methylobacterium*, “C” refers to control, and “I” refers to inoculated drinking water cultures.

The third critical question was, did the shaking or stagnant conditions influence the aggregation in the drinking water culture? It was unexpected that no significant differences were found in aggregation between the shaking and stagnant conditions. Shaking conditions have a number of effects on bacteria; they keep the particulates in suspension, break down any long-distance gradients in chemical concentration and hence, inhibit long-range bacterial chemotaxis, and increase the probability of bacteria colliding by chance (Lee et al., 2002, Son et al., 2015). Our result might suggest that the bacteria were sufficiently motile to gain little benefit from the random mixing and the increased proximity that shaking conditions afford. It might also suggest that short steep gradients in any chemical signals were more important in co-opting new bacteria into the aggregates.

The fourth question was, did the time period of growth influence the aggregation in the drinking water culture? There were again no significant differences in aggregation between the different time periods of growth at 24, 48 and 72 hours. This showed that the most important time period for the formation of aggregates was the first 24 hours. This suggested that the aggregation occurred relatively quickly and plateaued once it had occurred.

4.4 Conclusions

Aggregation in drinking water was studied for the *Methylobacterium* strain DSM 18358. The results from the experiments conducted suggested that the *Methylobacterium* actively formed aggregates in the drinking water culture rather than it being a passive mixing process. It was revealed that the *Methylobacterium*, inoculated at 1% relative abundance in the drinking water culture, was a key strain in aggregation in this experiment. Modest differences in aggregation were found for 1%-10% and 10%-20% inoculations. So, the behaviour of the *Methylobacterium* was qualitatively the same for all tested concentrations.

From the different environmental conditions tested, it was found that the addition of 1% glucose in drinking water significantly enhanced aggregation. This suggested that aggregation was an energy intensive process. No significant differences were found between the stagnant and shaking conditions, which suggested that the bacteria were sufficiently motile and that the short steep gradients in chemical signals were the important ones for the formation of aggregates. Finally, there were no significant differences in aggregation beyond 24 hours. This indicated that the *Methylobacterium* initiated the aggregation process and then played a less important role as time proceeded.

5 The role of *Methylobacterium* in aggregation in drinking water under two distinct flow regimes

5.1 Introduction

In Chapter 3 it was shown that differences in early biofilm formation in drinking water can be detected even over a limited time period of a few hours between three different flow regimes. Subsequently, in Chapter 4 it was shown that a *Methylobacterium* strain was able to enhance bacterial aggregation in drinking water. This leads naturally to the question addressed in this Chapter: does the flow regime influence the aggregation ability of the *Methylobacterium* in drinking water, and if it does, how this influences biofilm formation? Evidence from the freshwater environment has shown that at higher shear rates, higher number of autoaggregating bacteria (same species) was found (Rickard et al., 2004). Also, at intermediate shear rates it was shown that higher number of coaggregating bacteria (different species) occurred. This showed that autoaggregation interactions were stronger than coaggregation interactions at high shear rates. Within these autoaggregating and coaggregating bacteria there were species of *Methylobacterium* with a high visual aggregation score (Rickard et al., 2004).

It has been suggested that there is an 'on and off' switching of the coaggregation ability of bacteria in the freshwater environment and that could indicate some form of environmental control of this coaggregation process through starvation and stress (Rickard et al., 2000). If flow dependence with aggregation does exist in oligotrophic stressful conditions like that of complex mixed drinking water microbial communities then perhaps the interaction between the aggregation ability of the *Methylobacterium* and the flow regime is critical for biofilm formation.

The interaction between hydrodynamics and biofilm growth and morphology has received significant attention. Both modelling (Duddu et al., 2009, Barai et al., 2016) and experimental studies (Percival et al., 1999, Curran and Black, 2005, Garny et al., 2008) have revealed the important roles that, for example, shear-stress induced detachment of cells or increased oxygen transport to a biofilm in turbulent flow conditions play on the structure and growth of an established

biofilm. From engineering perspective, this does give some inkling of ways of managing the flow of water distribution system to control the sloughing of biofilm material into the bulk water that ultimately emerges at the tap. However, more attractive, but currently more elusive, solutions to the problems of biofilms in DWDS would involve intervention that prevents the biofilms ever forming on the pipe surfaces. The solutions could take many forms; novel pipe materials, chemical interventions, disruption of the cell biology, but all would share a common goal of disrupting the initial colonisation of surfaces; a process that may start with bacterial aggregation and for which there is little knowledge for complex mixes of bacteria in environments with different physicochemical conditions. In this study, the *Methylobacterium* strain DSM 18358 was inoculated into drinking water and aggregation was studied under two distinct flow regimes: the laminar and turbulent one.

5.2 Materials and Methods

5.2.1 Operating system

Bacterial aggregation in the bulk water of reactor was studied at 0, 24, 48 and 72 hours and the subsequent initial biofilm formation on the exposed surfaces was studied at 24, 48 and 72 hours in turbulent and laminar flows. The drinking water culture without addition of *Methylobacterium* is described as “control” culture, and the drinking water culture with the addition of *Methylobacterium* is described as “inoculated” culture, similarly to Chapter 4. The inoculated culture included *Methylobacterium* at 1% relative abundance in drinking water. This is a more realistic concentration for a strain in drinking water and it was found that there were modest differences in aggregation for 1%-10% and 10%-20% relative abundances, so the behaviour of *Methylobacterium* was qualitatively the same. Thus, the discernible effects that are described below are adequately demonstrated with the lowest inoculated level, 1%, of *Methylobacterium*.

As in the experiments described in 3.2.1, the same bioreactor was used in order to develop the turbulent and laminar flow conditions. The jacket maintained the temperature again at 16°C. The inner drum of the reactor was rotated again at 30 rpm, which corresponds to laminar flow and at 217 rpm, which corresponds to turbulent flow. The reactor was filled with only one litre of drinking water that

was sampled from a domestic tap in Glasgow (the same as the one in Section 3.2.2). Finally, the reactor was covered again with aluminium foil in order to achieve dark conditions for biofilm growth. In order to create the control and the inoculated drinking water cultures in the reactor, the same process described earlier in 4.2.3 was followed. The concentration of cells in the bulk water and on the reactor slides was determined using fluorescence microscopy (Olympus IX71, Japan, Asia) and was found to be $(5.1 \pm 2.3) \times 10^8$ cells/ml and $(5.3 \pm 2.2) \times 10^5$ cells/cm², respectively.

5.2.2 Analysis of samples

The concentration microcolonies in 5 ml liquid samples was determined by fluorescence microscopy using DAPI staining and the UPlanFLN objective lens with 10X magnification/0.30 numerical aperture (see Section 4.2.1 for the analytical process; the Triton solution is not used for the microcolonies measurements). Also, the number of aggregates from 10 ml liquid samples was determined directly by visual observation after the samples were filtered on cellulose nitrate filters of 0.2 µm pore size with 3 mm² squares (Sartorius, England, UK). Aggregates were found again to have a yellowish colour and a rectangular-like shape (see Appendix 10.2.3). Finally, 5 ml samples were filtered on 47 mm Whatman® 0.2 µm membrane filters (Sigma-Aldrich, Irvine, UK) and subsequently the percentage of surface area that biofilms from the bulk water covered on the membrane filters was calculated by fluorescence microscopy using the oil immersion UPlanFLN objective lens with 100X magnification/1.30 numerical aperture as described in Section 3.2.6. All measurements were performed in triplicates.

The number of microcolonies that were attached on the reactor slides was determined by fluorescence microscopy using the UPlanFLN objective lens with 10X magnification/0.30 numerical aperture as described in Section 3.2.5. Also, the number of aggregates on the reactor slides was determined directly by visual observation. Finally, the percentage of surface area that biofilms occupied on the reactor slides was calculated by fluorescence microscopy using the oil immersion UPlanFLN objective lens with 100X magnification/1.30 numerical aperture as described in Section 3.2.6. Again, all measurements were performed in triplicates.

5.2.3 Statistical analysis

The statistical analysis was conducted again in SPSS as described in Section 3.2.7. First goal was to determine for each flow regime whether there were significant differences between the control and inoculated culture regarding the number of microcolonies, the number of aggregates and the surface area of biofilms. It was also tested if there were significant differences in these measures between the laminar and turbulent flow. Finally, the effect of the different time periods of growth on those measures was studied.

To compare the measures between the control and inoculated culture the following tests were used. In turbulent flow, for the number of microcolonies in the bulk water, and the number of aggregates on the slides the Kruskal-Wallis test, and the one-way ANOVA test in conjunction with the Tukey's and Duncan-Waller's tests, respectively were used. In laminar flow, for both these measures the Pearson's Chi-squared and Phi and Cramer's tests were used. In turbulent flow, for the surface area of biofilms from the bulk water the one-way ANOVA test in conjunction with the Tukey's and Duncan-Waller's tests were used.

To compare the measures between the turbulent and laminar flow the following tests were used. To compare the microcolonies in the bulk water the Pearson's Chi-squared and Phi and Cramer's tests were used. Also, to compare the aggregates on the reactor slides, and the surface area of biofilms from the bulk water the one-way ANOVA test in conjunction with the Tukey's and Duncan-Waller's tests were followed.

Finally, to compare the measures between the different time periods the following tests were used. In laminar flow, the Pearson's Chi-squared and Phi and Cramer's tests were used. In turbulent flow, for the microcolonies in the bulk water, and the aggregates on the slides the Pearson's Chi-squared and Phi and Cramer's tests were used, and for the surface area of biofilms from the bulk water the Kruskal-Wallis test was used.

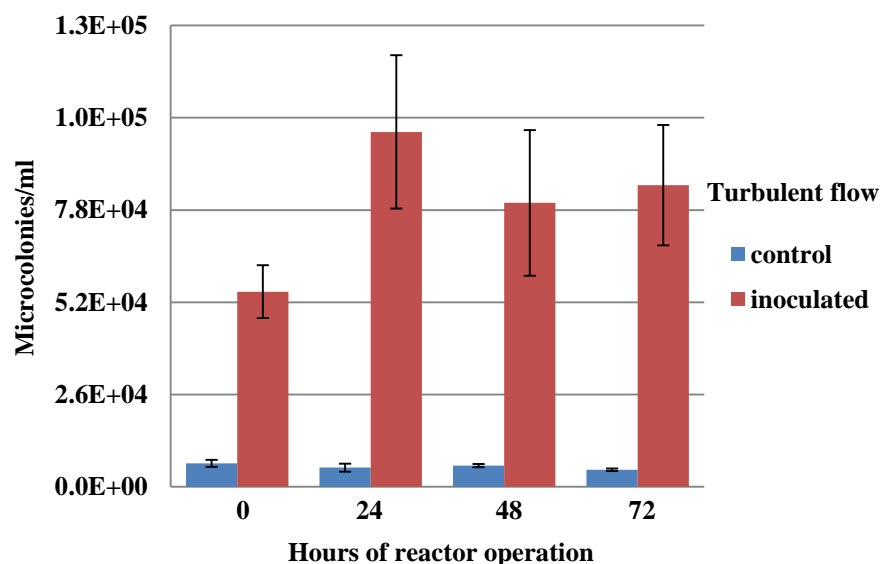
5.3 Results

5.3.1 Differences between control and inoculated cultures

It was found that the number of microcolonies in the bulk water (Figure 5-1) and the number of aggregates on the slides of the reactor (Figure 5-2) were significantly higher ($P < 0.05$) in the inoculated culture than in the control one in turbulent flow. The same result for the microcolonies in the bulk water and the aggregates on the reactor slides was found for laminar flow. There were no aggregates found in the bulk water in both laminar and turbulent flow. The percentage of surface area of biofilms from the bulk water (Figure 5-3) was found to be significantly higher ($P < 0.05$) in the inoculated culture than in the control one only in turbulent flow. The summary for those differences is presented in Table 5-1.

$P < 0.05 = X$	Control versus Inoculated		
	microcolonies/ml	aggregates on slides	biofilms% from the bulk
Turbulent	X	X	X
Laminar	X	X	

Table 5-1 Significant differences that were found in the various measures between control and inoculated drinking water cultures in turbulent and laminar flow.



a.

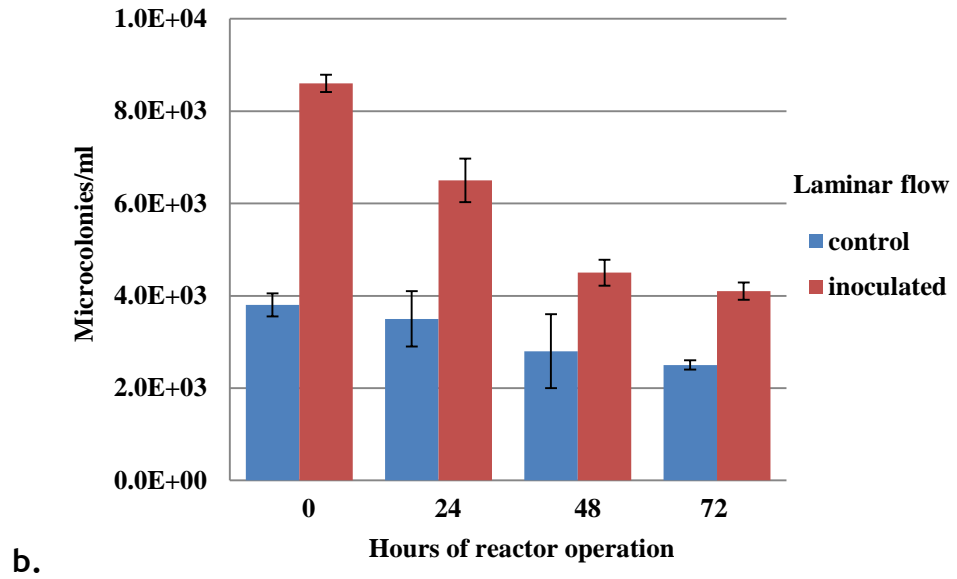
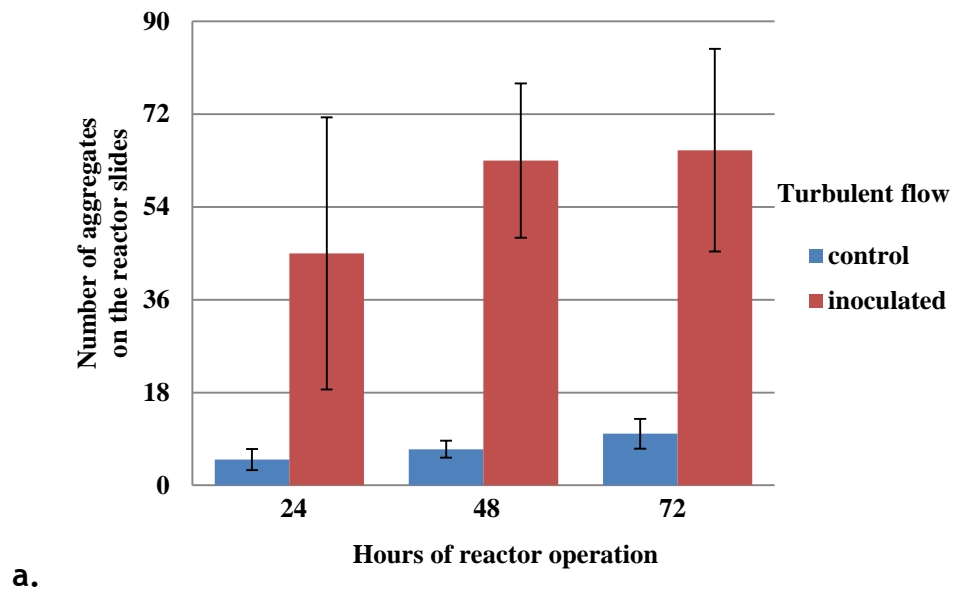
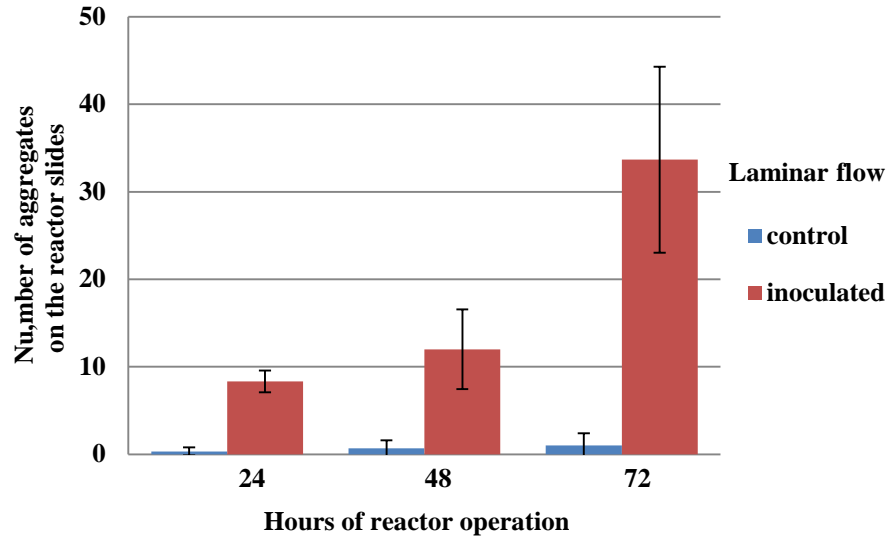


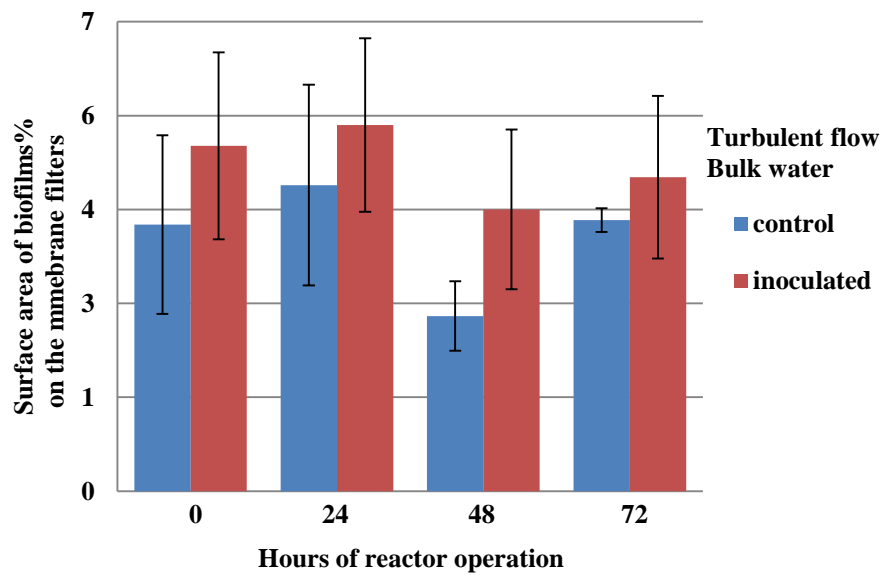
Figure 5-1 Concentration of microcolonies in the bulk water of reactor for both the control and inoculated drinking water cultures at 0, 24, 48 and 72 hours. (a) In turbulent flow and (b) in laminar flow. The error bars represent the standard deviation of the measurements.



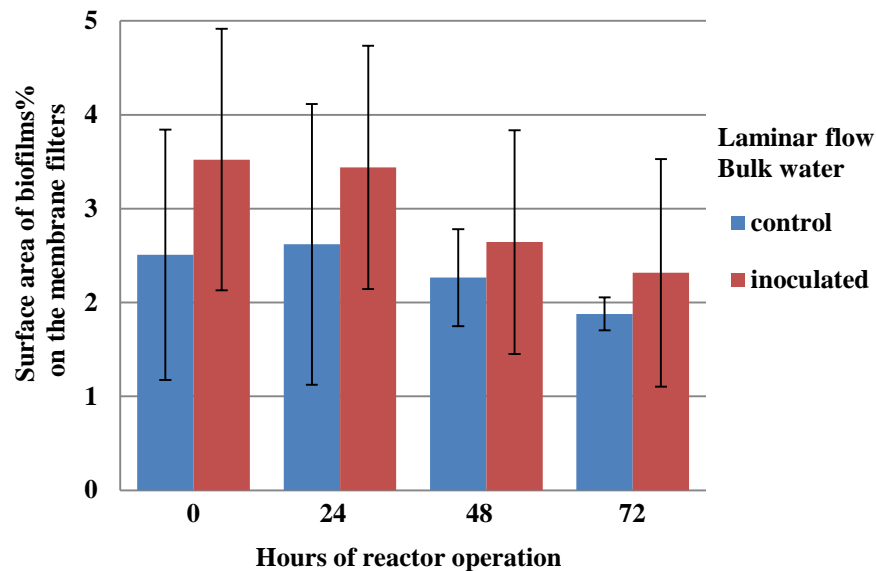


b.

Figure 5-2 Number of aggregates on the reactor slides for both the control and inoculated drinking water cultures at 24, 48 and 72 hours. (a) In turbulent flow and (b) in laminar flow. The error bars represent the standard deviation of the measurements.



a.



b.

Figure 5-3 Percentage of surface area of biofilms from the bulk water of reactor on the membrane filters for both the control and inoculated drinking water cultures at 0, 24, 48 and 72 hours.

(a) In turbulent flow and (b) in laminar flow. The error bars represent the standard deviation of the measurements.

5.3.2 Differences between turbulent and laminar flow

It was found that the number of microcolonies in the bulk water (Figure 5-1), the number of aggregates on the slides of the reactor (Figure 5-2), and the percentage of surface area of biofilms from the bulk water (Figure 5-3) were significantly higher ($P < 0.05$) in turbulent than laminar flow for the control culture. The same result for the microcolonies in the bulk water, the aggregates on the reactor slides and the surface area of biofilms from the bulk water was found for the inoculated culture. The summary for those differences is presented in Table 5-2.

$P < 0.05 = X$	Turbulent versus Laminar		
	microcolonies/ml	aggregates on slides	biofilms% from the bulk
Control	X	X	X
Inoculated	X	X	X

Table 5-2 Significant differences that were found in the various measures between turbulent and laminar flow for the control and inoculated drinking water cultures.

5.3.3 Differences between the time periods of growth

Significant differences were found in the various measures between the different time periods of growth. The most significant differences ($P < 0.05$)

were found between 24-48 hours, which shows that this was the most important time period for bacterial aggregation in the reactor. The summary for those differences is presented in Table 5-3 (see Appendix 10.3 for those measures in which no significant differences were found).

$P < 0.05 = X$		microcolonies/ml	aggregates on slides	biofilms% from the bulk
0-24 h	Turbulent C/I	/X		/X
	Laminar C/I	/X		
24-48 h	Turbulent C/I	/X	/X	X/X
	Laminar C/I	/X	/X	X/X
48-72 h	Turbulent C/I			X/X
	Laminar C/I		/X	

Table 5-3 Significant differences that were found in the various measures in turbulent and laminar flow between the different time periods.

“C” refers to control and “I” refers to inoculated drinking water cultures.

5.4 Discussion

Motility, stress and quorum sensing are all known to play an important role in triggering the switch from planktonic to biofilm mode of life in bacteria (Harshey, 2003, Liu et al., 2016). In the oligotrophic conditions in DWDS, where chemical stresses like chlorination are imposed, biofilms unsurprisingly seem to be the favoured mode of life for microorganisms. Yet, there is evidence that colonisation of biofilms on surfaces does not progress as a random uniformly distributed deposition of bacteria from the bulk liquid onto the surface (Saur et al., 2017).

Recently, in one of the few studies to explore the colonisation of complex biofilms under high-shear flows, it was demonstrated, for a complex mix of bacteria harvested from an activated sludge plant in a rotating annular reactor, heterogeneous clusters of bacteria, size and number of clusters (Saur et al., 2017). Surprisingly, the number and size of clusters was positively correlated with shear stress on the surface of the slides; one might have expected that higher shear would make it more difficult for bacteria to adhere. Flocs that are important in successful wastewater treatment were removed and then, a mixed supernatant, comprising planktonic bacteria, was cultured for 24 hours before it was inoculated into the high-shear bioreactor. The clustering patterns observed

were also observed in previous studies (Bos et al., 1995, Perni et al., 2006, Brugnoli et al., 2011), but the positive and strong correlation between clustering and shear is novel and the level of turbulence in the flow developed to induce such high shear flows is unique in biofilm colonisation studies. The mechanisms suggested to be important for the clustering patterns are co-adhesion (Bos et al., 1994), which occurs on the substratum and describes the propensity for bacteria to attach in proximity to those that have already attached, and coaggregation (Kolenbrander et al., 2010), which is the coming-together of bacteria in clumps in the bulk water prior to adhesion onto the surface.

Part of the motivation for this research was that bacterial aggregation has been studied only for simple mono- and dual-cultures (Simões et al., 2007, Simões et al., 2008, Ramalingam, 2012). These studies, which were performed in batch cultures, were motivated by biofilm formation but did not extend as far as the formation of complex multi-species biofilms on surfaces in realistic flow conditions. Nonetheless, the critical finding was that not all bacteria contribute equally to aggregation; some bacterial species such as *Methylobacterium* seem to promote aggregation. They go onto suggest that QS may play a role in aggregation (Purevdorj et al., 2002, Kirisits et al., 2007, Simões et al., 2007, Ramalingam, 2012). Quorum sensing can be influenced by the hydrodynamic environment. It has been shown that signals do not remain the same under different shear stress conditions due to mass transfer properties in the local environment. Biofilm thickness and density may be altered due to hydrodynamic environment and subsequently, QS signals can be also affected (Kirisits et al., 2007).

Our experiments indicated that in laminar flow aggregation was enhanced in the inoculated drinking water culture compared to the control one. In the inoculated laminar flow experiment, as time progressed the number of microcolonies in the bulk water and the surface area of biofilms from the bulk water were diminished and subsequently, the number of aggregates on the slides was increased. Interestingly, when the rotational speed of reactor was increased to take the flow into a fully turbulent regime there was no such gradual increase in aggregates on the reactor slides. Instead, there was a rapid accumulation within

the first 24 hours and then, a much slower accumulation. Aggregation was found to be enhanced in turbulent flow compared to laminar flow; inoculating with the *Methylobacterium* further enhanced the aggregation. Contrary to stagnant conditions, visible aggregates were not observed in the bulk water for either flow regimes. This suggests that the hydrodynamics ensures that aggregates are moved onto the reactor surfaces before they become large enough to be visible.

Finally, as it was mentioned in Section 4.3.2 for the stagnant conditions, the aggregation that was found in the drinking water culture when the *Methylobacterium* was inoculated into it under the different flow conditions can be attributed to either autoaggregation of *Methylobacterium* or coaggregation of *Methylobacterium* with other drinking water bacteria. At this stage, an additional control experiment including *Methylobacterium* inoculated into autoclaved drinking water would again help in the interpretation of the kind of aggregation that occurred; if it occurred for all drinking water bacteria or just for the added *Methylobacterium*. However, in the next chapter of this study this issue was investigated using microscopy techniques.

5.5 Conclusions

The *Methylobacterium* DSM 18358 was found to be able to cause substantial changes to drinking water microbial aggregation and that changed with the application of different flow regimes. The statistical analysis proved that its ability to form aggregates was enhanced in turbulent flow over that in laminar flow. In turbulent flow the number of microcolonies formed in the bulk water and the number of aggregates on the reactor slides were significantly higher than in laminar flow. These measures were even higher when *Methylobacterium* was present. In turbulent flow the surface area of biofilms from the bulk water was significantly higher when *Methylobacterium* was present. The most important time period for aggregation was found to be the 24-48 hours. These results, combined with the results of aggregation under stagnant conditions (Chapter 4), revealed that the *Methylobacterium* studied is a key strain in aggregation in drinking water in this experiment. Thus, disrupting the formation of biofilms by targeting the key species that initiate the aggregation process rather than acting on all species equally may be a beneficial strategy to drinking water industry.

6 The structures of drinking water aggregates under stagnant and flow conditions

For this work, Dr Jillian Couto designed the PCR primers described in Section 6.2.2 and Dr Ciara Keating conducted the training for the *in situ* hybridization process.

6.1 Introduction

The development of methods in order to study multi-species biofilms has allowed the identification of the various architectures and compositions of a biofilm (Hall-Stoodley et al., 2004). Fluorescence *in situ* hybridization (FISH) is an effective and simple technique based on specific probes, which anneal to specific target sequences of samples. Also, fluorescent reporter molecules are attached to the probes. This technique has been used for the detection of the presence of chromosomal abnormalities due to its high sensitivity and specificity and has provided significant advances in the research of leukemia (Dohner et al., 2000, Cui et al., 2016).

This method extends fluorescence microscopy and allows for the fast detection and enumeration of specific microorganisms. It has been successfully used to characterise microorganisms within biofilms and to detect pathogens in drinking water (Douterelo et al., 2014a). A limitation of the method is that when it is used to detect cells with low ribosomal content, an increased sensitivity must be obtained. Low ribosomal content is often seen in organisms of oligotrophic environments such as drinking water (Nielsen et al., 2006). The use of FISH in order to characterise structures of bacteria in drinking water is rare (Wilhartitz et al., 2007). Most often, DAPI staining (Simões et al., 2008) and catalysed reporter deposition-FISH (CARD-FISH) are used (Nielsen et al., 2006, Deines et al., 2010, Ramalingam, 2012, Kubota, 2013, Douterelo et al., 2014a). However, FISH has been used to detect *Methylobacterium* in various environments, such as plants (Hardoim et al., 2015) and bathrooms (Yano et al., 2013).

In Chapters 4 and 5 it was shown that the *Methylobacterium* DSM 18358 is a key strain in promoting the formation of drinking water aggregates under different

flow conditions. Here, it is attempted to ascertain whether the *Methylobacterium* is arranged in coherent spatial structures in the bulk water and on the exposed surfaces. Thus, aggregates were here visualised for samples taken from stagnant conditions (Chapter 4), laminar and turbulent flow conditions (Chapter 5) using *in situ* hybridization, in order to characterise the aggregation ability of the *Methylobacterium* and its effect on the structure of the total bacterial population.

6.2 Materials and Methods

To conduct *in situ* hybridization it was necessary to perform DNA extraction and polymerase chain reaction (PCR) in order to be able to target the *Methylobacterium* DSM 18358 in the drinking water structures.

6.2.1 DNA extraction

For PCR, genomic DNA was extracted from the pure *Methylobacterium* DSM 18358 culture at the exponential phase of growth at a series of different OD values (see Section 4.2.1) using the Maxwell® 16 LEV Blood DNA kit and quantified based on the Qubit® DNA assay using the Qubit® Fluorometer (ThermoFisher Scientific, England, UK) (see Appendix 10.4.1 for the analytical DNA extraction protocol). The extracted DNA from the pure *Methylobacterium* DSM 18358 culture was stored at -80°C until used for the PCR process as described below.

6.2.2 PCR for *Methylobacterium* DSM 18358

To track the *Methylobacterium* DSM 18358 and distinguish it from naturally occurring members of *Methylobacterium*, specific primers were designed using a two-step approach outlined below.

6.2.2.1 Initial amplification of a 369 bp region of the 16S gene from *Methylobacterium* DSM 18358 via general primers

Species information and DNA sequence was unavailable for *Methylobacterium* DSM 18358, making it impossible to design *Methylobacterium* DSM 18358-specific primers. Instead we opted to use more general published primers, which could

pick up *Methylobacterium* species. Nishio *et al.* had reported multiple primers, which were specific to 7 species of *Methylobacterium* (Nishio *et al.*, 1997). Of these, the authors reported that the Mb4 set, comprised of 4F (5'-CTT-GAG-ACC-GGA-AGA-GGA-C-3') and 4R (5'-CCG-ATC-TCT-CGA-GGT-AAC-A-3'), were the best at identifying the genus *Methylobacterium* only (Nishio *et al.*, 1997). As their study had only utilized a small number of *Methylobacterium* species, we further validated their primers via *in silico* alignments of these published primers and additional available 16S sequence of species from the genus *Methylobacterium* via the BLAST tool. These analyses confirmed their results by also singled out the Mb4 set as the most 'promising' primer pairs. Therefore, this primer pair was used in an initial PCR to amplify the 369 base pairs (bp) 16S gene fragment from *Methylobacterium* DSM 18358.

6.2.2.2 Designing *Methylobacterium* DSM 18358-specific primers

The Mb4 set was a general primer for *Methylobacterium*. As we desired a primer pair specific to this *Methylobacterium* DSM 18358, we opted to clone and sequence this particular 369 bp amplicon. This would enable us to compare primer annealing regions of this sequence with other *Methylobacterium* via a fine-scale multiple sequence alignment analysis. Therefore, this 369 bp amplicon was then cloned via the TOPO TA cloning kit (Invitrogen, Thermo Fisher Scientific, England, UK) and 8-10 clones were mini-prepped and sequenced via the Sanger method. A multiple sequence alignment was then conducted via Clustal OMEGA with this cloned sequence and 26 additional 16S gene sequences from species of both *Methylobacterium* and a few closely related non-*Methylobacterium* organisms. Sequence information was only extracted from species with publically available completed and validated fully sequenced genomes. We focused on the 4F and 4R primer regions and found that in addition to common base pairs, each of these species contained unique bases too. Bases that were specific to the *Methylobacterium* DSM 18358 were then used to design the following primers: MethF (5'-CTT GAG TGT GGT AGA GGT T-3') and MethR (5'-TGT ATC TCT CCA GGT AAC A-3'). These primers were designed by Dr Jillian Couto. The forward primer MethF corresponded to *Methylobacterium populi* BJ001 positions 589 to 606 targeting the 16S *rRNA* V4 region. The reverse primer MethR corresponded to *Methylobacterium populi* BJ001 positions 939 to 958 targeting the 16S *rRNA* V5 region.

6.2.2.3 PCR amplification of the 16S rRNA gene

Initially, the Meth4F (5'-CTT-GAG-ACC-GGA-AGA-GGA-C-3') and Meth4R (5'-CCG-ATC-TCT-CGA-GGT-AAC-A-3') primers (Nishio et al., 1997) were tested to see if they can amplify the 16S rRNA gene of *Methylobacterium* DSM 18358, but this set of primers did not finally amplify the 16S rRNA gene of *Methylobacterium* DSM 18358. The PCR mixtures contained 0.5 µl of 10 µM of each Meth4F and Meth4R primers, 0.2 µl of 5 U KAPA Taq Standard DNA Polymerase, 5 µl of 5X KAPA Taq Buffer containing 10 mM deoxynucleoside triphosphates (dNTPs) and 25 mM magnesium chloride (MgCl₂), and 1 µl of 15 ng/µl template genomic DNA isolated from the *Methylobacterium* DSM 18358 in a final volume of 25 µl (Douris et al., 2017). The PCR products were purified using a PCR purification kit with magnetic beads (AmPure XP, Beckman Coulter, California, US) and stored at -20°C until used for sequencing. Mrs Julie Russel performed this purification process. The purified PCR products were sent for Sanger sequencing (Source Bioscience, Glasgow, UK) to get the sequence of the 16S rRNA gene.

The 16S rRNA gene was finally amplified using the primer sets MethF (5'-CTT GAG TGT GGT AGA GGT T-3') and MethR (5'-TGT ATC TCT CCA GGT AAC A-3') designed by Dr Jillian Couto. The PCR mixtures contained 0.5 µl of 10 µM of each MethF and MethR primers, 0.2 µl of 1 U Bioline MyTaqTM DNA polymerase, 5 µl of 5X MyTaqTM Buffer containing 5 mM dNTPs and 15 mM MgCl₂ and 1 µl of 4.6 ng/µl template genomic DNA isolated from the *Methylobacterium* DSM 18358 in a final volume of 20 µl (Ragot et al., 2015). The optimum annealing temperature was experimentally determined in a single PCR run using a temperature gradient across the reaction block (48.7°C, 50.7°C, 53.1°C, 54.4°C, 55.3°C, 57.4°C, 58.2°C, 59.9°C and 61.3°C). The optimal annealing temperature was found to be the 55.3°C. The PCR was carried out in the Techne TC-5000 gradient thermal cycler (Suffern, US), with an initial denaturation step at 95°C for 5 minutes followed by 35 cycles of 95°C for 15 seconds, 55°C for 15 seconds and 72°C for 15 seconds (see Appendix 10.4.2 for the PCR protocol). Triplicates of samples were used in PCR and 3 negative controls with no template DNA.

The PCR products were finally visualised by agarose gel electrophoresis to ensure that the correct size fragment was amplified and imaged using the Molecular Imager® Gel DocTM with the Image LabTM Software (Bio-Rad Laboratories, Perth,

UK). The 1xTAE buffer was used that contained 40 mM tris(hydroxymethyl)aminomethane (Tris), 20 mM acetic acid and 1 mM ethylenediaminetetraacetic acid (EDTA), and 1% agarose. The SYBR® Safe DNA gel stain was used to stain the buffer and the PCR products (see Appendix 10.4.3 for the agarose gel electrophoresis protocol).

6.2.3 *In situ* hybridization

Samples that were analysed using *in situ* hybridization were obtained from the 24-hour time point of stagnant conditions (Chapter 4), laminar flow (Chapter 5) and turbulent flow (Chapter 5). The samples under stagnant conditions were liquid samples, whereas those in laminar and turbulent flow included samples from both the bulk water and the slides of the reactor. For the samples that were obtained from the slides of the reactor, all the material was gently scraped from them and then it was diluted in 10 ml of distilled water. The *in situ* hybridization process was carried out following the steps described below (Hugenholtz et al., 2002)(see Appendix 10.4.4 for the analytical protocol). Dr Ciara Keating conducted the training for the *in situ* hybridization process.

6.2.3.1 Fixation, storage and preparation of samples

All samples were firstly filtered on 47 mm Whatman® 0.2 µm membrane filters (Sigma-Aldrich, Irvine, UK). Then, they were fixed using 2% paraformaldehyde for 8 hours and stored at -20°C (Herndl, 2007). The samples were dehydrated in an aqueous ethanol dilution series (50, 80, 90-96%) for 3 minutes each and then, the membrane filters were cut into pieces of 2 mm² squares.

6.2.3.2 Hybridization with oligonucleotide probes

To specifically target the *Methylobacterium* DSM 18358 the oligonucleotide sequence (5'-CTT-GAG-ACC-GGA-AGA-GGA-C-3'), which was specific for this strain as described in 6.2.1.2 was labelled with digoxigenin (DIG) (Pirttila et al., 2000, Podolich et al., 2009). For the detection of the total bacterial drinking water population the universal 16S *rRNA* bacterial probe EUB338 (5'-GCT GCC TCC CGT AGG AGT-3') was used targeting the 16S *rRNA* V3 region of all cells (Amann et al., 1990). The EUB338 probe was labelled with cyanine dye (CY3) (Stoecker et al., 2010). Both the 5'-DIG labelled probe MethF and the 5'-CY3

labelled probe EUB338 were purchased from Eurofins (Eurofins Scientific, Bavaria, Germany).

The hybridization buffer included 5 M sodium chloride (NaCl), 1 M tris - hydrochloride (Tris-HCL) at pH= 8, 30% formamide (CH₃NO), 10% sodium dodecyl sulphate (SDS) at pH= 7.2. Other CH₃NO concentrations that were tested but they did not work for our samples were 40% and 50%. Hybridization was carried out through the addition of 8 µl of hybridization buffer and 1 µl of 50 ng/µl of each probe to each sample. Samples were hybridised at 46°C for 2 hours in a water circulator (Isotemp Bath Circulator, Fisher Scientific, England, UK). Other hybridization temperatures that were tested but they did not work for our samples were 50°C and 55°C.

6.2.3.3 Washing and microscopy

Unbound oligonucleotides were removed by rinsing the samples with 2 ml of washing buffer. This buffer included 1 M Tris-HCL at pH= 8, 5 M NaCl, 0.5 M EDTA at pH= 8 and 10% SDS at pH= 7.2. The samples were washed at 48°C for 15 minutes in the same water circulator as in the previous step and then, they were deposited on gelatin coated slides (Marienfeld, Baden-Württemberg, Germany), which contained 10 reaction wells. The slides were then dried at room temperature in the dark overnight. All the DNA of the samples was then stained using 10 µg/ml of DAPI for 20 minutes in the dark. Other DAPI concentrations that were tested but they did not work for our samples were 1 µg/ml and 5 µg/ml. Remaining DAPI was removed afterwards by rinsing the slides gently with distilled water. After air drying, cover glasses were mounted with 2 µl of Ever Brite™ mounting medium (Biotium, Cambridge Bioscience, Cambridge, UK).

Samples were finally analysed using fluorescence microscopy with the oil immersion UPlanFLN objective lens with 100X magnification/1.30 numerical aperture. The filters used was the DAPI filter with excitation at 358 nm and emission at 461 nm for total DNA visualisation, the Nile red filter with excitation at 485 nm and emission at 525 nm for total cells visualisation, and finally the TRITC filter with excitation at 557 nm and emission at 576 nm for the *Methylobacterium* strain DSM 18358 visualisation. The composite images included all 3 staining channels: DAPI for all DNA, Cy3 for all drinking water

bacteria and digoxigenin for the *Methylobacterium* strain DSM 18358 only. The images were analysed using Matlab whereby the command called “cat” was used that concatenates arrays along a specified dimension.

6.2.3.4 Control reactions

Digoxigenin is not technically a fluorophore; however, it has been successfully used for *in situ* hybridization reactions (Bartsch and Schwinger, 1991, Robbins et al., 1991, Komminoth, 1992, Miyazaki et al., 1994, Schroder et al., 2000, Schumacher et al., 2014). In this study a modified preparation of DIG was used. In order to ensure the accuracy and efficiency of the 5'-DIG labelled probe MethF to target only the *Methylobacterium* DSM 18358, various controls were performed. As a positive control reaction the 5'-DIG labelled probe MethF was tested for the pure *Methylobacterium* DSM 18358 culture (Figure 6-1). It was shown that the 5'-DIG labelled probe MethF can detect the *Methylobacterium* DSM 18358. Also, the pure *Methylobacterium* DSM 18358 culture was visualised with DAPI using fluorescence microscopy (Figure 6-2).

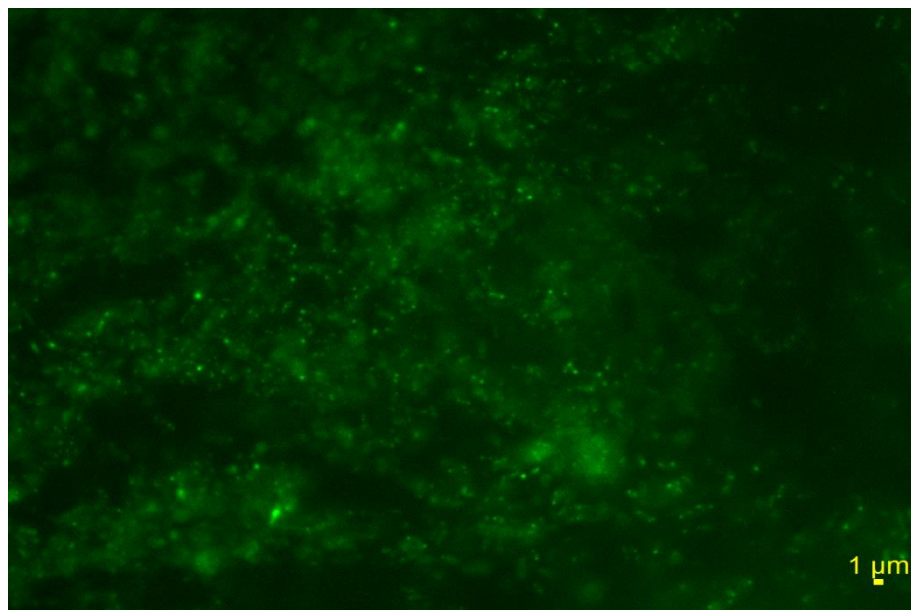


Figure 6-1 Positive control image for 5'-DIG labelled probe MethF in pure *Methylobacterium* DSM 18358 culture as revealed by *in situ* hybridization using the 100X objective lens. *Methylobacterium* DSM 18358-green colour.

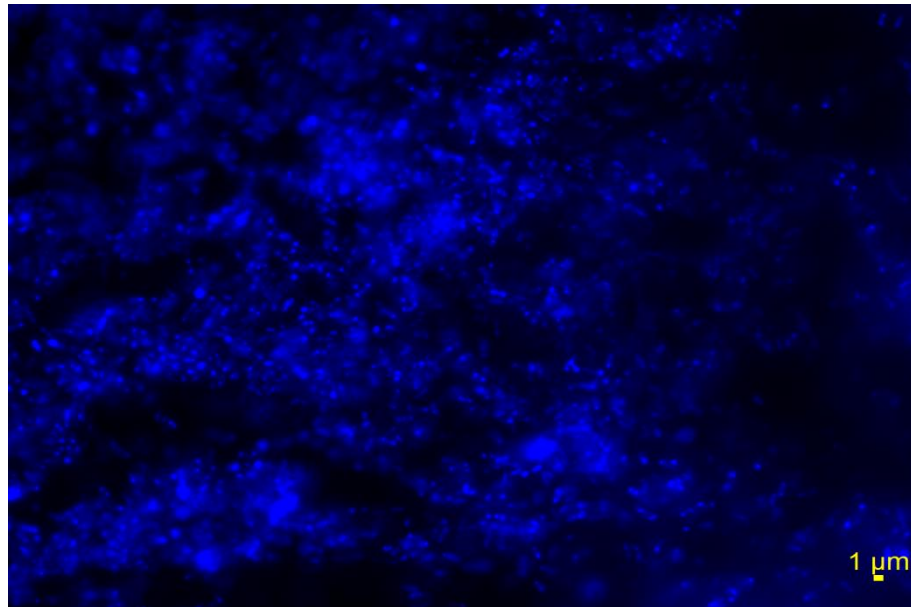


Figure 6-2 Pure *Methylobacterium* DSM 18358 culture stained with DAPI as revealed by fluorescence microscopy using the 100X objective lens.

In order to calculate the efficiency of the 5'-DIG labelled probe MethF the surface areas of the biomaterial on the images were calculated for the case of the 5'-DIG labelled probe MethF in the pure *Methylobacterium* DSM 18358 culture using *in situ* hybridization (SA_1) (i.e. the one in Figure 6-1) and for the case of DAPI staining in the pure *Methylobacterium* DSM 18358 culture using fluorescence microscopy (SA_2) (i.e. the one in Figure 6-2). The efficiency (EF) of the 5'-DIG labelled probe MethF was calculated for at least 30 images from each case using the Equation 6-1. It was found that the efficiency of the 5'-DIG labelled probe MethF was high at 82.25%.

$$(EF)\% = 100 - \frac{SA_1 - SA_2}{SA_1} * 100 \quad 6-1$$

As a negative control to ensure that the 5'-DIG labelled probe MethF was specific only for *Methylobacterium* DSM 18358 and also did not demonstrate autofluorescence the probe was tested for *Escherichia coli* MG 1655 culture (Figure 6-3). It was found that the 5'-DIG labelled probe MethF did not detect the *E. coli* MG 1655. The *E. coli* MG 1655 grew overnight in Luria-Bertani agar at 37°C. Then, a single colony was picked from the agar and diluted in Luria-Bertani broth at 37°C at 90 RPM for 3.50 hours. This *E. coli* MG 1655 culture (approximately 10^8 cells/ml) had also been stained with DAPI and visualised using the TRITC filter to rule out excitation carry over from the DAPI stained

cells (Figure 6-4). It was found that *E. coli* MG 1655 was not detected using the TRITC filter. The *E. coli* MG 1655 culture, which was stained with DAPI using fluorescence microscopy, can be seen in Figure 6-5.

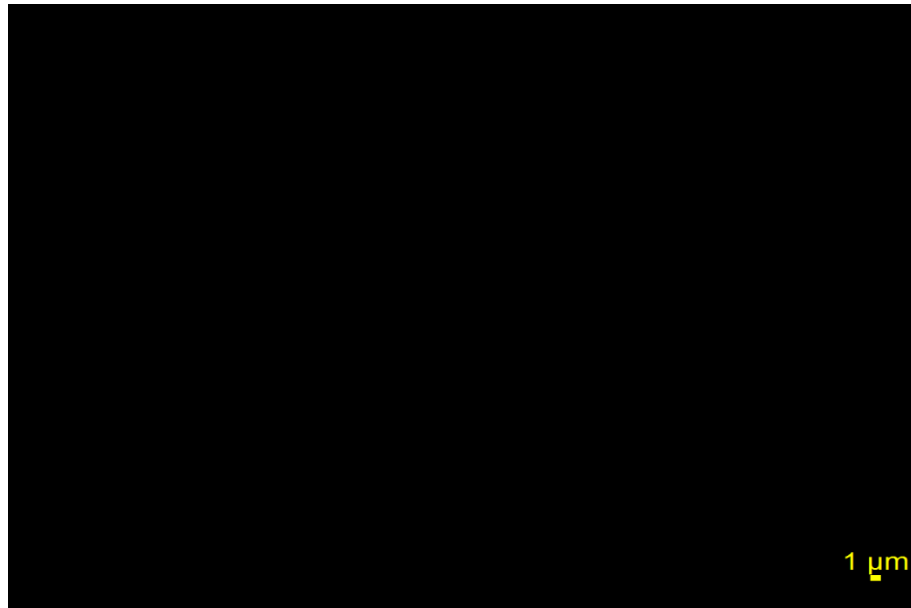


Figure 6-3 Negative control image for 5'-DIG labelled probe MethF in pure *E. coli* MG 1655 culture as revealed by *in situ* hybridization using the 100X objective lens.

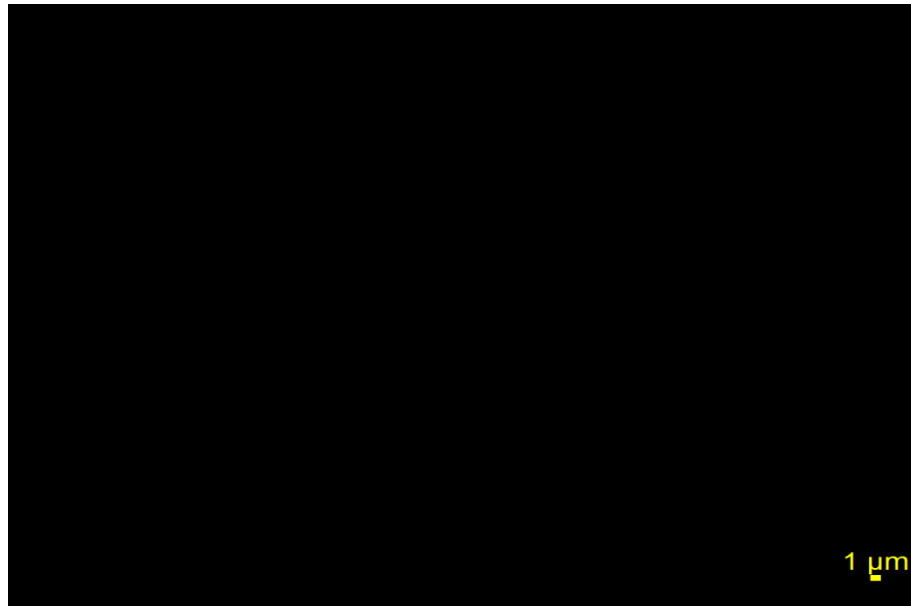


Figure 6-4 Pure *E. coli* MG 1655 culture stained with DAPI and visualised using the TRITC filter as revealed by fluorescence microscopy using the 100X objective lens.

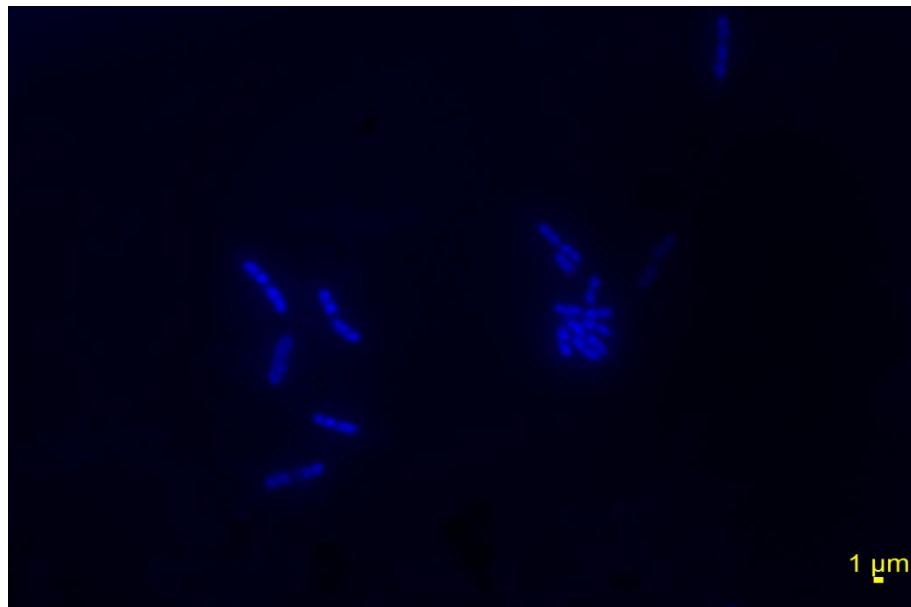


Figure 6-5 Pure *E. coli* MG 1655 culture stained with DAPI as revealed by fluorescence microscopy using the 100X objective lens.

The same procedure was carried out to test the specificity of the 5'-CY3 labelled probe EUB338. As a positive control the 5'-CY3 labelled probe EUB338 was tested for a drinking water culture without any added *Methylobacterium* (Figure 6-6). It was found that the 5'-CY3 labelled probe EUB338 can detect the drinking water bacteria. The 5'-CY3 labelled probe EUB338 was also tested for the pure *Methylobacterium* DSM 18358 culture (Figure 6-7). It was shown that the 5'-CY3 labelled probe EUB338 can detect the *Methylobacterium* DSM 18358. Finally, as a negative control to ensure that the 5'-CY3 labelled probe EUB338 was specific only for bacteria the probe was tested for a pure culture consisting of protozoa (Figure 6-8). It was found that the 5'-CY3 labelled probe EUB338 did not detect the protozoa. The protozoa culture (approximately $1.2 \pm 0.3 \times 10^8$ protozoa/ml), which was stained with DAPI using fluorescence microscopy, can be seen in Figure 6-9. The way this culture was created can be found in Appendix 10.4.5.

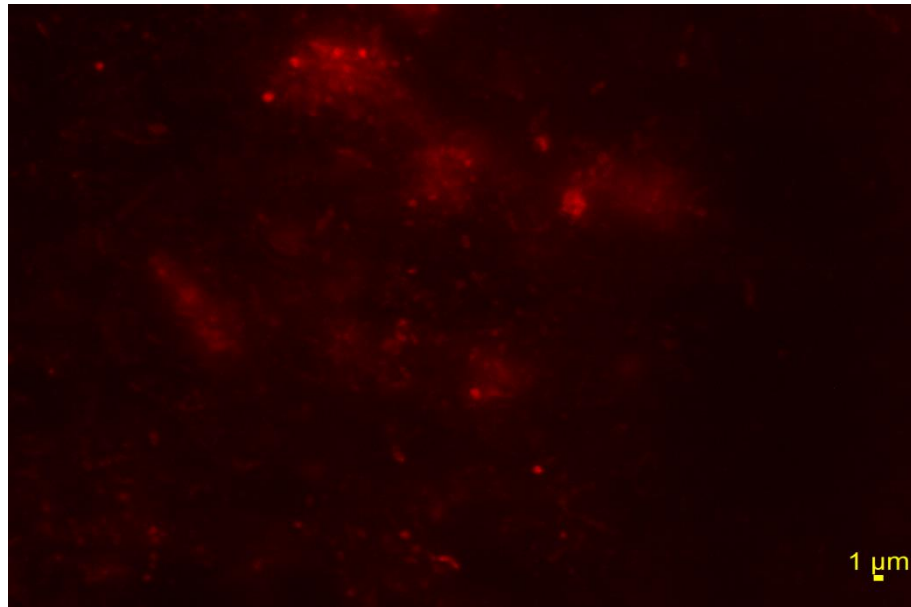


Figure 6-6 Positive control image for 5'-CY3 labelled EUB338 probe in drinking water culture without any added *Methylobacterium* as revealed by *in situ* hybridization using the 100X objective lens.
Drinking water bacteria-red colour.

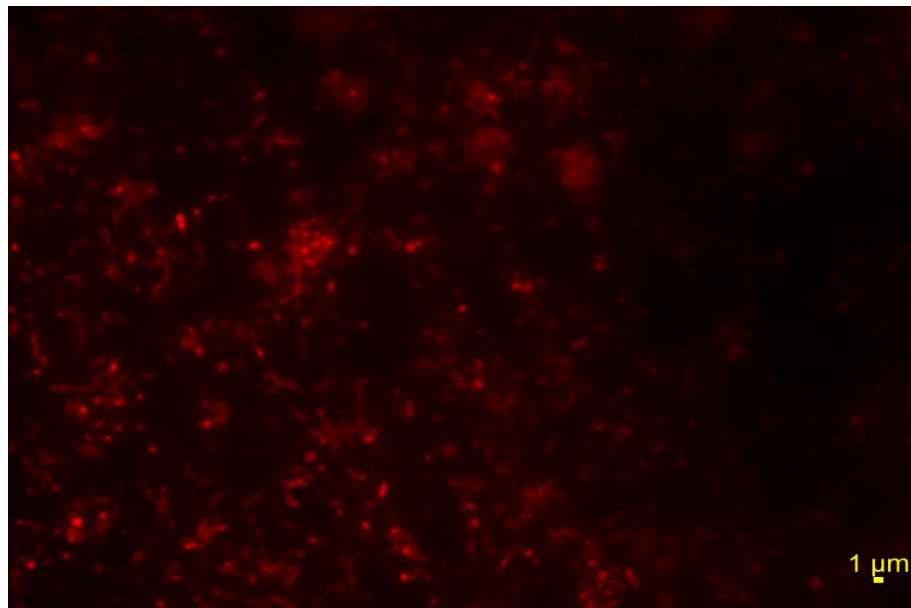


Figure 6-7 Positive control image for 5'-CY3 labelled EUB338 probe in pure *Methylobacterium* DSM 18358 culture as revealed by *in situ* hybridization using the 100X objective lens.
Methylobacterium DSM 18358-red colour.

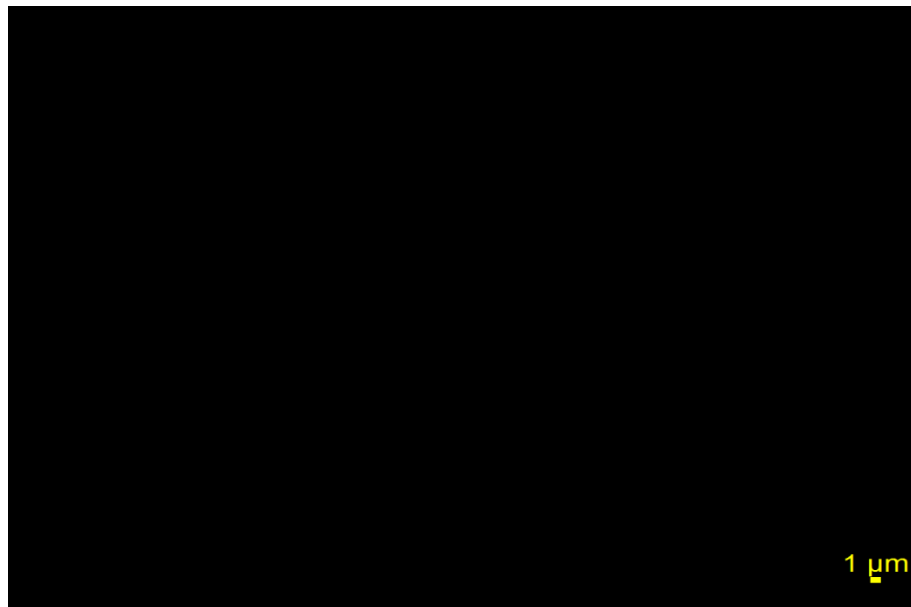


Figure 6-8 Negative control image for 5'-CY3 labelled probe EUB338 in protozoa culture as revealed by *in situ* hybridization using the 100X objective lens.

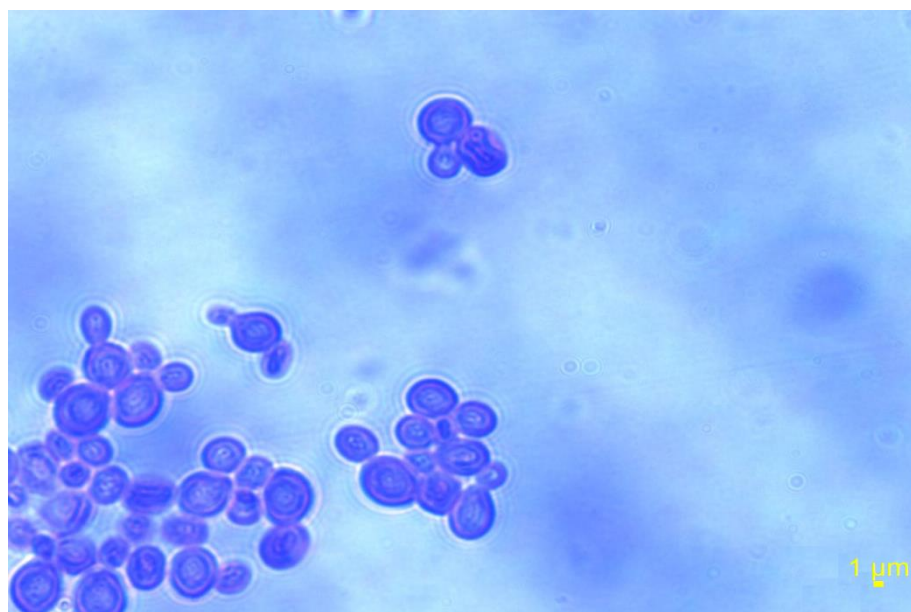


Figure 6-9 Protozoa culture stained with DAPI as revealed by fluorescence microscopy using the 100X objective lens.

6.3 Results

The relationship between the OD values and the amounts of extracted DNA for the pure *Methylobacterium* culture is shown in Figure 6-10; the sample illustrated as the fourth point (OD at 0.32 and DNA at 46 ng/μl) was the one used for PCR. From agarose gel electrophoresis, the DNA fragment size was found at about 200-400 bp.

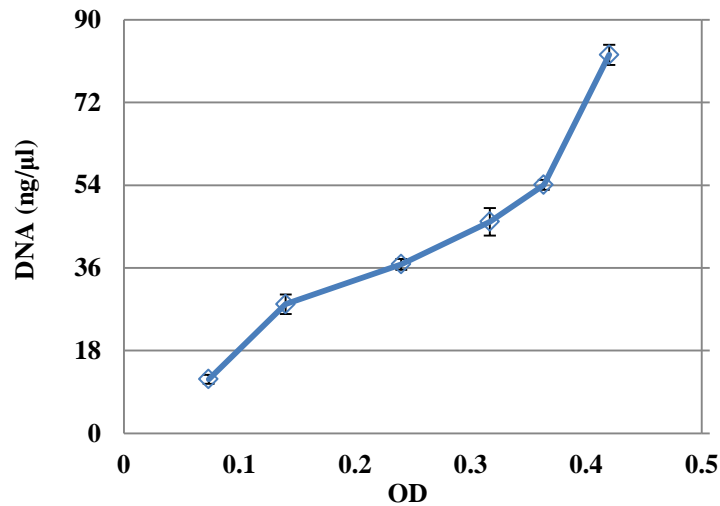


Figure 6-10 Amount of DNA from the pure *Methylobacterium* DSM 18358 culture quantified based on the Qubit® DNA assay for different optical densities.

Below, the first set of images that are presented includes only those areas in which the *Methylobacterium* strain was present. These were selected as being the most representative images from those obtained for stagnant, laminar and turbulent flow conditions. The second set of images includes only those areas in which the *Methylobacterium* was not present. These were again selected as being the most representative images from those obtained from stagnant, laminar and turbulent flow conditions.

6.3.1 Areas in which *Methylobacterium* was present

Under stagnant conditions, it was found that the *Methylobacterium* strain DSM 18358 was dominant within the forming aggregates (Figure 6-11). Specifically, the *Methylobacterium* created its own large aggregates excluding the rest of the drinking water bacteria.

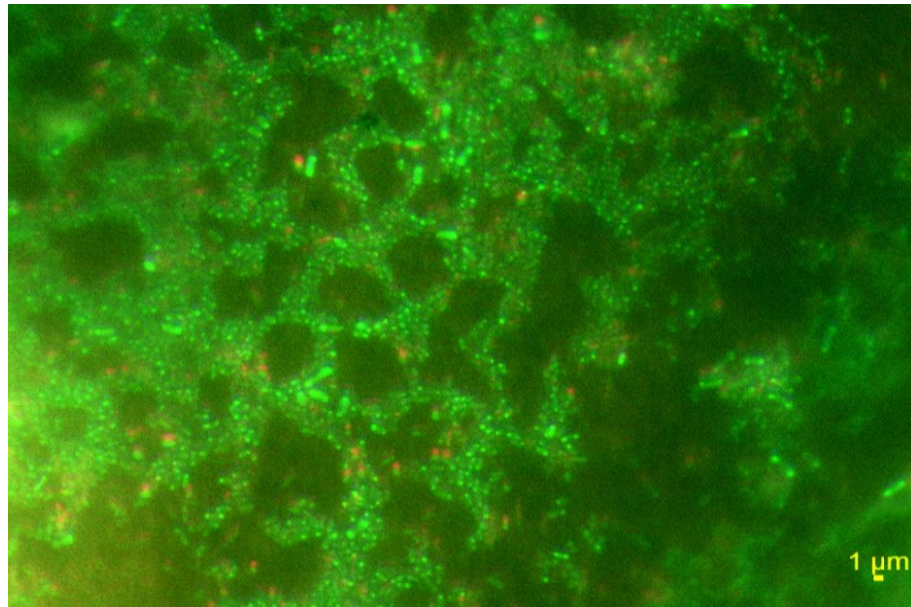


Figure 6-11 Structures of drinking water aggregates under stagnant conditions as revealed by *in situ* hybridization using the 100X objective lens. *Methylobacterium* DSM 18358-green, all bacteria-red, all DNA-blue.

Similarly to stagnant conditions, in laminar flow the *Methylobacterium* was dominant within the forming aggregates in both liquid samples (Figure 6-12) and samples from the reactor slides (Figure 6-13). In addition, there were more aggregates detected for the samples from the reactor slides than for the liquid samples. The aggregates detected in laminar flow for the liquid samples were less than those under stagnant conditions. However, in laminar flow the aggregates were not solely formed of the *Methylobacterium* DSM 18358 aggregates, but there was a co-location of other drinking water bacteria in the abundant *Methylobacterium* aggregates.

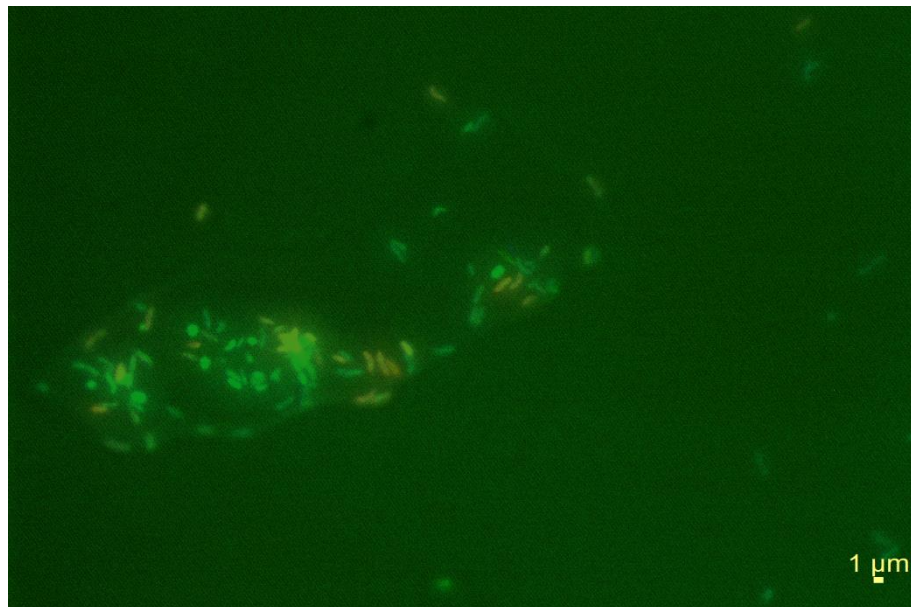


Figure 6-12 Structures of drinking water aggregates in laminar flow as revealed by *in situ* hybridization using the 100X objective lens - Liquid sample.
Methylobacterium DSM 18358-green, all bacteria-red, all DNA-blue.

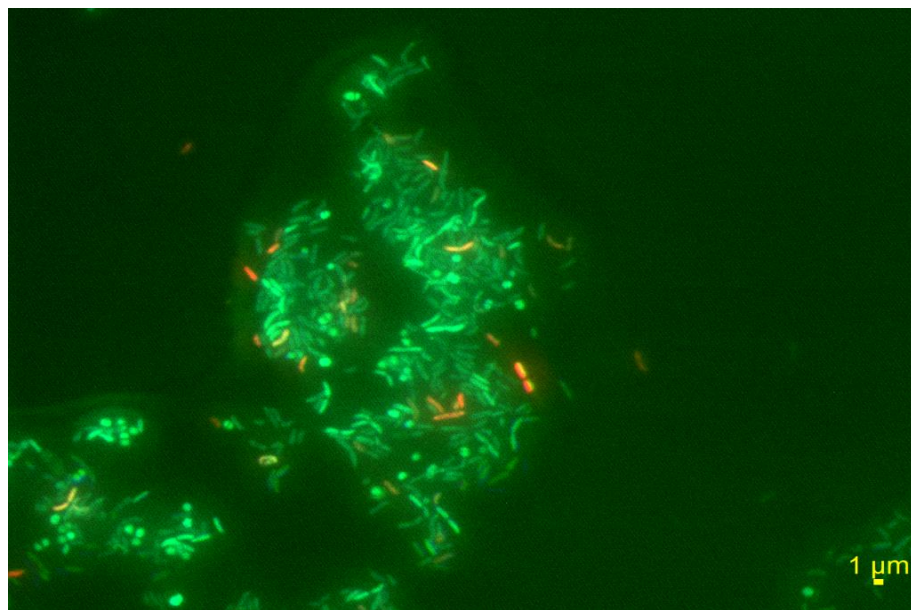


Figure 6-13 Structures of drinking water aggregates in laminar flow as revealed by *in situ* hybridization using the 100X objective lens - Slide sample.
Methylobacterium DSM 18358-green, all bacteria-red, all DNA-blue.

In turbulent flow, the *Methylobacterium* was found to create a tightly knit core of its own aggregates and the rest of the drinking water bacteria were found to create a large mantle that surrounded this *Methylobacterium* aggregates core. It was shown that the *Methylobacterium* stain DSM 18358 acted as a “flocculant” picking up the rest drinking water bacteria around it. Similarly to laminar flow, there were more aggregates detected for the samples from the reactor slides (Figure 6-15) than for the liquid samples (Figure 6-14). In the rapid mixing and

high shear describing turbulent flow conditions there were more aggregates found than in laminar flow.

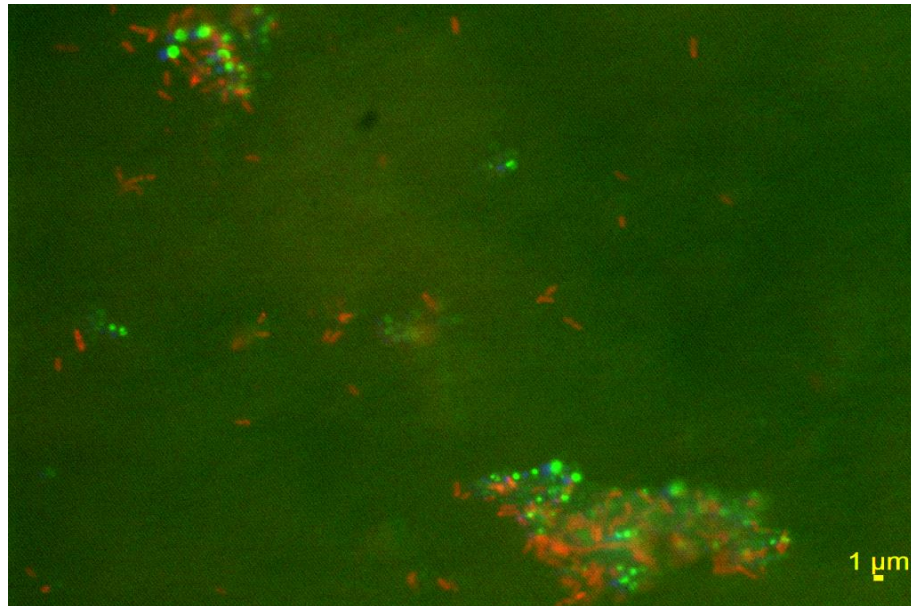


Figure 6-14 Structures of drinking water aggregates in turbulent flow as revealed by *in situ* hybridization using the 100X objective lens - Liquid sample.
Methylobacterium DSM 18358-green, all bacteria-red, all DNA-blue

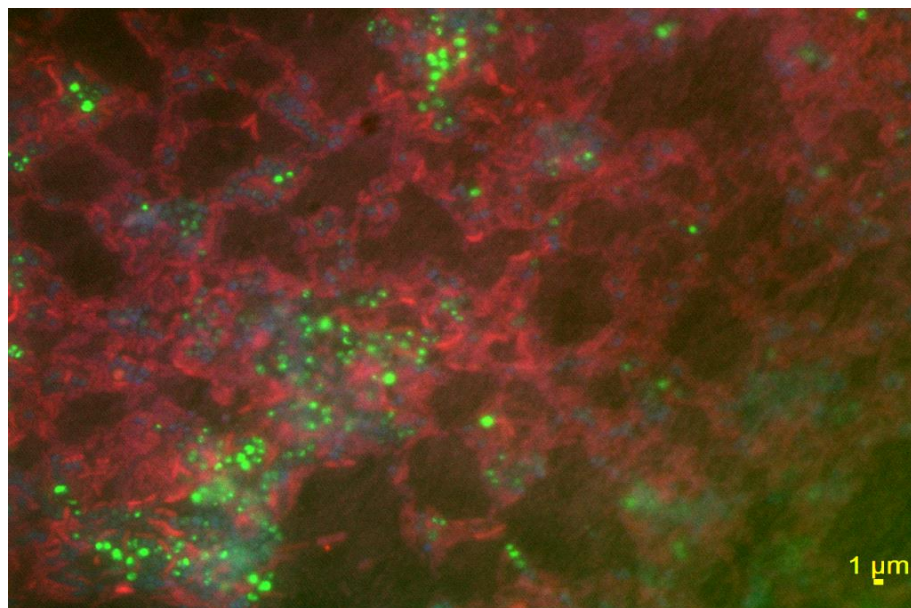


Figure 6-15 Structures of drinking water aggregates in turbulent flow as revealed by *in situ* hybridization using the 100X objective lens - Slide sample.
Methylobacterium DSM 18358-green, all bacteria-red, all DNA-blue.

6.3.2 Areas in which *Methylobacterium* was not present

Below, the areas in which there was no *Methylobacterium* detected are demonstrated for stagnant conditions (Figure 6-16), laminar flow for a liquid sample (Figure 6-17) and for a sample from the reactor slides (Figure 6-18), and

finally, turbulent flow for a liquid sample (Figure 6-19) and for a slide sample (Figure 6-20). Again, it was shown that there were more aggregates for the samples from the reactor slides than for the liquid samples in both laminar and turbulent flow. In addition, more aggregates were found again in turbulent than in laminar flow.

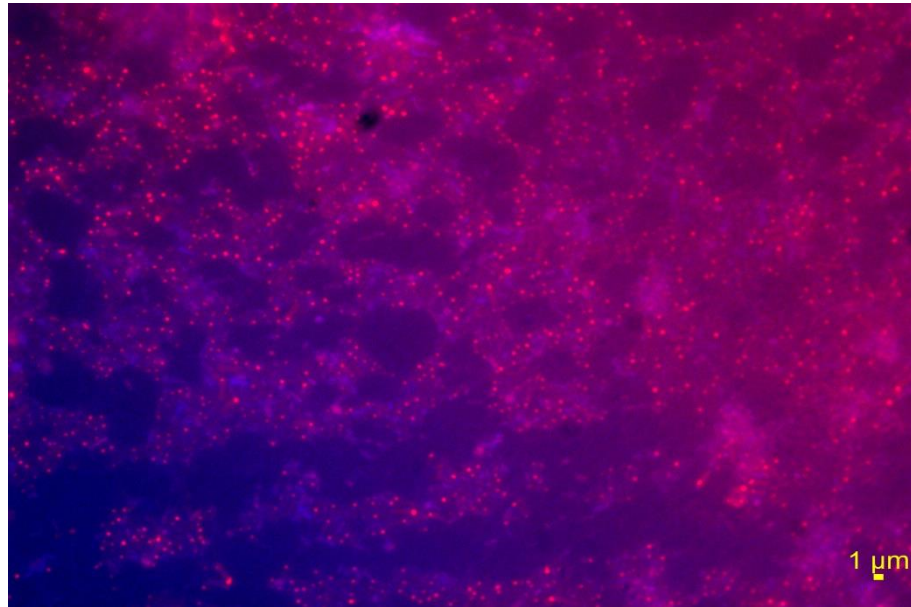


Figure 6-16 Structures of drinking water aggregates under stagnant conditions as revealed by *in situ* hybridization using the 100X objective lens. All bacteria-red and all DNA-blue.

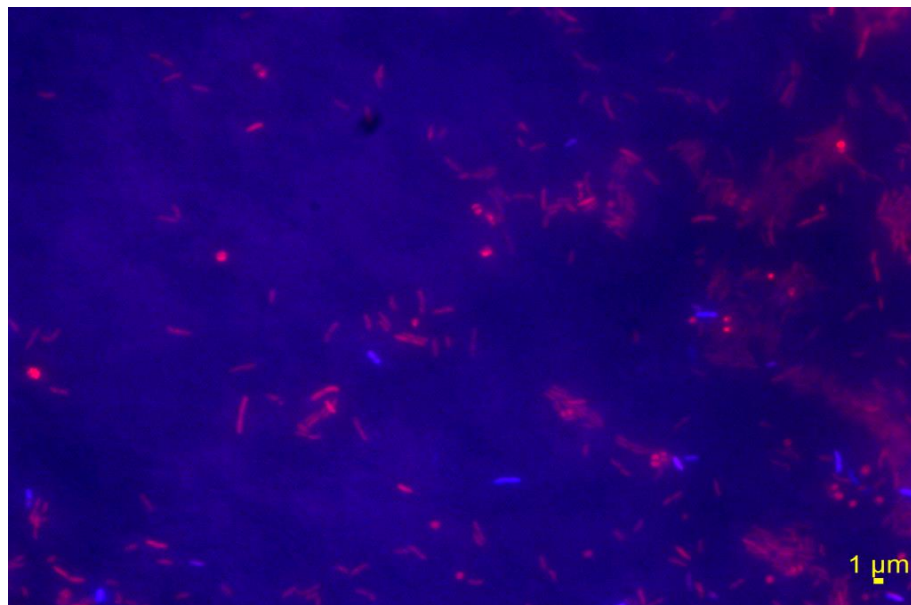


Figure 6-17 Structures of drinking water aggregates in laminar flow as revealed by *in situ* hybridization using the 100X objective lens - Liquid sample. All bacteria-red and all DNA-blue.

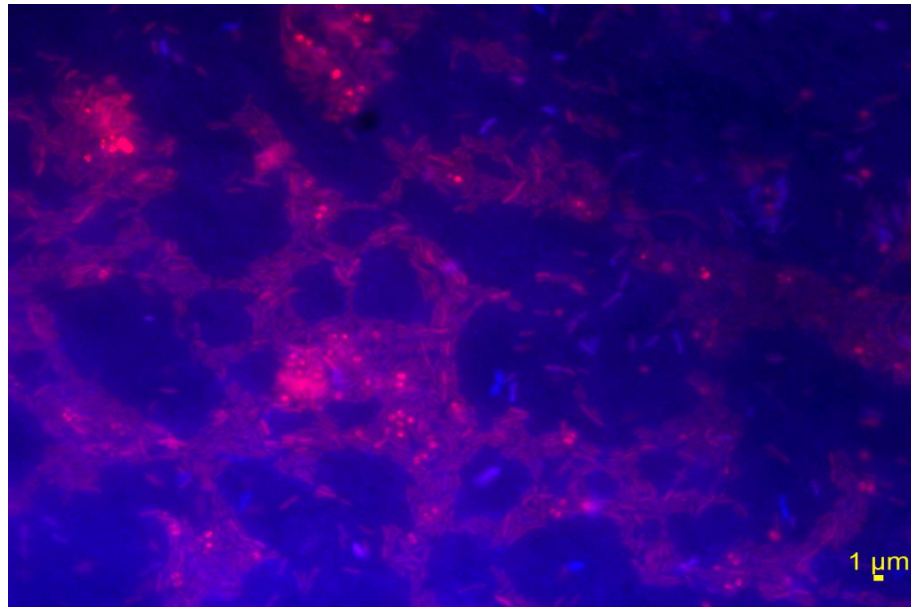


Figure 6-18 Structures of drinking water aggregates in laminar flow as revealed by *in situ* hybridization using the 100X objective lens - Slide sample. All bacteria-red and all DNA-blue.

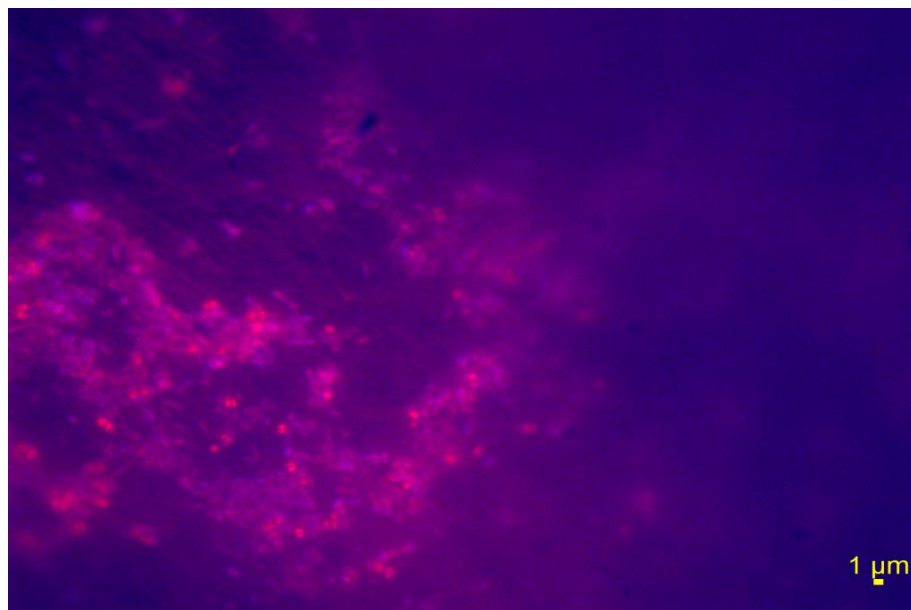


Figure 6-19 Structures of drinking water aggregates in turbulent flow as revealed by *in situ* hybridization using the 100X objective lens - Liquid sample. All bacteria-red and all DNA-blue.

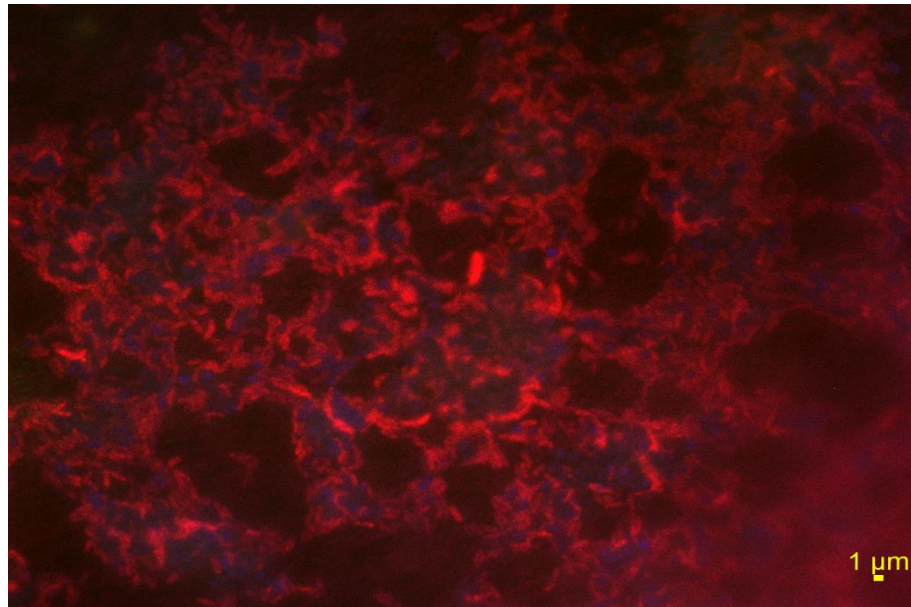


Figure 6-20 Structures of drinking water aggregates in turbulent flow as revealed by *in situ* hybridization using the 100X objective lens - Slide sample. All bacteria-red and all DNA-blue.

6.4 Discussion

In this study we successfully used the 5'-DIG labelled probe MethF to target only the *Methylobacterium* DSM 18358 within the structures of drinking water aggregates. Even though digoxigenin is not a fluorophore, it was successfully used for our *in situ* hybridization reactions after conducting a number of control experiments that are described in Section 6.2.3.4. It was found that aggregation did occur for general drinking water bacteria other than the *Methylobacterium* strain DSM 18358. It might be that these aggregates were created by other key species in bacterial aggregation that were not targeted with *in situ* hybridization. The findings from this study agreed with the previous findings in Chapter 5. Similarly to Chapter 5, here it was found that in turbulent flow aggregation was enhanced compared to laminar flow. Under both flow conditions aggregates were most apparent for the slide samples than for the liquid samples. This suggests that once aggregates were formed in the bulk water they were moved onto the surfaces. In Chapter 5, it was found that there were no visible aggregates in the liquid samples for both flow conditions. Here, it was shown that aggregates did occur in the bulk water but those aggregates were detectable by microscopy and not by visual observation. It was finally shown that there were more aggregates under stagnant conditions than under flow conditions in the bulk water, which again suggests that the flow conditions enable their move onto the surfaces.

The experiments lend weight to the speculation that coaggregation in the bulk liquid is an important precursor to biofilm colonisation and that the formation of aggregates at various scales is enhanced by turbulence (Saur et al., 2017). The increase in mass transport with increasing turbulence is a very well documented phenomenon (Hughmark, 1975, Jischa, 1976, Jaber and Colucci, 2003b, Jaber and Colucci, 2003a) and thus, it is unsurprising that movement of biomass from the bulk liquid onto the surfaces with increases in shear stress. What is surprising is that the propensity for aggregation in the bulk liquid is maintained as the flow speeds increase and turbulence is induced.

If there are groups of bacteria that produce a chemical signal to induce aggregation, then one might expect the dispersal caused by turbulent flow would homogenise the concentration of signalling molecule and thus, make chemotaxis difficult. It has been suggested that individual bacterial cells can feel turbulence and modify their phenotype in response to it (Hondzo and Wuest, 2009). So, it could be that the drinking water bacteria modify their cell surfaces to promote adhesion in turbulent flow conditions and that the mechanical mixing and the consequent increased likelihood of collisions form aggregates. Yet, this does not explain why the core of the aggregates was made up of the *Methylobacterium* in turbulent flow; the *Methylobacterium* must firstly form single-species core and then, the other bacterial species adhere to this core. Thus, it looks like even in turbulent flows some sort of signalling occurs between the *Methylobacterium* cells that causes them to rapidly adhere to one another. The same it is speculated for the rest drinking water bacteria that were found to surround this core of the *Methylobacterium* aggregates. If this is chemical signalling, then it is a mystery how the chemical gradients are maintained in highly mixed turbulent flows.

6.5 Conclusions

It is particularly interesting that the spatial distribution of bacterial aggregates, revealed by fluorescence *in situ* hybridization, was changed with the flow regime. Under all studied conditions, the *Methylobacterium* strain DSM 18358 was found to firstly form its own aggregates, which suggests some form of strong communication between the *Methylobacterium* cells.

The main difference between the stagnant and flow conditions was that there was a co-location of the other drinking water bacteria in the forming *Methylobacterium* aggregates under the flow conditions only, which suggests again that cell communication in drinking water might be enhanced by the flow conditions. This was more obvious in turbulent flow, in which the *Methylobacterium* aggregates were found to be surrounded by the aggregates that the rest drinking water bacteria formed. Overall, aggregation in the bulk water was more apparent for stagnant conditions, as once big aggregates were formed under flow conditions they were moved onto the surfaces. However, the higher was the mixing and shear applied, the higher was the aggregation detected on the surfaces.

7 The role of motility of *Methylobacterium* in aggregation

7.1 Introduction

Motility is an important factor for biofilm formation by which bacteria overcome the electrostatic forces between them and the surfaces they colonise. It is also critical in the aggregation of bacteria into free-floating biofilms (O'Toole and Kolter, 1998, Pratt and Kolter, 1998, Mireles et al., 2001, Recht and Kolter, 2001). Cell motility regulates the production of genes that control the expression of virulence determinants; these enable bacteria to invade host cells (Macfarlane et al., 2001, Fraser et al., 2002, Mattick, 2002, Senesi et al., 2002). Chemotaxis is important for the regulation and control of the direction of cell movement and the extent of bacterial colonisation, as it plays key role in the nutrient consumption and cycling in the surrounding environment (Harshey, 2003, Son et al., 2015). Quorum sensing has been shown to coordinate the motility of bacteria and trigger specific behavioural responses in a bacterial population that presumably benefit the bacteria in a particular environment (Huber et al., 2001, Riedel et al., 2001, Poonguzhali et al., 2007).

One of the conditions affecting bacterial motility is the moisture of the substrate. Thus, the viscosity of the substrate is often tested for affecting bacterial motility and different agar concentrations have been used to create substrates of different viscosities (Mattick, 2002). Bacterial motility is also an energy intensive process and bacteria need to have enough energy to move. So, some bacteria will only move in energy rich environments (Mattick, 2002). On the other hand, bacteria will often expend energy they have stored when the environment cannot provide sufficient energy, so that they can transport themselves to a more favourable environment (Martinez et al., 1999).

Another factor influencing bacterial motility is the slime of bacteria, which consists of polysaccharides and other surface-active components, such as amino acids and peptides (Matsuyama et al., 1993). These components offer bacteria protection from desiccation by water retention providing a hydrated milieu within which cell appendages function and thus, promote cell motility (Toguchi et al., 2000, Harshey, 2003). They also serve as cell density signals that regulate

the expression of genes and thus, coordinate cell movements (Fraser and Hughes, 1999, Harshey, 2003). Finally, the temperature is a factor that affects motility in most bacterial species (Matsuyama et al., 1995).

There are several types of surface motility; swarming motility, which requires flagella organelles; twitching motility, which requires type IV pili organelles; gliding motility, which requires a group of bacteria and; sliding motility, which requires a growing colony of bacteria (Harshey, 2003). These types of surface motility enable bacteria to establish symbiotic and pathogenic associations with plants and animals (Rashid and Kornberg, 2000). Most bacterial species are motile by means of flagella; the structure and arrangement of these appendages are different from species to species and are related to the specific environment in which the species live. Flagella can be arranged on the cell body by single polar, multiple polar and peritrichous or lateral configurations (Soutourina et al., 2001).

Swimming motility, on the other hand, is a beneficial trait for bacteria in fluid environments as it enables cell movements towards favourable environmental conditions (Stocker et al., 2008, Dennis et al., 2013), which are away from toxins and predators (Samad et al., 2017). It also enables cell survival in changing environmental conditions (Galajda et al., 2007). Swimming motility is powered by rotating flagella similarly to the swarming motility on the surfaces (Kearns, 2010). Whereas swarming is a movement of a group of bacteria that requires many flagella, possibly because of the surface friction, swimming is an individual endeavour that requires less flagella. Some bacteria have distinct flagella for these two modes of motility, whereas others have only one kind of flagella for both.

It has been shown that some species of *Methylobacetrrium* such as *Methylobacterium goesingense* are motile on semi-solid agar media forming small fimbriae-like structures (Schauer and Kutschera, 2011). Also, other *Methylobacterium* species such as *Methylobacterium marchantiae* have been found to assemble a polar flagellum in liquid media (Doerges and Kutschera, 2014). In a variety of environments, such as drinking water, seawater, soil and air, it has been shown that there are motile *Methylobacterium* species including *Methylobacterium variabile* (Gallego et al., 2005c), *Methylobacterium salsuginis*

(Wang et al., 2007), *Methylobacterium tarhaniae* (Veyisoglu et al., 2013) and *Methylobacterium iners* (Weon et al., 2008). Here, the motility of the *Methylobacterium* strain DSM 18358 and its role in the interactions with other drinking water bacteria were explored, as an attempt to understand its enhanced ability to form aggregates in drinking water.

7.2 Materials and Methods

Two sets of experiments were conducted. In the first set of experiments, it was attempted to answer whether the motility of *Methylobacterium* was affected by the viscosity of the substrate, the temperature, the available energy and the type of substrate. Therefore, the motility of pure colonies of *Methylobacterium* was studied on agar plates under different concentrations of agar, different temperatures and different substrate conditions in order to understand whether these conditions would impact the extent and direction of movement of *Methylobacterium* cells. In the second set of experiments, the role of *Methylobacterium* in the interactions between mixed drinking water bacteria was tested. To do that, both pure *Methylobacterium* and mixed drinking water bacterial colonies were inoculated into agar plates.

7.2.1 Pure *Methylobacterium* colonies

The first set of experiments included 3 motility experiments. The total volume of medium in all of them was 30 ml for each agar plate. At 4 symmetric points of each plate there was injection of 5 μ l of the pure *Methylobacterium* culture (Hauwaerts et al., 2002, Rasmussen et al., 2011), which was at the exponential phase of growth (see Section 4.2.1). The 4 *Methylobacterium* colonies in each agar plate had an initial diameter of 2.5 mm. All agar plates were Petri dishes with a diameter of 8.60 cm. The distances between the pure colonies of *Methylobacterium* were equal to half of the radius of the Petri dish. All experiments were performed in triplicates.

The maximum linear movement of *Methylobacterium* was firstly measured, with starting point the centre of injection, at a particular time and by dividing them the maximum velocity of *Methylobacterium* was calculated. An additional measurement was to determine the diameter of the pure colonies of

Methylobacterium at specific time periods. Finally, images of the agar plates were obtained at each of these time periods using the Molecular Imager® Gel Doc™ and the Image Lab™ Software (Bio-Rad Laboratories, Perth, UK). Motility was assessed after 12, 24, 48 and 72 hours of incubation (Simões et al., 2007).

In the first motility experiment, the medium used was 3 g/l R2A, as this medium was previously used for the growth of *Methylobacterium* (see Section 4.2.1). Here, it was used because it is mainly composed of glucose and starch, which provide carbon for adequate energy to cells, and of amino acids and peptides, which provide favourable conditions for the bacterial slime (Harshey, 2003). In the same experiment, in order to explore the effect of viscosity, different concentrations of agar at 0.2%, 0.3% and 1% were tested (Wolfe and Berg, 1989, Ben-Jacob et al., 1994, Simões et al., 2007). To explore the effect of temperature, two different temperatures were tested. The first temperature tested was 28°C, as this was the optimal growth temperature for the *Methylobacterium* strain (see Section 4.2.1), and the other temperature was 16°C, as this was the temperature chosen previously in our experiments (see Sections 3.2.1 and 5.2.1).

In the second motility experiment, it was explored whether a change in the energy available to the *Methylobacterium* cells would affect their motility. This was achieved by testing R2A medium concentrations at 3 g/l and 3 mg/l. In order to ensure that neither viscosity nor temperature would limit motility, in this experiment only 0.2% agar and 28°C temperature were used, as from the first motility experiment it was shown that the higher agar concentrations (0.3% and 1%) and the lower temperature (16°C) had detrimental effects on the motility of *Methylobacterium*.

In the third motility experiment, it was attempted to explore whether the change of substrate and the absence of energy from the R2A medium would affect the motility of *Methylobacterium*. The substrate used here was drinking water that was sampled from a domestic tap in Glasgow (the same as the one in Section 3.2.2). This is most akin to real world conditions, admittedly with a slightly higher viscosity (again at 0.2%), which is needed in order to the plates can be safely moved without disturbing any motility patterns formed. The

temperature of incubation was again at 28°C. The conditions for all 3 motility experiments are summarised in Table 7-1.

First set of experiments	Colonies	Medium	Agar%	Temperature (°C)
1	4 pure <i>Methylobacterium</i>	3 g/l R2A	0.2, 0.3, 1	28, 16
2	4 pure <i>Methylobacterium</i>	3 g/l R2A & 3 mg/l R2A	0.2	28
3	4 pure <i>Methylobacterium</i>	Drinking water	0.2	28

Table 7-1 Summary of conditions of the first set of experiments.

7.2.2 Mixed drinking water and pure *Methylobacterium* colonies

The second set of experiments includes both colonies of mixed drinking water and pure *Methylobacterium* colonies inoculated at discrete points onto plates that comprise 30 ml of drinking water with 0.2% agar at 28°C. As in the first set of experiments, each inoculated colony occupied 5 µl and had a surface diameter of 2.5 mm. The distances between the colonies were the same as previously. The mixed population that was inoculated onto the plates was drawn from a drinking water culture (see Section 4.2.2). The pure *Methylobacterium* colonies were inoculated onto the plates as described previously. Here, only images of the agar plates were obtained after 12, 24, 48 and 72 hours of incubation as described previously. All experiments were again performed in triplicates.

In the first experiment, it was explored whether the presence of *Methylobacterium* within mixed drinking water colonies would impact the interactions between cells. Therefore, 4 colonies of mixed drinking water bacteria were compared with 4 colonies of mixed drinking water bacteria with the *Methylobacterium* inoculated at 1% relative abundance.

In the second experiment, it was tested whether the presence of pure *Methylobacterium* colonies in the same plate with mixed drinking water colonies would result in different findings from those of the first experiment. Therefore, 2 colonies of mixed drinking water bacteria and 2 pure colonies of *Methylobacterium* in a plate were compared with 2 colonies of mixed drinking

water with the *Methylobacterium* inoculated at 1% relative abundance and 2 pure colonies of *Methylobacterium* in another plate. The conditions of these experiments are summarised in Table 7-2.

Second set of experiments	Colonies	Medium	Agar%	Temperature (°C)
1	4 DW colonies to be compared with 4 DW colonies with 1% M.	DW	0.2	28
2	2 DW colonies + 2 M. colonies to be compared with 2 DW colonies with 1% M. + 2 M. colonies	DW	0.2	28

Table 7-2 Summary of conditions of the second set of experiments.
“DW” refers to drinking water and “M” refers to *Methylobacterium*.

7.3 Results and Discussion

7.3.1 Motility of pure *Methylobacterium* colonies

In the first motility experiment, it was found that the viscosity and the temperature had significant effects on the motility of *Methylobacterium*. The bacteria only moved in the lowest agar concentration (0.2%) and only at 28°C; at agar concentrations above the 0.2% and at 16°C temperature, there was no motility observed on the plates. This is unsurprising as the drag is related to both the viscosity and the velocity, and the energy required to overcome the viscous drag force increases with viscosity. Also, it was expected to find this result regarding the temperature, as the 16°C is a much lower temperature from the optimum for the *Methylobacterium* at 28°C. Thus, all subsequent motility experiments were conducted for the lowest viscosity environment at 28°C.

In the second motility experiment, in which the concentration of R2A was varied to ascertain the effect of different levels of energy on the motility of *Methylobacterium*, it was found that the motility was enhanced for the higher concentration of R2A at 3g/l. In the third motility experiment, it was found that the absence of energy affected the motility of *Methylobacterium*, which was found to be further decreased when drinking water was used as available medium.

Overall, the motility of *Methylobacterium* was decreased with time with the maximum velocity of *Methylobacterium* cells be at the first 12 hours. The medium with the highest offered energy to cells was the one for which the highest velocity of *Methylobacterium* was found. These results are shown in Figure 7-1. The maximum diameter of *Methylobacterium* colonies was determined at the first 12 hours for all the tested conditions. After 12 hours of incubation, the diameter of the colonies was not changed and thus, no further measurements were recorded. These results are shown in Figure 7-2.

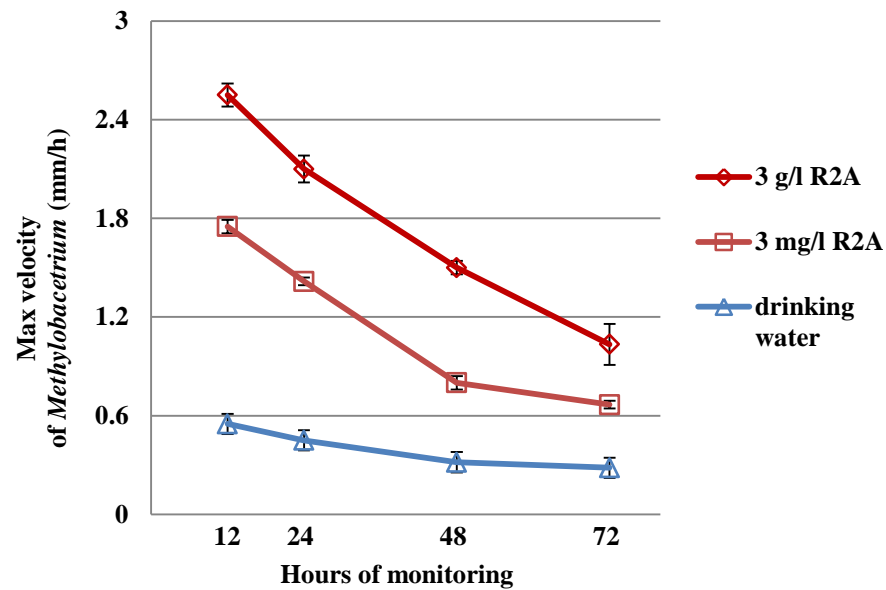


Figure 7-1 Motility of *Methylobacterium* at 0.2% agar medium after 12, 24, 48 and 72 hours of incubation at 28°C.

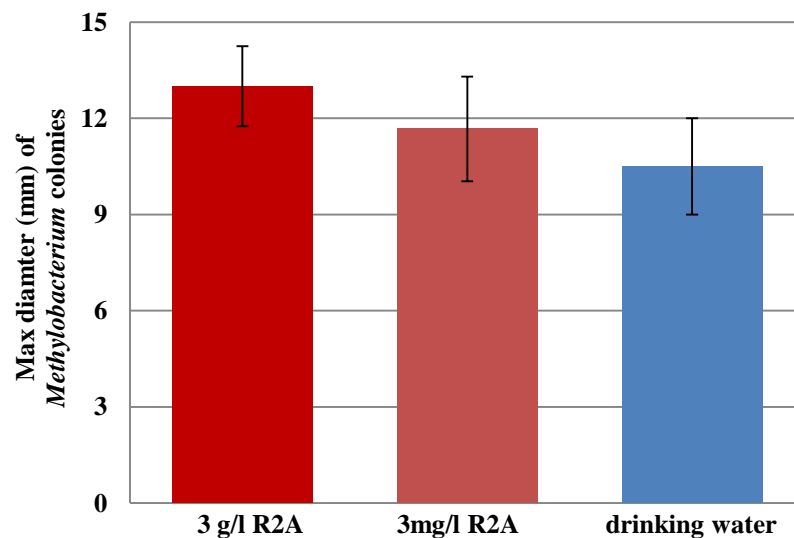
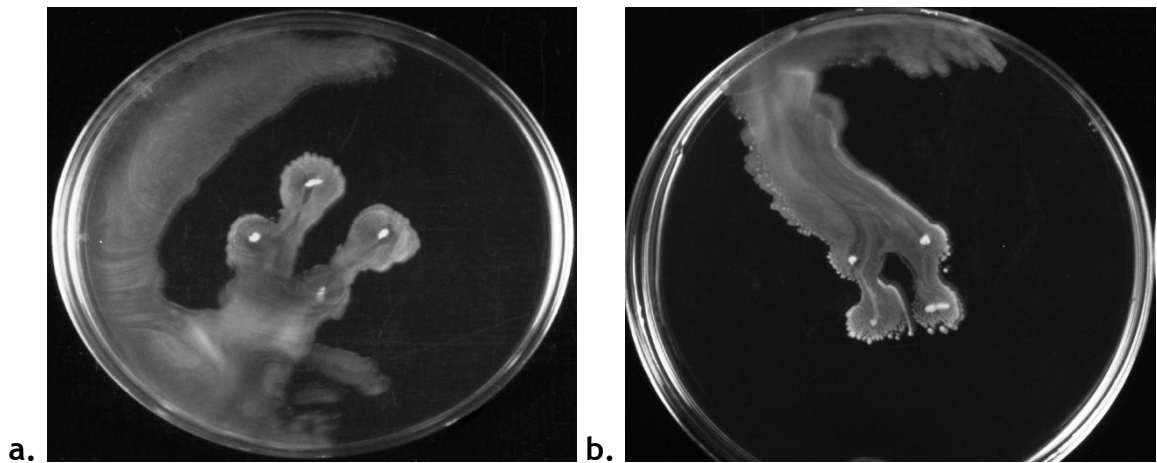


Figure 7-2 Maximum diameter of pure *Methylobacterium* colonies at 0.2% agar medium after 12 hours of incubation at 28°C.

From Figure 7-3a and Figure 7-3b, it can be seen that the *Methylobacterium* colonies had the same behaviour when R2A was the available medium. The colonies were migrated towards the centre of the dish and then moved off “en masse” towards the wall to the dish. The fact that they firstly moved in a coordinated manner towards the centre suggests that the organisms can sense one-another, perhaps through chemotaxis, and that there is some benefit to aggregating. The fact that once congregated in the centre of the plate they moved off together rather than spreading radially suggests that once aggregated they acted in a coordinated way perhaps driven by some sort of quorum sensing.

From Figure 7-3c, it was shown that the behaviour of the *Methylobacterium* colonies in drinking water was clearly different from that in R2A medium. The colonies here appeared to move away from one another. This pattern shows that there was no aggregation between cells. The fact that the bacteria moved away from one another suggests that chemotaxis may well be at play, but it is chemotaxis in search of resources. Thus, the bacteria moved away from where the population was dense and resources were depleted.



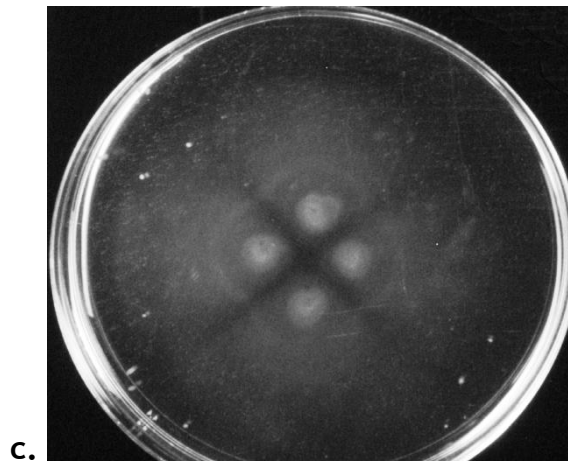


Figure 7-3 Motility of *Methylobacterium* in different substrate conditions at 0.2% agar medium after 12 hours of incubation at 28°C. (a) in 3 g/l R2A, (b) in 3 mg/l R2A and (c) in drinking water.

7.3.2 Interactions of mixed drinking water and pure *Methylobacterium* colonies

In the first experiment, it was observed that in the mixed drinking water colonies in which *Methylobacterium* was inoculated at 1% relative abundance, there were more bacterial movements observed on the agar plates and bacteria tended to communicate more with each other (Figure 7-4b) compared to the mixed drinking water colonies in which there was no *Methylobacterium* inoculated (Figure 7-4a).

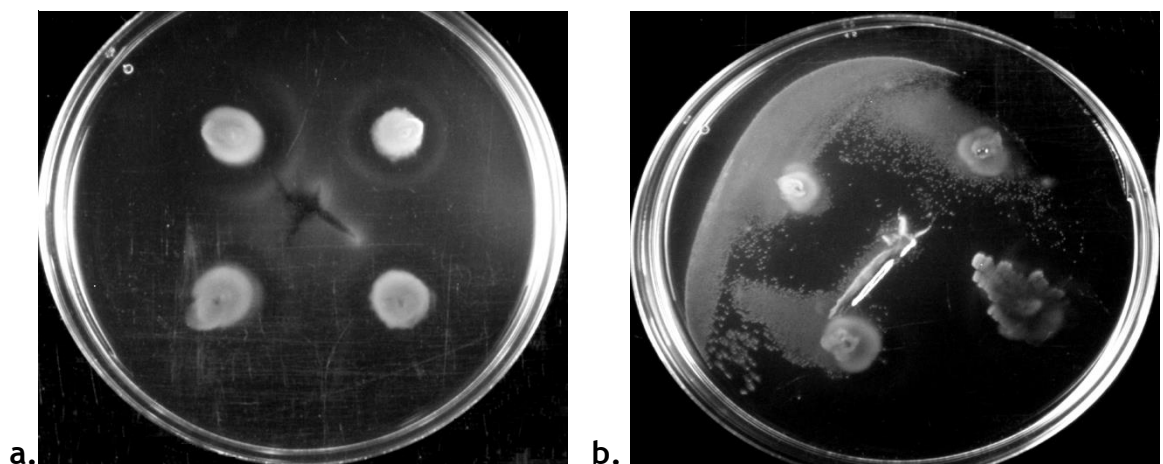


Figure 7-4 Interactions of mixed drinking water colonies with and without *Methylobacterium* addition after 12 hours of incubation. (a) Four mixed drinking water colonies and (b) four mixed drinking water colonies with 1% *Methylobacterium* inoculated.

In the second experiment, in which there was presence of both pure colonies of *Methylobacterium* and mixed drinking water colonies in the same plate, it was

found that the pure *Methylobacterium* colonies were not able to grow in the plate as the mixed drinking water colonies did (Figure 7-5). However, it was again obvious that in the two mixed drinking water colonies in which there was *Methylobacterium* inoculated at 1% relative abundance, there were more bacterial movements observed on the agar plates (Figure 7-5b) compared those in which there was no addition of *Methylobacterium* in the two mixed drinking water colonies (Figure 7-5a). The most important difference of this experiment with the previous one is that here there were cell interactions between the 2 mixed drinking water colonies without the inoculated 1% *Methylobacterium* (Figure 7-5a), which were not observed in the 4 mixed drinking water colonies, which were again without the inoculated 1% *Methylobacterium* in the first experiment (Figure 7-4a). This suggests that the presence of pure *Methylobacterium* colonies in the plate triggered the communication between the mixed drinking water colonies.

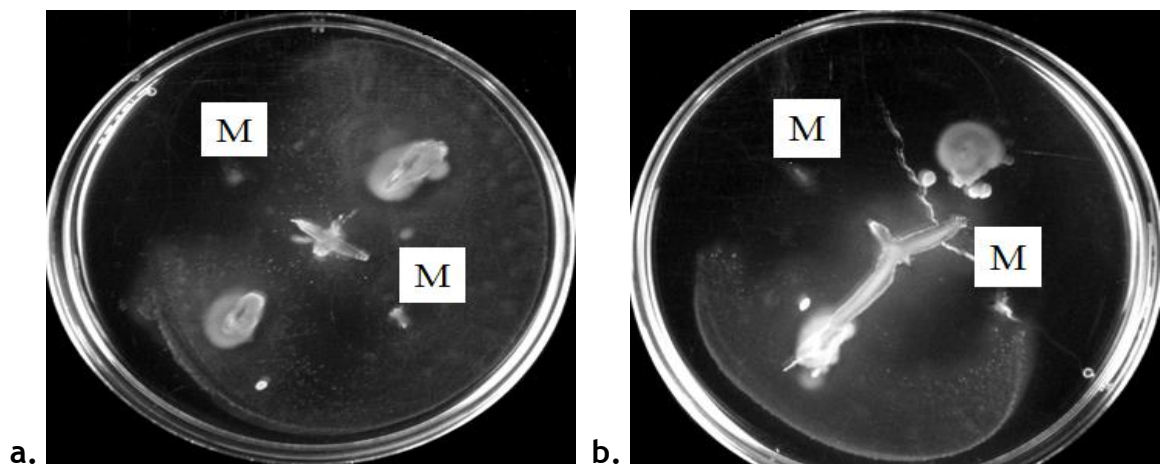


Figure 7-5 Interactions of mixed drinking water colonies with and without *Methylobacterium*, and of pure *Methylobacterium* colonies after 12 hours of incubation. (a) Two mixed drinking water colonies and two pure colonies of *Methylobacterium* (indicated with “M”) and (b) two mixed drinking water colonies with 1% *Methylobacterium* inoculated, and two pure colonies of *Methylobacterium* (indicated with “M”).

7.4 Conclusions

From the first set of experiments in which the *Methylobacterium* DSM 18358 was the only present species on the plates, it was shown that the *Methylobacterium* was motile only for the lowest agar concentration at 0.2% and the higher temperature tested at 28°C. This indicated the important role that the viscosity of the substrate and the temperature play in the motility of the *Methylobacterium*. The most favourable conditions for the motility of the

Methylobacterium were those in which the highest energy was provided to cells. This was found in R2A medium, in which cells were communicating with each other and tending to aggregate. When the medium switched from energy sufficient conditions to drinking water, the motility of *Methylobacterium* was decreased and the pure colonies tended to spread away from each other in the search for nutrients.

From the second set of experiments in which the *Methylobacterium* was inoculated into mixed drinking water bacterial colonies at 1% relative abundance, it was found that its presence significantly enhanced the communication between drinking water bacteria even in a nutrient poor environment like drinking water. It was also found that the presence of pure *Methylobacterium* colonies on the same plate with mixed drinking water colonies enhanced the ability of the drinking water bacteria to interact with each other and aggregate. The patterns observed from both sets of experiments were obvious even from the first 12 hours. Overall, this work proved again the important role of the *Methylobacterium* DSM 18358 in drinking water.

8 Effect of *Methylobacterium* on trihalomethanes concentration in drinking water

8.1 Introduction

Disinfectants that are routinely used in DWDS include chlorine (Cl_2), chloramines (NH_2Cl) and chlorine dioxide (ClO_2). Where chlorine or chloramines are used as disinfectants, trihalomethanes (THM) and haloacetic acids (HAA) emerge as by-products (Rodriguez et al., 2004, Zhang et al., 2009, Simoes and Simoes, 2013). Trihalomethanes are produced when the hydrogen atoms (H) in methane (CH_4) are replaced by halogen atoms: chlorine, fluorine (F), bromine (Br), iodine (I) and astatine (At). Haloacetic acids are produced when the hydrogen atoms in acetic acids (CH_3COOH) are replaced by halogen atoms. These two classes of disinfection by-products, THM and HAA, are the most common and have demonstrated carcinogenic activity in animals (Pereira, 2000). Other chlorine disinfection by-products include haloacetonitriles, haloketones and chloropicrin (Chen and Weisel, 1998).

In water treatment, chlorine is applied in one of three forms: as a compressed gas under pressure, which is dissolved in water at the point of application, as sodium hypochlorite solution or as calcium hypochlorite solution. The rate of decay of chlorine concentration in the bulk water is primarily a function of the concentration of organic matter in drinking water, the water temperature and the initial chlorine concentration. However, chlorine can also decay through its interactions with the materials of pipes, wall tanks and fittings, or with the adhering on them biofilms (Brown et al., 2011). New and alternative techniques for disinfection, such as the combination of ultra violet irradiation and direct electrolysis (Bergmann et al., 2002), the combination of acoustic (Jyoti and Pandit, 2001) and hydrodynamic cavitation (Mezule et al., 2009), and hybrid cavitation (Jyoti and Pandit, 2003), have the advantage that neither THM nor HAA are produced (Simoes and Simoes, 2013).

The THM that are mostly present in drinking water are chloroform (CHCl_3), bromoform (CHBr_3), dibromochloromethane (CHBr_2Cl) and bromodichloromethane (CHBrCl_2) (Rodriguez and Serodes, 2001). Chloroform is the most common of THM (Lebel and Williams, 1995). The HAA that are mostly

present in drinking water are monochloroacetic acid ($C_2H_3ClO_2$), dichloroacetic acid ($C_2H_2Cl_2O_2$), trichloroacetic acid ($C_2HCl_3O_2$), monobromoacetic acid ($C_2H_3BrO_2$) and dibromoacetic acid ($C_2H_2Br_2O_2$) (Chang et al., 2001). In general, high concentrations of THM correlate with high concentrations of free and total chlorine, high concentrations of humic and non-humic substances, high temperature, high pH, and finally, high concentrations of bromide ions (Chen and Weisel, 1998, Sadiq and Rodriguez, 2004, Deborde and von Gunten, 2008, Brown et al., 2011). Levels of THM vary seasonally; concentrations have been found to be higher in summer, that the temperature of water is higher than in winter (Dyck et al., 2015).

In a DWDS it was shown that spatial changes of THM and HAA were important and the pattern of these changes was different for them. In particular, the concentrations of THM were increased and finally stabilised in the distribution system extremities, but this was not the case for HAA, the concentrations of which were decreased approaching the extremities probably because of microbiological degradation of these substances (Rodriquez et al., 2004). However, due to the complexity and uncertainty of reactions between chlorine and organic matter, no successful models of predicting THM formation have been developed; most existing models are empirical and therefore, include a number of constants, with no physical meaning, which must be determined by experiments (Brown et al., 2011).

Chloroform, the most common THM, is found in a variety of environments, such as the outdoor air of urban areas, the indoor air by release from water, a variety of food and soft drinks, and drinking water (WHO, 2008). Examples of anthropogenic chloroform sources are pulp and paper mills, water treatment plants, chemical manufacturing plants and waste incinerators (Cappelletti et al., 2012). Acute health problems from exposure to chloroform are rare and associated with high concentrations. For instance, anaesthesia using chloroform can result in respiratory and cardiac arrhythmias. Occupational exposure to chloroform can cause renal tubular necrosis and liver toxicity (WHO, 2008). There is evidence that the chronic effects of long-term exposure to chloroform might cause cancer and reproductive problems (Melnick et al., 1994, Gallagher et al., 1998, Waller et al., 1998).

For most of the human population their greatest exposure to chloroform at low concentrations is as a disinfection by-product in drinking water. The primary source of chloroform in chlorinated drinking water has been found to be the reaction between chlorine and naturally occurring organic compounds (Brown et al., 2011). Examples of organic compounds that can be found in drinking water supplies come from pharmaceuticals, fragrances, flame retardants, plasticizers, components of personal care products, etc. Some of these compounds may not be completely degraded or removed during wastewater treatment (Stackelberg et al., 2007).

Microbial chloroform degradation occurs under both anaerobic and aerobic conditions and has been mostly studied as a cometabolic process with chloroform used by bacteria as carbon and energy source. Alkanes, hydrocarbons and ammonia have been used as growth substrates to support chloroform cometabolism via the activity of enzymes produced by microorganisms (Cappelletti et al., 2012). Methane is a common substrate used for chloroform cometabolism. By the oxidation of methane via the activity of methane monooxygenases, methanol is firstly produced and then methanol is oxidized in three consecutive steps to formaldehyde, formate, and carbon dioxide (Jahng and Wood, 1994, Semrau et al., 1995, Lieberman and Rosenzweig, 2004). Methylophiles under aerobic conditions and methanogens under anaerobic conditions have been associated with the biodegradation of chloroform (Cappelletti et al., 2012, Zamani et al., 2015).

Methylobacterium species have been found to be able to utilize chlorinated methanes as the sole carbon and energy source (Leisinger and Braus-Stromeyer, 1995, Kayser, 2001, Trotsenko and Doronina, 2003). Drinking water bacteria including *Methylobacterium* isolated from DWDS have been shown to be capable of degrading HAA after they grew in high concentrations of HAA enrichment cultures (Zhang et al., 2009). The *Methylobacterium* CRL-26 strain was found to be able to degrade chloroform with methane used as available substrate (Patel et al., 1982, Cappelletti et al., 2012). These findings motivated our research to study if the inoculation of *Methylobacterium* DSM 18358 in drinking water might have a significant effect on the concentration of THM. Thus, THM concentrations were conducted in raw drinking water and in drinking water with the

Methylobacterium inoculated at different relative abundances. In addition, the role of the organic compounds and chlorine concentrations in THM concentration was studied as these are two key factors affecting THM formation in drinking water.

8.2 Materials and Methods

Drinking water was sampled again from a domestic tap in Glasgow (the same as the one in Section 3.2.2). The *Methylobacterium* DSM 18358 strain was chosen again as previously in this study (Chapters 4-7). The pure *Methylobacterium* culture was created as described in Section 4.2.1. The *Methylobacterium* cells were then harvested at the exponential phase of growth and used as inoculum into the drinking water as described in Section 4.2.3, in order to inoculate the drinking water with different relative abundances of *Methylobacterium* at 1% and 10%.

The USEPA DPD Method 8167 (Chamberlain and Adams, 2006) was followed to measure the total chlorine concentration in drinking water using the DR 900 Hach colorimeter (Colorado, US). A total chlorine reagent powder pillow (Hach, Colorado, US) was used for each measurement. During this measurement, combined chlorine, which is part of the total chlorine, oxidizes iodide. Then, iodine and free chlorine, which is the other part of total chlorine, react with DPD (N,N-diethyl-p-phenylenediamine) to form a pink colour, which is proportional to the total chlorine concentration. The measurements were performed in triplicates in 10 ml samples and the wavelength of the measurements was at 520 nm (see Appendix 10.5.1 for the analytical protocol).

The concentration of THM was measured following the THM PlusTM Method 10132 (Fujiwara, 1916, Khan et al., 2014) using the DR 2800 Hach spectrophotometer. Four chemical solutions from Hach were used for each measurement; the 27539-29 THM Plus reagent, the 27540-48 THM Plus reagent, the 27541-42 THM Plus reagent and the 2756559 pH storage solution. During this measurement, trihalomethanes present in the sample react firstly with N, N,-diethylnicotinamide under heated alkaline conditions to form a dialdehyde intermediate using the first 2 reagents. The sample is then cooled and acidified using the third reagent. Then, the dialdehyde intermediate reacts with 7-amino-

1,3 naphthalene disulfonic acid to form a coloured Schiff base using the last Hach solution. The colour formed is proportional to the total amount of THM present in the sample. The measurements were performed in triplicates in 10 ml samples and the wavelength of the measurements was at 515 nm (see Appendix 10.5.2 for the analytical protocol). Some additional disinfection by-products, which are included in the result from this test are: 1,1,1-trichloro-2-propanone, 1,1,1-trichloroacetonitrile, chloral hydrate and the HAA: dichlorobromoacetic acid, dibromochloroacetic acid, tribromoacetic acid and trichloroacetic acid.

8.2.1 Chlorine and trihalomethanes measurements at different times of water sampling

Chlorine and THM concentrations were measured in raw drinking water from 8.00 hours to 18.00 hours every 2 hours in order to study if there were differences in their concentrations depending on the time of water sampling. There was no control of the temperature in those measurements because the samples were processed immediately after water sampling. Therefore, the temperature of the samples at the time of measurement was the same as that of drinking water that was sampled from the tap.

8.2.2 Chlorine and trihalomethanes measurements under different *Methylobacterium* concentrations

Chlorine and THM concentrations were measured in raw drinking water and in drinking water with the *Methylobacterium* strain DSM 18358 inoculated at relative abundances of 1% and 10%, to study the effect that *Methylobacterium* might have on their concentrations. The role of *Methylobacterium* in THM concentration was also studied in a solution, in which there was no chlorine or any organic matter other than *Methylobacterium* cells. The goal of this measurement was to exclude the effect of chlorine and organic matter on THM concentration, and only focus on the potential effect of *Methylobacterium*. This solution was a standard THM solution of 100 µg/l THM concentration. *Methylobacterium* cells were injected into that standard solution at 10⁵ cells/ml concentration and THM concentrations were then measured after 0, 1, 3, 6 and 24 hours. The temperature of the samples was maintained at 4°C as THM are volatile chlorination by-products (Nikolaou et al., 2002).

8.2.3 Chlorine and trihalomethanes measurements in drinking water under different organic matter concentrations

In order to understand the role of organic matter in chlorine and THM concentrations, the raw drinking water and the one with *Methylobacterium* inoculated at 1% and 10% relative abundances were autoclaved so that there are no active bacteria that could affect the measurements. The samples were autoclaved at 121°C for approximately 60 minutes and then, chlorine and THM concentrations were measured after 0, 1, 3, 6 and 24 hours at 4°C.

Extracellular polymeric substances are important polymers of high molecular weight secreted by microorganisms (Staudt et al., 2004). The potential change of the amount of EPS in drinking water might explain the change in the concentration of THM in drinking water. The surface area of EPS was measured as described in Section 3.2.6 for 10 ml samples from the 3 samples (the raw drinking water and the one with *Methylobacterium* inoculated at 1% and 10% relative abundances) after 0, 1, 3, 6 and 24 hours at 4°C.

Finally, the effect of glucose on the concentrations of chlorine and THM in drinking water was studied in order to further explore the role of organic matter in THM formation. That allowed us to test if chlorine would react with this additional organic matter added from the glucose to drinking water so that THM be formed. Chlorine and THM concentrations were measured in raw drinking water after 0, 1 and 3 hours, and after the 3-hour measurement 1% glucose was added to drinking water. Measurements of chlorine and THM concentrations were conducted after 3 and 21 hours from the glucose addition. The temperature was maintained at 4°C.

8.2.4 Trihalomethanes measurements in drinking water under different chlorine concentrations

Here, the effect of chlorine concentration on THM concentration was studied for the raw drinking water and for the one with *Methylobacterium* inoculated at 1% and 10% relative abundances. Specifically, sodium thiosulfate ($\text{Na}_2\text{S}_2\text{O}_3$) was added to the 3 samples in order to reduce chlorine concentration (Jarroll et al., 1981, Barbera et al., 2012). The effect of that chlorine decay on THM concentration in drinking water was studied. A crystal of $\text{Na}_2\text{S}_2\text{O}_3$ at 0.1 N

(248.18 g/mol) concentration (WaterCommittee, 1953) was added to the samples and then, chlorine and THM concentrations were measured after 5 and 10 minutes at 4°C.

8.3 Results

8.3.1 Chlorine and trihalomethanes concentrations in raw drinking water

The time of sampling of drinking water from the tap was found to affect the concentration of chlorine. The lowest chlorine concentration was found at 8.00 hours, then it was increased until 14.00 hours and finally, it was decreased until 18.00 hours. Also, the time of sampling affected the concentration of THM, which was generally decreased from 8.00 hours to 18.00 hours (Figure 8-1).

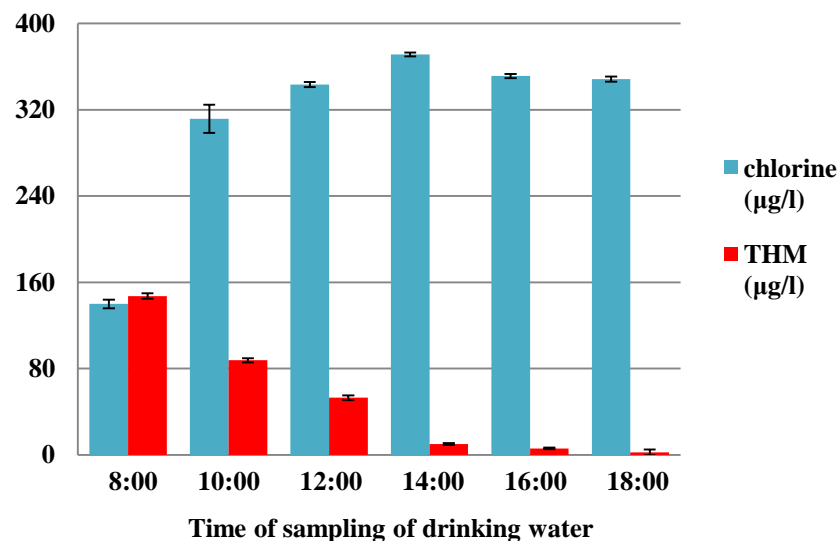


Figure 8-1 Chlorine and THM concentrations in raw drinking water at different times of water sampling from 8.00 hours to 18.00 hours every 2 hours. The error bars represent the standard deviation of the measurements.

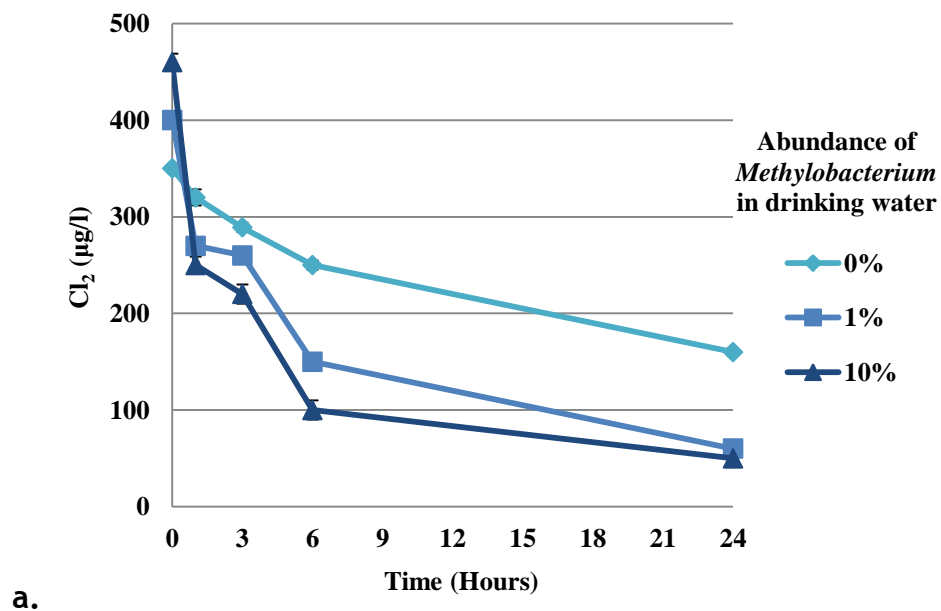
8.3.2 The role of *Methylobacterium* in chlorine and trihalomethanes concentrations

It was found that the chlorine concentration in raw drinking water was decreased over the 24-hour period (Figure 8-2a). The THM concentration in raw drinking water was initially decreased sharply, but after the first 3 hours there

was a steady and slow increase for the remaining 21 hours for which measurements were taken (Figure 8-2b).

Chlorine concentration was found to be decreased with time in drinking water with the presence of the *Methylobacterium*. The rate of decline was marginally affected by the relative abundance at which the *Methylobacterium* was inoculated into drinking water (Figure 8-2a). Also, when *Methylobacterium* was added to drinking water, the change in the concentration of THM over time displayed the opposite behaviour from that in raw drinking water; an initial sharp increase up to the first 3 hours followed by a steady decline. The THM concentration at the last measurement was almost the half from the initial one (Figure 8-2b).

Finally, the addition of *Methylobacterium* in the THM standard solution was found to have a profound effect on the concentration of THM. Specifically, the concentration of THM was decreased over the 24-hour period. The concentration of THM at the last measurement was less than the half from the initial one (Figure 8-3).



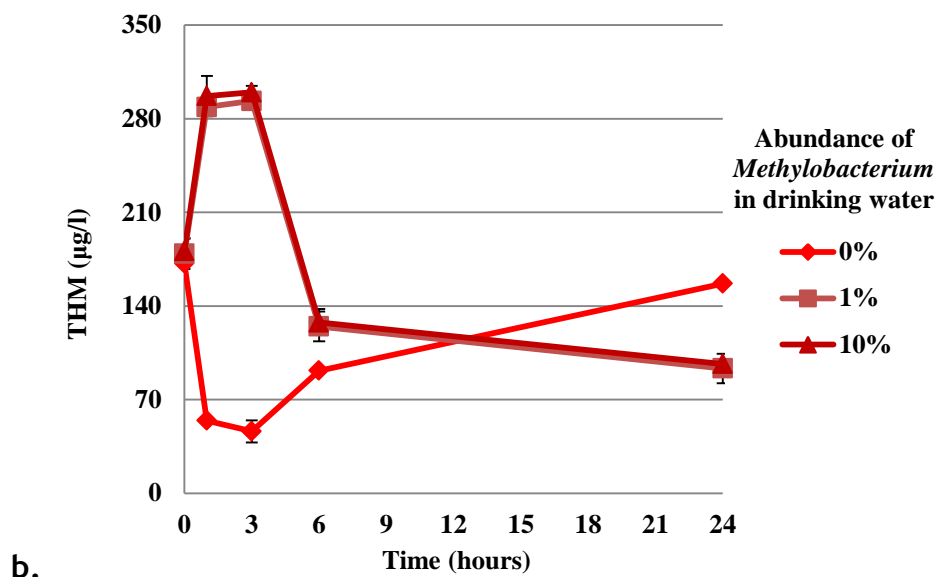


Figure 8-2 Chlorine and THM concentrations in drinking water with *Methylobacterium* after 0, 1, 3, 6 and 24 hours at 4°C.

(a) Chlorine and (b) THM concentrations in raw drinking water and in drinking water with *Methylobacterium* inoculated at 1% and 10% relative abundances. The error bars represent the standard deviation of the measurements.

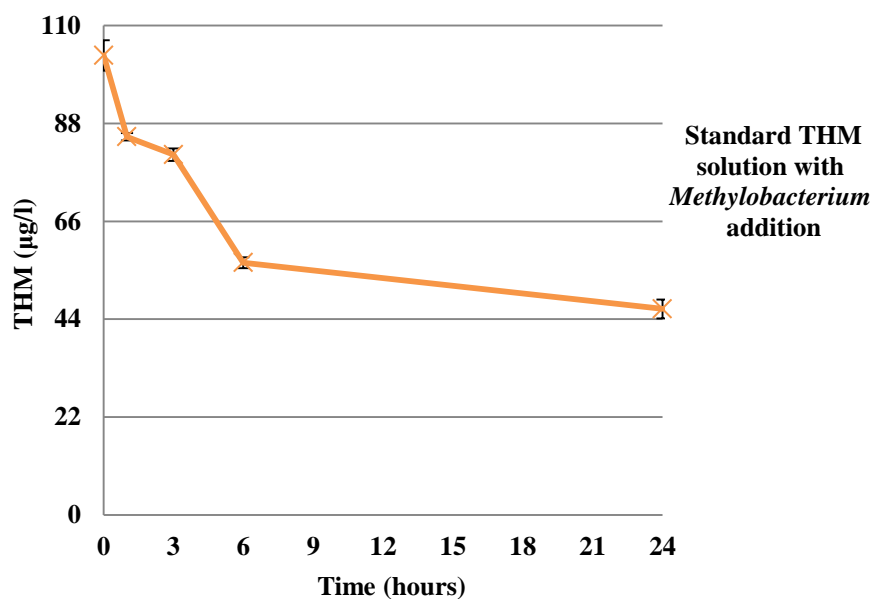
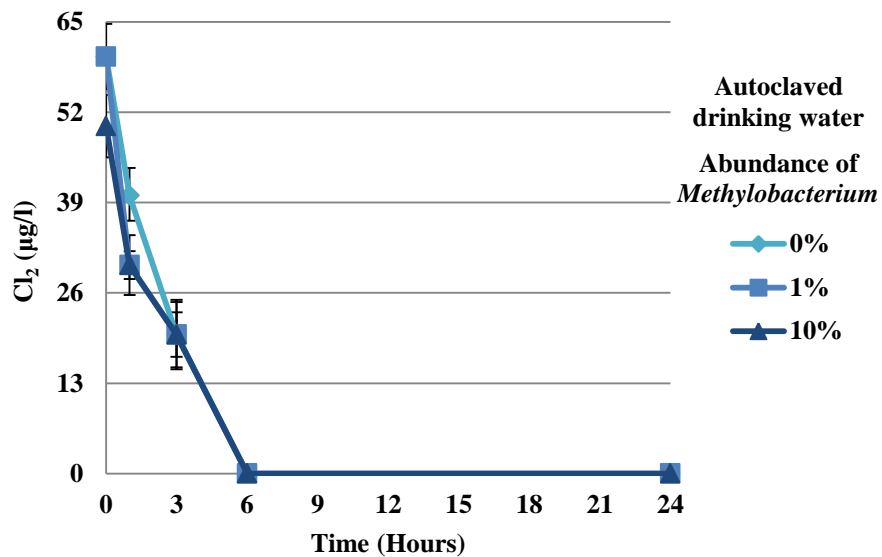


Figure 8-3 Concentration of THM in a THM standard solution with *Methylobacterium* addition after 0, 1, 3, 6 and 24 hours at 4°C.

Methylobacterium was added to the THM solution with a concentration of 10^5 cells/ml at the 0-hour measurement. The error bars represent the standard deviation of the measurements.

8.3.3 The role of organic matter in chlorine and trihalomethanes concentrations

The chlorine concentration from the first measurement at 0 hour was found to be very low in the autoclaved samples and its concentration was equal to zero after the 6-hour measurement. In addition, it was shown that the presence of the dead *Methylobacterium* cells in the samples accelerated the decrease of chlorine concentration. Again, the rate of decline was marginally affected by the relative abundance at which the *Methylobacterium* was inoculated (Figure 8-4a). Also, THM were found to be formed only up to the first 6 hours that chlorine was still present in the sample. The higher was the amount of organic matter, depending on the number of dead cells in each of the 3 samples, the higher was the THM formation (Figure 8-4b).



a.

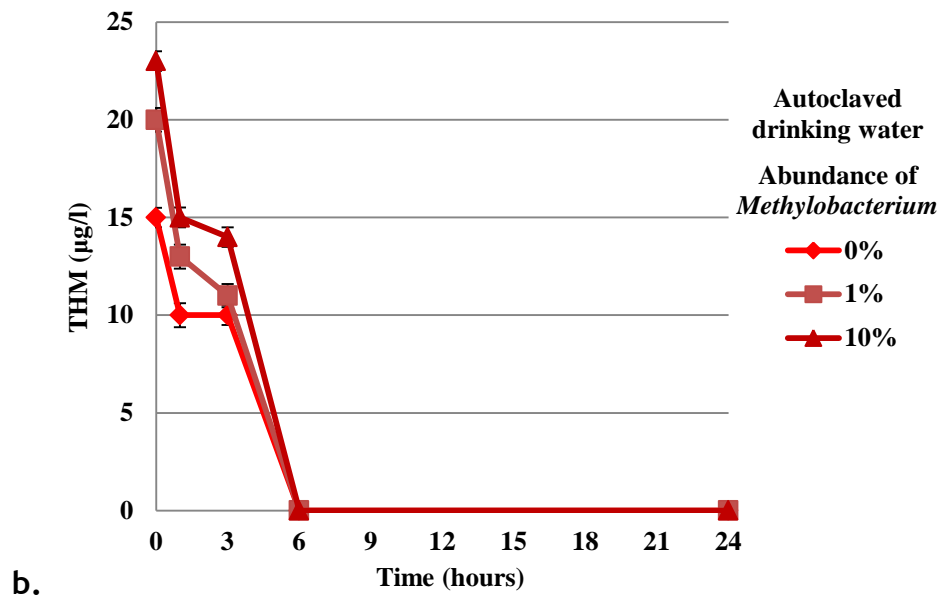


Figure 8-4 Chlorine and THM concentrations in autoclaved drinking water after 0, 1, 3, 6 and 24 hours at 4°C.
(a) Chlorine and (b) THM concentrations in autoclaved samples of raw drinking water and of drinking water with *Methylobacterium* inoculated at 1% and 10% relative abundances. The error bars represent the standard deviation of the measurements.

In raw drinking water only modest differences were found in the surface area of EPS during the 24-hour period. However, in the drinking water with inoculated *Methylobacterium* a shift increase in the surface area of EPS was found that was most evident up to the first 3 hours, regardless the concentration of *Methylobacterium* (Figure 8-5).

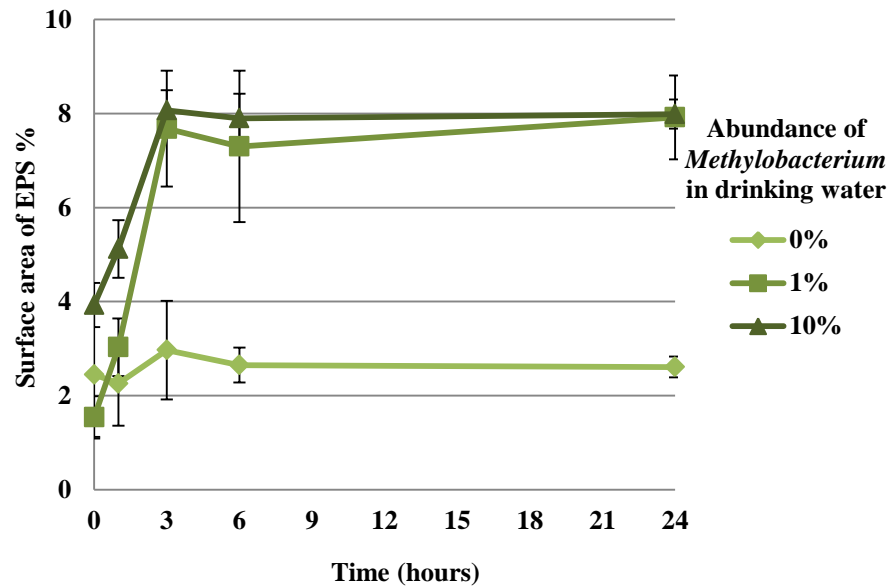


Figure 8-5 Percentage of surface area of EPS in drinking water after 0, 1, 3, 6 and 24 hours at 4°C.

Samples from raw drinking water and from drinking water with *Methylobacterium* inoculated at 1% and 10% relative abundances were taken. The error bars represent the standard deviation of the measurements.

The addition of 1% glucose to drinking water caused a sharp decrease in the concentration of chlorine with time; the concentration of chlorine was equal to zero at the 24-hour measurement. The concentration of THM displayed the opposite behaviour of that of chlorine; THM concentration was increased with time up to a final concentration which was more than 3 times higher than the initial one (Figure 8-6). Also, the behaviour of chlorine and THM in raw drinking water up to the first 3 hours, before the addition of glucose to drinking water, was the same as it was previously shown (Figure 8-2).

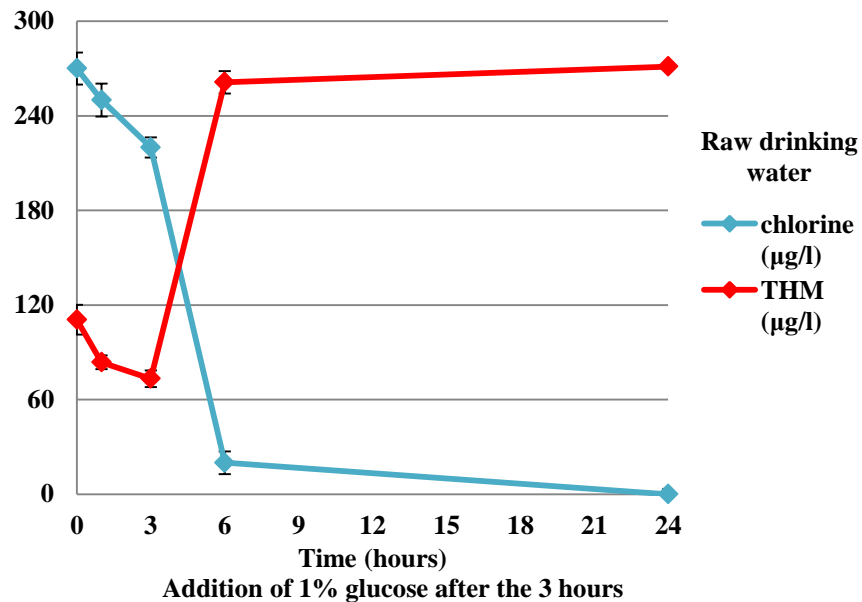
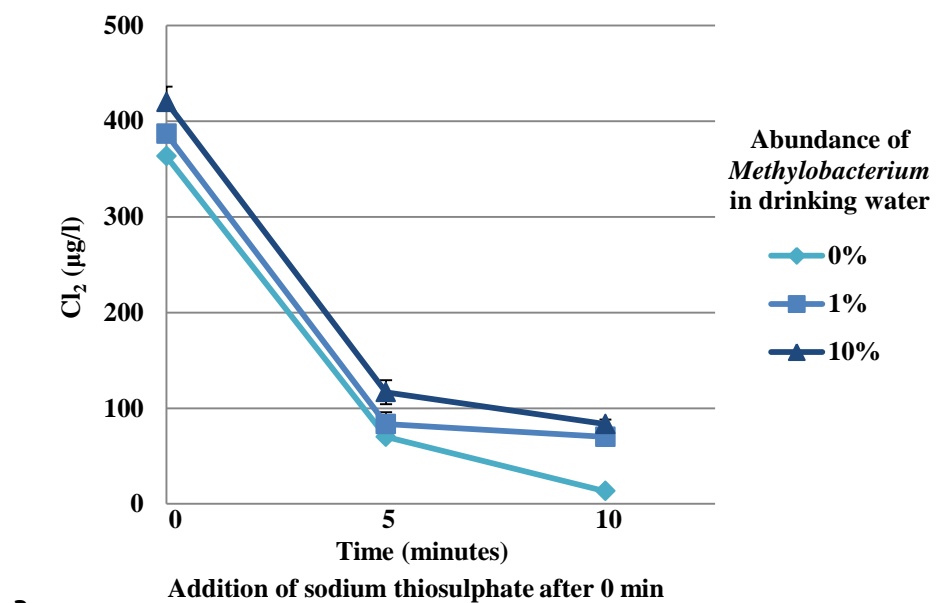


Figure 8-6 Chlorine and THM concentrations in drinking water with 1% glucose addition after 0, 1, 3, 6 and 24 hours at 4°C. The error bars represent the standard deviation of the measurements.

8.3.4 The role of chlorine in trihalomethanes concentration

After the addition of sodium thiosulphate to drinking water the concentration of chlorine was sharply decreased in all 3 drinking water samples regardless the presence or absence of *Methylobacterium* (Figure 8-7a). This decrease of chlorine concentration was found to affect the concentration of THM only in raw drinking water, in which the concentration of THM was decreased (Figure 8-7b).



a.

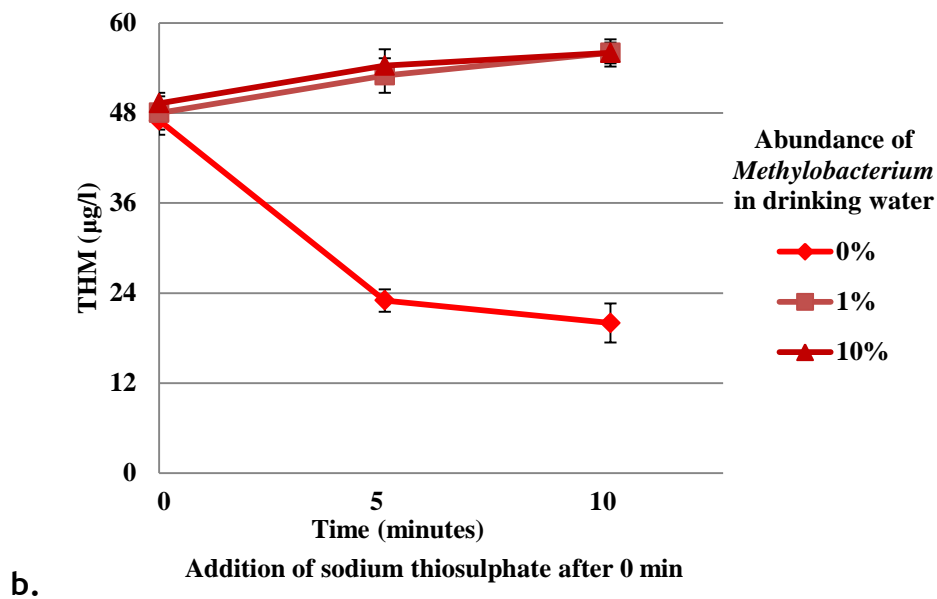


Figure 8-7 Chlorine and THM concentrations in drinking water with sodium thiosulphate addition after 0, 5 and 10 minutes at 4°C.
(a) Chlorine and (b) THM concentrations in raw drinking water and in drinking water with *Methylobacterium* inoculated at 1% and 10% relative abundances. The error bars represent the standard deviation of the measurements.

8.4 Discussion

During the hours in which people do not use the tap often, biofilms may be formed at the inner surfaces of the pipes in stagnant waters (Momba and Kaleni, 2002, Beech and Sunner, 2004, Simoes and Simoes, 2013). This can cause decrease in the concentration of chlorine in drinking water through its interaction with the bacteria in the bulk water or with the adhering on them biofilms (Brown et al., 2011). This was shown in our experiments, where chlorine concentration was low early in the morning and later in the afternoon. It was also shown that early in the morning the concentration of THM was high. This might happen because even this low amount of chlorine that was still present in water had enough time during the night in order to react with the organics and form THM. This should not be a surprising result since it has been previously shown that the longer time the chlorine has available to react with the organic compounds in drinking water, the higher is the formation of THM (Rodriguez and Serodes, 2001, Sadiq and Rodriguez, 2004).

When chlorine concentration was monitored over time in raw drinking water, it was found that there was a stable decrease in its concentration for the first 3 hours, and the same was found for the concentration of THM. This happened

because as chlorine concentration was decreased there was less available chlorine to react with the organic compounds and form THM. After the first 3 hours, even though chlorine concentration was again decreased with time, it was found that THM concentration was increased. Over the last 21 hours of measurements the remaining chlorine in drinking water reacted with the organics that were available in drinking water and that caused the formation of THM.

When the *Methylobacterium* was added to drinking water the decrease in the concentration of chlorine with time was enhanced. Regarding the concentration of THM, it was found that during the first 3 hours, the *Methylobacterium* caused the increase in the concentration of THM. The EPS measurements showed that the first 3 hours were critical as the *Methylobacterium* produced EPS, which suggests the formation of aggregates in drinking water (Sheng et al., 2010). This agrees with our previous findings about the enhanced ability of the *Methylobacterium* to form aggregates in drinking water. The formation of these aggregates caused the formation of EPS, which caused the increase in the formation of organic matter and that subsequently caused the increase in the concentration of THM in drinking water.

After the first 3 hours there was significant decrease in the concentration of THM with a final concentration equal to almost the half of the initial one. This may suggest that the formation of aggregates by the *Methylobacterium* accelerated the decrease of THM concentration. This ability of the *Methylobacterium* to decrease the concentration of THM was also proved by the measurements in the THM standard solution, in which the *Methylobacterium* was found to be able to decrease the concentration of THM with a final concentration equal to less than the half of the initial one. The reason why the *Methylobacterium* was found to be able to decrease THM concentration might be that it utilised them as an energy and carbon source in order to grow and form aggregates in drinking water.

The addition of glucose to drinking water was proved to be important as chlorine concentration was rapidly decreased with time to a final concentration equal to zero. This happened because chlorine reacted with glucose and this caused THM formation. The formation of THM was shown by the rapid increase of their

concentration with a final concentration equal to 2 times higher than the initial one. Similarly, the higher organic matter, derived from the dead *Methylobacterium* cells in the autoclaved inoculated drinking water, resulted to higher concentrations of THM than that in the autoclaved raw drinking water. The decrease of the concentration of chlorine here resulted in the decrease of the concentration of THM.

This positive correlation in the concentrations of chlorine and THM was also proved in the measurements with the sodium thiosulphate, in which the rapid decrease of the concentration of chlorine resulted in the decrease of the concentration of THM in raw drinking water. On the other hand, in the inoculated with the *Methylobacterium* drinking water, this did not happen as again the *Methylobacterium* proved to increase the concentration of THM in the initial phase. Finally, the results from this work proved again that the behaviour of *Methylobacterium* DSM 18358 was qualitatively the same when it was inoculated into drinking water at either low (1%) or high (10%) relative abundance.

8.5 Conclusions

In this study, it was shown that the *Methylobacterium* strain DSM 18358 played an important role in the concentration of THM in drinking water. When it was inoculated into drinking water, even at 1% relative abundance, it was found to be able to decrease the concentration of THM after 24 hours to almost the half of their initial concentration. After the conduction of various experiments, which included changes in the concentrations of chlorine and organic matter, the role of this *Methylobacterium* strain in the concentration of THM in drinking water was revealed.

At the first 3 hours, the *Methylobacterium* accelerated the decrease of chlorine concentration and caused the THM concentration to be increased. That happened because of the formation of aggregates in drinking water by *Methylobacterium*, the formation of which resulted in the increase of EPS, the subsequent reaction of chlorine with them and finally, the formation of THM. After the first 3 hours, it was found that the *Methylobacterium* was able to decrease the concentration of THM to a high extent. This is an important

knowledge for drinking water industries, which continuously search for cheap and effective ways to improve drinking water quality because introducing specific key species like *Methylobacterium* in the flow of drinking water systems, even at low concentrations, might lead to safer drinking water.

9 Conclusions and Future Work

9.1 Conclusions

Biofilms are ubiquitous and can be beneficial or detrimental depending on the circumstances and locations. The received wisdom is that they are problematic in drinking water systems where they cause loss of disinfectants, corrosion and harbour pathogens. Thus, it is imperative that we gain a deeper understanding of the behaviour of biofilms and develop effective strategies for their removal or control. The present study was focused on the interactions between physical and biological processes in biofilms in drinking water.

After biofilms were grown in a bioreactor filled with drinking water under three different flow regimes: turbulent, transition and laminar, it was found that turbulence enhanced both the initial formation and the development of biofilms in drinking water. Biofilms were found to be densest, thickest and most extensive in turbulent flow compared to the rest two flow regimes and to stagnant conditions. The structures of biofilms were also studied and it was shown to be different under the different flow conditions; the most heterogenous, complex and irregular biofilm structures were found in turbulent flow. These findings were contrary to most of the previous studies in which the high shear stresses, which are experienced in most engineering applications, were correlated with a reduction in biofilms. The knowledge that turbulence promotes biofilm formation in drinking water can be useful for water companies as they might search for ways to control the high shear and mixing conditions at specific parts of the DWDS, which might be important, and especially where the service lines start. Overall, this part of the thesis highlighted the important role that flow conditions play in the formation of biofilms and indicated that turbulent flow promoted the formation of biofilms in drinking water.

Throughout my research, I have also suggested that *Methylobacterium* DSM 18358 is a key strain in the formation of aggregates in drinking water. Bacterial aggregation was studied for mixed natural drinking water cultures inoculated with different relative abundances of this *Methylobacterium* strain; previous research in the field was focused only on single- or dual-species mixes. The

results of this study clearly indicated that the *Methylobacterium*, even when it was inoculated into drinking water at the lowest tested relative abundance of 1%, significantly increased bacterial aggregation even at the first 24 hours. That was proved for both stagnant and shaking conditions and for both oligotrophic and eutrophic conditions.

The aggregation ability of this *Methylobacterium* strain was further studied in complex mixed drinking water bacterial communities for different flow regimes. It was shown that the *Methylobacterium*, even when it was inoculated into drinking water at the lowest tested relative abundance of 1%, enhanced bacterial aggregation under flow conditions. This ability was enhanced in turbulent flow compared to laminar flow. Thus, it is suggested that the presence of *Methylobacterium* in drinking water systems, even at a low concentration, might be very important for biofilm formation under both stagnant and flow conditions.

The structures of aggregates formed by this *Methylobacterium* strain were visualised using fluorescence *in situ* hybridization for both liquid samples and samples from the reactor surfaces, taken from stagnant, laminar and turbulent flow conditions. It was found that the spatial arrangement and size of those aggregates was different for the different samples and for the different flow conditions. The main difference between them was that there were more aggregates found in the samples from the reactor surfaces than in the liquid samples, which suggested that the presence of the *Methylobacterium* triggered the movement of those aggregates from the bulk water onto the surfaces. Under stagnant conditions, the *Methylobacterium* was found to form its own aggregates excluding the rest of the drinking water bacteria, but that changed as the shear stresses increased in the bioreactor. The increased shear stresses triggered the co-location of the other drinking water bacteria that were found to surround those *Methylobacterium* aggregates. The study suggests that the high mixing conditions that describe turbulent flows enhanced the interactions between the *Methylobacterium* cells and between the rest drinking water bacteria. This part of the study suggested that it is very important that we focus on key species in bacterial aggregation and study their behaviour under different flow conditions.

Since it has been previously suggested that bacterial motility might play an important role in biofilm formation, the motility of this *Methylobacterium* strain was studied on agar plates. The experiments suggested that the given energy from the R2A medium, enhanced the communication and motility of *Methylobacterium* cells. In contrast, in drinking water the *Methylobacterium* colonies were found to spread away from one another in the search of energy. These results suggested that the *Methylobacterium* might quorum sense and move depending on the available energy in the surrounding environment. Finally, when *Methylobacterium* was inoculated into mixed drinking water bacterial colonies at 1% relative abundance, it significantly enhanced the communication and interactions between drinking water bacteria on drinking water agar plates. The knowledge that there might be key species in aggregation in drinking water that play an important role in the initiation of biofilm formation at the inner surface of pipes can be useful for drinking water companies as they might search for ways to eradicate those bacteria or at least eliminate their concentration in the main water flow.

Driven by the fact that *Methylobacterium* species were previously found between other drinking water bacteria to be able to degrade haloacetic acids, in the last part of this thesis, this *Methylobacterium* strain was studied for its ability to impact the fate of trihalomethanes. It was shown that when the *Methylobacterium* was inoculated into drinking water at 1% relative abundance, a significant decrease in THM concentration in drinking water was found. That was an important finding since THM consist a major class of chlorine disinfection by-products in drinking water and their presence at high concentrations constitute a serious threat for human health. Thus, *Methylobacterium* species might have a beneficial effect on the quality of drinking water. The knowledge that there might be other species in drinking water such as the *Methylobacterium* strain DSM 18358 that play a key role in the removal of THM, and are not key in bacterial aggregation, can be useful for drinking water companies as they might search for ways to identify those species and probably introduce them or increase their concentration in the main water flow.

9.2 Future Work

Based on the experimental work conducted and the results obtained from this study there are a few perspectives for future work to be carried out. Only a small number of bacterial species have been implicated in promoting the formation of aggregates in pure or simple mixed cultures, but have not been studied in complex mixed bacterial communities that typify industrial biofilms. Thus, it is currently unknown whether there are key strains like the *Methylobacterium* studied here in aggregation and, if there are, whether they share similar mechanisms in promoting biofilm formation.

A part of my thesis suggests that the studied *Methylobacterium* strain could quorum sense by sending chemical signals to one-another and other species to trigger the bacterial aggregation. However, the interaction of quorum sensing with flow regime for a suite of potentially key biofilm formers in complex mixed cultures has never been studied. This is a potential study to be carried out under a realistic range of flow conditions for complex mixed bacterial communities inoculated with different mixes of key organisms in aggregation. Quorum sensing molecules have been previously reported by releasing specific bacteria into the system that help to detect these signalling molecules. Indicator bacteria, such as *Chromobacterium violaceum* and *Pseudomonas aureofaciens*, have been used to detect QS molecules by regulating pigment production of purple-coloured violacein and orange-coloured phenazine, respectively on agar plates (McLean et al., 2004, Simões et al., 2007).

The studies that have been conducted so far regarding the role of QS in drinking water are few and limited (Simões et al., 2007, Ramalingam, 2012). They were focused on the QS ability of a particular bacterial strain in a monoculture (Purevdorj et al., 2002, Kirisits et al., 2007, Simões et al., 2007) or in a simple mixed culture (Ramalingam, 2012). Identifying other key species and their generic modes of aggregation under the application of physical forces will allow us to target them.

One promising avenue is the use of predatory bacteria, which kill other microbes and consume them as a nutritional resource. These bacteria have the ability to degrade the polymeric compounds that their prey is composed of. Bacteria such

as *Bdellovibrio bacteriovorus* (Velicer and Mendes-Soares, 2009), which will prey upon a wide variety of Gram-negative bacteria (Nunez et al., 2003), can be used. Many other less well studied predatory bacteria exist in nature, such as *Vampirovibrio* species and *Daptobacter* species (Velicer and Mendes-Soares, 2009). There is some evidence that there is cell density dependence akin to QS in *Bdellovibrio bacteriovorus* (Shilo and Bruff, 1965).

If the key in biofilm formation species are profligate signallers (Jurkevitch, 2006, Capeness et al., 2013), then perhaps we can use the chemical signals to guide specific predators to them and disrupt the biofilm formation. Thus, rather than chemical control, which is costly and only partially successful, an alternative and cheap method can be applied where predatory bacteria are unleashed and the challenge is to obtain species specific predators and guide them towards these key species under the application of physical forces.

10 Appendix

10.1 Chapter 3

10.1.1 Protocol for fixation of biofilms on surfaces

The biofilms on the surfaces were fixed using the protocol below (Chao and Zhang, 2011):

1. Fill a beaker with 200 ml of distilled water and add two 1xPBS tablets.
2. Weigh 8 g of paraformaldehyde and assure cleaning powder particles after use. Once the paraformaldehyde is weighed it is added to the 1xPBS solution.
3. Place the beaker on a hot plate and adjust the temperature at 80°C and turn on the magnetic stirrer.
4. Add few drops of 1 M sodium hydroxide (NaOH) and leave it for approximately 1 hour until the PBS and the paraformaldehyde are completely dissolved and the solution becomes transparent.
5. Once the solution is ready, remove it from the hot plate and let it to cool until it reaches room temperature.
6. Place the samples in a clean Petri dish and then rinse them with 1xPBS.
7. Place the samples in another clean Petri dish and cover them with 0.5 ml of 4% paraformaldehyde for 30 minutes at room temperature.
8. Rinse them again with 1xPBS and leave to dry.

10.1.2 Microcolonies and entropy measurements in the changes of flow regime process

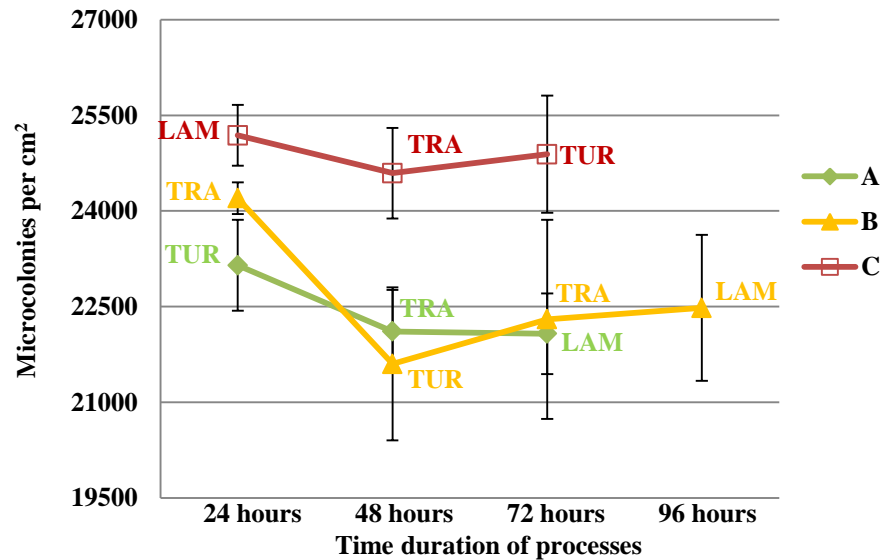


Figure 10-2 Concentration of microcolonies on the reactor surfaces in the changes of flow regime process.

“TUR” refers to turbulent flow regime, “TRA” refers to transition flow regime and “LAM” refers to laminar flow regime in all three experiments (A, B & C). The error bars represent the standard deviation of the measurements.

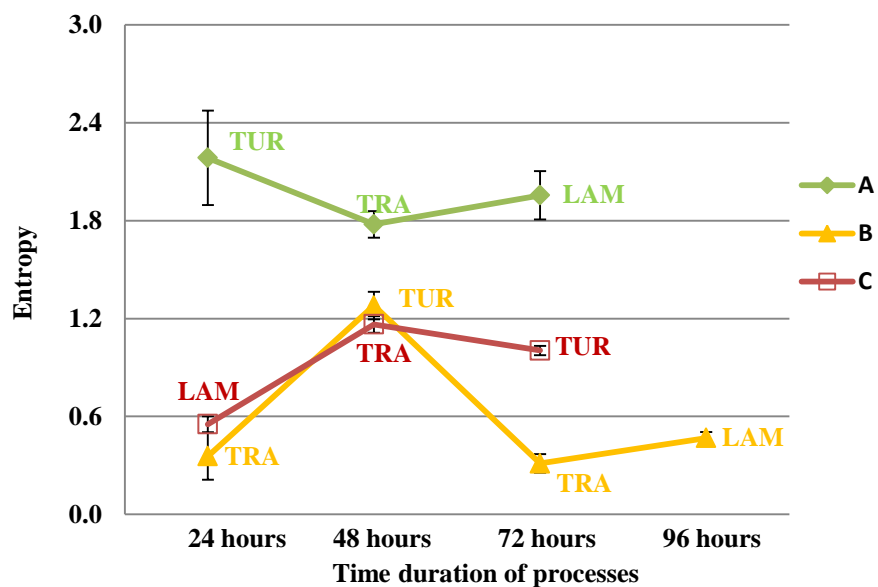


Figure 10-3 Entropy of biofilms in the changes of flow regime process.

“TUR” refers to turbulent flow regime, “TRA” refers to transition flow regime and “LAM” refers to laminar flow regime in all three experiments (A, B & C). The error bars represent the standard deviation of the measurements.

10.1.3 Semi-Variograms

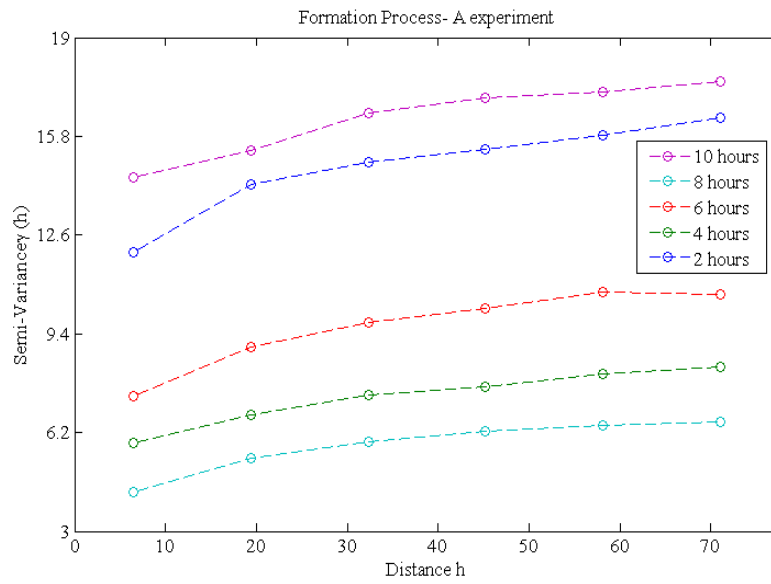


Figure 10-4 Semi-variograms for A experiment for the formation process. “A” describes turbulent flow.

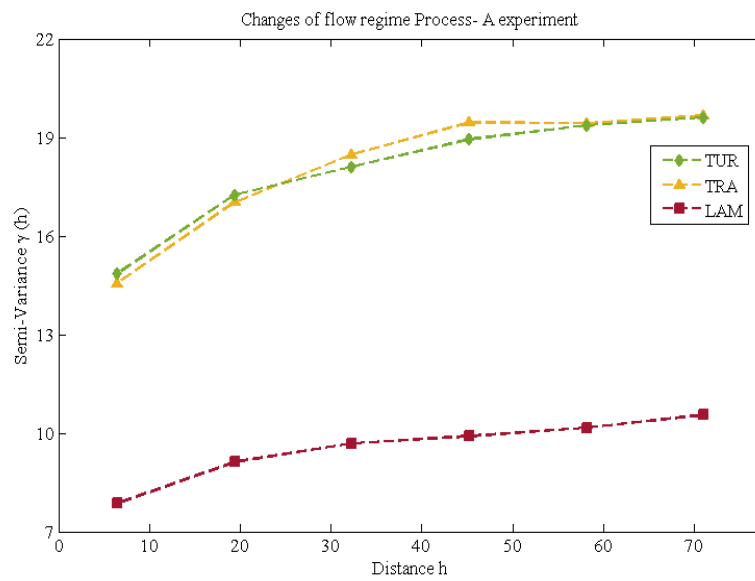


Figure 10-5 Semi-variograms for A experiment for the changes of flow regime process. “TUR” refers to turbulent flow regime, “TRA” refers to transition flow regime and “LAM” refers to laminar flow regime.

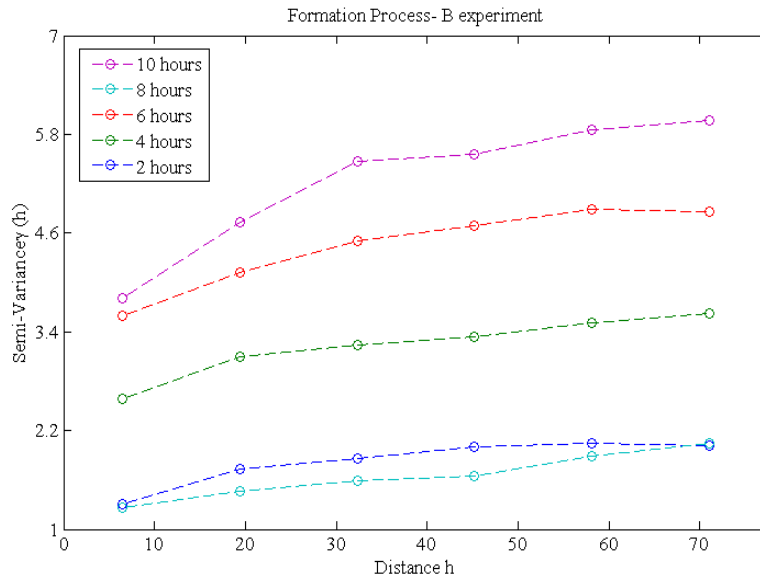


Figure 10-6 Semi-variograms for B experiment for the formation process. “B” describes transition flow.

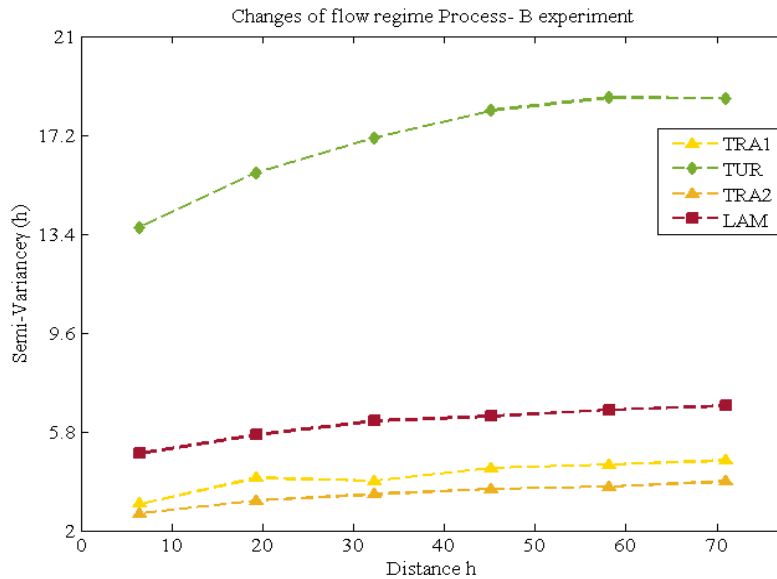


Figure 10-7 Semi-variograms for B experiment for the changes of flow regime process. “TRA1” refers to first transition flow regime, “TUR” refers to turbulent flow regime, “TRA2” refers to the second transition flow regime and “LAM” refers to laminar flow regime.

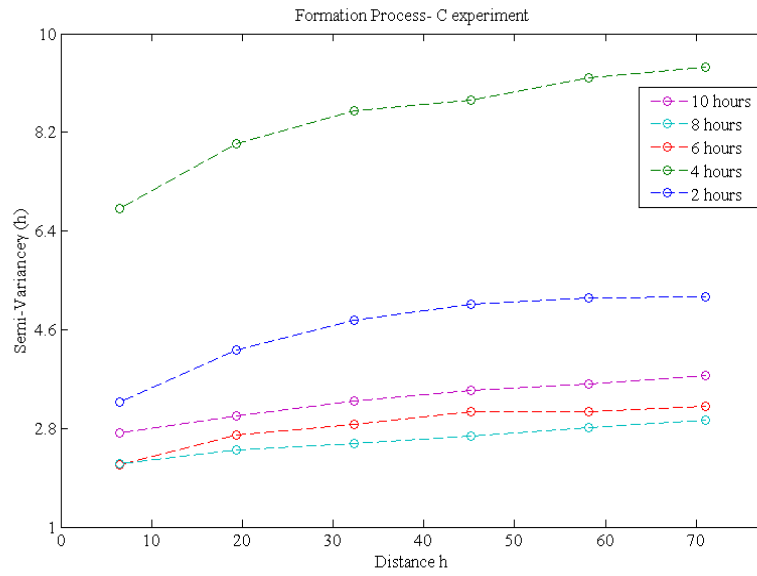


Figure 10-8 Semi-variograms for C experiment for the formation process. “C” describes laminar flow.

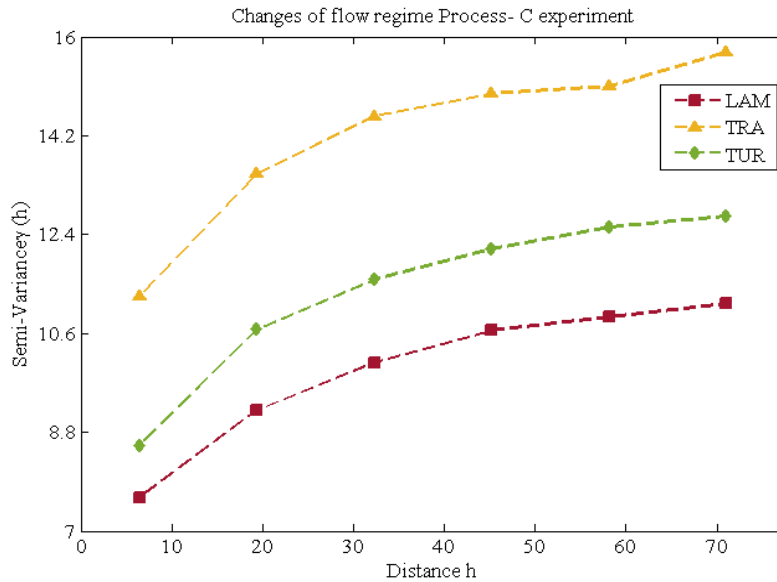
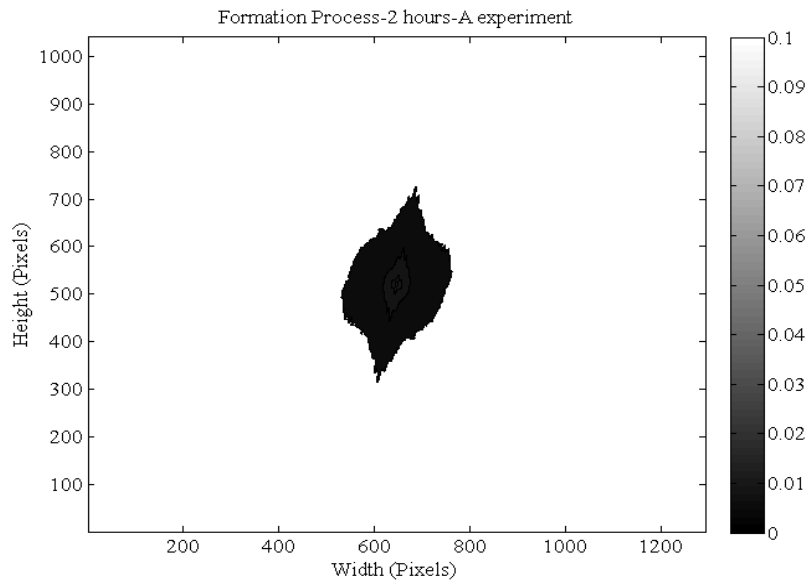
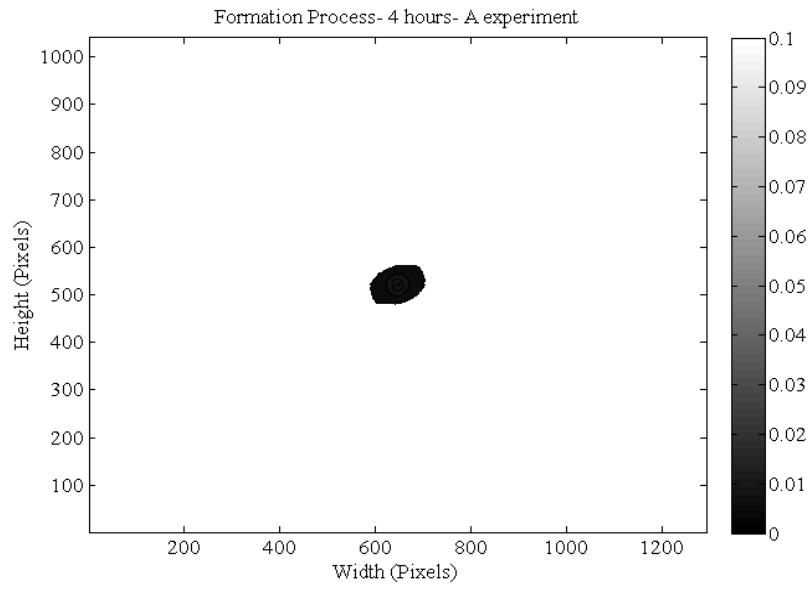


Figure 10-9 Semi-variograms for C experiment for the changes of flow regime process. “LAM” refers to laminar flow regime, “TRA” refers to transition flow regime and “TUR” refers to turbulent flow regime.

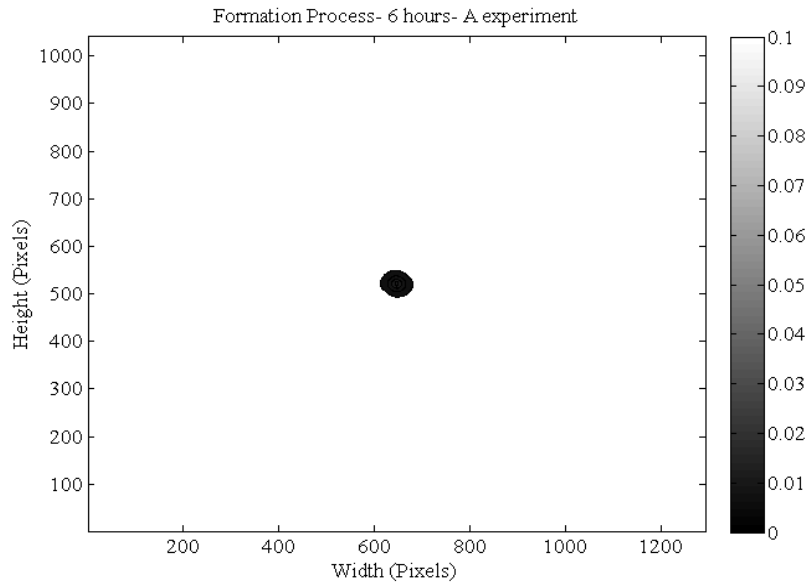
10.1.4 Autocorrelation function diagrams



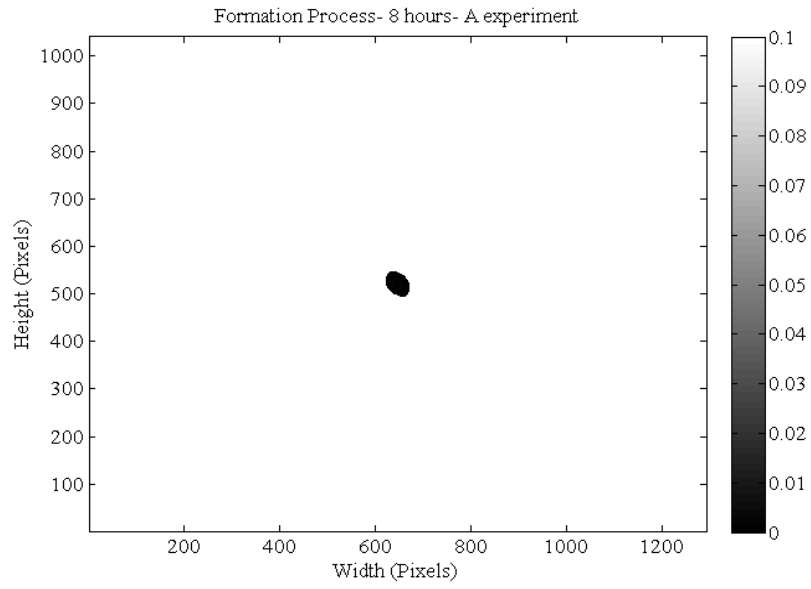
a.



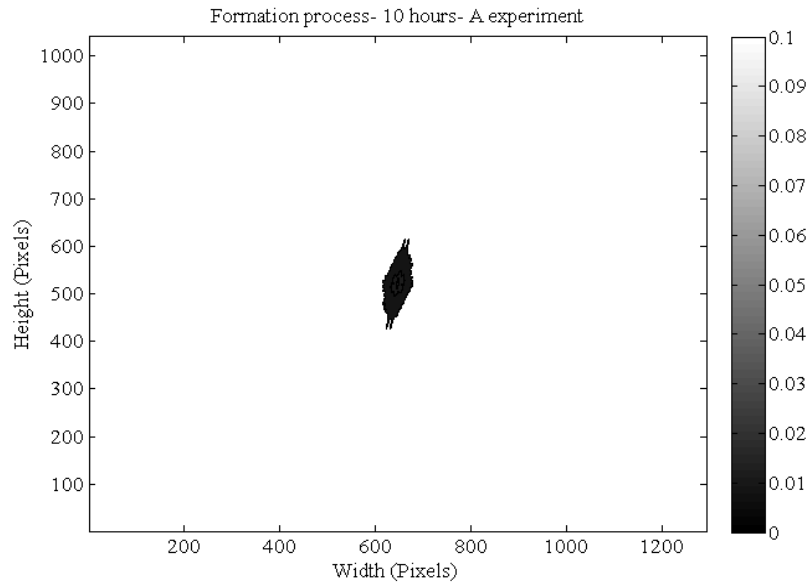
b.



c.

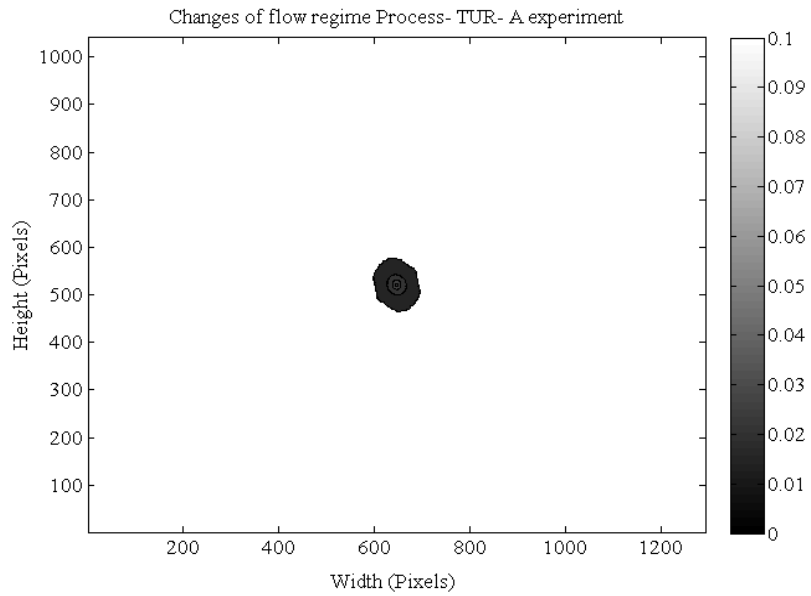


d.

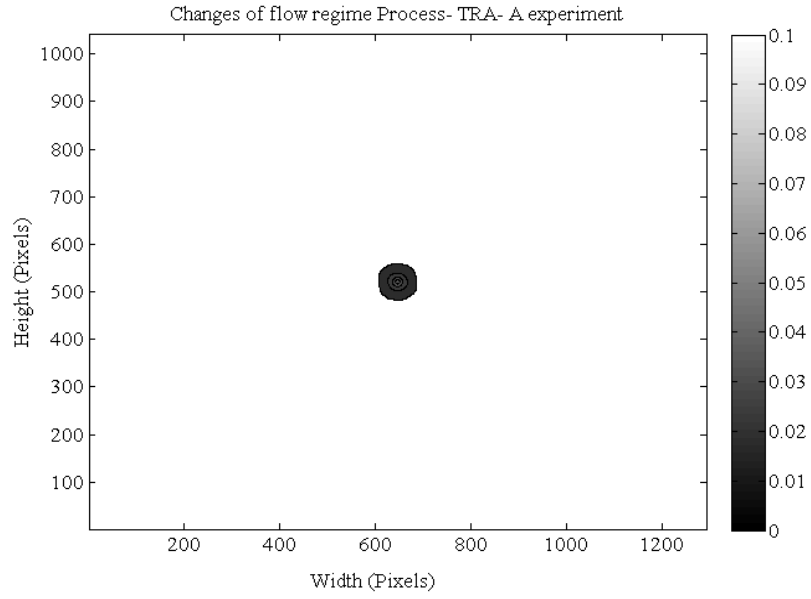


e.

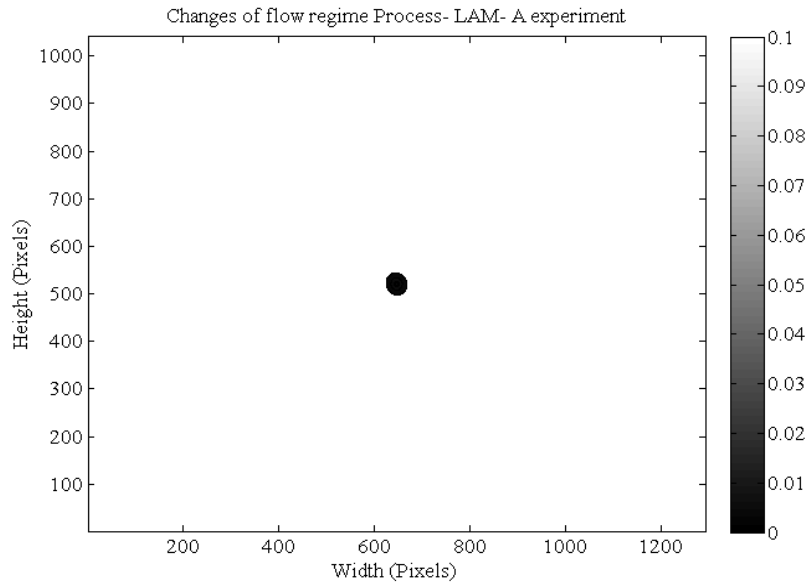
Figure 10-10 Autocorrelation function diagrams for A experiment for the formation process. "A" describes turbulent flow. (a) 2, (b) 4, (c) 6, (d) 8 and (e) 10 hours.



a.

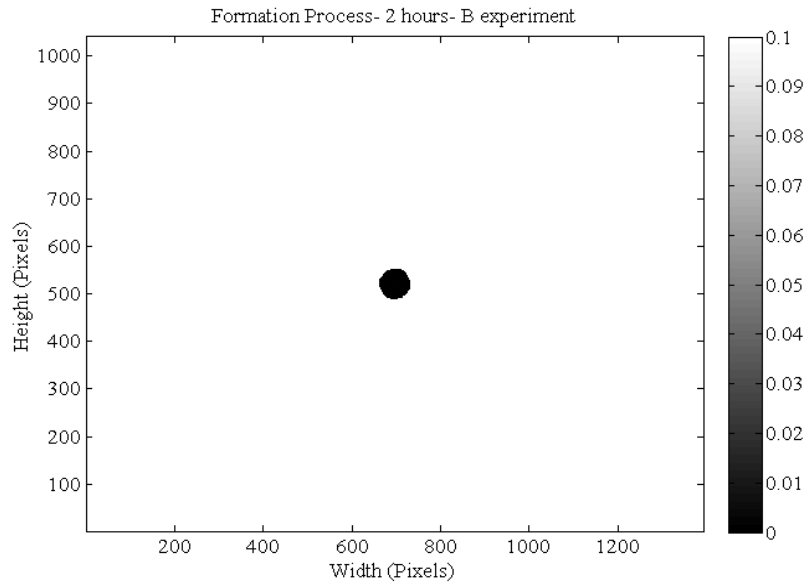


b.

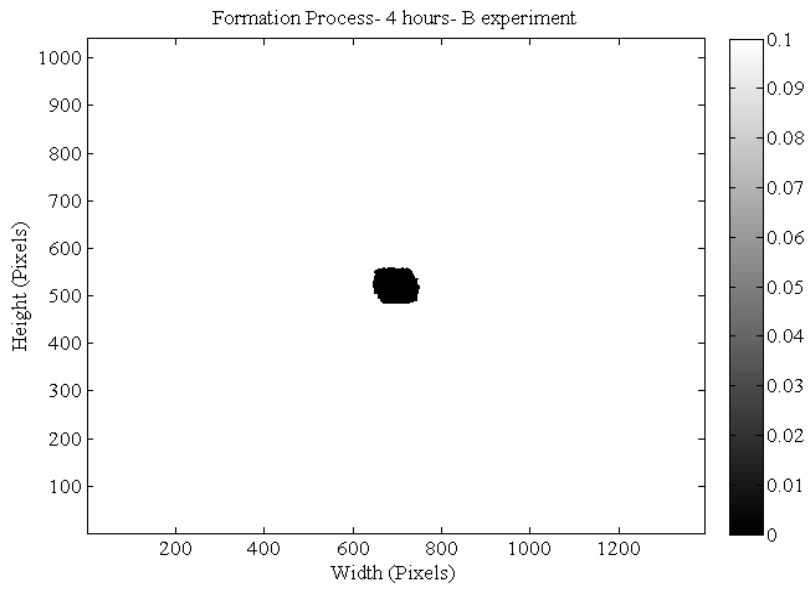


c.

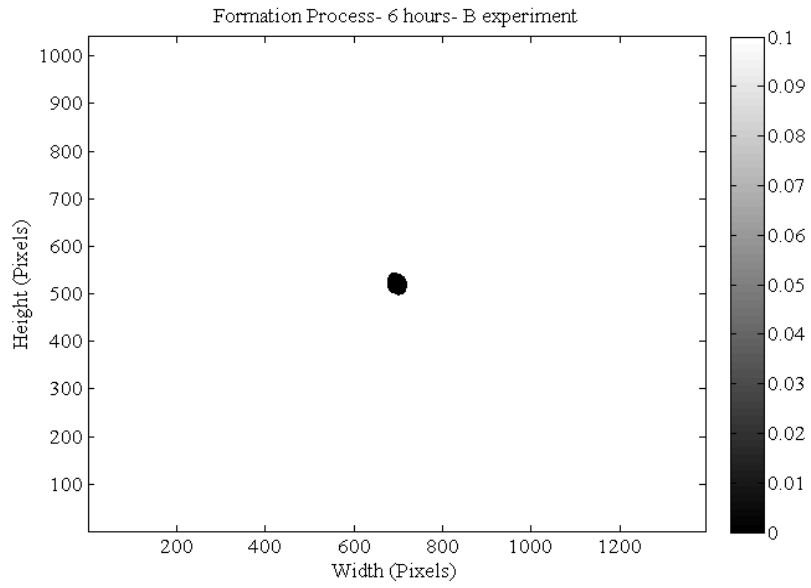
Figure 10-11 Autocorrelation function diagrams for A experiment for the changes of flow regime process.
“TUR” refers to turbulent flow regime, “TRA” refers to transition flow regime and “LAM” refers to laminar flow regime.



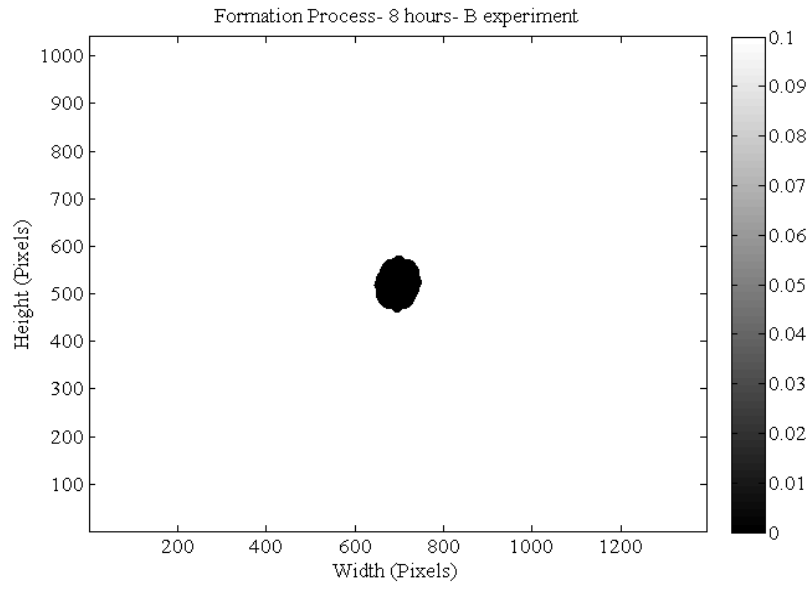
a.



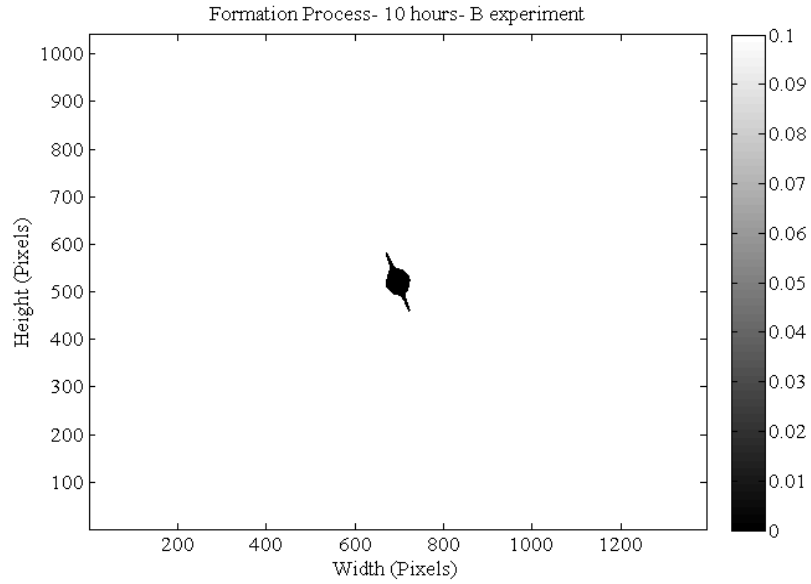
b.



c.

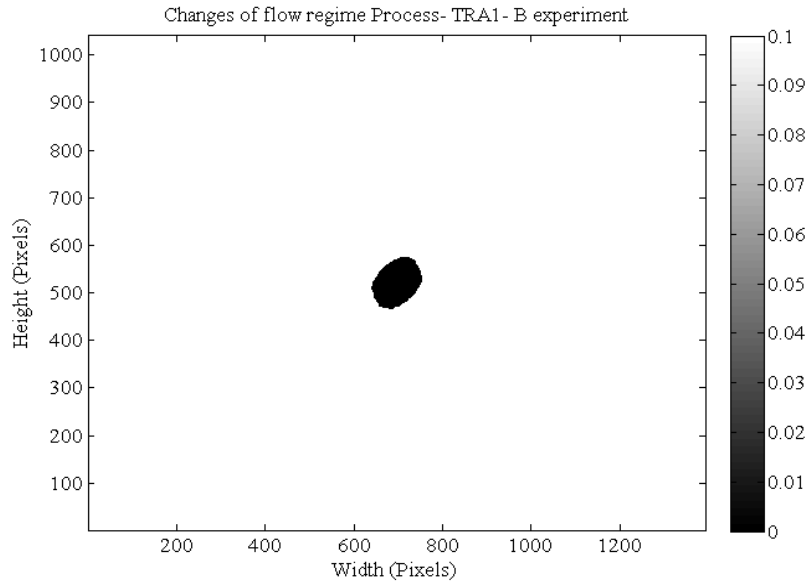


d.

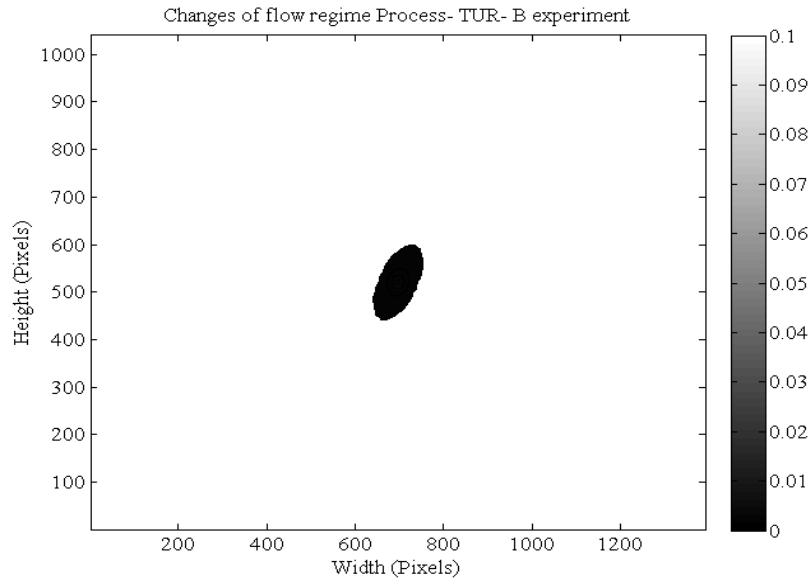


e.

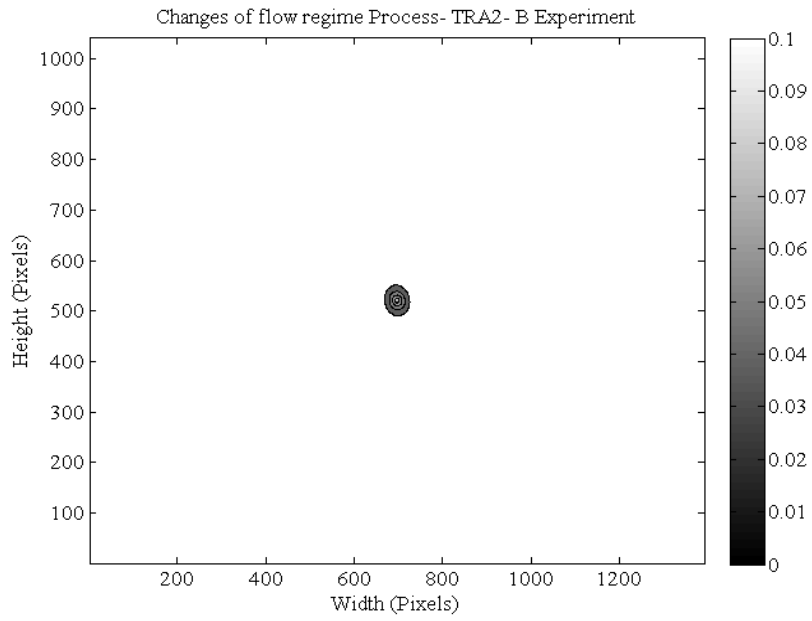
Figure 10-12 Autocorrelation function diagrams for B experiment for the formation process. "B" describes transition flow. After (a) 2, (b) 4, (c) 6, (d) 8 and (e) 10 hours.



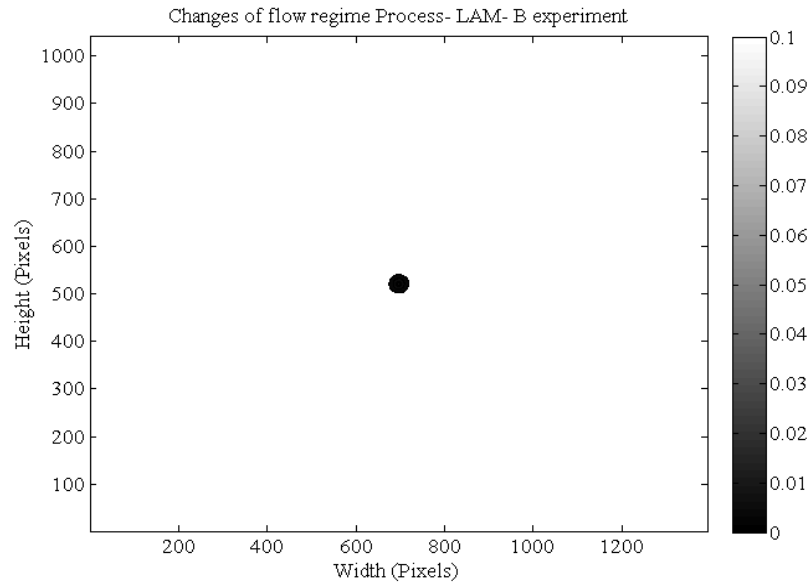
a.



b.



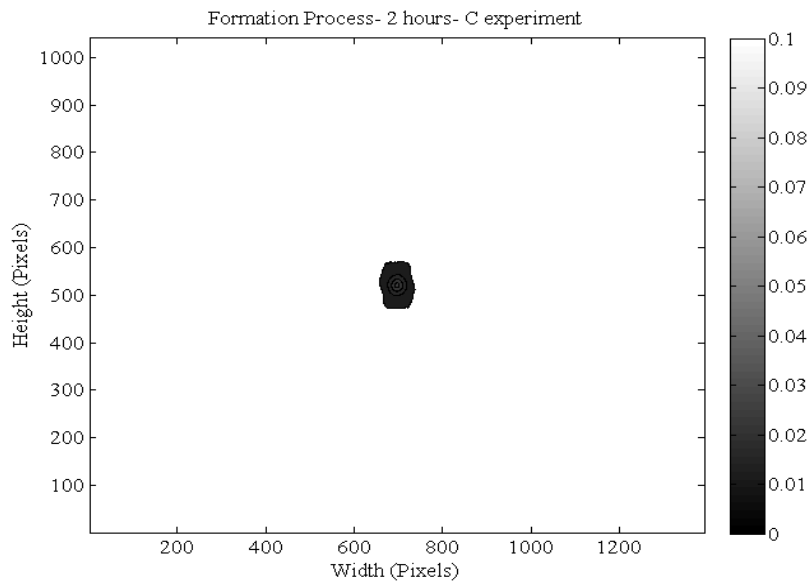
c.



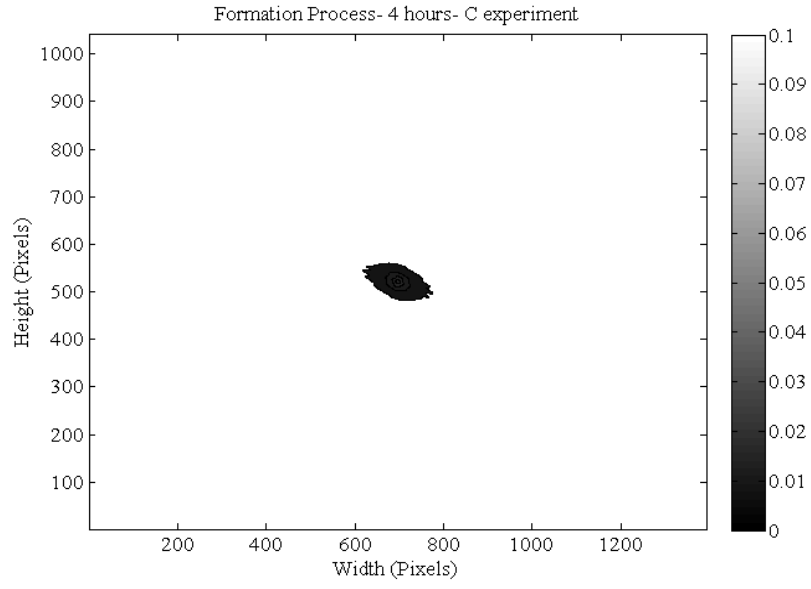
d.

Figure 10-13 Autocorrelation function diagrams for B experiment for the changes of flow regime process.

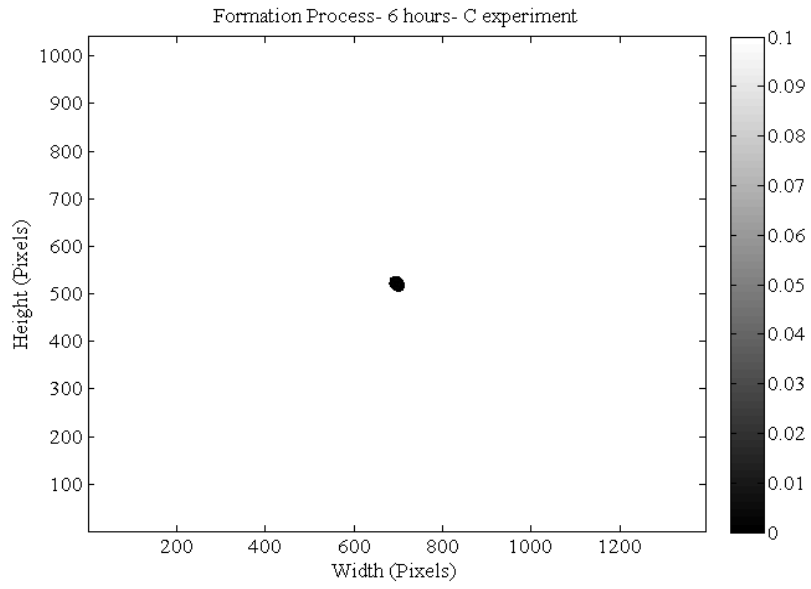
“TRA1” refers to first transition flow regime, “TUR” refers to turbulent flow regime, “TRA2” refers to the second transition flow regime and “LAM” refers to laminar flow regime.



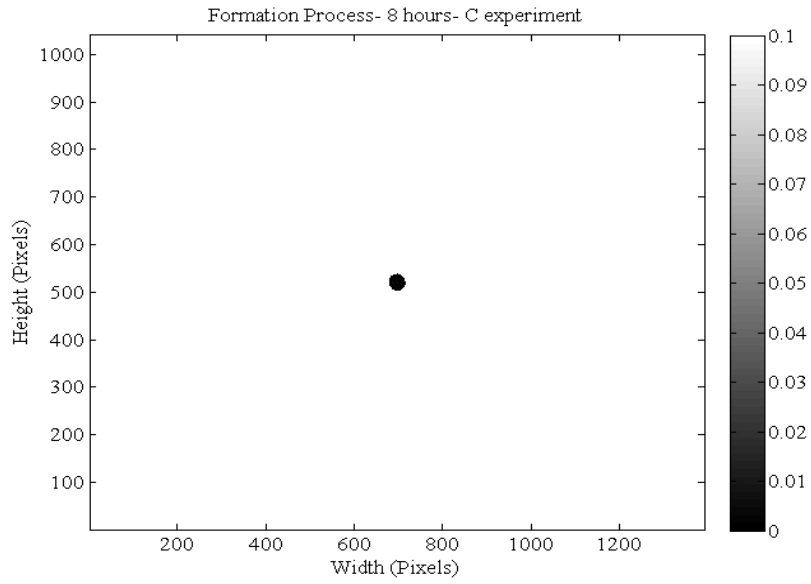
a.



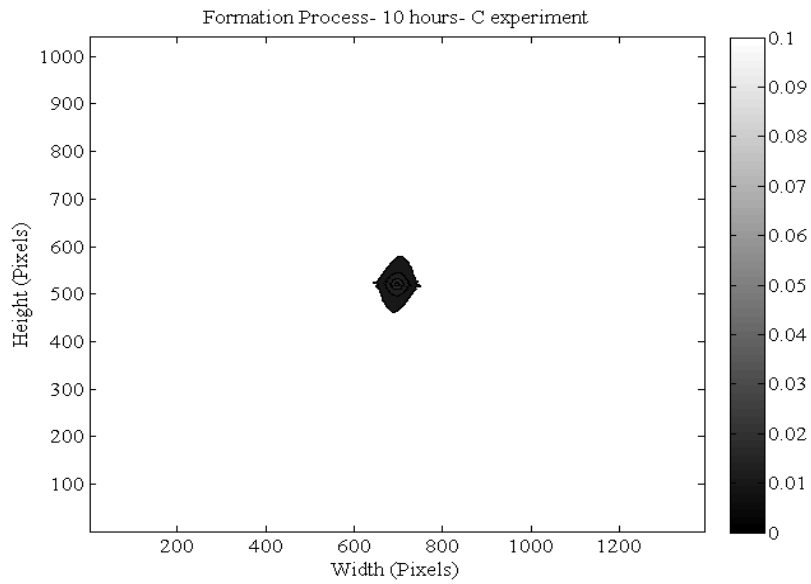
b.



c.

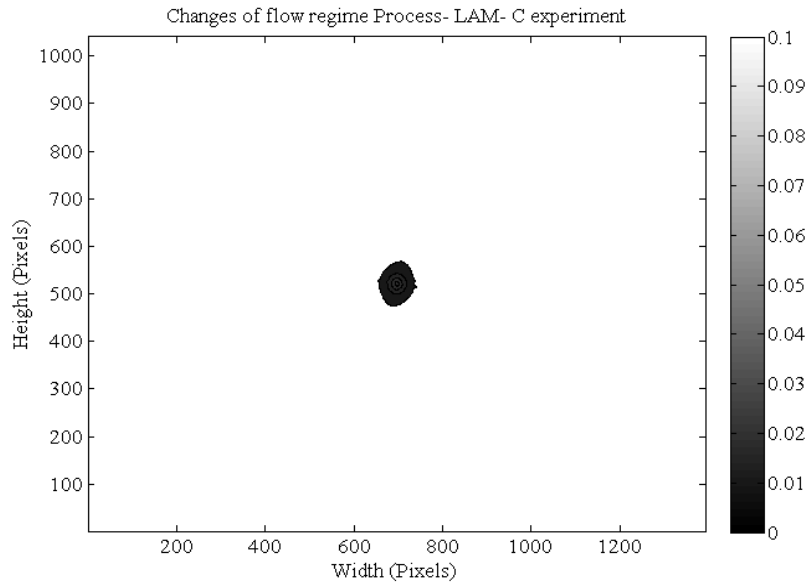


d.

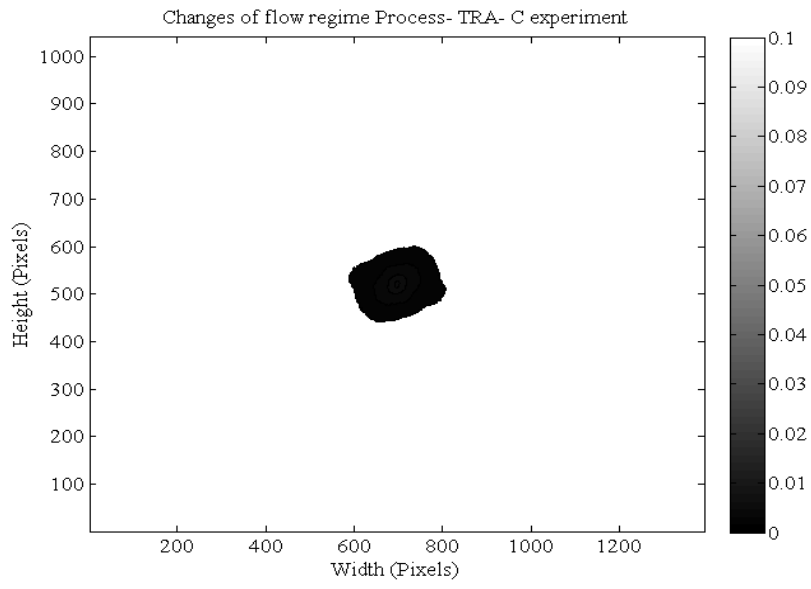


e.

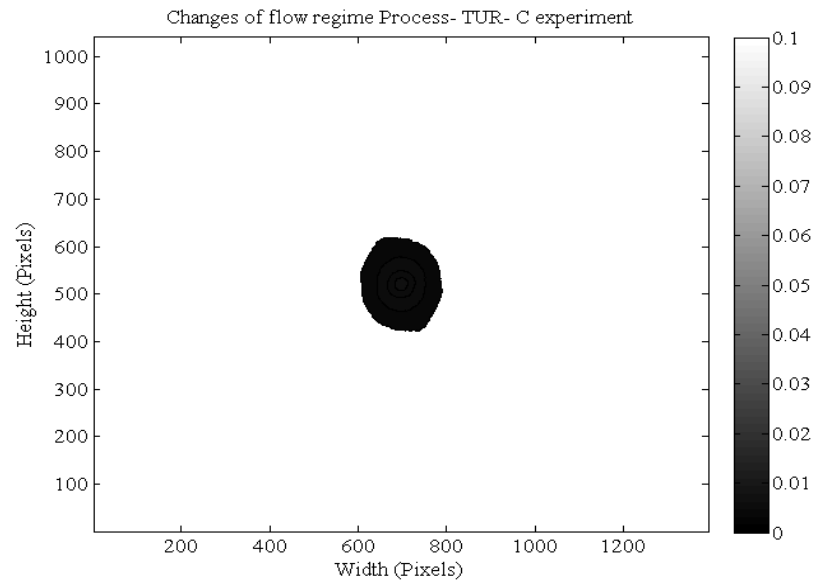
Figure 10-14 Autocorrelation function diagrams for C experiment for the formation process. "C" describes laminar flow. After (a) 2, (b) 4, (c) 6, (d) 8 and (e) 10 hours.



a.



b.



C.

Figure 10-15 Autocorrelation function diagrams for C experiment for the changes of flow regime process.

“LAM” refers to laminar flow regime, “TRA” refers to transition flow regime, and “TUR” refers to turbulent flow regime.

10.2 Chapter 4

10.2.1 Protocol for the revival of the freeze-dried *Methylobacterium* culture

The following protocol was used to reactivate and culture the *Methylobacterium* strain received from DSMZ (Leibniz-Institute, Braunschweig, Germany):

1. Remove the glass ampoule from plastic tube.
2. Check the indicator to ensure an intact seal.
3. Heat the tip of glass ampoule over a Bunsen burner flame thoroughly.
4. Drop some water onto the tip to crack glass all around.
5. Carefully strike the glass tip with forceps to break off the tip.
6. Remove the insulation material and extract the smaller vial with forceps.
7. Remove the cotton plug from vial and keep it sterile.
8. Add 0.5 ml of recommended medium to the dehydrated culture and insert cotton plug back into the vial. Allow the culture to rehydrate for about 30 minutes.
9. Remove the cotton plug again. Mix very gently with an inoculation loop and transfer to the recommended liquid medium in a 15 ml tube.
10. Pipette 100 µl of liquid culture onto plate as a spot and make a streak plate.

10.2.2 Culture medium R2A

The R2A medium was prepared and autoclaved at 121°C for approximately 60 minutes. Its composition is: yeast extract of 0.5 g/l, sodium pyruvate of 0.3 g/l, peptone of 0.5 g/l, di-potassium phosphate of 0.3 g/l, casamino acids of 0.5 g/l, magnesium sulphate of 0.05 g/l, glucose of 0.5 g/l and starch of 0.5 g/l. In the

case in which R2A agar medium was created, 15 g/l of agar was added to R2A liquid medium.

10.2.3 Images from the analysis of aggregates



Figure 10-16 BRAND[®] culture tube (Sigma-Aldrich, Irvine, UK) containing 10 ml of drinking water bacterial culture.

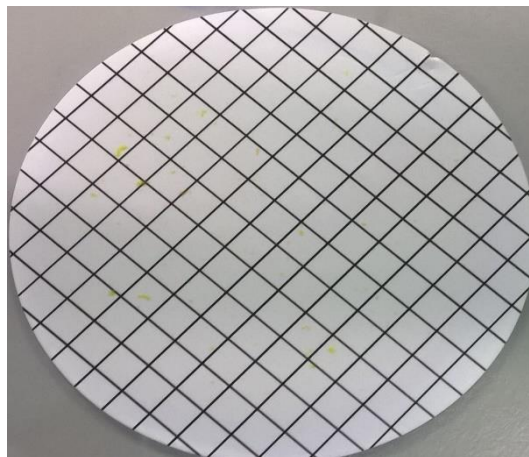


Figure 10-17 Cellulose nitrate filter of 0.2 μm pore size with 3 mm² squares (Sartorius, England, UK) used for the analysis of aggregates.

10.3 Chapter 5

10.3.1 Microcolonies attached on the reactor slides

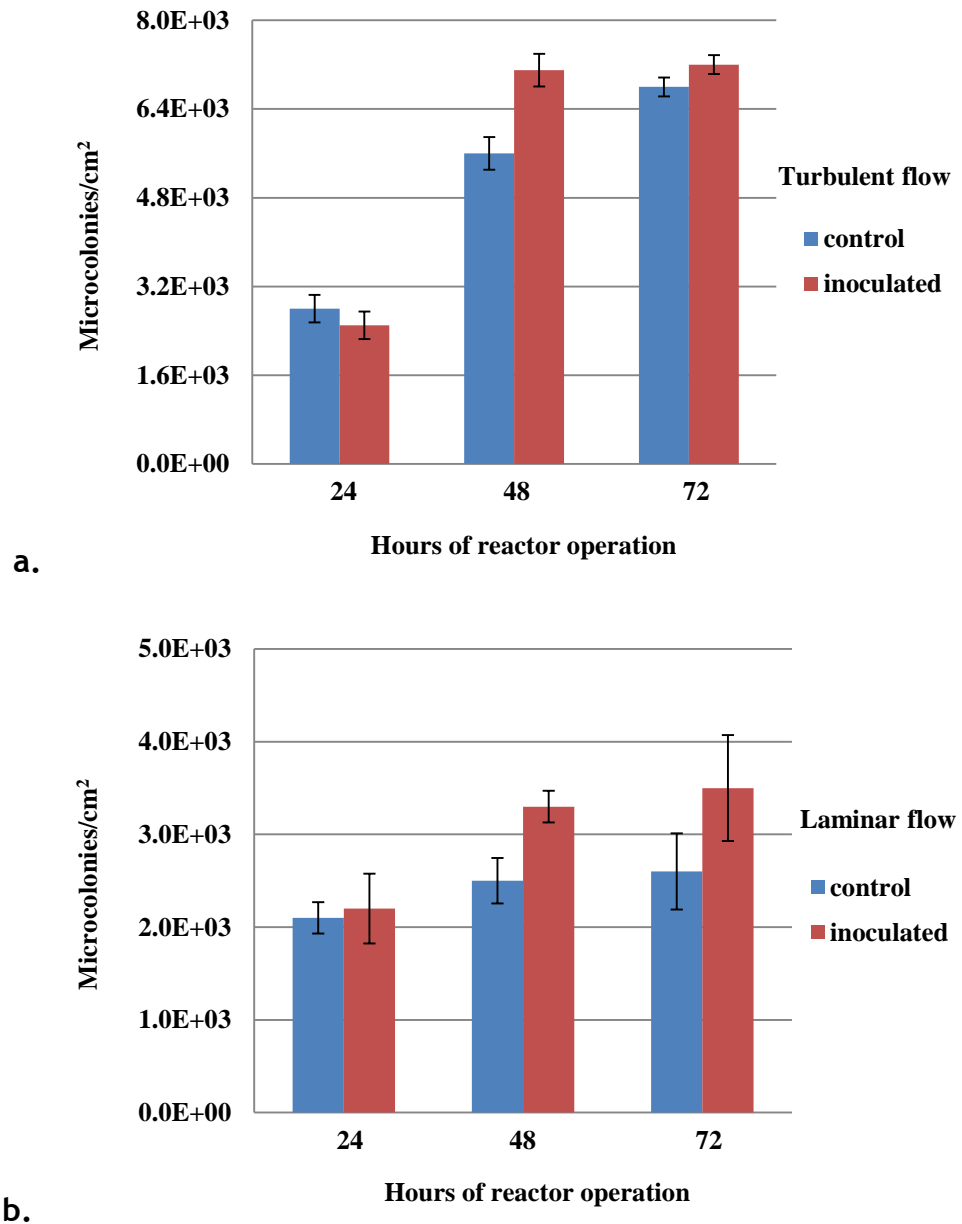


Figure 10-18 Concentration of microcolonies on the reactor slides for both the control and inoculated drinking water cultures at 24, 48 and 72 hours. (a) In turbulent flow and (b) in laminar flow. The error bars represent the standard deviation of the measurements.

10.3.2 Surface area of biofilms on the reactor slides

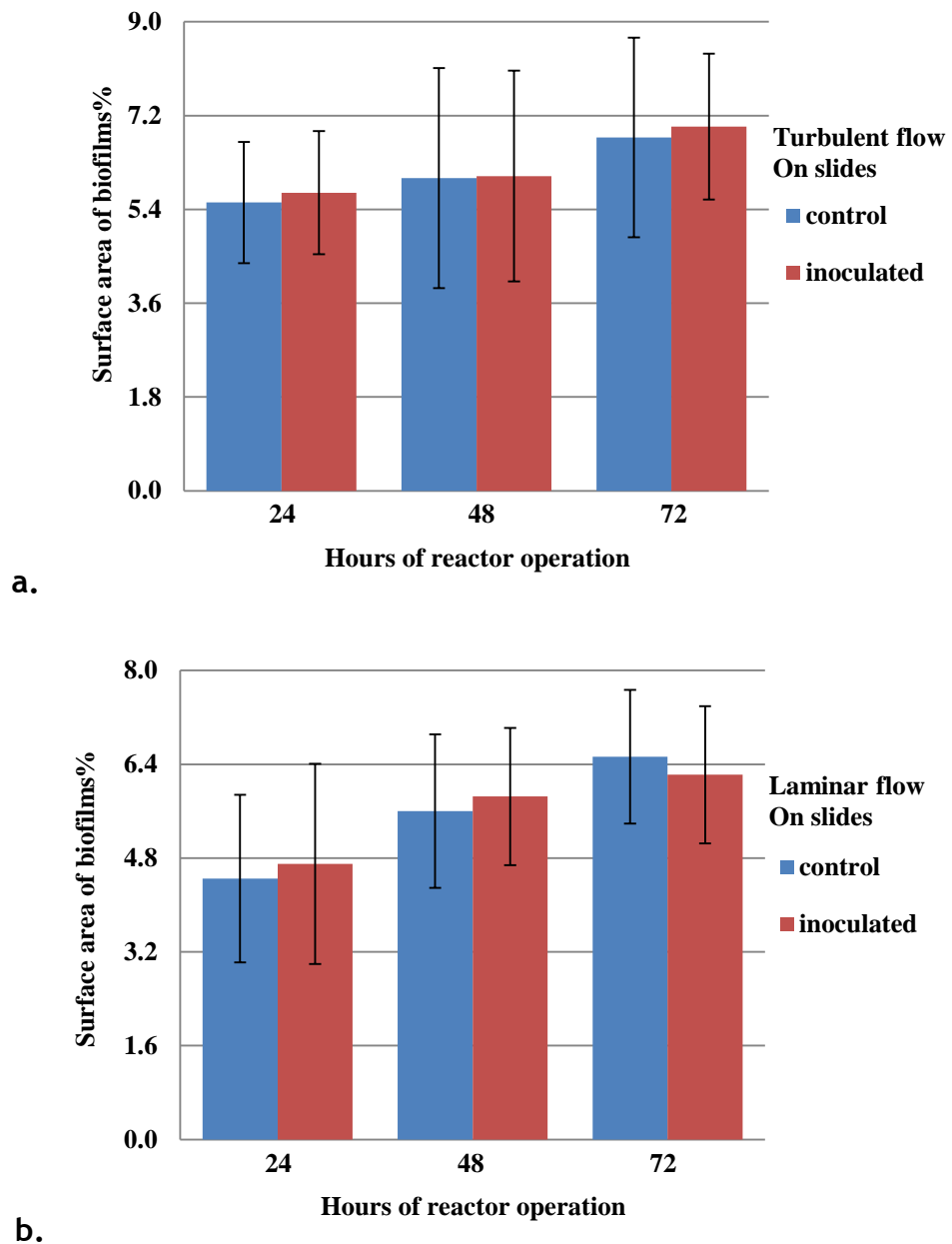


Figure 10-19 Percentage of surface area of biofilms on the reactor slides for both the control and inoculated drinking water cultures at 24, 48 and 72 hours. (a) In turbulent flow and (b) in laminar flow. The error bars represent the standard deviation of the measurements.

10.4 Chapter 6

10.4.1 Protocol for DNA extraction

The Maxwell® 16 LEV Blood DNA Kit was used that involves the following steps:

1. To a lysing matrix tube E containing the sample and a 0.22 µm filter, add 300 µl of lysis buffer.
2. Add 30 µl of Proteinase K.
3. Incubate for 20 minutes at 56°C.
4. Add 500 µl of chloroform: isoamyl alcohol and vortex.
5. Bead beat at setting 6 for 40 seconds.
6. Centrifuge for 10 minutes at 14,000xg.
7. Transfer supernatant to a clean 2 ml tube.
8. Add 75 µl of lysis buffer to the lysing matrix E tube and vortex.
9. Bead beat at setting 6 for 40 seconds.
10. Centrifuge for 10 minutes at 12,500xg.
11. Transfer supernatant to 2 ml tube.
12. Add 50 µl of lysis buffer to the lysing matrix E tube and vortex.
13. Bead beat at setting 6 for 40 seconds.
14. Centrifuge for 10 minutes at 12,500xg
15. Transfer supernatant to 2 ml tube.
16. Add 500 µl of chloroform: isoamyl alcohol to a 2 ml tube.

17. Centrifuge the 2 ml tube for 5 minutes at 14,000xg.
18. Use supernatant (630 μ l approximately) as a sample for the Maxwell Blood DNA kit.
19. Change gloves before handling cartridges, LEV Plungers and Elution Tubes. Place the cartridges to be used in the Maxwell 16 LEV Cartridge Rack. Place each cartridge in the rack with the label side facing away from the Elution Tubes. Press down on the cartridge to snap it into position. Carefully peel back the seal so that all plastic comes off the top of the cartridge.
20. Place one plunger into well with number 8 of each cartridge.
21. Place an empty Elution Tube into the Elution Tube position for each cartridge in the cartridge Rack. Add 50 μ l of Elution Buffer to the bottom of each Elution Tube.
22. Add supernatant from 2 ml tube (630 μ l approximately) in well with number 1 of the cartridge.
23. Run the Maxwell machine in low elution volume mode, select DNA, blood protocol and follow the instructions on the screen.

10.4.2 Protocol for PCR

1. Spray the inside surface of cabinet, the pipette barrels and wipe the racks that are used for PCR. Use ethanol 70% for all the cleaning.
2. Turn on the ultraviolet light for at least 10 minutes.
3. Assemble the pipettes and start preparing the master mix.
4. Thaw the reagents that are stored in the freezer at -20°C and then give the tubes a few flicks to make sure that everything is re-suspended. Then, give tubes a quick spin for 20-30 seconds in the centrifuge at 13000 rpm.
5. Mix all of the components in the respective chip.

6. Put them into the appropriate device, select the appropriate method and run the appropriate program.

10.4.3 Protocol for agarose gel electrophoresis

1. Create a small gel using 50 ml of 1xTAE buffer and 0.5 g of agarose.
2. Place the bottle with the buffer and the agarose in the microwave for 2-3 minutes with its button loose. Look if there are any particles visible in the bottle. If there are, then put it back to the microwave.
3. Let the mixture cool down and add 1 μ l of SYBR® Safe DNA gel stain (Invitrogen, Thermo Fisher Scientific, England, UK) for 10 ml of gel. Centrifuge the gel stain before with pulse for 10 seconds.
4. Place the liquid to the gel cast, check its level and if there is need to add some buffer and leave it for half an hour to solidify. Then remove the comb from the gel; the wells are created.
5. In each of the tubes of PCR products, add 2.5 μ l of SYBR® Safe DNA gel stain. Mix well with the pipette the dye with the PCR product.
6. Place 10 μ l of the mixture to each of the created wells. Go up to the middle of the depth of the well so as not to destroy the gel.
7. In the last well place 10 μ l of 1 μ g/ μ l of 1 kb Plus DNA Ladder dye (Thermo Fisher Scientific, England, UK).
8. Place the gel to the gel tank and set the system at 80 Volts for 30 minutes.

10.4.4 Protocol for *in situ* hybridization

This protocol was used to fix the samples (Herndl, 2007):

1. Deposit samples on 47 mm Whatman® 0.2 μ m membrane filters (Sigma-Aldrich, Irvine, UK).

2. Fix samples with 2% paraformaldehyde for 8 hours.
3. Filter 10 ml sample of approximately 10^8 cells/ml concentration on 47 mm Whatman® 0.2 µm membrane filters (Sigma-Aldrich, Irvine, UK) with a 0.45 µm cellulose nitrate support filter (Sartorius, England, UK).
4. Wash with 10 ml of distilled water.
5. Air-dry filters.
6. Store at -20°C until processing.

The final protocol created for our samples after conducting various tests to find the optimum conditions was the following:

1. Prepare the following chemical solutions:
 - i. EDTA, 0.5 M, pH 8
 - ii NaCl, 5 M
 - iii. SDS 10%, pH 7.2
 - iv. Tris-HCl, 1 M, pH 8
2. Prepare the following two solutions for the glass slides upon which the samples (filter pieces) are placed:
 - i. Gelatin solution for glass slides: Add 2.5 g of gelatine and fill up to 500 ml of distilled water. Heat the solution on a hot block to 60°C by stirring to dissolve the gelatine. Allow solution to cool down at room temperature and then add 0.25 g of chromium potassium sulphate ($\text{CrK}_2\text{O}_8\text{S}_2$).
 - ii. Washing solution for glass dishes: Add 145 ml of distilled water to 350 ml of absolute ethanol and 5 ml of 25% HCl.
3. Prepare the glass slides that are used for microscopy:

- i. Wash the slides with the washing solution in a glass dish for 30 seconds.
- ii. Let the slides to air dry for a few minutes in a vertical position.
- iii. Coat the slides with the gelatin solution for 30 seconds.
- iv. Let the slides to air dry for a few minutes in a vertical position.
- v. Place the slides in the oven for 1 hour at 60°C with a steel holder.
- vi. Store the slides at -20°C until next use.

4. Prepare the filters that contain the samples:

- i. Dehydrate the filters in an ethanol dilution series of 50, 80 and 90-96% concentration by pulling the ethanol solutions through the vacuum manifold for 3 minutes each and let them dry for other 3 minutes.
- ii. Cut the filters into small squares of 2 mm².
- iii. Place the filter sections on the gelatin coated slides.

5. Prepare the buffers:

- i. *In situ* hybridization buffer: Add 9 ml of 5 M NaCl, 1 ml of 1 M Tris-HCl at pH 8, and 15 ml of 30% CH₃NO. Fill up to 50 ml of distilled water. Add 50 µl 10% SDS that is filter sterilised.
- ii. *In situ* washing buffer: Add 25.5 ml of 5 M NaCl, 1 ml of 1 M Tris-HCl of pH 8 and 12.5 ml of 0.5 M EDTA if 30% CH₃NO was used for the hybridization buffer. Fill up to 50 ml of distilled water. Add 50 µl of 10% SDS that is filter sterilised.

6. Follow the hybridization steps:

- i. Place the filters into a small Petri dish with a bed tissue underneath.

- ii. Use 8 μl of the hybridization buffer to filter piece and add 2 ml to the tissue underneath the filter.
- iii. Take working solutions of each probe out of the freezer and allow them to thaw for 5 minutes in dark.
- iv. Add 1 μl of 50 ng/ μl of each probe that it is used to each filter piece.
- v. Incubate the Petri dishes containing the filter pieces at 46°C for 2 hours.

7. Follow the washing steps:

- i. Preheat the tubes containing the washing buffer to 48°C in a water bath (Isotemp Bath Circulator, Fisher Scientific, England, UK).
- ii. Remove the filters from the hybridization Petri dishes and place them into the washing tubes containing 2 ml of washing buffer each. Place them in a water bath for 15 minutes at 48°C.

8. Follow the final steps:

- i. Take out the filters from the washing tubes and place them on the gelatin coated slides to dry overnight in dark.
- ii. The next day add 10 μl of 10 $\mu\text{g}/\text{ml}$ DAPI onto each filter piece and stain for 20 minutes in the dark.
- iii. Embed the gelatin coated slide with 1 μl of EverBride mounting medium (Biotium) and put a cover slip onto the slide.

10.4.5 Amoeba protozoa

A Petri dish was filled with 20 ml of glucose (10 mg/l) and 5 ml of water that was sampled from a tap in Glasgow, which was fed by an old tank. A polycarbonate slide was introduced as potential surface area for growth in the Petri dish. The slide was left for 4 weeks inside the dish in dark conditions at room temperature. After the 4 weeks, the slide was sampled and the attached

on it material was manually detached using a sterile cell scraper of 30 mm blade length and 390 mm handle length (ThermoFisher Scientific, England, UK) that was sterilised by 70% ethanol before, and diluted in sterile water. The sample was filtered on a Whatman® 0.2 µm membrane filters (Sigma-Aldrich, Irvine, UK) in order any cells be removed from the filtered sample. Then, 2 ml filtered sample was taken for DNA extraction according to Maxwell Blood DNA quantification protocol described in 10.4.1. The DNA was quantified at 0.181 ng/µl.

After that, PCR was carried out using the KAPA HiFi HotStart PCR Kit. We used 3 µl of 5X KAPA HiFi Buffer, 0.45 µl of 10 mM KAPA dNTP Mix, 0.3 µl of 1 µl KAPA HiFi HotStart DNA Polymerase, 0.5 µl of each 18S primer of 10 µM, which were the EukA and EukB, and 10 µl of 5 ng/µl of template DNA in 15 µl final total volume (Bazin et al., 2014). The PCR was carried out in the Techne TC-5000 gradient thermal cycler (Suffern, US), with an initial denaturation step at 95°C for 5 minutes followed by 35 cycles of 98°C for 20 seconds, 59°C for 40 seconds and 72°C for 40 seconds. Triplicates of samples were used in PCR and 3 negative controls with no template DNA. The PCR products were visualised by agarose gel electrophoresis to ensure that the correct size fragment was amplified and imaged using the Molecular Imager® Gel Doc™ with the Image Lab™ Software (Bio-Rad Laboratories, Perth, UK). The 1xTAE buffer was used that contained 40 Tris, 20 mM acetic acid and 1 mM EDTA, and 1% agarose. The SYBR® Safe DNA gel stain was used to stain the buffer and the PCR products. The PCR product was found at about 1500-2000 bp.

10.5 Chapter 8

10.5.1 Protocol for total chlorine concentration measurements

1. Start program 80 Chlorine F&T PP.
2. Fill a sample cell with 10 ml of sample.
3. Prepare the sample by adding the contents of one DPD total chlorine reagent powder pillow (Hach, Colorado, US) to the sample cell.
4. Swirl the sample cell for 20 seconds to mix. A pink colour shows if chlorine is present in the sample.
5. Start the instrument timer. A 3-minute reaction time starts. Prepare the sample blank and set the instrument to zero during the reaction time.
6. Prepare the sample by filling a second sample cell with 10 ml of sample.
7. Clean the blank sample cell.
8. Insert the blank into the cell holder.
9. Push zero; the display shows 0.00 mg/l Cl₂.
10. Clean the prepared sample cell.
11. Within 3 minutes after the timer expires, insert the prepared sample into the cell holder.
12. Push read; results show in mg/l Cl₂.

10.5.2 Protocol for trihalomethanes concentration measurements

1. Prepare a hot water bath by adding 500 ml of water to an evaporating dish. Put the dish on a hot plate and turn the heater on high.

2. Prepare a cooling bath by adding 500 ml of cold (18-25°C) tap water to a second evaporating dish. Maintain the temperature in this range.
3. Fill one round sample cell to the 10 ml mark with sample. Then cap and label as "sample".
4. Fill another sample cell to the 10 ml mark with distilled water. Then cap and label as "blank".
5. Add 3 drops of THM Plus Reagent 1 (27539-29) to each cell. Cap tightly and mix gently by swirling each cell 3 times.
6. Add 3 ml of THM Plus Reagent 2 (27540-48) to each cell. Avoid excess agitation of the sample when dispensing the reagent.
7. Place the sample cells in the cell holder assembly and then place the assembly in the hot water bath when the water is boiling rapidly.
8. Start the instrument timer. A 5-minute reaction period will begin. Heat for 7 minutes if refrigerated samples are being analysed.
9. When the timer expires, remove the sample cells from the hot water bath. Place them in the cooling bath. Use ice to cool the tap water if it is necessary.
10. Start the instrument timer. A 3-minute cooling period will begin. When the timer expires, remove the cells from the cooling bath.
11. Add 1 ml of THM Plus Reagent 3 (27541-42) to each cell. The sample and blank will become warm.
12. Replace the cooling water with cold tap water. Place the assembly that contains the sample and blank cells into the cooling bath. Use ice to cool the tap water if necessary.

13. Start the instrument timer. A 3-minute cooling period will begin. When the timer expires, remove the cells from the cooling bath. The temperature of the sample should be 15-25°C.
14. Add the contents of one THM Plus Reagent 4 (2756559) Powder Pillow to the sample cell and one to the blank. Cap each cell tightly and mix by shaking until all the powder dissolves.
15. Start the instrument timer. A 15-minute development time will begin. The colour is stable for at least 30 minutes after the 15-minute development time.
16. After the timer expires, pour the prepared sample and blank into two square sample cells. Allow the solution to settle in the square cells for 30 seconds to enable any turbidity that may be present to settle.
17. When the timer expires, wipe the blank and insert it into the cell holder.
18. Zero the instrument; the display will show 0 ppb.
19. Wipe the prepared sample and insert it into the cell holder. Read the results in ppb.

References

- Abe, Y., Skali-Lami, S., Block, J. C. and Francius, G. 2012. Cohesiveness and hydrodynamic properties of young drinking water biofilms. *Water Res*, 46, 1155-66.
- Abu-Lail, N. I. and Camesano, T. A. 2003. Role of ionic strength on the relationship of biopolymer conformation, DLVO contributions, and steric interactions to bioadhesion of *Pseudomonas putida* KT2442. *Biomacromolecules*, 4, 1000-1012.
- Amann, R. I., Krumholz, L. and Stahl, D. A. 1990. Fluorescent-Oligonucleotide Probing of Whole Cells for Determinative, Phylogenetic, and Environmental-Studies in Microbiology. *J Bacteriol*, 172, 762-770.
- Amann, R. I., Ludwig, W. and Schleifer, K. H. 1995. Phylogenetic Identification and in-Situ Detection of Individual Microbial-Cells without Cultivation. *Microbiological Reviews*, 59, 143-169.
- Andersson, S., Rajarao, G. K., Land, C. J. and Dalhammar, G. 2008. Biofilm formation and interactions of bacterial strains found in wastewater treatment systems. *FEMS Microbiol Lett*, 283, 83-90.
- Armitano, J., Mejean, V. and Jurlin-Castelli, C. 2014. Gram-negative bacteria can also form pellicles. *Environ Microbiol Rep*, 6, 534-544.
- Banin, E., Vasil, M. L. and Greenberg, E. P. 2005. Iron and *Pseudomonas aeruginosa* biofilm formation. *Proc Natl Acad Sci U S A*, 102, 11076-11081.
- Barai, P., Kumar, A. and Mukherjee, P. P. 2016. Modeling of Mesoscale Variability in Biofilm Shear Behavior. *PLoS One*, 11.
- Barbera, J. J., Metzger, A. and Wolf, M. 2012. Sulfites, Thiosulfates, and Dithionites. *Ullmann's Encyclopedia of Industrial Chemistry 2012*. Wiley-VCH, Weinheim.
- Bartsch, O. and Schwinger, E. 1991. A Simplified Protocol for Fluorescence Insitu Hybridization with Repetitive DNA Probes and Its Use in Clinical Cytogenetics. *Clinical Genetics*, 40, 47-56.
- Batté, M., Appenzeller, B. M. R., Grandjean, D., Fass, S., Gauthier, V., Jorand, F., Mathieu, L., Boualam, M., Saby, S. and Block, J. C. 2003. Biofilms in drinking water distribution systems. *Reviews in Environmental Science and Bio/Technology*, 2, 147-168.
- Battin, T. J., Sloan, W. T., Kjelleberg, S., Daims, H., Head, I. M., Curtis, T. P. and Eberl, L. 2007. Microbial landscapes: new paths to biofilm research. *Nature Reviews Microbiology*, 5, 76-81.
- Bautista-de Los Santos, Q. M., Schroeder, J. L., Blakemore, O., Moses, J., Haffey, M., Sloan, W. and Pinto, A. J. 2016a. The impact of sampling, PCR, and sequencing replication on discerning changes in drinking water bacterial community over diurnal time-scales. *Water Res*, 90, 216-24.
- Bautista-de los Santos, Q. M., Schroeder, J. L., Sevillano-Rivera, M. C., Sungthong, R., Ijaz, U. Z., Sloan, W. T. and Pinto, A. J. 2016b. Emerging investigators series: microbial communities in full-scale drinking water distribution systems - a meta-analysis. *Environmental Science-Water Research & Technology*, 2, 631-644.
- Bazin, P., Jouenne, F., Deton-Cabanillas, A. F., Perez-Ruzafa, A. and Veron, B. 2014. Complex patterns in phytoplankton and microeukaryote diversity along the estuarine continuum. *Hydrobiologia*, 726, 155-178.
- Beech, W. B. and Sunner, J. 2004. Biocorrosion: towards understanding interactions between biofilms and metals. *Curr Opin Biotechnol*, 15, 181-186.

- Ben-Jacob, E., Schohet, O., Tenenbaum, A., Cohen, I., Czirók, A. and T., V. 1994. Generic modelling of cooperative growth patterns in bacterial colonies. *Nature*, 368, 46-49.
- Bergmann, H., Iourtchouk, T., Schops, K. and Bouzek, K. 2002. New UV irradiation and direct electrolysis - promising methods for water disinfection. *Chemical Engineering Journal*, 85, 111-117.
- Besemer, K., Hodl, I., Singer, G. and Battin, T. J. 2009. Architectural differentiation reflects bacterial community structure in stream biofilms. *Isme Journal*, 3, 1318-1324.
- Beyenal, H., Donovan, C., Lewandowski, Z. and Harkin, G. 2004. Three-dimensional biofilm structure quantification. *J Microbiol Methods*, 59, 395-413.
- Bird, R. B., Steward, E. W. and Lightfoot, N. E. 1960. Transport phenomena, New York, Wiley.
- Bishop, P. L., Gibbs, J. T. and Cunningham, B. E. 1997. Relationship between concentration and hydrodynamic boundary layers over biofilms. *Environmental Technology*, 18, 375-385.
- Boe-Hansen, R. 2001. Microbial growth in drinking water distribution systems. PhD Thesis, Environment & Resources, Technical University of Denmark.
- Bos, R., Vandermei, H. C. and Busscher, H. J. 1995. A Quantitative Method to Study Co-Adhesion of Microorganisms in a Parallel-Plate Flow Chamber .2. Analysis of the Kinetics of Co-Adhesion. *J Microbiol Methods*, 23, 169-182.
- Bos, R., Vandermei, H. C., Meinders, J. M. and Busscher, H. J. 1994. A Quantitative Method to Study Co-Adhesion of Microorganisms in a Parallel-Plate Flow Chamber - Basic Principles of the Analysis. *J Microbiol Methods*, 20, 289-305.
- Brown, D., Bridgeman, J. and West, J. R. 2011. Predicting chlorine decay and THM formation in water supply systems. *Reviews in Environmental Science and Bio-Technology*, 10, 79-99.
- Brugnoni, L. I., Cubitto, M. A. and Lozano, J. E. 2011. Role of shear stress on biofilm formation of *Candida krusei* in a rotating disk system. *Journal of Food Engineering*, 102, 266-271.
- Brunk, C. F., Jones, K. C. and James, T. W. 1979. Assay for Nanogram Quantities of DNA in Cellular Homogenates. *Analytical Biochemistry*, 92, 497-500.
- Byrd, J. J., Xu, H. S. and Colwell, R. R. 1991. Viable but Nonculturable Bacteria in Drinking-Water. *Appl Environ Microbiol*, 57, 875-878.
- Campos, L. C., Su, M. F. J., Graham, N. J. D. and Smith, S. R. 2002. Biomass development in slow sand filters. *Water Res*, 36, 4543-4551.
- Capeness, M. J., Lambert, C., Lovering, A. L., Till, R., Uchida, K., Chaudhuri, R., Alderwick, L. J., Lee, D. J., Swarbreck, D., Liddell, S., Aizawa, S. I. and Sockett, R. E. 2013. Activity of *Bdellovibrio* Hit Locus Proteins, Bd0108 and Bd0109, Links Type IVa Pilus Extrusion/Retraction Status to Prey-Independent Growth Signalling. *PLoS One*, 8.
- Cappelletti, M., Frascari, D., Zannoni, D. and Fedi, S. 2012. Microbial degradation of chloroform. *Appl Microbiol Biotechnol*, 96, 1395-1409.
- Carr, J. R. and de Miranda, F. P. 1998. The semivariogram in comparison to the co-occurrence matrix for classification of image texture. *IEEE Transactions on Geoscience and Remote Sensing*, 36, 1945-1952.
- Chamberlain, E. and Adams, C. 2006. Oxidation of sulfonamides, macrolides, and carbadox with free chlorine and monochloramine. *Water Res*, 40, 2517-2526.

- Chan, K. Y., Xu, L. C. and Fang, H. H. P. 2002. Anaerobic electrochemical corrosion rug of mild steel in the presence of extracellular polymeric substances produced by a culture enriched in sulfate-reducing bacteria. *Environ Sci Technol*, 36, 1720-1727.
- Chang, E. E., Lin, Y. P. and Chiang, P. C. 2001. Effects of bromide on the formation of THMs and HAAs. *Chemosphere*, 43, 1029-1034.
- Chao, Y. Q. and Zhang, T. 2011. Optimization of fixation methods for observation of bacterial cell morphology and surface ultrastructures by atomic force microscopy. *Appl Microbiol Biotechnol*, 92, 381-392.
- Characklis, W. G., M.H., T. and Zilver, N. 1990. Transport and interfacial transfer phenomena. In: Characklis, W. G., Marshall, K.C. (ed.) *Biofilms*. New York: John Wiley & Sons.
- Characklis, W. G. and Marshall, K. C. 1990. *Biofilms*, New York: John Wiley and Sons.
- Chen, L., Jia, R. B. and Li, L. 2013. Bacterial community of iron tubercles from a drinking water distribution system and its occurrence in stagnant tap water. *Environmental Science-Processes & Impacts*, 15, 1332-1340.
- Chen, W. J. and Weisel, C. P. 1998. Halogenated DBP concentrations in a distribution system. *Journal American Water Works Association*, 90, 151-163.
- Childs, P., R.,N. 2011. Rotating Cylinders, Annuli, and Spheres. Chapter 6. In: Elsevier (ed.) *Rotating Flow*. China: Elsevier Science & Technology Books.
- Chowdhury, S. 2012. Heterotrophic bacteria in drinking water distribution system: a review. *Environ Monit Assess*, 184, 6087-6137.
- Cogan, N. G., Harro, J. M., Stoodley, P. and Shirtliff, M. E. 2016. Predictive Computer Models for Biofilm Detachment Properties in *Pseudomonas aeruginosa*. *MBio*, 7.
- Cohen, W. B., Spies, T. A. and Bradshaw, G. A. 1990. Semivariograms of Digital Imagery for Analysis of Conifer Canopy Structure *Remote Sens. Environ.*, 34, 167-178.
- Colwell, R. R., Brayton, P. R., Grimes, D. J., Roszak, D. B., Huq, S. A. and Palmer, L. M. 1985. Viable but Non-Culturable *Vibrio-Cholerae* and Related Pathogens in the Environment - Implications for Release of Genetically Engineered Microorganisms. *Bio-Technology*, 3, 817-820.
- Craig, L., Pique, M. E. and Tainer, J. A. 2004. Type IV pilus structure and bacterial pathogenicity. *Nat Rev Microbiol*, 2, 363-78.
- CRChandbook 1984. Handbook of Chemistry and Physics. Sixtyfourth. Edition. CRC Press.
- Cressie, N. 1993. Statistics for spatial data, Wiley series in probability and mathematical statistics, Revised Edition, New York, Wiley.
- Cui, C., Shu, W. and Li, P. 2016. Fluorescence In situ Hybridization: Cell-Based Genetic Diagnostic and Research Applications. *Front Cell Dev Biol*, 4, 89.
- Curran, S. J. and Black, R. A. 2005. Oxygen transport and cell viability in an annular flow bioreactor: comparison of laminar Couette and Taylor-vortex flow regimes. *Biotechnol Bioeng*, 89, 766-74.
- De Beer, D. and Stoodley, P. 2006. Microbial Biofilms. Chapter 3.10. . In: Springer (ed.) *The Prokaryotes. Volume 7: Proteobacteria: Delta, Epsilon Subclass. Third Edition*.
- De Beer, D., Stoodley, P., Roe, F. and Lewandowski, Z. 1994. Effects of biofilm structures on oxygen distribution and mass transport. *Biotechnol Bioeng*, 43, 1131-8.

- Deborde, M. and von Gunten, U. 2008. Reactions of chlorine with inorganic and organic compounds during water treatment-Kinetics and mechanisms: a critical review. *Water Res*, 42, 13-51.
- Deighton, M. A. and Balkau, B. 1990. Adherence Measured by Microtiter Assay as a Virulence Marker for Staphylococcus-Epidermidis Infections. *J Clin Microbiol*, 28, 2442-2447.
- Deines, P., Sekar, R., Husband, P. S., Boxall, J. B., Osborn, A. M. and Biggs, C. A. 2010. A new coupon design for simultaneous analysis of in situ microbial biofilm formation and community structure in drinking water distribution systems. *Appl Microbiol Biotechnol*, 87, 749-756.
- Dennis, P. G., Seymour, J., Kumbun, K. and Tyson, G. W. 2013. Diverse populations of lake water bacteria exhibit chemotaxis towards inorganic nutrients. *Isme Journal*, 7, 1661-1664.
- DePas, W. H., Hufnagel, D. A., Lee, J. S., Blanco, L. P., Bernstein, H. C., Fisher, S. T., James, G. A., Stewart, P. S. and Chapman, M. R. 2013. Iron induces bimodal population development by Escherichia coli. *Proc Natl Acad Sci U S A*, 110, 2629-2634.
- Derlon, N., Masse, A., Escudie, R., Bernet, N. and Paul, E. 2008. Stratification in the cohesion of biofilms grown under various environmental conditions. *Water Res*, 42, 2102-2110.
- Doerges, L. and Kutschera, U. 2014. Assembly and loss of the polar flagellum in plant-associated methylobacteria. *Naturwissenschaften*, 101, 339-346.
- Dohner, H., Stilgenbauer, S., Benner, A., Leupolt, E., Krober, A., Bullinger, L., Dohner, K., Bentz, M. and Lichter, P. 2000. Genomic aberrations and survival in chronic lymphocytic leukemia. *N Engl J Med*, 343, 1910-6.
- Donlan, R. M. 2002. Biofilms: Microbial life on surfaces. *Emerg Infect Dis*, 8, 881-890.
- Douris, V., Papapostolou, K. M., Ilias, A., Roditakis, E., Kounadi, S., Riga, M., Nauen, R. and Vontas, J. 2017. Investigation of the contribution of RyR target-site mutations in diamide resistance by CRISPR/Cas9 genome modification in Drosophila. *Insect Biochem Mol Biol*, 87, 127-135.
- Douterelo, I., Boxall, J. B., Deines, P., Sekar, R., Fish, K. E. and Biggs, C. A. 2014a. Methodological approaches for studying the microbial ecology of drinking water distribution systems. *Water Res*, 65, 134-156.
- Douterelo, I., Husband, S. and Boxall, J. B. 2014b. The bacteriological composition of biomass recovered by flushing an operational drinking water distribution system. *Water Res*, 54, 100-114.
- Douterelo, I., Sharpe, R. and Boxall, J. 2014c. Bacterial community dynamics during the early stages of biofilm formation in a chlorinated experimental drinking water distribution system: implications for drinking water discolouration. *J Appl Microbiol*, 117, 286-301.
- Douterelo, I., Sharpe, R. L. and Boxall, J. B. 2013. Influence of hydraulic regimes on bacterial community structure and composition in an experimental drinking water distribution system. *Water Res*, 47, 503-16.
- Duddu, R., Chopp, D. L. and Moran, B. 2009. A Two-Dimensional Continuum Model of Biofilm Growth Incorporating Fluid Flow and Shear Stress Based Detachment. *Biotechnol Bioeng*, 103, 92-104.
- Dunne, W. M. 2002. Bacterial adhesion: Seen any good biofilms lately? *Clinical Microbiology Reviews*, 15, 155-166.
- Dyck, R., Cool, G., Rodriguez, M. and Sadiq, R. 2015. Treatment, residual chlorine and season as factors affecting variability of trihalomethanes in

- small drinking water systems. *Frontiers of Environmental Science & Engineering*, 9, 171-179.
- Edwards, K. J., Bond, P. L., Gihring, T. M. and Banfield, J. F. 2000. An archaeal iron-oxidizing extreme acidophile important in acid mine drainage. *Science*, 287, 1796-1799.
- Else, T. A., Pantle, C. R. and Amy, P. S. 2003. Boundaries for biofilm formation: Humidity and temperature. *Appl Environ Microbiol*, 69, 5006-5010.
- Emtiazi, F., Schwartz, T., Marten, S. M., Krolla-Sidenstein, P. and Obst, U. 2004. Investigation of natural biofilms formed during the production of drinking water from surface water embankment filtration. *Water Res*, 38, 1197-1206.
- Escobar, I. C. and Randall, A. A. 2001. Assimilable organic carbon (AOC) and biodegradable dissolved organic carbon (BDOC): Complementary measurements. *Water Res*, 35, 4444-4454.
- Espeso, D. R., Carpio, A. and Einarsson, B. 2015. Differential growth of wrinkled biofilms. *Physical Review E*, 91.
- Falkinham, J. O., Williams, M. D., Kwait, R. and Lande, L. 2016. *Methylobacterium* spp. as an indicator for the presence or absence of *Mycobacterium* spp. *International Journal of Mycobacteriology*, 5, 240-243.
- Fang, H. H. P., Chan, K. Y. and Xu, L. C. 2000. Quantification of bacterial adhesion forces using atomic force microscopy (AFM). *J Microbiol Methods*, 40, 89-97.
- Fish, K. E., Osborn, A. M. and Boxall, J. 2016. Characterising and understanding the impact of microbial biofilms and the extracellular polymeric substance (EPS) matrix in drinking water distribution systems. *Environmental Science-Water Research & Technology*, 2, 614-630.
- Flemming, H. C. 2011. The perfect slime. *Colloids Surf B Biointerfaces*, 86, 251-9.
- Flemming, H. C., Percival, S. L. and Walker, J. T. 2002. Contamination potential of biofilms in water distribution systems. *Innovations in Conventional and Advanced Water Treatment Processes*, 2, 271-280.
- Flemming, H. C. and Wingender, J. 2010. The biofilm matrix. *Nature Reviews Microbiology*, 8, 623-633.
- Florjanic, M. and Kristl, J. 2011. The control of biofilm formation by hydrodynamics of purified water in industrial distribution system. *International Journal of Pharmaceutics*, 405, 16-22.
- Fraser, G. M., Claret, L., Furness, R., Gupta, S. and Hughes, C. 2002. Swarming-coupled expression of the *Proteus mirabilis* hpmBA haemolysin operon. *Microbiology*, 148, 2191-201.
- Fraser, G. M. and Hughes, C. 1999. Swarming motility. *Current Opinion in Microbiology*, 2, 630-5.
- Fuhrman, J. A. 2009. Microbial community structure and its functional implications. *Nature*, 459, 193-9.
- Fujiwara, K. 1916. New reaction for the detection of chloroform. *Sitzungsberichte der Naturforschenden Gesellschaft zu Rostock*, 6, 33-43.
- Galajda, P., Keymer, J., Chaikin, P. and Austin, R. 2007. A wall of funnels concentrates swimming bacteria. *J Bacteriol*, 189, 8704-8707.
- Gallagher, M. D., Nuckols, J. R., Stallones, L. and Savitz, D. A. 1998. Exposure to trihalomethanes and adverse pregnancy outcomes. *Epidemiology*, 9, 484-489.

- Gallego, V., Garcia, M. T. and Ventosa, A. 2005a. *Methylobacterium hispanicum* sp nov and *Methylobacterium aquaticum* sp nov., isolated from drinking water. *Int J Syst Evol Microbiol*, 55, 281-287.
- Gallego, V., Garcia, M. T. and Ventosa, A. 2005b. *Methylobacterium isbiliense* sp nov., isolated from the drinking water system of Sevilla, Spain. *Int J Syst Evol Microbiol*, 55, 2333-2337.
- Gallego, V., Garcia, M. T. and Ventosa, A. 2005c. *Methylobacterium variabile* sp nov., a methylotrophic bacterium isolated from an aquatic environment. *Int J Syst Evol Microbiol*, 55, 1429-1433.
- Garny, K., Horn, H. and Neu, T. R. 2008. Interaction between biofilm development, structure and detachment in rotating annular reactors. *Bioprocess Biosyst Eng*, 31, 619-629.
- Garrett, T. R., Bhakoo, M. and Zhang, Z. 2008. Bacterial adhesion and biofilms on surfaces. *Progress in Natural Science*, 18, 1049-1056.
- Gehring, A. G., Albin, D. M., Bhunia, A. K., Kim, H., Reed, S. A. and Tu, S. I. 2012. Mixed culture enrichment of *Escherichia coli* O157:H7, *Listeria monocytogenes*, *Salmonella enterica*, and *Yersinia enterocolitica*. *Food Control*, 26, 269-273.
- Gjaltema, A., Arts, P. A. M., Vanloosdrecht, M. C. M., Kuenen, J. G. and Heijnen, J. J. 1994. Heterogeneity of Biofilms in Rotating Annular Reactors - Occurrence, Structure, and Consequences. *Biotechnol Bioeng*, 44, 194-204.
- Gomes, I. B., Simões, M. and Simões, L. C. 2014. An overview on the reactors to study drinking water biofilms. *Water Res*, 62, 63-87.
- Hall-Stoodley, L., Costerton, J. W. and Stoodley, P. 2004. Bacterial biofilms: from the natural environment to infectious diseases. *Nat Rev Microbiol*, 2, 95-108.
- Hall-Stoodley, L. and Stoodley, P. 2005. Biofilm formation and dispersal and the transmission of human pathogens. *Trends Microbiol*, 13, 7-10.
- Hall, J., Szabo, J., Panguluri, S. and Meiners, G. 2009. Distribution System Water Quality Monitoring: Sensor Technology Evaluation Methodology and Results; A Guide for Sensor Manufacturers and Water Utilities. Environmental Protection Agency. USA.
- Hallberg, K. B., Coupland, K., Kimura, S. and Johnson, D. B. 2006. Macroscopic streamer growths in acidic, metal-rich mine waters in north wales consist of novel and remarkably simple bacterial communities. *Appl Environ Microbiol*, 72, 2022-2030.
- Hardoim, P. R., van Overbeek, L. S., Berg, G., Pirttila, A. M., Compant, S., Campisano, A., Doring, M. and Sessitsch, A. 2015. The Hidden World within Plants: Ecological and Evolutionary Considerations for Defining Functioning of Microbial Endophytes. *Microbiology and Molecular Biology Reviews*, 79, 293-320.
- Harshey, R. M. 2003. Bacterial motility on a surface: Many ways to a common goal. *Annual Review of Microbiology*, 57, 249-273.
- Hausler, S. and Fuqua, C. 2013. Biofilms 2012: New Discoveries and Significant Wrinkles in a Dynamic Field. *J Bacteriol*, 195, 2947-2958.
- Hauwaerts, D., Alexandre, G., Das, S. K., Vanderleyden, J. and Zhulin, I. B. 2002. A major chemotaxis gene cluster in *Azospirillum brasilense* and relationships between chemotaxis operons in alpha-proteobacteria. *FEMS Microbiol Lett*, 208, 61-67.
- Heilbronner, R. and Barrett, S. 2014. Image Analysis in Earth Sciences. Springer.

- Hermansson, M. 1999. The DLVO theory in microbial adhesion. *Colloids and Surfaces B-Biointerfaces*, 14, 105-119.
- Herndl, G. 2007. CARD-FISH and Microautoradiography Protocol for Bacteria and Archaea.
- Heydorn, A., Nielsen, A. T., Hentzer, M., Sternberg, C., Givskov, M., Ersboll, B. K. and Molin, S. 2000. Quantification of biofilm structures by the novel computer program COMSTAT. *Microbiology-Uk*, 146, 2395-2407.
- Hiraishi, A., Furuhashi, K., Matsumoto, A., Koike, K. A., Fukuyama, M. and Tabuchi, K. 1995. Phenotypic and Genetic Diversity of Chlorine-Resistant *Methylobacterium* Strains Isolated from Various Environments. *Appl Environ Microbiol*, 61, 2099-2107.
- Holman, J. P. 2002. Heat transfer. Tenth Edition. Department of Mechanical Engineering. Southern Methodist University.
- Hondzo, M. and Wuest, A. 2009. Do Microscopic Organisms Feel Turbulent Flows? *Environ Sci Technol*, 43, 764-768.
- Hope, C. K. and Wilson, M. 2006. Biofilm structure and cell vitality in a laboratory model of subgingival plaque. *J Microbiol Methods*, 66, 390-398.
- Horemans, B., Breugelmans, P., Hofkens, J., Smolders, E. and Springael, D. 2013. Environmental Dissolved Organic Matter Governs Biofilm Formation and Subsequent Linuron Degradation Activity of a Linuron-Degrading Bacterial Consortium. *Appl Environ Microbiol*, 79, 4534-4542.
- Hori, K. and Matsumoto, S. 2010. Bacterial adhesion: From mechanism to control. *Biochemical Engineering Journal*, 48, 424-434.
- Hsieh, M. K., Li, H., Chien, S. H., Monnell, J. D., Chowdhury, I., Dzombak, D. A. and Vidic, R. D. 2010. Corrosion Control When Using Secondary Treated Municipal Wastewater as Alternative Makeup Water for Cooling Tower Systems. *Water Environment Research*, 82, 2346-2356.
- Huber, B., Riedel, K., Hentzer, M., Heydorn, A., Gotschlich, A., Givskov, M., Molin, S. and Eberl, L. 2001. The *cep* quorum-sensing system of *Burkholderia cepacia* H111 controls biofilm formation and swarming motility. *Microbiology-Sgm*, 147, 2517-2528.
- Hugenholtz, P., Tyson, G. W. and Blackall, L. L. 2002. Design and evaluation of 16S rRNA-targeted oligonucleotide probes for fluorescence in situ hybridization. *Methods Mol Biol*, 179, 29-42.
- Hughmark, G. A. 1975. Heat, Mass, and Momentum Transport with Turbulent-Flow in Smooth and Rough Pipe. *Aiche Journal*, 21, 1033-1035.
- Hung, C., Zhou, Y. Z., Pinkner, J. S., Dodson, K. W., Crowley, J. R., Heuser, J., Chapman, M. R., Hadjifrangiskou, M., Henderson, J. P. and Hultgren, S. J. 2013. *Escherichia coli* Biofilms Have an Organized and Complex Extracellular Matrix Structure. *MBio*, 4.
- Husband, S. and Boxall, J. B. 2010. Field Studies of Discoloration in Water Distribution Systems: Model Verification and Practical Implications. *Journal of Environmental Engineering-Asce*, 136, 86-94.
- Jaberi, F. A. and Colucci, P. J. 2003a. Large eddy simulation of heat and mass transport in turbulent flows. Part 1: Velocity field. *International Journal of Heat and Mass Transfer*, 46, 1811-1825.
- Jaberi, F. A. and Colucci, P. J. 2003b. Large eddy simulation of heat and mass transport in turbulent flows. Part 2: Scalar field. *International Journal of Heat and Mass Transfer*, 46, 1827-1840.
- Jackson, C. R., Churchill, P. F. and Roden, E. E. 2001. Successional changes in bacterial assemblage structure during epilithic biofilm development. *Ecology*, 82, 555-566.

- Jackson, C. R., Roden, E. E. and Churchill, P. F. 1998. Changes in bacterial species composition in enrichment cultures with various dilutions of inoculum as monitored by denaturing gradient gel electrophoresis. *Appl Environ Microbiol*, 64, 5046-5048.
- Jahng, D. J. and Wood, T. K. 1994. Trichloroethylene and Chloroform Degradation by a Recombinant Pseudomonad Expressing Soluble Methane Monooxygenase from Methylosinus-Trichosporium Ob3b. *Appl Environ Microbiol*, 60, 2473-2482.
- Jan-Roblero, J., Romero, J. M., Amaya, M. and Le Borgne, S. 2004. Phylogenetic characterization of a corrosive consortium isolated from a sour gas pipeline. *Appl Microbiol Biotechnol*, 64, 862-867.
- Jarroll, E. L., Bingham, A. K. and Meyer, E. A. 1981. Effect of Chlorine on Giardia-Lambliia Cyst Viability. *Appl Environ Microbiol*, 41, 483-487.
- Jefferson, K. K. 2004. What drives bacteria to produce a biofilm? *FEMS Microbiol Lett*, 236, 163-173.
- Jischa, M. 1976. Transfer of Momentum, Heat and Mass in Turbulent Flows of Binary-Mixtures .1. Reynolds Equations and Transport-Equations. *Warme Und Stoffubertragung-Thermo and Fluid Dynamics*, 9, 173-178.
- Jurkevitch, E. 2006. The Genus Bdellovibrio, Chapter 3.4. In: Springer (ed.) *The Prokaryotes. Volume 7: Proteobacteria: Delta, Epsilon Subclass. Third Edition*.
- Jyoti, K. K. and Pandit, A. B. 2001. Water disinfection by acoustic and hydrodynamic cavitation. *Biochemical Engineering Journal*, 7, 201-212.
- Jyoti, K. K. and Pandit, A. B. 2003. Hybrid cavitation methods for water disinfection: simultaneous use of chemicals with cavitation. *Ultrasonics Sonochemistry*, 10, 255-264.
- Kalmbach, S., Manz, W. and Szewzyk, U. 1997. Isolation of new bacterial species from drinking water biofilms and proof of their in situ dominance with highly specific 16S rRNA probes. *Appl Environ Microbiol*, 63, 4164-4170.
- Kaplan, J. B. 2010. Biofilm dispersal: mechanisms, clinical implications, and potential therapeutic uses. *J Dent Res*, 89, 205-18.
- Karunakaran, E., Mukherjee, J., Ramalingam, B. and Biggs, C. A. 2011. "Biofilmology": a multidisciplinary review of the study of microbial biofilms. *Appl Microbiol Biotechnol*, 90, 1869-1881.
- Kaye, J. and Elgar, E., C. 1957. Modes of adiabatic and diabatic fluid flow in an annulus with an inner rotating cylinder. Massachusetts Institute of Technology. Research Laboratory of heat transfer in electronics.: Cambridge, Mass., M.I.T. Research Laboratory of Heat Transfer in Electronics.
- Kayser, M. 2001. Genes and proteins associated with dichloromethane metabolism in *Methylobacterium dichloromethanicum* DM4.
- Kearns, D. B. 2010. A field guide to bacterial swarming motility. *Nature Reviews Microbiology*, 8, 634-644.
- Kepner, R. L. and Pratt, J. R. 1994. Use of Fluorochromes for Direct Enumeration of Total Bacteria in Environmental-Samples - Past and Present. *Microbiological Reviews*, 58, 603-615.
- Khan, F., Hossain, M. D. and Kafi, A. 2014. Treatment of Textile Liquid Waste by Chlorination Process and Evaluation of the Formation of Trihalomethane *Journal of Modern Science and Technology*, 2, 69-77.
- Kirisits, M. J., Margolis, J. J., Purevdorj-Gage, B. L., Vaughan, B., Chopp, D. L., Stoodley, P. and Parsek, M. R. 2007. Influence of the hydrodynamic

- environment on quorum sensing in *Pseudomonas aeruginosa* biofilms. *J Bacteriol*, 189, 8357-8360.
- Klausen, M., Aaes-Jorgensen, A., Molin, S. and Tolker-Nielsen, T. 2003a. Involvement of bacterial migration in the development of complex multicellular structures in *Pseudomonas aeruginosa* biofilms. *Molecular Microbiology*, 50, 61-68.
- Klausen, M., Gjermansen, M., Kreft, J. U. and Tolker-Nielsen, T. 2006. Dynamics of development and dispersal in sessile microbial communities: examples from *Pseudomonas aeruginosa* and *Pseudomonas putida* model biofilms. *FEMS Microbiol Lett*, 261, 1-11.
- Klausen, M., Heydorn, A., Ragas, P., Lambertsen, L., Aaes-Jorgensen, A., Molin, S. and Tolker-Nielsen, T. 2003b. Biofilm formation by *Pseudomonas aeruginosa* wild type, flagella and type IV pili mutants. *Molecular Microbiology*, 48, 1511-1524.
- Kloc, J. and González, I. M. 2012. The Study of Biological Wastewater Treatment through Biofilm Development on Synthetic Material vs. Membranes. Worcester Polytechnic Institute.
- Kokare, C. R., Chakraborty, S., Khopade, A. N. and Mahadik, K. R. 2009. Biofilm: Importance and applications. *Indian Journal of Biotechnology*, 8, 159-168.
- Kolenbrander, P. E., Palmer, R. J., Periasamy, S. and Jakubovics, N. S. 2010. Oral multispecies biofilm development and the key role of cell-cell distance. *Nature Reviews Microbiology*, 8, 471-480.
- Komminoth, P. 1992. Digoxigenin as an alternative probe labeling for in situ hybridization. *Diagn Mol Pathol*, 1, 142-50.
- Kormas, K. A., Neofitou, C., Pachiadaki, M. and Koufostathi, E. 2010. Changes of the bacterial assemblages throughout an urban drinking water distribution system. *Environ Monit Assess*, 165, 27-38.
- Kornaros, M. and Lyberatos, G. 2006. Biological treatment of wastewaters from a dye manufacturing company using a trickling filter. *Journal of Hazardous Materials*, 136, 95-102.
- Korvick, J. A., Rihs, J. D., Gilardi, G. L. and Yu, V. L. 1989. A pink-pigmented, oxidative, nonmotile bacterium as a cause of opportunistic infections. *Arch Intern Med*, 149, 1449-51.
- Kraigsley, A., Ronney, P. D. and Finkel, S. E. 2014. Hydrodynamic influences on biofilm formation and growth. University of Southern California. <http://ronney.usc.edu/research/biophysics/Biofilms4Web.html>.
- Kubota, K. 2013. CARD-FISH for Environmental Microorganisms: Technical Advancement and Future Applications. *Microbes and Environments*, 28, 3-12.
- Kumarasamy, M. V. and Maharaj, P. M. 2015. The Effect of Biofilm Growth on Wall Shear Stress in Drinking Water PVC Pipes. *Polish Journal of Environmental Studies*, 24, 2479-2483.
- Lebel, G. L. and Williams, D. T. 1995. Differences in Chloroform Levels from Drinking-Water Samples Analyzed Using Various Sampling and Analytical Techniques. *International Journal of Environmental Analytical Chemistry*, 60, 213-220.
- Lee, S. H., Lee, S. S. and Kim, C. W. 2002. Changes in the cell size of *Brevundimonas diminuta* using different growth agitation rates. *PDA J Pharm Sci Technol*, 56, 99-108.
- Leisinger, T. and Braus-Stromeyer, S. A. 1995. Bacterial growth with chlorinated methanes. *Environmental Health Perspectives*, 103, 33-36.

- Lewandowski, Z. and Beyenal, H. 2013. *Fundamentals of Biofilm Research*, Second Edition, CRC Press, Taylor and Francis Group.
- Lidstrom, M. E. and Chistoserdova, L. 2002. Plants in the pink: cytokinin production by methylobacterium. *J Bacteriol*, 184, 1818.
- Lieberman, R. L. and Rosenzweig, A. C. 2004. Biological methane oxidation: Regulation, biochemistry, and active site structure of particulate methane monooxygenase. *Critical Reviews in Biochemistry and Molecular Biology*, 39, 147-164.
- Liu, S., Gunawan, C., Barraud, N., Rice, S. A., Harry, E. J. and Amal, R. 2016. Understanding, Monitoring, and Controlling Biofilm Growth in Drinking Water Distribution Systems. *Environ Sci Technol*, 50, 8954-8976.
- Liu, Y. and Tay, J. H. 2001. Metabolic response of biofilm to shear stress in fixed-film culture. *J Appl Microbiol*, 90, 337-342.
- Liu, Y. and Tay, J. H. 2002. The essential role of hydrodynamic shear force in the formation of biofilm and granular sludge. *Water Res*, 36, 1653-1665.
- Macfarlane, S., Hopkins, M. J. and Macfarlane, G. T. 2001. Toxin synthesis and mucin breakdown are related to swarming phenomenon in *Clostridium septicum*. *Infect Immun*, 69, 1120-1126.
- Machell, J. and Boxall, J. 2014. Modeling and Field Work to Investigate the Relationship between Age and Quality of Tap Water. *Journal of Water Resources Planning and Management*, 140.
- Machell, J., Boxall, J., Saul, A. and Bramley, D. 2009. Improved Representation of Water Age in Distribution Networks to Inform Water Quality. *Journal of Water Resources Planning and Management-Asce*, 135, 382-391.
- Manuel, C. M. 2007. *Biofilm Dynamics and Drinking Water Stability: Effects of Hydrodynamics and Surface Materials*. PhD Thesis, University of Porto, Portugal.
- Manuel, C. M., Nunes, O. C. and Melo, L. F. 2007. Dynamics of drinking water biofilm in flow/non-flow conditions. *Water Res*, 41, 551-562.
- Martinez, A., Torello, S. and Kolter, R. 1999. Sliding motility in mycobacteria. *J Bacteriol*, 181, 7331-8.
- Martiny, A. C., Jorgensen, T. M., Albrechtsen, H. J., Arvin, E. and Molin, S. 2003. Long-term succession of structure and diversity of a biofilm formed in a model drinking water distribution system. *Appl Environ Microbiol*, 69, 6899-6907.
- Matsuyama, T., Bhasin, A. and Harshey, R. M. 1995. Mutational analysis of flagellum-independent surface spreading of *Serratia marcescens* 274 on a low-agar medium. *J Bacteriol*, 177, 987-91.
- Matsuyama, T., Harshey, R. M. and Matsushita, M. 1993. Self-similar colony morphogenesis by bacteria as the experimental model of fractal growth by a cell population. *Fractals-Complex Geometry Patterns and Scaling in Nature and Society*, 1, 302-11.
- Mattick, J. S. 2002. Type IV pili and twitching motility. *Annual Review of Microbiology*, 56, 289-314.
- McDougald, D., Rice, S. A., Weichert, D. and Kjelleberg, S. 1998. Nonculturability: adaptation or debilitation? *FEMS Microbiol Ecol*, 25, 1-9.
- McLean, R. J. C., Pierson, L. S. and Fuqua, C. 2004. A simple screening protocol for the identification of quorum signal antagonists. *J Microbiol Methods*, 58, 351-360.
- Melnick, R. L., Dunnick, J. K., Sandler, D. P., Elwell, M. R. and Barrett, J. C. 1994. Trihalomethanes and Other Environmental-Factors That Contribute to Colorectal-Cancer. *Environmental Health Perspectives*, 102, 586-588.

- Mezule, L., Tsyfansky, S., Yakushevich, V. and Juhna, T. 2009. A simple technique for water disinfection with hydrodynamic cavitation: Effect on survival of *Escherichia coli*. *Desalination*, 248, 152-159.
- Milferstedt, K., Pons, M. N. and Morgenroth, E. 2006. Optical method for long-term and large-scale monitoring of spatial biofilm development. *Biotechnol Bioeng*, 94, 773-782.
- Mireles, J. R., Toguchi, A. and Harshey, R. M. 2001. *Salmonella enterica* serovar typhimurium swarming mutants with altered biofilm-forming abilities: Surfactin inhibits biofilm formation. *J Bacteriol*, 183, 5848-5854.
- Miyazaki, M., Nikolicpaterson, D. J., Endoh, M., Nomoto, Y., Sakai, H., Atkins, R. C. and Koji, T. 1994. A Sensitive Method of Nonradioactive in-Situ Hybridization for Messenger-Rna Localization within Human Renal Biopsy Specimens - Use of Digoxigenin-Labeled Oligonucleotides. *Internal Medicine*, 33, 87-91.
- Momba, M. N. B. and Kaleni, P. 2002. Regrowth and survival of indicator microorganisms on the surfaces of household containers used for the storage of drinking water in rural communities of South Africa. *Water Res*, 36, 3023-3028.
- Momba, M. N. B., Kfir, R., Venter, S. N. and Cloete, T. E. 2000. An overview of biofilm formation in distribution systems and its impact on the deterioration of water quality. *Water SA*, 26, 59-66.
- Morgenroth, E. and Wilderer, P. A. 2000. Influence of detachment mechanisms on competition in biofilms. *Water Res*, 34, 417-426.
- Munson B. R., Young D. F. and Okiishi, T. H. 1998. *Fundamentals of Fluid Mechanics*.
- Neria-Gonzalez, I., Wang, E. T., Ramirez, F., Romero, J. M. and Hernandez-Rodriguez, C. 2006. Characterization of bacterial community associated to biofilms of corroded oil pipelines from the southeast of Mexico. *Anaerobe*, 12, 122-33.
- Nicewarner-Pena, S. R., Freeman, R. G., Reiss, B. D., He, L., Pena, D. J., Walton, I. D., Cromer, R., Keating, C. D. and Natan, M. J. 2001. Submicrometer metallic barcodes. *Science*, 294, 137-141.
- Niederdorfer, R., Peter, H. and Battin, T. J. 2016. Attached biofilms and suspended aggregates are distinct microbial lifestyles emanating from differing hydraulics. *Nat Microbiol*, 1, 16178.
- Nielsen, J. L., Klausen, C., Nielsen, P. H., Burford, M. and Jorgensen, N. O. G. 2006. Detection of activity among uncultured Actinobacteria in a drinking water reservoir. *FEMS Microbiol Ecol*, 55, 432-438.
- Nikolaou, A. D., Lekkas, T. D., Golfinopoulos, S. K. and Kostopoulou, M. N. 2002. Application of different analytical methods for determination of volatile chlorination by-products in drinking water. *Talanta*, 56, 717-26.
- Nishio, T., Yoshikura, T. and Itoh, H. 1997. Detection of *Methylobacterium* species by 16S rRNA gene-targeted PCR. *Appl Environ Microbiol*, 63, 1594-1597.
- NRCouncil 2006. *Drinking Water Distribution Systems: Assessing and Reducing Risks*. National Research (NR) Council. The National Academies Press. USA.
- Nunez, M., Martin, M. O., Duong, L. K., Ly, E. and Spain, E. M. 2003. Investigations into the life cycle-of the bacterial predator *Bdeliovibrio bacteriovorus* 109J at an interface by atomic force microscopy. *Biophysical Journal*, 84, 3379-3388.

- O'Toole, G. A. and Kolter, R. 1998. Flagellar and twitching motility are necessary for *Pseudomonas aeruginosa* biofilm development. *Molecular Microbiology*, 30, 295-304.
- O'Neal, J. and Guillemot, G. 2010. Online Monitoring of Biofilm in Cooling Tower Systems. The Analyst Technology Supplement.
- Olea, R. A. 1999. Geostatistics for Engineers and Earth Scientists. Boston: Kluwer Academic Publishers.
- Oliver, J. D., Nilsson, L. and Kjelleberg, S. 1991. Formation of Nonculturable *Vibrio-Vulnificus* Cells and Its Relationship to the Starvation State. *Appl Environ Microbiol*, 57, 2640-2644.
- Olson, B. H. and Nagy, L. A. 1984. Microbiology of Potable Water. *Adv Appl Microbiol*, 30, 73-132.
- Omer, Z. S., Tombolini, R. and Gerhardson, B. 2004. Plant colonization by pink-pigmented facultative methylotrophic bacteria (PPFMs). *FEMS Microbiol Ecol*, 47, 319-26.
- Parsek, M. R. and Tolker-Nielsen, T. 2008. Pattern formation in *Pseudomonas aeruginosa* biofilms. *Current Opinion in Microbiology*, 11, 560-566.
- Patel, R. N., Hou, C. T., Laskin, A. I. and Felix, A. 1982. Microbial Oxidation of Hydrocarbons - Properties of a Soluble Methane Mono-Oxygenase from a Facultative Methane-Utilizing Organism, *Methylobacterium* Sp Strain Crl-26. *Appl Environ Microbiol*, 44, 1130-1137.
- Paul, E., Ochoa, J. C., Pechaud, Y., Liu, Y. and Line, A. 2012. Effect of shear stress and growth conditions on detachment and physical properties of biofilms. *Water Res*, 46, 5499-5508.
- Penalver, C. G. N., Cantet, F., Morin, D., Haras, D. and Vorholt, J. A. 2006. A plasmid-borne truncated luxI homolog controls quorum-sensing systems and extracellular carbohydrate production in *Methylobacterium extorquens* AM1. *J Bacteriol*, 188, 7321-7324.
- Percival, S. L., Knapp, J. S., Wales, D. S. and Edyvean, R. G. J. 1999. The effect of turbulent flow and surface roughness on biofilm formation in drinking water. *J Ind Microbiol Biotechnol*, 22, 152-159.
- Percival, S. L., Malic, S., Cruz, H. and Williams, D. W. 2011. Introduction to Biofilms. In: Springer (ed.) *Biofilms and Veterinary Medicine*.
- Pereira, M. A. 2000. Health Risk of the Trihalomethanes Found in Drinking Water Carcinogenic Activity and Interactions. Environmental Protection Agency (EPA). USA.
- Pereira, M. O., Kuehn, M., Wuertz, S., Neu, T. and Melo, L. F. 2002. Effect of flow regime on the architecture of a *Pseudomonas fluorescens* biofilm. *Biotechnol Bioeng*, 78, 164-171.
- Perni, S., Jordan, S. J., Andrew, P. W. and Shama, G. 2006. Biofilm development by *Listeria innocua* in turbulent flow regimes. *Food Control*, 17, 875-883.
- Picioreanu, C., Kreft, J. U., Klausen, M., Haagensen, J. A. J., Tolker-Nielsen, T. and Molin, S. 2007. Microbial motility involvement in biofilm structure formation - a 3D modelling study. *Water Science & Technology*, 55, 337.
- Picioreanu, C., van Loosdrecht, M., C., M. and Heijnen, J., J. 2000. Modelling and predicting biofilm structure. In: Allison, D., J., Gilbert, P., Lappin-Scott, H., M. & Wilson, M. (eds.) *Community Structure and Co-operation in Biofilms*. Cambridge University Press.
- Pirttila, A. M., Laukkanen, H., Pospiech, H., Myllyla, R. and Hohtola, A. 2000. Detection of intracellular bacteria in the buds of Scotch pine (*Pinus sylvestris* L.) by in situ hybridization. *Appl Environ Microbiol*, 66, 3073-3077.

- Podolich, O., Laschevskyy, V., Ovcharenko, L., Kozyrovska, N. and Pirttila, A. M. 2009. *Methylobacterium* sp resides in unculturable state in potato tissues in vitro and becomes culturable after induction by *Pseudomonas fluorescens* IMGB163. *J Appl Microbiol*, 106, 728-737.
- Poonguzhali, S., Madhaiyan, M. and Sa, T. 2007. Production of acyl-homoserine lactone quorum-sensing signals is widespread in gram-negative *Methylobacterium*. *Journal of Microbiology and Biotechnology*, 17, 226-233.
- Pratt, L. A. and Kolter, R. 1998. Genetic analysis of *Escherichia coli* biofilm formation: roles of flagella, motility, chemotaxis and type I pili. *Molecular Microbiology*, 30, 285-293.
- Purevdorj, B., Costerton, J. W. and Stoodley, P. 2002. Influence of Hydrodynamics and Cell Signaling on the Structure and Behavior of *Pseudomonas aeruginosa* Biofilms. *Appl Environ Microbiol*, 68, 4457-4464.
- Purevdorj, B. and Stoodley, P. 2004. Biofilm structure, behavior, and hydrodynamics. *Microbial Biofilms*.
- Ragot, S. A., Kertesz, M. A. and Bunemann, E. K. 2015. *phoD* Alkaline Phosphatase Gene Diversity in Soil. *Appl Environ Microbiol*, 81, 7281-7289.
- Ramalingam, B. 2012. The role of cell to cell interactions and quorum sensing in formation of biofilms by drinking water bacteria. PhD Thesis, Univeristy of Sheffield, United Kingdom.
- Ramalingam, B., Sekar, R., Boxall, J. B. and Biggs, C. A. 2013. Aggregation and biofilm formation of bacteria isolated from domestic drinking water. *Water Science and Technology-Water Supply*, 13, 1016-1023.
- Rashid, M. H. and Kornberg, A. 2000. Inorganic polyphosphate is needed for swimming, swarming, and twitching motilities of *Pseudomonas aeruginosa*. *Proc Natl Acad Sci U S A*, 97, 4885-90.
- Rasmussen, L., White, E. L., Pathak, A., Ayala, J. C., Wang, H. X., Wu, J. H., Benitez, J. A. and Silva, A. J. 2011. A High-Throughput Screening Assay for Inhibitors of Bacterial Motility Identifies a Novel Inhibitor of the Na⁺-Driven Flagellar Motor and Virulence Gene Expression in *Vibrio cholerae*. *Antimicrob Agents Chemother*, 55, 4134-4143.
- Read, S. T., Dutta, P., Bond, P. L., Keller, J. and Rabaey, K. 2010. Initial development and structure of biofilms on microbial fuel cell anodes. *BMC Microbiol*, 10.
- Reasoner, D. J. and Geldreich, E. E. 1985. A New Medium for the Enumeration and Subculture of Bacteria from Potable Water. *Appl Environ Microbiol*, 49, 1-7.
- Recht, J. and Kolter, R. 2001. Glycopeptidolipid acetylation affects sliding motility and biofilm formation in *Mycobacterium smegmatis*. *J Bacteriol*, 183, 5718-5724.
- Reysenbach, A. L. and Cady, S. L. 2001. Microbiology of ancient and modern hydrothermal systems. *Trends Microbiol*, 9, 79-86.
- Rickard, A. H., Leach, S. A., Buswell, C. M., High, N. J. and Handley, P. S. 2000. Coaggregation between aquatic bacteria is mediated by specific-growth-phase-dependent lectin-saccharide interactions. *Appl Environ Microbiol*, 66, 431-434.
- Rickard, A. H., McBain, A. J., Ledder, R. G., Handley, P. S. and Gilbert, P. 2003. Coaggregation between freshwater bacteria within biofilm and planktonic communities. *FEMS Microbiol Lett*, 220, 133-140.

- Rickard, A. H., McBain, A. J., Stead, A. T. and Gilbert, P. 2004. Shear rate moderates community diversity in freshwater biofilms. *Appl Environ Microbiol*, 70, 7426-7435.
- Riedel, K., Hentzer, M., Geisenberger, O., Huber, B., Steidle, A., Wu, H., Hoiby, N., Givskov, M., Molin, S. and Eberl, L. 2001. N-acylhomoserine-lactone-mediated communication between *Pseudomonas aeruginosa* and *Burkholderia cepacia* in mixed biofilms. *Microbiology-Sgm*, 147, 3249-3262.
- Robbins, E., Baldino, F., Jr., Roberts-Lewis, J. M., Meyer, S. L., Grega, D. and Lewis, M. E. 1991. Quantitative non-radioactive in situ hybridization of preproenkephalin mRNA with digoxigenin-labeled cRNA probes. *Anat Rec*, 231, 559-62.
- Rochex, A., Godon, J. J., Bernet, N. and Escudie, R. 2008. Role of shear stress on composition, diversity and dynamics of biofilm bacterial communities. *Water Res*, 42, 4915-4922.
- Rodriguez, M. J. and Serodes, J. B. 2001. Spatial and temporal evolution of trihalomethanes in three water distribution systems. *Water Res*, 35, 1572-1586.
- Rodriquez, M. J., Serodes, J. B. and Levallois, P. 2004. Behavior of trihalomethanes and haloacetic acids in a drinking water distribution system. *Water Res*, 38, 4367-4382.
- Rollins, D. M. and Colwell, R. R. 1986. Viable but Nonculturable Stage of *Campylobacter-jejuni* and Its Role in Survival in the Natural Aquatic Environment. *Appl Environ Microbiol*, 52, 531-538.
- Romero-Gomez, P. and Choi, C. Y. 2011. Axial Dispersion Coefficients in Laminar Flows of Water-Distribution Systems. *Journal of Hydraulic Engineering-Asce*, 137, 1500-1508.
- Roszak, D. B. and Colwell, R. R. 1987. Survival Strategies of Bacteria in the Natural-Environment. *Microbiological Reviews*, 51, 365-379.
- Roszak, D. B., Grimes, D. J. and Colwell, R. R. 1984. Viable but Nonrecoverable Stage of *Salmonella-Enteritidis* in Aquatic Systems. *Canadian Journal of Microbiology*, 30, 334-338.
- Rusconi, R., Lecuyer, S., Guglielmini, L. and Stone, H. A. 2010. Laminar flow around corners triggers the formation of biofilm streamers. *Journal of the Royal Society Interface*, 7, 1293-1299.
- Russ, J. C. 2011. The image processing handbook, Sixth Edition, North Carolina State University, Materials Science and Engineering Department, Raleigh, North Carolina, CRC Press.
- Sadiq, R. and Rodriguez, M. J. 2004. Disinfection by-products (DBPs) in drinking water and predictive models for their occurrence: a review. *Science of the Total Environment*, 321, 21-46.
- Sager, B. and Kaiser, D. 1994. Intercellular C-Signaling and the Traveling Waves of *Myxococcus*. *Genes & Development*, 8, 2793-2804.
- Samad, T., Billings, N., Birjiniuk, A., Cruzier, T., Doyle, P. S. and Ribbeck, K. 2017. Swimming bacteria promote dispersal of non-motile staphylococcal species. *ISME J*.
- Sanders, J. W., Martin, J. W., Hooke, M. and Hooke, J. 2000. *Methylobacterium mesophilicum* infection: Case report and literature review of an unusual opportunistic pathogen. *Clinical Infectious Diseases*, 30, 936-938.
- Sandle, T. 2004. An approach for the reporting of microbiological results from water systems. *Pda Journal of Pharmaceutical Science and Technology*, 58, 231-237.

- Saur, T., Morin, E., Habouzit, F., Bernet, N. and Escudie, R. 2017. Impact of wall shear stress on initial bacterial adhesion in rotating annular reactor. *PLoS One*, 12, e0172113.
- SAWater 2011. Allowable pipe size, class and materials for water mains. South Australian (SA) Water Corporation.
- Schauer, S. and Kutschera, U. 2011. A novel growth-promoting microbe, *Methylobacterium funariae* sp. nov., isolated from the leaf surface of a common moss. *Plant Signal Behav*, 6, 510-5.
- Schroder, S., Hain, M. and Sterflinger, K. 2000. Colorimetric in situ hybridization (CISH) with digoxigenin-labeled oligonucleotide probes in autofluorescent hyphomycetes. *International Microbiology*, 3, 183-6.
- Schumacher, J. A., Zhao, E. J., Kofron, M. J. and Sumanas, S. 2014. Two-color fluorescent in situ hybridization using chromogenic substrates in zebrafish. *Biotechniques*, 57, 254-256.
- Scoaris, D. D., Colacite, J., Nakamura, C. V., Ueda-Nakamura, T., de Abreu, B. A. and Dias, B. P. 2008. Virulence and antibiotic susceptibility of *Aeromonas* spp. isolated from drinking water. *Antonie Van Leeuwenhoek International Journal of General and Molecular Microbiology*, 93, 111-122.
- Sekar, R., Deines, P., Machell, J., Osborn, A. M., Biggs, C. A. and Boxall, J. B. 2012. Bacterial water quality and network hydraulic characteristics: a field study of a small, looped water distribution system using culture-independent molecular methods. *J Appl Microbiol*, 112, 1220-1234.
- Semrau, J. D., Chistoserdov, A., Lebron, J., Costello, A., Davagnino, J., Kenna, E., Holmes, A. J., Finch, R., Murrell, J. C. and Lidstrom, M. E. 1995. Particulate Methane Monooxygenase Genes in Methanotrophs. *J Bacteriol*, 177, 3071-3079.
- Senesi, S., Celandroni, F., Salvetti, S., Beecher, D. J., Wong, A. C. L. and Ghelardi, E. 2002. Swarming motility in *Bacillus cereus* and characterization of a *fliY* mutant impaired in swarm cell differentiation. *Microbiology-Sgm*, 148, 1785-1794.
- Sheng, G. P., Yu, H. Q. and Li, X. Y. 2010. Extracellular polymeric substances (EPS) of microbial aggregates in biological wastewater treatment systems: A review. *Biotechnology Advances*, 28, 882-894.
- Shilo, M. and Bruff, B. 1965. Lysis of Gram-Negative Bacteria by Host-Independent Ectoparasitic *Bdellovibrio* Bacteriovorus Isolates. *Journal of General Microbiology*, 40, 317-8.
- Simões, L. C. 2012. Biofilms in drinking water. *Biofilms in drinking water: formation and control*. LAMBERT Academic Publishing.
- Simoës, L. C. and Simoes, M. 2013. Biofilms in drinking water: problems and solutions. *Rsc Advances*, 3, 2520-2533.
- Simoës, L. C., Simoes, M., Oliveira, R. and Vieira, M. J. 2007a. Potential of the adhesion of bacteria isolated from drinking water to materials. *Journal of Basic Microbiology*, 47, 174-183.
- Simões, L. C., Simões, M. and Vieira, M. J. 2007. Biofilm interactions between distinct bacterial genera isolated from drinking water. *Appl Environ Microbiol*, 73, 6192-6200.
- Simões, L. C., Simões, M. and Vieira, M. J. 2008. Intergeneric coaggregation among drinking water bacteria: Evidence of a role for *Acinetobacter calcoaceticus* as a bridging bacterium. *Appl Environ Microbiol*, 74, 1259-1263.

- Simoës, M., Pereira, M. O., Sillankorva, S., Azeredo, J. and Vieira, M. J. 2007b. The effect of hydrodynamic conditions on the phenotype of *Pseudomonas fluorescens* biofilms. *Biofouling*, 23, 249-258.
- Singla, A., Verma, D., Lal, B. and Sarma, P. M. 2014. Enrichment and optimization of anaerobic bacterial mixed culture for conversion of syngas to ethanol. *Bioresour Technol*, 172, 41-49.
- Soge, O. O., Giardino, M. A., Ivanova, I. C., Pearson, A. L., Meschke, J. S. and Roberts, M. C. 2009. Low prevalence of antibiotic-resistant gram-negative bacteria isolated from rural south-western Ugandan groundwater. *Water SA*, 35, 343-347.
- Son, K., Brumley, D. R. and Stocker, R. 2015. Live from under the lens: exploring microbial motility with dynamic imaging and microfluidics. *Nature Reviews Microbiology*, 13, 761-775.
- Soutourina, O. A., Semenova, E. A., Parfenova, V. V., Danchin, A. and Bertin, P. 2001. Control of bacterial motility by environmental factors in polarly flagellated and peritrichous bacteria isolated from Lake Baikal. *Appl Environ Microbiol*, 67, 3852-9.
- Srinivasan, S., Harrington, G. W., Xagorarakis, I. and Goel, R. 2008. Factors affecting bulk to total bacteria ratio in drinking water distribution systems. *Water Res*, 42, 3393-3404.
- Stackelberg, P. E., Gibs, J., Furlong, E. T., Meyer, M. T., Zaugg, S. D. and Lippincott, R. L. 2007. Efficiency of conventional drinking-water-treatment processes in removal of pharmaceuticals and other organic compounds. *Science of the Total Environment*, 377, 255-272.
- Staudt, C., Horn, H., Hempel, D. C. and Neu, T. R. 2004. Volumetric measurements of bacterial cells and extracellular polymeric substance glycoconjugates in biofilms. *Biotechnol Bioeng*, 88, 585-592.
- Stepanovic, S., Vukovic, D., Dakic, I., Savic, B. and Svabic-Vlahovic, M. 2000. A modified microtiter-plate test for quantification of staphylococcal biofilm formation. *J Microbiol Methods*, 40, 175-179.
- Stewart, P. S. and Franklin, M. J. 2008. Physiological heterogeneity in biofilms. *Nature Reviews Microbiology*, 6, 199-210.
- Stickler, D. J. 2008. Bacterial biofilms in patients with indwelling urinary catheters. *Nat Clin Pract Urol*, 5, 598-608.
- Stocker, R., Seymour, J. R., Samadani, A., Hunt, D. E. and Polz, M. F. 2008. Rapid chemotactic response enables marine bacteria to exploit ephemeral microscale nutrient patches. *Proc Natl Acad Sci U S A*, 105, 4209-4214.
- Stoecker, K., Dorninger, C., Daims, H. and Wagner, M. 2010. Double labeling of oligonucleotide probes for fluorescence in situ hybridization (DOPE-FISH) improves signal intensity and increases rRNA accessibility. *Appl Environ Microbiol*, 76, 922-6.
- Stoodley, P., Boyle, J. D., Dodds, I. and Lappin-Scott, H. M. 1997. Consensus model of biofilm structure. In: Wimpenny, J. W. T., Handley, P. S., Gilbert, P., Lappin-Scott, H. M. & Jones, M. (eds.) *Biofilms: Community Interactions and Control*. Cardiff, United Kingdom.
- Stoodley, P., Dodds, I., Boyle, J. D. and Lappin-Scott, H. M. 1999a. Influence of hydrodynamics and nutrients on biofilm structure. *J Appl Microbiol*, 85, 19S-28S.
- Stoodley, P., Lewandowski, Z., Boyle, J. D. and Lappin-Scott, H. M. 1999b. The formation of migratory ripples in a mixed species bacterial biofilm growing in turbulent flow. *Environ Microbiol*, 1, 447-455.

- Stoodley, P., Wilson, S., Hall-Stoodley, L., Boyle, J. D., Lappin-Scott, H. M. and Costerton, J. W. 2001. Growth and detachment of cell clusters from mature mixed-species biofilms. *Appl Environ Microbiol*, 67, 5608-5613.
- Szabo, J. G., Rice, E. W. and Bishop, P. L. 2007. Persistence and decontamination of *Bacillus atrophaeus* subsp. *globigii* spores on corroded iron in a model drinking water system. *Appl Environ Microbiol*, 73, 2451-7.
- Szewzyk, U., Szewzyk, R., Manz, W. and Schleifer, K. H. 2000. Microbiological safety of drinking water. *Annual Review of Microbiology*, 54, 81-127.
- Thiel, T. 1999. Streaking Microbial Cultures on Agar Plates. *Science in the Real World: Microbes in Action*. Department of Biology, University of Missouri-St. Louis.
- Thomas, V., Herrera-Rimann, K., Blanc, D. S. and Greub, G. 2006. Biodiversity of amoebae and amoeba-resisting bacteria in a hospital water network. *Appl Environ Microbiol*, 72, 2428-2438.
- Toguchi, A., Siano, M., Burkart, M. and Harshey, R. M. 2000. Genetics of swarming motility in *Salmonella enterica* serovar typhimurium: critical role for lipopolysaccharide. *J Bacteriol*, 182, 6308-21.
- Tolker-Nielsen, T., Brinch, U. C., Ragas, P. C., Andersen, J. B., Jacobsen, C. S. and Molin, S. 2000. Development and dynamics of *Pseudomonas* sp biofilms. *J Bacteriol*, 182, 6482-6489.
- Trejo, M., Douarche, C., Bailleux, V., Poulard, C., Mariot, S., Regeard, C. and Raspaud, E. 2013. Elasticity and wrinkled morphology of *Bacillus subtilis* pellicles. *Proc Natl Acad Sci U S A*, 110, 2011-2016.
- Trotsenko, Y. A. and Doronina, N. V. 2003. The biology of methylobacteria capable of degrading halomethanes. *Microbiology*, 72, 121-131.
- Ude, S., Arnold, D. L., Moon, C. D., Timms-Wilson, T. and Spiers, A. J. 2006. Biofilm formation and cellulose expression among diverse environmental *Pseudomonas* isolates. *Environ Microbiol*, 8, 1997-2011.
- Van Aken, B., Yoon, J. M. and Schnoor, J. L. 2004. Biodegradation of nitro-substituted explosives 2,4,6-trinitrotoluene, hexahydro-1,3,5-trinitro-1,3,5-triazine, and octahydro-1,3,5,7-tetranitro-1,3,5-tetrazocine by a phytosymbiotic *Methylobacterium* sp. associated with poplar tissues (*Populus deltoides* x *nigra* DN34). *Appl Environ Microbiol*, 70, 508-17.
- van Loosdrecht, M. C. M., Eikelboom, D., Gjaltema, A., Tjihuis, L. and Heijnen, J. J. 1995. Biofilm structures. *Water Science and Technology*, 32, 35-43.
- Vanloosdrecht, M. C. M., Lyklema, J., Norde, W. and Zehnder, A. J. B. 1989. Bacterial Adhesion - a Physicochemical Approach. *Microb Ecol*, 17, 1-15.
- Vanoss, C. J. 1993. Acid-Base Interfacial Interactions in Aqueous-Media. *Colloids and Surfaces a-Physicochemical and Engineering Aspects*, 78, 1-49.
- Velicer, G. J. and Mendes-Soares, H. 2009. Bacterial predators. *Current Biology*, 19, R55-R56.
- Veyisoglu, A., Camas, M., Tatar, D., Guven, K., Sazaki, A. and Sahin, N. 2013. *Methylobacterium tarhaniae* sp nov., isolated from arid soil. *Int J Syst Evol Microbiol*, 63, 2823-2828.
- Vijayakumar, A., Kashter, Y., Kelner, R. and Rosen, J. 2016. Coded aperture correlation holography-a new type of incoherent digital holograms. *Optics Express*, 24, 2430-2441.
- Visick, K. L., Quirke, K. P. and McEwen, S. M. 2013. Arabinose Induces Pellicle Formation by *Vibrio fischeri*. *Appl Environ Microbiol*, 79, 2069-2080.
- Vu, B., Chen, M., Crawford, R. J. and Ivanova, E. P. 2009. Bacterial Extracellular Polysaccharides Involved in Biofilm Formation. *Molecules*, 14, 2535-2554.

- Waller, K., Swan, S. H., DeLorenze, G. and Hopkins, B. 1998. Trihalomethanes in drinking water and spontaneous abortion. *Epidemiology*, 9, 134-140.
- Wang, J. M., Liu, M., Xiao, H. J., Wu, W., Xie, M. J., Sun, M. J., Zhu, C. L. and Li, P. F. 2013. Bacterial community structure in cooling water and biofilm in an industrial recirculating cooling water system. *Water Science and Technology*, 68, 940-947.
- Wang, X. and Melchers, R. E. 2017. Corrosion of carbon steel in presence of mixed deposits under stagnant seawater conditions. *Journal of Loss Prevention in the Process Industries*, 45, 29-42.
- Wang, X., Sahr, F., Xue, T. and Sun, B. 2007. *Methylobacterium* *salsuginis* sp nov., isolated from seawater. *Int J Syst Evol Microbiol*, 57, 1699-1703.
- WaterCommittee 1953. The Effect of Sodium Thiosulphate on the Coliform and Bacterium-Coli Counts of Non-Chlorinated Water Samples. Public Health Laboratory Service (PHLS). *Journal of Hygiene*, 51 572-577.
- Waters, C. M. and Bassler, B. L. 2005. Quorum sensing: Cell-to-cell communication in bacteria. *Annual Review of Cell and Developmental Biology*, 21, 319-346.
- Weon, H. Y., Kim, B. Y., Joa, J. H., Son, J. A., Song, M. H., Kwon, S. W., Go, S. J. and Yoon, S. H. 2008. *Methylobacterium iners* sp nov and *Methylobacterium aerolatum* sp nov., isolated from air samples in Korea. *Int J Syst Evol Microbiol*, 58, 93-96.
- WHO 2004. Biosafety Manual. World Health Organization (WHO) Laboratory. Third Edition. Geneva, Switzerland.
- WHO 2008. Guidelines for Drinking-water Quality. World Health Organisation (WHO). Volume 1. Third Edition. Geneva, Switzerland.
- Wiener, N. 1930. Generalized harmonic analysis. *Acta Mathematica*, 55, 117-258.
- Wilhartitz, I., Mach, R. L., Teira, E., Reinthaler, T., Herndl, G. J. and Farnleitner, A. H. 2007. Prokaryotic community analysis with CARD-FISH in comparison with FISH in ultra-oligotrophic ground- and drinking water. *J Appl Microbiol*, 103, 871-881.
- Williams, M. M., Domingo, J. W. S., Meckes, M. C., Kelty, C. A. and Rochon, H. S. 2004. Phylogenetic diversity of drinking water bacteria in a distribution system simulator. *J Appl Microbiol*, 96, 954-964.
- Wimpenny, J., Manz, W. and Szewzyk, U. 2000. Heterogeneity in biofilms. *Fems Microbiology Reviews*, 24, 661-671.
- Wingender, J. and Flemming, H. C. 2004. Contamination potential of drinking water distribution network biofilms. *Water Science and Technology*, 49, 277-286.
- Wolfe, A. J. and Berg, H. C. 1989. Migration of Bacteria in Semisolid Agar. *Proc Natl Acad Sci U S A*, 86, 6973-6977.
- Wu, W., Giese, R. F. and van Oss, C. J. 1999. Stability versus flocculation of particle suspensions in water - correlation with the extended DLVO approach for aqueous systems, compared with classical DLVO theory. *Colloids and Surfaces B-Biointerfaces*, 14, 47-55.
- Xu, F. F., Morohoshi, T., Wang, W. Z., Yamaguchi, Y., Liang, Y. and Ikeda, T. 2014. Evaluation of intraspecies interactions in biofilm formation by *Methylobacterium* species isolated from pink-pigmented household biofilms. *Microbes Environ*, 29, 388-92.
- Xu, H. S., Roberts, N., Singleton, F. L., Attwell, R. W., Grimes, D. J. and Colwell, R. R. 1982. Survival and Viability of Nonculturable *Escherichia-*

- Coli and Vibrio-Cholerae in the Estuarine and Marine-Environment. *Microb Ecol*, 8, 313-323.
- Yang, X. M., Beyenal, H., Harkin, G. and Lewandowski, Z. 2000. Quantifying biofilm structure using image analysis. *J Microbiol Methods*, 39, 109-119.
- Yano, T., Kubota, H., Hanai, J., Hitomi, J. and Tokuda, H. 2013. Stress Tolerance of Methylobacterium Biofilms in Bathrooms. *Microbes and Environments*, 28, 87-95.
- Yotsumoto, H. and Yoon, R. H. 1993a. Application of Extended DLVO Theory .1. Stability of Rutile Suspensions. *Journal of Colloid and Interface Science*, 157, 426-433.
- Yotsumoto, H. and Yoon, R. H. 1993b. Application of Extended DLVO Theory .2. Stability of Silica Suspensions. *Journal of Colloid and Interface Science*, 157, 434-441.
- Zamani, I., Bouzari, M., Emtiazi, G. and Fanaei, M. 2015. Rapid Quantitative Estimation of Chlorinated Methane Utilizing Bacteria in Drinking Water and the Effect of Nanosilver on Biodegradation of the Trichloromethane in the Environment. *Jundishapur Journal of Microbiology*, 8.
- Zhang, P., Lapara, T. M., Goslan, E. H., Xie, Y. F., Parsons, S. A. and Hozalski, R. M. 2009. Biodegradation of Haloacetic Acids by Bacterial Isolates and Enrichment Cultures from Drinking Water Systems. *Environ Sci Technol*, 43, 3169-3175.
- Zhang, T., Fang, H. H. P. and Ko, B. C. B. 2003. Methanogen population in a marine biofilm corrosive to mild steel. *Appl Microbiol Biotechnol*, 63, 101-106.
- Zheng, M. Z., He, C. G. and He, Q. 2015. Fate of free chlorine in drinking water during distribution in premise plumbing. *Ecotoxicology*, 24, 2151-2155.
- Zhu, X. Y., Lubeck, J. and Kilbane, J. J. 2003. Characterization of microbial communities in gas industry pipelines. *Appl Environ Microbiol*, 69, 5354-5363.